Louisiana State University
LSU Digital Commons

LSU Doctoral Dissertations | Graduate School

2007

Synthesis of Quaternary Dendronized Cellulose Derivatives and Their Potential Biological Applications

Changde Zhang
Louisiana State University and Agricultural and Mechanical College

Follow this and additional works at: https://digitalcommons.lsu.edu/gradschool_dissertations

Part of the Chemistry Commons

Recommended Citation
Zhang, Changde, "Synthesis of Quaternary Dendronized Cellulose Derivatives and Their Potential Biological Applications" (2007). *LSU Doctoral Dissertations*. 2168.
https://digitalcommons.lsu.edu/gradschool_dissertations/2168

This Dissertation is brought to you for free and open access by the Graduate School at LSU Digital Commons. It has been accepted for inclusion in LSU Doctoral Dissertations by an authorized graduate school editor of LSU Digital Commons. For more information, please contactgradetd@lsu.edu.

SYNTHESIS OF QUATERNARY DENDRONIZED CELLULOSE DERIVATIVES AND THEIR POTENTIAL BIOLOGICAL APPLICATIONS

A Dissertation

Submitted to the Graduate Faculty of the
Louisiana State University and
Agriculture and Mechanical College
in partial fulfillment of the
requirements for the degree of
Doctor of Philosophy

In

The Department of Chemistry

by
Changde Zhang
B.S., Liaocheng Teacher College, China, 1986
M.S., Xi'an Jiaotong University, China, 1989
M.S., Case Western Reserve University, USA, 2002
August 2007

To my wife, Wenju Wu, for her love and support

and

To my child, my parents, and my parents-in-law for their love and support

ACKNOWLEDGEMENTS

First of all, I want to express my sincere appreciation to my adviser and mentor, Professor William H. Daly, for his guidance, patience, encouragement, kindness, and financial support. His wealth of knowledge has been a fortune in my research. His advice and support has encouraged me to go through many challenging times I have faced during my academic pursuit and my life in America. It would be impossible for me to finish this dissertation without his strong support. His tough questions have promoted me to analyze my research more critically and more profoundly. His advice will always benefit my career and my life in the future.

I would also like to thank my committee members: Professor Ioan I. Negulescu, Professor M. Graca H. Vicente, Professor David A. Spivak, Professor G. Wayne, and Professor Gundrum Schmidt for reviewing my research, and giving me valuable suggestions. I would especially like to thank professor Ioan I. Negulescu for his teaching on using thermo analysis technique in polymer characterization and data analysis. I will remember their kindness and care to me forever. Their help and advice are very valuable for my dissertation research and for stimulating the growth of my graduate career at LSU.

I would like to further thank Professor Paul S. Russo for instructing me on the usage of GPC-Light scattering technique, Dr. Rafael Cueto and Dr. Dale Treleaven for the help in my work in the fluorescence and NMR experiment, Dr. Martha Juban for her instruction in antibacterial tests, and Professor Marcia Newcomer for the advise in the preparation of phospholipid vesicles.

I would like to thank the fellow members in Dr Daly's group for their support and friendship during my graduate study. I deeply appreciate Professor Steve Watkins, the director of the Graduate Program in the Chemistry Department; Sherry Wilkes, the secretary of the Graduate

Program in the Chemistry Department; Vickie Thornton, and Genell Bodoin for their help during my graduate life at LSU.

Finally I am grateful to my wife Wenju Wu, my child Can (Jane) Zhang, and my whole family for their sacrifice and support for my graduate studies in America.

TABLE OF CONTENTS

ACKNOWLEDGEMENTS iii

LIST OF TABLES ix

LIST OF FIGURES x

LIST OF ABBREVIATIONS xiii

ABSTRACT xviii

CHAPTER 1. INTRODUCTION 1
1.1 Cellulose and Its Derivatives 1
1.1.1 Fundamentals of Cellulose Chemistry 1
1.1.2 Cellulose Derivatives 3
1.1.3 Cellulose Applications in Industry 5
1.2 Polymeric Antimicrobial Agents 8
1.3 Polysaccharide Chemistry Research in Dr. William H. Daly's Group 10
1.4 Dendrimers 11
1.5 Dendronization of Cellulose 15
1.5.1 Proposed Advantages of Dendronized Cellulose Derivatives 15
1.5.2 Newkome's AB3 Monomer Dendron 16
1.5.3 Our Design of Dendronized Cellulose Derivatives: Dendrigraft-polyamino and Dendrigraft-polyquat 16
1.6 Present Project 19

CHAPTER 2. SYNTHESIS AND CHARACTERIZATION OF NEWKOME'S DENDRON 20
2.1 Introduction 20
2.2 Experimental 22
2.2.1 Synthesis of Behera's Amine 22
2.2.2 Synthesis of 2nd Generation Newkome's Dendron 23
2.3 Results and Discussions 25
2.3.1 Synthesis of Behera's Amine 25
2.3.2 Synthesis of 2nd Generation Newkome's Dendron 28
2.3.3 FTIR Characterization 33
2.3.4 Thermo-analysis Characterization 33
2.4 Conclusions 36

CHAPTER 3. SYNTHESIS AND CHARACTERIZATION OF WATER SOLUBLE AMIDOAMINE DENDRONIZED CELLULOSE DERIVATIVES 37
3.1 Introduction 37
3.2 Experimental 39
3.2.1 Synthesis of CMCDMPDA 40
3.2.2 Synthesis of CMCBADMPDA 41
3.2.3 Synthesis of CMCBABADMPDA 43
3.3 Results and Discussion 44
3.3.1 Synthesis of CMCDMPDA 44
3.3.2 Synthesis of CMCBA 47
3.3.3 Control of DS of CMCBA 50
3.3.4 Synthesis of CMCBABA 53
3.3.5 Synthesis of CMCBADMPDA 56
3.3.6 Synthesis of CMCBABADMPDA 58
3.3.7 FTIR Characterization of CMC, CMCBA, CMCBABA, CMCBADMPDA, and CMCBABADMPDA 60
3.3.8 TGA Characterization of CMC, CMCBA, CMCBADMPDA, and CMCBABADMPDA 61
3.3.9 Intrinsic Viscosity Characterization of CMCBADMPDA and CMCBABADMPDA 63
3.3.10 Molecular Weight and Molecular Size Characterization of CMC, CMCDMPDA, CMCBADMPDA, and CMCBABADMPDA by GPC-LS 65
3.4 Conclusions 68

CHAPTER 4. HYDROPHOBICITY/HYDROPHILICITY STUDY OF WATER SOLUBLE AMIDOAMINE DENDRONIZED CELLULOSE DERIVATIVES 70
4.1 Introduction 70
4.2 Experimental 72
4.2.1 Solution Preparation 72
4.2.2 Fluorescence Measurement 72
4.3 Results and Discussions 72
4.3.1 The Hydrophobicity of CMCBADMPDA in Its Aqueous Solutions with Different Concentrations 72
4.3.2 The Hydrophobicity of CMCBABADMPDA in Its Aqueous Solutions with Different Concentrations 74
4.3.3 Effect of Saline Condition on the Hydrophobicity of the Microenviroments in Aqueous CMCBADMPDA and CMCBABADMPDA Solutions 75
4.4 Conclusions 75

CHAPTER 5. SYNTHESIS OF DENDRONIZED CELLULOSE DERIVATIVES WITH QUATERNARY AMMONIUM FUNCTIONAL GROUPS 77
5.1 Introduction 77
5.2 Experimental 82
5.2.1 Synthesis of CMCDMPDA-Quat188 82
5.2.2 Synthesis of CMCBADMPDA-Quat188 82
5.2.3 Synthesis of CMCBADMPDA-C1 83

5.2.4 Synthesis of CMCBADMPDA-R 83
5.2.5 Synthesis of CMCDMPDA-R 85
5.2.6 Synthesis of CMCBADMPDA-C10 with Different DS of C10 86
5.2.7 Synthesis of CMCBADMPDA-C10-quat188 86
5.2.8 Synthesis of CMCBADMPDA-C10-PO 87
5.2.9 Determination of Quat Content of Quaternary Ammonium Dendronized Cellulose Derivatives 87
5.3 Results and Discussions 88
5.3.1 Synthesis and Characterization of CMCBADMPDA-Quat188 88
5.3.2 Synthesis and Characterization of CMCBADMPDA-R 90
5.3.3 Control of the Degree of Quaternization (DQ) of CMCBADMPDA-C10 95
5.3.4 Synthesis and Characterization of CMCBADMPDA-C10-quat188 98
5.3.5 Synthesis and Characterization of CMCBADMPDA-R-PO 99
5.3.6 FTIR Characterization 101
5.3.7 Thermo Analysis Characterization 102
5.4 Conclusions 110

CHAPTER 6. ANTIMICROBIAL ASSESSMENT OF WATER SOLUBLE DENDRONIZED CELLULOSE DERIVATIVES WITH QUATERNARY AMMONIUM FUNCTIONAL GROUPS 112
6.1 Introduction 112
6.2 Experimental 114
6.2.1 Materials 114
6.2.2 Evaluation of Antimicrobial Activity 115
6.2.3 Dye Release in Encapsulated Phospholipid Vesicles 118
6.3 Results and Discussion 119
6.3.1 Dendritic Effect on the Antibacterial Properties of Dendronized Cellulose 119
6.3.2 Effect of Di-quaternary Nitrogens and Chain Lengths on the Antibacterial Properties of Dendronized Cellulose 120
6.3.3 Effects of Degree of Quaternization on the Antibacterial Properties of CMCBADMPDA-C10 121
6.3.4 Effect of Degree of Quaternization of C10 on the Antibacterial Properties of CMCBADMPDA-C10-Quat188 123
6.3.5 The Antimicrobial Property of CMCBADMPDA-C10-PO 124
6.3.6 The Mode of Antimicrobial Action of Dendronized Cellulose Derivatives 124
6.3.7 Phospholipid Vesicle Leakage Releasing Encapsulated Dye 126
6.4 Conclusions 128

CHAPTER 7. SYNTHESIS OF DENDRONIZED CELLULOSE DERIVATIVES BY NUCLEOPHILIC SUBSTITUTION OF TOSYLATED CELLULOSE OR BROMOPROPYLCELLULOSE 129
7.1 Introduction 129
7.2 Experimental 131
7.2.1 Synthesis of Tosylated Cellulose 131
7.2.2 Synthesis of N,N-dimethylaminopropylcarbomoylmethyl Modified Cellulose (Cellulose-DMPDA) from Tosylated Cellulose 131

7.2.3 Synthesis of Bromopropylcellulose 132
7.2.4 Synthesis of Cellulose-BA from Bromopropylcellulose 132
7.3 Results and Discussion 133
7.3.1 Attempted Synthesis of Cellulose-BA via Tosylated Cellulose 133
7.3.2 Synthesis of Dendronized Cellulose through Bromopropylcellulose 135
7.4 Conclusions 136

CHAPTER 8. SUMMARY AND FUTURE WORK 137
8.1 Conclusions 137
8.2 Future Work 139

REFERENCES 140

APPENDIX: PERMISSION LETTER. 148

VITA 150

LIST OF TABLES

Table 2.1. TGA peaks of nitrotriester, BA, and G-2-amine 36

Table 3.1. Influence of DS of CMC on DS of CMCBA [a] 51

Table 3.2. Influence of MW of CMC on DS of CMCBA [a] 51

Table 3.3. Influence of relative concentration of CMPI on DS of CMCBA 52

Table 3.4. Synthesis of CMCBADMPDA 58

Table 3.5. Weight loss, residue of CMC, CMCBA, CMCBABA, CMCBADMPDA, and CMCBABADMPDA 63

Table 3.6. Intrinsic viscosity of CMC, CMCDMPDA, CMCBADMPDA 65

Table 3.7. The molecular size, molecular weight, and distribution of CMC, CMADMPDA, and CMCBADMPDA from GPC-LS 67

Table 4.1. The ratio of I_{373}/I_{384} of pyrene (2μM) in aqueous solutions 73

Table 5.1. Preparation of CMCBADMPDA-R 93

Table 5.2. The DQ of CMCBADMPDA-C10 measured by titration 96

Table 5.3. The synthesis of CMCBADMPDA-C10-Quat188 99

Table 5.4. The synthesis of CMCBADMPDA-C10-PO 101

Table 5.5. The TGA analysis of quaternary ammonium dendronized cellulose derivatives 105

Table 6.1. The compositions in the wells in the three zones on 96-well plates 118

Table 6.2. Effect of dendritic structure on the antimicrobial activity of cellulose derivatives ... 119

Table 6.3. Effect of chain lengths and diquat on the antibacterial properties of dendronized cellulose 121

Table 6.4. Effect of DQ on the antibacterial properties of dendronized cellulose CMCBADMPDA-C10 122

Table 6.5. Effect of DQ of C10 on the antibacterial properties of CMCBADMPDA-C10-Quat188 123

Table 6.6. The antimicrobial properties of dendronized cellulose CMCBADMPDA-C10-PO .. 124

LIST OF FIGURES

Figure 2.1. ^{1}H NMR spectrum of nitrotriester. 26

Figure 2.2. ^{13}C NMR spectrum of nitrotriester. 27

Figure 2.3. ^{1}H NMR spectrum of Behera amine. 27

Figure 2.4. ^{13}C NMR spectrum of Behera amine. 28

Figure 2.5. ^{1}H NMR spectrum of G-2-nitro. 30

Figure 2.6. ^{13}C NMR spectrum of G-2-nitro. 30

Figure 2.7. MALDI-TOF mass spectra of G-2-nitro. 31

Figure 2.8. ^{1}H NMR spectrum of G-2-amine. 31

Figure 2.9. ^{13}C NMR spectrum of G-2-amine. 32

Figure 2.10. MALDI-TOF mass spectra of G-2-amine. 32

Figure 2.11. FTIR spectra of nitrotriester, BA, G-2-nitro, and G-2-amine. 33

Figure 2.12. TGA and DSC spectra of BA. 34

Figure 2.13. TGA spectra of nitrotriester, BA, and G-2-amine. 35

Figure 3.1. ^{1}H NMR of CMCDMPDA. 46

Figure 3.2. ^{13}C NMR of CMCDMPDA. 46

Figure 3.3. Deconvoluted TGA weight derivative curves of CMCBA for DS calculation of CBCBA based on the weight loss. 49

Figure 3.4. The corresponding peaks of the DSC curve and TGA curve of CMCBA. 49

Figure 3.5. Influence of DS of CMC on DS of CMCBA. 50

Figure 3.6. CMCBA with different DS produced using different concentration CMPI. 53

Figure 3.7. TGA of CMCBABA. 55

Figure 3.8. ^{1}H NMR Spectrum of CMCBADMPDA. 57

Figure 3.9. ^{13}C NMR Spectrum of CMCBADMPDA. 57

Figure 3.10. ^{1}H NMR Spectrum of CMCBABADMPDA. 59

Figure 3.11. ^{13}C NMR Spectrum of CMCBABADMPDA by divergent approach. 60

Figure 3.12. FTIR Spectrum of CMC, CMCBA, CMCBABA, CMCBADMPDA, and CMCBABADMPDA. 61

Figure 3.13. Thermo analysis plots of CMCBA and CMCBABA. 62

Figure 3.14. Thermo analysis plots of CMC, CMCBADMPDA, and CMCBABADMPDA. 62

Figure 3.15. Intrinsic viscosity of CMCBABADMPDA and CMCBADMPDA. 65

Figure 3.16. GPC-LS traces of CMC and CMCBADMPDA. 66

Figure 3.17. Relationship between RMS R_zs and molecular weights of CMCBADMPDA and CMC. 67

Figure 4.1. Solvent dependence of Vibronic band intensities in pyrene monomer fluorescence: [pyrene] = 2μM; λ_{excit} = 310nm.[90] 71

Figure 4.2. Fluorescence emission of pyrene in different concentration of CMCBADMPDA. ...73

Figure 4.3. Fluorescence emission of pyrene in different concentration of CMCBABADMPDA. 74

Figure 4.4. Influence of saline condition on fluorescence emission of pyrene in aqueous CMCBADMPDA solution. 75

Figure 4.5. Influence of saline condition on fluorescence emission of pyrene in aqueous CMCBABADMPDA solution. 76

Figure 5.1. ^{1}H NMR Spectrum of CMCBADMPDA-quat188. 89

Figure 5.2. ^{13}C NMR Spectrum of CMCBADMPDA-Quat188. 89

Figure 5.3. ^{13}C NMR of CMCBADMPDA-C1. 90

Figure 5.4. ^{1}H NMR of CMCBADMPDA-R with R=C4~C12. 92

Figure 5.5. FTIR of CMCBADMPDA-R. 93

Figure 5.6. FTIR of CMCBADMPDA-C10 with different DS of C10. 97

Figure 5.7. ^{1}H NMR of CMCBADMPDA-R-Quat188. 99

Figure 5.8. ^{1}H NMR of CMCBADMPDA-R-PO. 101

Figure 5.9. FTIR of quaternary ammonium dendronized cellulose derivatives with different functional groups 102

Figure 5.10. TGA curves of CMCBADMPDA, CMCBADMPDA-C10, and CMCBADMPDA-C10-PO..... 104

Figure 5.11. TGA curves of CMCBADMPDA, CMCBADMPDA-quat188, and CMCBADMPDA-C10-quat188. 105

Figure 5.12. DSC curve, weight loss curve, and deconvoluted TGA weight derivative curve of CMCBADMPDA-quat188. 108

Figure 5.13. DSC curve, weight loss curve, and deconvoluted TGA weight derivative curve of CMCBADMPDA-C10… 108

Figure 5.14. DSC curve, weight loss curve, and deconvoluted TGA weight derivative curve of CMCBADMPDA-C10-Quat188. 109

Figure 5.15. DSC curve, weight loss curve, and deconvoluted TGA weight derivative curve of CMCBADMPDA-C10-PO..... 110

Figure 6.1. Dye release profile from PG/PE vesicles encapsulated with calcein after adding CMCBADMPDA-C10 (17 μg/mL; MIC: 32 μg/mL against *E-Coli*), CMCBADMPDA-C10-Qaut188 (17 μg/mL; MIC: 256 μg/mL), and CMCBADMPDA-C10-PO (34 μg/mL, MIC>512 μg/mL). 127

Figure 7.1. ^{1}H NMR spectra of tosylated cellulose. 133

Figure 7.2. ^{1}H NMR spectrum of Cellulose-DMPDA. 134

Figure 7.3. ^{1}H NMR spectrum of dendronized cellulose in DMDO-d_6. 136

LIST OF ABBREVIATIONS

CMCBA

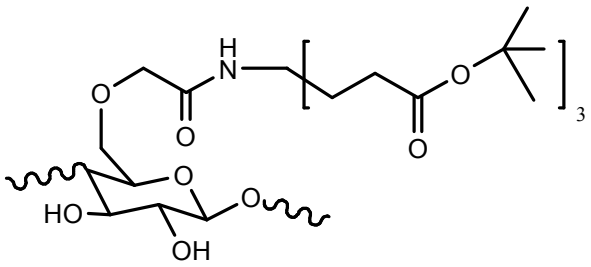

CMCBABA

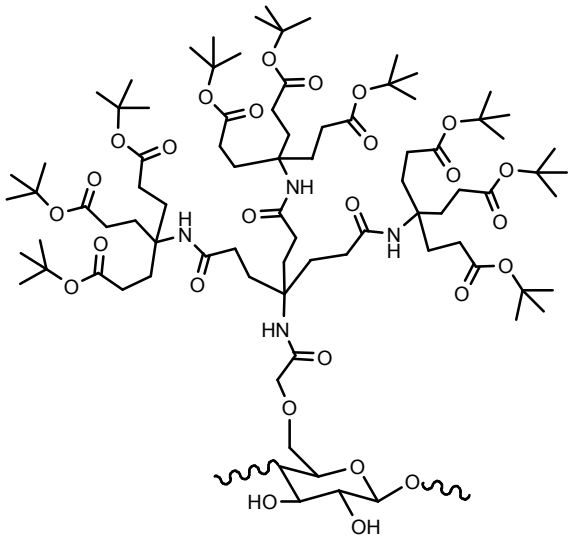

CMCDMPDA N,N-dimethylaminopropylcarbomoylmethyl cellulose

CMCBADMPDA

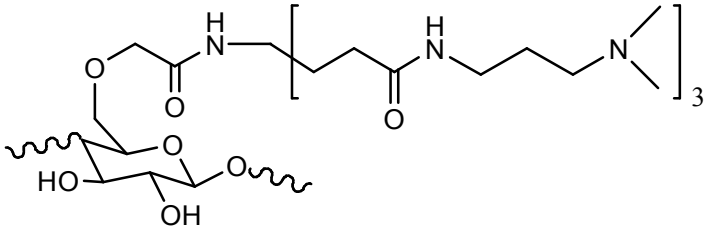

CMCBABADMPDA

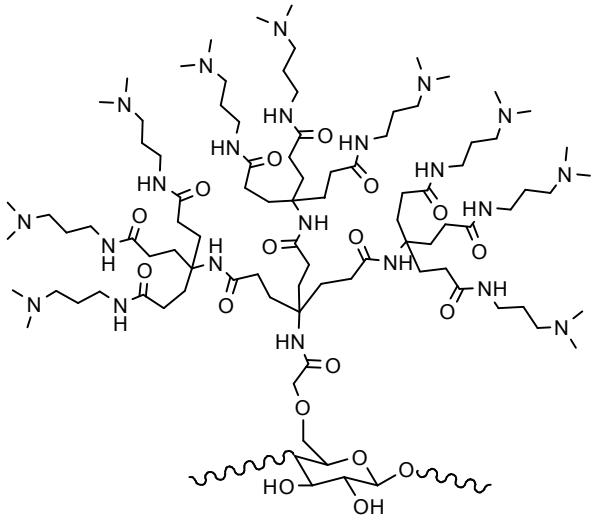

CMCBADMPDA-Quat188

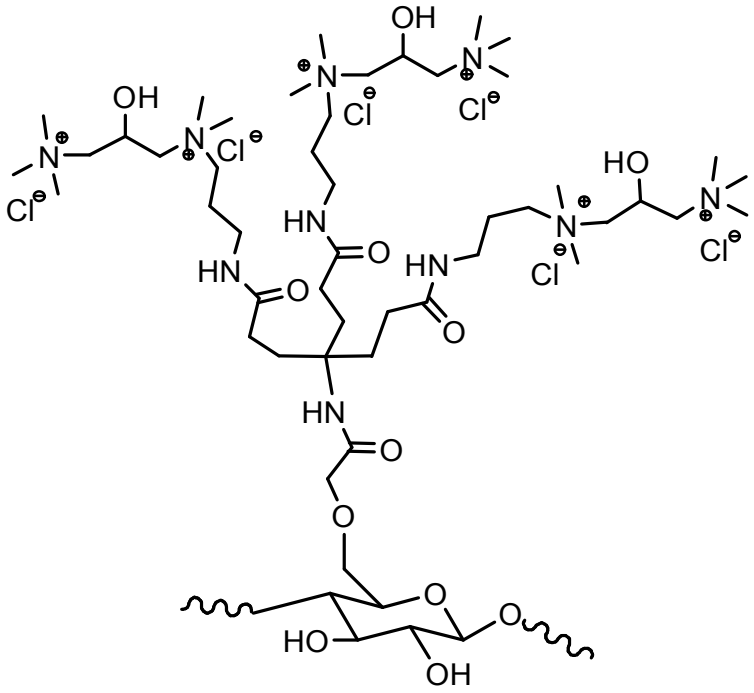

CMCBADMPDA-R

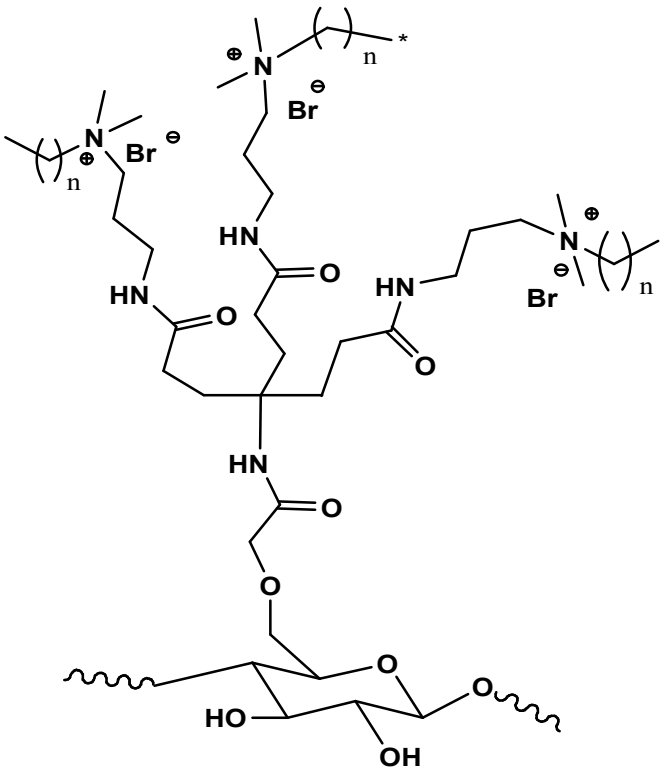

CMCBADMPDA-C10 CMCBADMPDA-R if the carbon chain length of R is ten

CMCBADMPDA-C10-PO

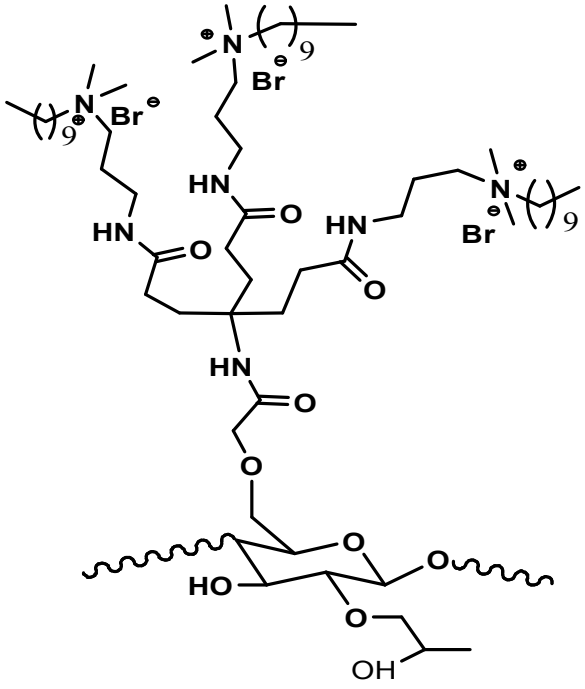

CMCBADMPDA-C10-Quat188

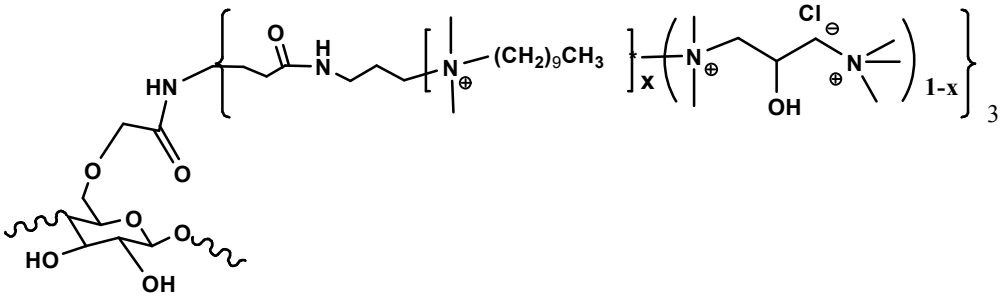

Cellulose-DMPDA

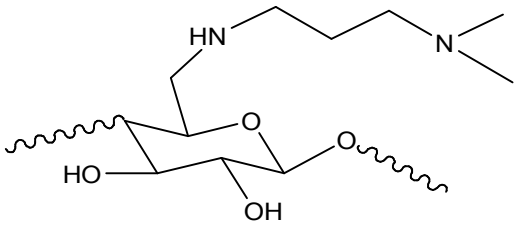

Cellulose-BA

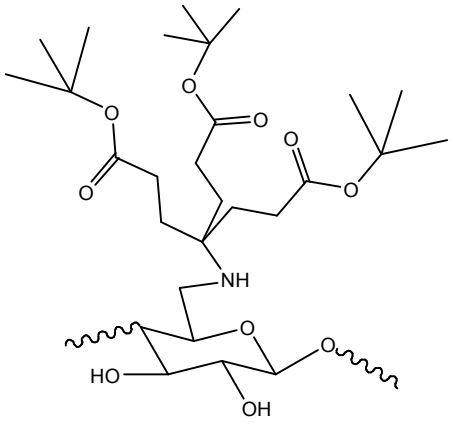

HPC-BA

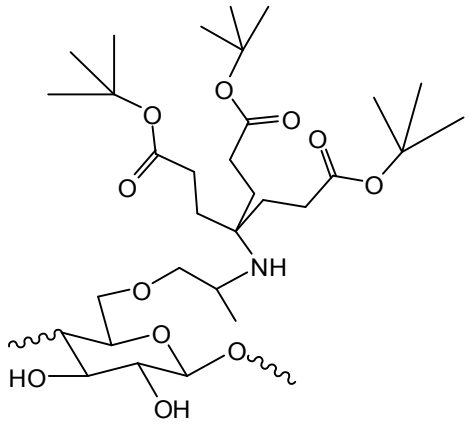

DQ	Degree of quaternization
DSC	Differential scanning calorimetry
MALDI-TOF	Matrix-assisted laser desorption/ionization-time of flight
MIC	Minimum inhibitory concentration
TGA	Thermogrametric analysis

ABSTRACT

In this dissertation, novel dendronized cellulose derivatives with biodegradable backbones were created by using sodium carboxymethyl cellulose (CMC) as the starting material. CMC was first transformed into its corresponding tetrabutyl ammonium salt, which reacted with 2-chloro-*N*-methylpyridinium iodide (CMPI) to produce an activated ester of [2-(N-methyl pyridium) carboxymethyl cellulose] iodide (MPCMCI). The reaction of MPCMCPI and di-*tert*-butyl 4-[2-(ter-butoxycarbonyl)ethyl]-4-aminoheptanedicarboxylate (BA) produced a new derivative with BA dendron elaborated on cellulose backbone (CMCBA). The degree of substitution (DS) of CMCBA was adjusted by controlling the relative concentration of CMPI and by choosing CMC with different DS or different molecular weights. Thermogrametric analysis (TGA) was used to estimate the DS of CMCBA. CMCBA was first hydrolyzed into its acid and further transformed into its corresponding tetrabutyl ammonium salt, activated ester (MPCMCBAI) with CMPI, and was further elaborated with BA to form the 2^{nd} generation dendronized cellulose derivative (CMCBABA). CMCBABA was transformed into its corresponding activated (MPCMCBABAI) using the same procedure used in forming MPCMCBAI. The reactions of MPCMCI, MPCMCBAI, or MPCMCBABAI with *N*,*N*-dimethyl-1,3-propanediamine (DMPDA) produced the water soluble N,N-dimethylaminopropylcarbamoylmethyl cellulose (CMCDMPDA), CMCBADMPDA, and CMCBABADMPDA respectively. Both CMCBADMPDA and CMCBABADMPDA showed lower intrinsic viscosities than CMCDMPDA due to their dendritic structure. The hydrophobicity of the microenviroments of CMCBADMPDA and CMCBABADMPDA was investigated by studying the fluorescence of pyrene in their aqueous solutions.

CMCBADMPDA was used to react with 3-chloro-2-hydroxypropyl trimethyl chloride (Quat188) or alkyl bromides to synthesize the dendronized cellulose with hydrophilic quaternary nitrogen periphery groups (CMCBADMPDA-Quat188) and the dendronized cellulose derivatives with hydrophobic alkyl chains with different carbon chain lengths on quaternary nitrogen (CMCBADMPDA-R). CMCBADMPDA-R with a carbon chain length of ten (CMCBADMPDA-C10) with high DS of C10 was further modified with Quat188 or propylene oxide to produce its water soluble form CMCBADMPDA-C10-Quat188 or CMCBADMPDA-C10-PO. The antimicrobial activity of these N-decyl,N,N-dimethyl quaternary dendronized cellulose derivatives was found using their minimum inhibitory concentration (MIC) against *E-coli* and *S-aureus* to be 32 μg/mL and 16 μg/mL respectively. The structure-antimicrobial property relations of quaternary ammonium cellulose derivatives were discussed by evaluating their MIC values and their molecular structures.

CHAPTER 1. INTRODUCTION

1.1 Cellulose and Its Derivatives

1.1.1 Fundamentals of Cellulose Chemistry

Cellulose composed of β-1,4-glycosidic units is the most abundant biodegradable polymer in nature. It was discovered by Anselme Payen in 1938 that the cell walls of many kinds of plants were constructed of the same substance. He named this substance as cellulose. The pyranose rings are in the $^4C1$ conformation (Scheme 1.1), which means that $–CH_2OH$, –OH groups, and glycosidic bonds are all equatorial with respect to the mean planes of rings. The repeating units (DP) of cellulose in different plant walls vary in a broad range from low 500 in the primary walls of protoplasts to as high as 18000 in the secondary walls of alga, Valonia;[1] but purification procedures usually reduce the DP of isolated cellulose to around 2500.[2] Cellulose exists as the structure component of cell walls of various types of plants such as cotton fiber (purest source), wood, plant stalks, leaves, and vegetable fibers.[3] Billions of tons of cellulose are produced annually by photosynthesis. The most common sources of cellulose for industrial use are wood pulp and cotton lint; other sources for industrial use include grasses such as esparto and bamboo.[4]

Scheme 1.1. Cellulose structure

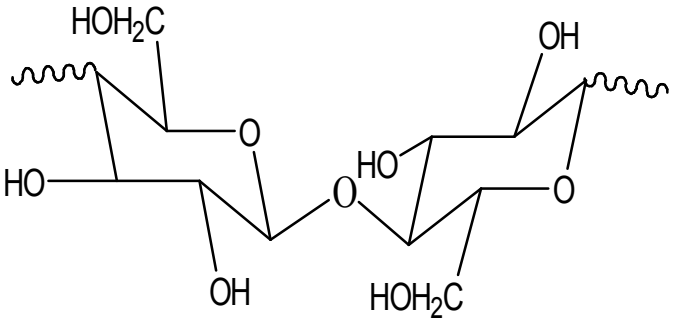

When the cellulose molecule is fully extended, it takes the form of a flat ribbon with hydroxyl groups protruding laterally and is capable of forming both inter-molecular and intra-molecular hydrogen bonds. (Scheme 1.2)[5] The surface of the ribbon consists mainly of hydrogen atoms linked directly to carbon and shows hydrophobic behavior. This leads to the formation of its supramolecular structure, microfibrils. Therefore, it often shows stiff-rod conformations and is water insoluble.[4]

Scheme 1.2. Intra-molecular and inter-molecular hydrogen bonding of cellulose

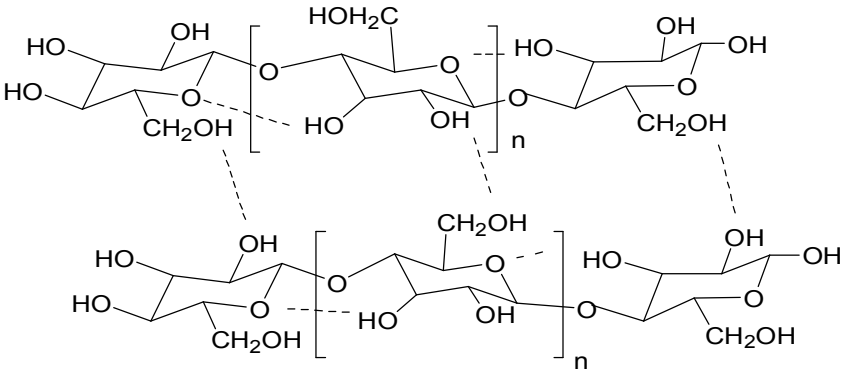

Cellulose in nature contains both amorphous and crystalline regions in its supramolecular structure. The two regions demonstrate different reactivity, solubility and other properties due to different accessibility[6] to various reactants and solvents with different molecular size, different hydrophobic or hydrophilic properties. The amorphous regions often show better reactivity than crystalline regions. To obtain uniformly distributed modified cellulose derivatives, it is important to use homogenous cellulose solutions in appropriate solvent systems.

There are three hydroxyl groups located at C2, C3, and C6 on one anhydroglucose unit. The essential features and chemical properties of cellulose molecules are related with the primary and secondary alcohol groups in each unit. The primary hydroxyl groups on C6 normally show greater reactivity than the other two secondary hydroxyl groups due to their more accessible location protruding out of the anhydroglucose ring. Many different groups can be attached to

C2, C3, and C6 and confer cellulose with different functions. The degree of substitution (DS) is defined as the average number of hydroxyl groups substituted in one anhydroglucose unit. The highest possible DS for cellulose is three because of the three hydroxyl groups on each anhydroglucose ring unit. Carboxymethyl cellulose (CMC) is one of the important commercialized cellulose ethers because of its water-solubility. It is normally prepared by reacting cellulose with $ClCH_2COONa$ under basic conditions. Scheme 1.3 shows the DS of a representative cellulose derivative where CMC acts as the example.

Scheme 1.3. The DS of CMC

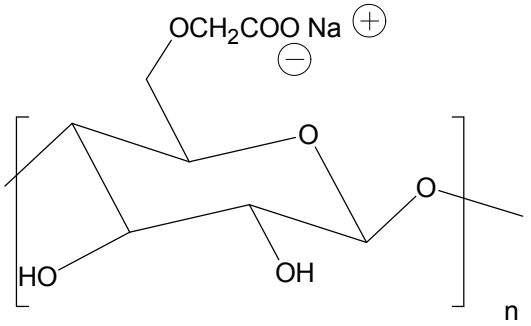

Formular: $[C_6H_7O_2(OH)x(OCH_2COONa)y]n$

$x + y = 3$

y = Degree of substitution

1.1.2 Cellulose Derivatives

The elaboration of various functional groups on cellulose has produced many useful derivatives in applications such as food additives, coatings, rheology modifiers, cosmetics, drug carriers, and controlled releasing drugs. The applications and properties of cellulose derivatives are greatly influenced by the category of functional groups elaborated on cellulose, their DS, crosslinking structure, and the degree of crosslinking. There are five categories of cellulose derivatives: inorganic esters, organic esters, cellulose ethers, cellulose graft copolymers, and

cross-linked cellulose. Cellulose can be oxidized, esterified, and converted into ethers. Scheme 1.4 shows some of the useful derivatives and the reactions for manufacturing them.[4]

Scheme 1.4. Cellulose derivatives formed based on reactions with hydroxyl groups of cellulose[7-9]

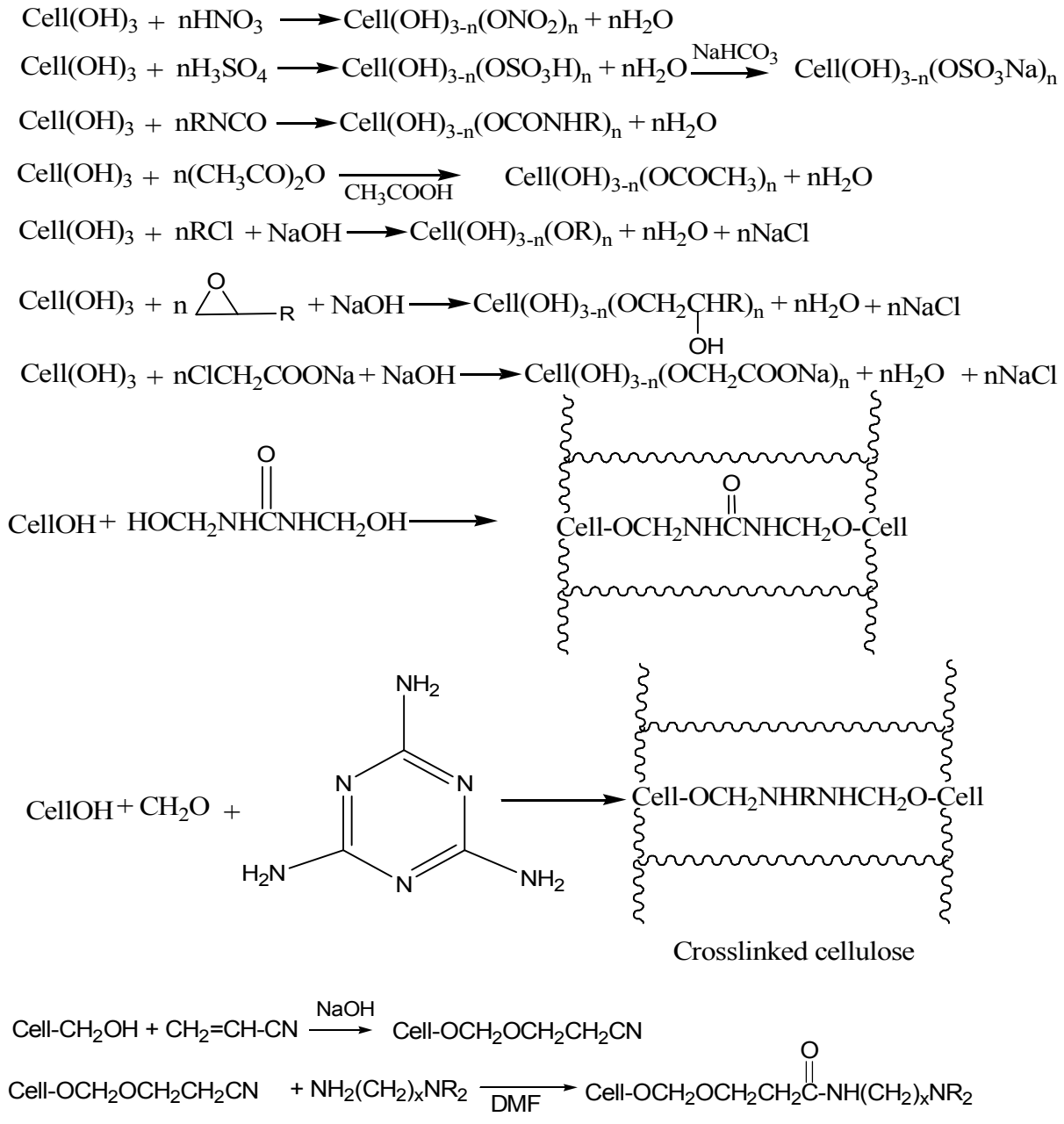

The esterification of cellulose with acid chlorides, anhydrides, and acids produces the esters of cellulose nitrate, cellulose sulfate, cellulose sulfonate, cellulose acetate, and cellulose phosphate.

The nucleophilic substitutions of cellulose with alkyl halides and nucleophilic addition with epoxides produce the ethers of ethylcellulose, methylcellulose, hydroxylpropylcellulose, hydroxyethylcellulose, and CMC. Michael addition to cellulose with acrylonitrile produces the ether of cynoethylcellulose. Oxidation of cellulose ether could introduce carboxylic acid groups or initiate free radical polymerization producing grafted cellulose. The reaction of cellulose with di, tri or more functional agents could produce a crosslinked cellulose structure. The varieties of structures of cellulose and its derivatives make them valuable in extremely broad areas.

1.1.3 Cellulose Applications in Industry

As the most abundant biodegradable polymer, cellulose is an important raw material. People have developed many ways to utilize this abundant natural resource. As I mentioned before, various chemical processes have been developed to modify cellulose. Cellulose and its derivatives have been produced in various forms beneficial for human use such as powder, solution, gel, cardboard, fiber, film, filter, and foam, etc. Cellulose has been used in every field of work. For example, cellulose is a natural fiber in cotton used in making clothes. Many types of paper products, which include fine papers for writing, printing, and copying, are based upon cellulose fibers. The absorption of cellulose is useful in diapers, feminine hygiene products, baby wipes, and other disposable wipes as well as in filters for automotive applications, coffee filters, cigarette filters, and tea bags. Crude cellulose is compressed into cardboard for packaging applications. Solutions of cellulose derivatives are employed in coatings, antibiotics, surfactants and viscosity thickeners for cosmetics, toothpaste, and personal care products. Films cast from dissolved cellulose are used in photography and food sealing packaging. Various forms of cellulose are important. It has also been used as insulation material, construction material for furniture, building, and recycled paper bags for shopping. Regenerated cellulose

fibers have been used in artificial mechanical hemodialyser organs and in dialysis for purifying polymers such as proteins.[10] Cellulose derivatives have also been commercialized as explosives, plastics, and flame retardants. Many companies are involved in this large business including International Paper, Atlas Paper Mills Ltd., Appleton, Brownville Specialty Paper Products Inc., Georgia-Pacific Corp., West Linn Paper Co., Innovia Films, Hercules, Celanese Corporation, BASF, and Cargill. A plethora of companies and research groups in academic institutes and government agencies have been actively involved in the development of better methods and new products utilizing this abundant, inexpensive, renewable, and recyclable natural resource.

New applications and novel ways of modifying and processing cellulose continue to be the interest of many research groups in academia and industry. Free radical polymerization was recently used to graft cellulose backbone with controlled lengths of vinyl polymers to modify the surface of cellulose. Sang Beon Lee treated cellulose paper with 2-bromoisobutyryl bromide and then immerged it in 2-dimethylaminoethyl methacrylate with CuBr in 1,2-dichlorbenzene at 80°C for 48 hours. The grafted polymer was then treated with methyl bromide and ethyl bromide to bear quaternary nitrogen groups. The grafted polymer exhibited antibacterial activities.[11] Debashish Roy grafted polystyrene onto cellulose paper via the reversible addition-fragmentation chain transfer (RAFT) technique with S-C=S thioester as chain transfer agent to confer cellulose with a hydrophobic surface.[12] A. Carlmark and E. V. Malmstrom created a block-copolymer graft layer of PMA-PHEMA on cellulose.[13] CMC with different DS has been tested for the application as cotton for healing wounds under moist conditions by D. P. Parikh. CMC with the DS which did not lose strength but maintained a certain amount of moisture showed a promise as swellable, highly water retentive cotton dressing.[14] Cellulose has been chemically modified with dimethylol-5,5-dimethylhydantion and 2-amino-4-chloro-6-hydroxy-s-

triazine for preparing antimicrobial textiles.[15-20] L. Chen et al. modified the surface of filter paper with pyridium groups to produce cellulose paper with antimicrobial properties.[15] Several cellulose derivatives with quaternized nitrogen have been commercialized for applications as viscosity thickeners, antimicrobial agents, cationic surfactant conditioners in cosmetics and body cleaning products. Polyquaternium 10 and polyquaternium 4 are two quaternized cellulose derivative examples used in shampoo (Scheme 1.5).

Scheme 1.5. Chemical structure of Polyquaternium 10 and Polyquaternium 4

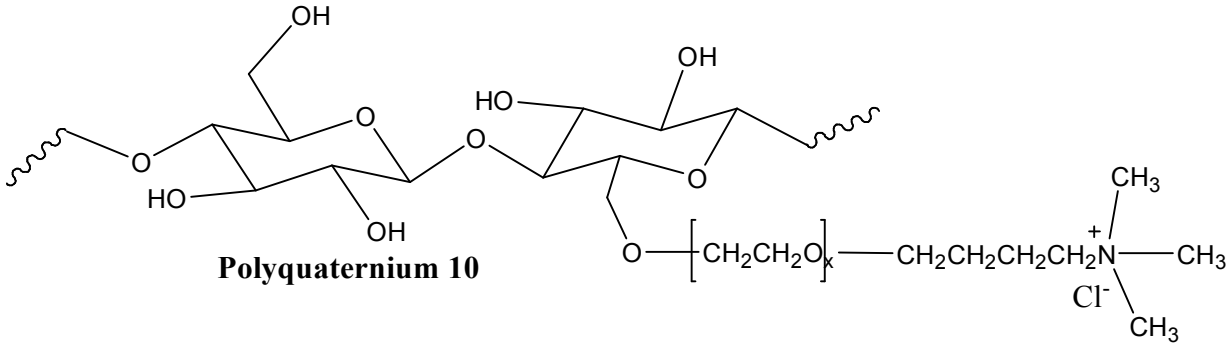

Polyquaternium 10

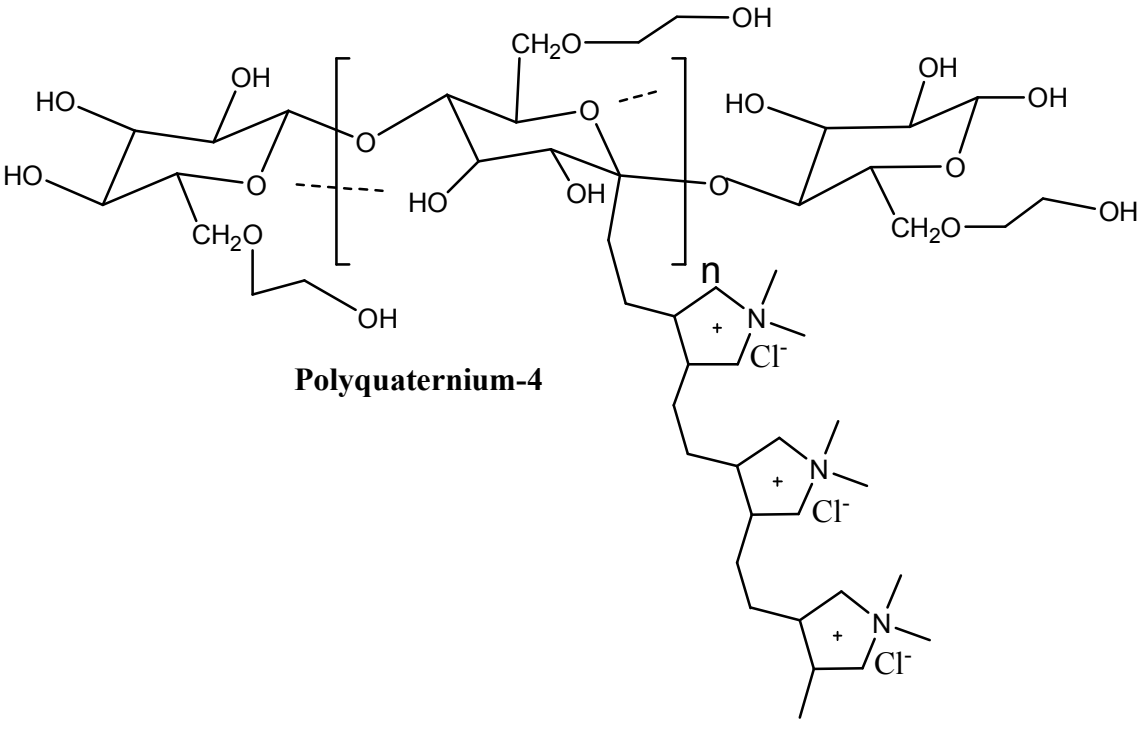

Polyquaternium-4

1.2 Polymeric Antimicrobial Agents

Before the discovery of antimicrobial agents, humanity has been severely plagued by various infection diseases throughout history. In 1865, Ingnaz Semmelweiss recommended the use of chlorine to control infection. Pasteur was the first one to demonstrate that a microorganism was responsible for a specific infection of cholera in chickens. It was Gerhard Domargk who first demonstrated antimicrobial activity of sulfamidochrysoidine in vivo in the treatment of experimental streptococcal septicemia in 1919. Sulfonamides were the first broad-spectrum antimicrobial agent medications. In 1929, Alexander Fleming published his studies on the antimicrobial activity of penicillin.[21] The discovery of penicillin was the turning point of anti-infective chemotherapy, which has saved millions of lives by killing the infectious microorganisms as antibiotics. There are numerous antimicrobial agents in today's world such as halogens, formalaldehyde, alcohols, phenols, and heavy metal.

Several approaches can be used to confer polymers with certain antimicrobial properties. Metal ions (for example tributyltin, zeolites), quaternary ammonium salts, phosphorium salts, biguanides, N-chlorinated sulfonamides, and N-halomines have been used to modify various polymers to develop antimicrobial polymeric materials.[16, 18, 19, 22] A quaternary nitrogen moiety is an essential component for many biologically active compounds such as Vitamins B involved in carbohydrate metabolism, choline involved in transmethylation reaction of fat metabolism, and acetylcholine which mediated the transmission of nerve impulses. Since 1915, many kinds of quaternary ammonium compounds (Scheme 1.6) have been synthesized and found to be able to mimic certain biological effects. R_1, R_2, R_3, and R_4 in the formula may be the same or different, cyclic or acyclic, alkyl or aromatic with various structures. Many low molecular weight compounds with quaternary ammonium moieties including pyridium type molecules have

been commercialized as germicides due to their outstanding germicidal performance, low foaming properties, and unusual tolerance for anionic surfactants, protein, and hard water.[23]

Since 1941, many polymeric quaternary ammonium compounds have been synthesized producing antimicrobial properties. The first polycation ammonium compound, polyionenes (Scheme 1.7) reported in 1941, was synthesized by a polycondensation reaction using diamine and dihalide.[24] Polymers with quaternary ammonium on their branches have also been developed by radical polymerization with monomers containing quaternized nitrogen, grafting polymers with short chains composed of quaternized nitrogen, and by modifying polymers with amine groups on the tips of branches by reacting with alkyl halides or epoxides to yield quaternized nitrogens. The famous polyquat examples include polyionenes, polyquaternium 10, poly(dimethyl diallyl ammonium chloride), and polyquaternium-4 etc. The polyquats often showed broad spectrums of antimicrobial activities, dual functionalities as microbiocides and polymer clarifiers effective for use in swimming pools due to their absence of foaming.

Scheme 1.6. Representative formula of general quaternary ammonium compound

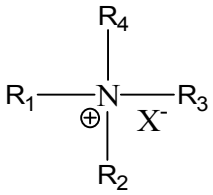

Scheme 1.7. PolyQuat structure

Biocidal groups on main chain arrangement

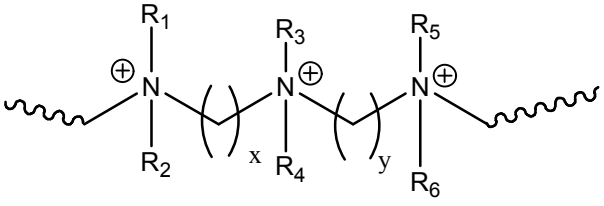

Pendent biocidal groups on comb-like arrangement

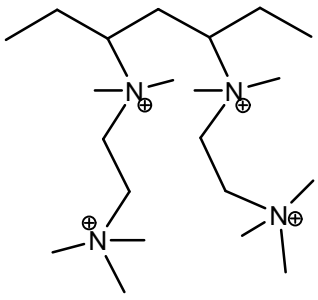

In Professor William H. Daly's groups, we are interested in developing polysaccharide polymeric antimicrobial material.

1.3 Polysaccharide Chemistry Research in Dr. William H. Daly's Group

Many kinds of chemistry have been used to modify different polysaccharides in Professor William H. Daly's group. D. A. Culberson in Dr. Daly's lab has intensively modified CMC by using many kinds of chemical reactions (Scheme 1.8). Melissa Manuszak Guerrini has studied their potential applications in cosmetics.

Scheme 1.8. The modification reactions of CMC and its derivatives[5, 25, 26]

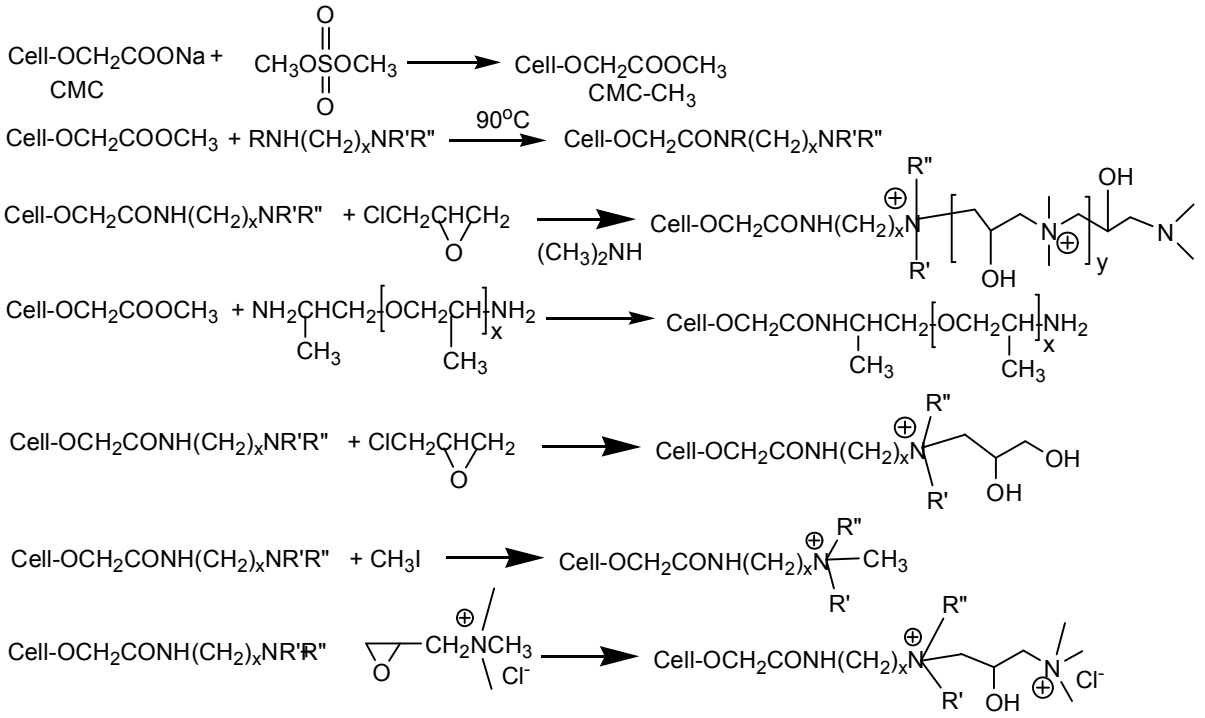

Chitosan, the second most abundant natural polysaccharide, has also been intensively modified in Dr. William H. Daly's group (Scheme 1.9). D. Logan has modified chitosan using quat-188[27]. Mrunal R. Thatte prepared quaternizaed chitosan derivatives with different hydrophobic or hydrophilic substitutes.[28] The quaternized chitosan derivatives showed good antimicrobial properties against *E-coli* and *S. aureus.*

Scheme 1.9. Reactions used in preparing quaternized chitosan derivatives in Dr. Daly's group

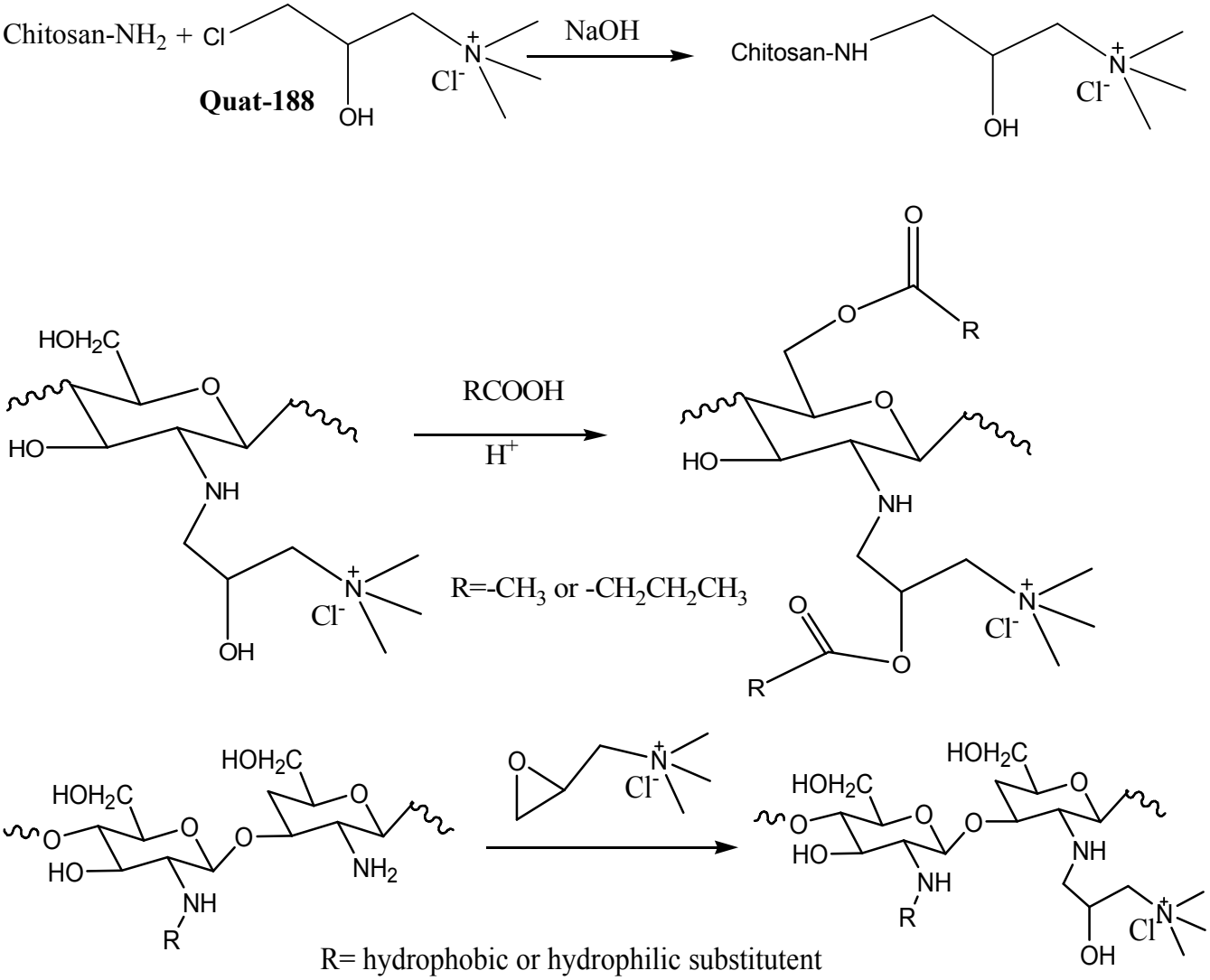

1.4 Dendrimers

Polymer scientists have long been dreaming of controlling the molecular architecture of polymers. A new structure of polymers can often bring new properties and applications to polymer systems. By controlling their chemical composition, stereoregularity, molecular weight and molecular weight distribution and by controlling the linear, branched, or cross-linked structure of their molecules,[29] numerous polymers with varieties of architecture structures have

been invented with specific properties for numerous applications. Modern civilized society would be in chaos and unimaginable without the inventions of various polymers.

Dendrimer synthesis is a challenging field for polymer chemists. It represents an evolutionary direction of polymer chemistry. Dendrimers are also named as cascade molecules, dendritic molecules, and hyperbranched polymers. In the early of 1950s, Paul J. Flory[30] predicted the dendritic growth of molecules and several structural variations. The pioneer work of F. Vögtle at the end of 1970s opened a new area, synthesis of polymers with dendritic structures.[31, 32] The works of Donald A. Tomalia,[33, 34] George Newkome,[35] Jean M. J. Fréchet,[36] and Virgil Percec*et al.*[37] have greatly enriched the diversities of dendrimer structures. Poly(amidoamine) (PAMAM) and poly(propylene imine) (PI) are two commercially available dendrimers. Different functional groups have been elaborated on various dendrimers to confer dendrimers with different functions. Dendrimers have been synthesized and modified for potential uses in encapsulation, targeted drug delivery,[38, 39] and light harvesting and emission for use in fiber-optic amplifier and optoelectronic devices.[40] G-4 PAMAM with PEG surface end functional groups has been investigated as carriers for carrying anticancer drugs like adriamycin and methotrexate.[41, 42] Hydrophilic quaternary ammonium groups were elaborated on the periphery of PI dendrimer for enhancing both its water solubility and release properties.[43] E. Murugan prepared PI dendrimer with quaternary ammonium and tertiary amine functionalities and these polymers exhibited catalytic activity for decarboxylation of 6-nitrobenzisoxazole-3-carboxylate.[44] The nanodevice of G-5 PAMAM dendrimer elaborated with folic acid, methotrexate, and fluorescein detecting agent has proven effective in dealing with tumor cells in both in vitro and in vivo rat animal model tests. The quaternization of G-5 and G-4 PI dendrimer produced effective

antimicrobials.[45-47] The simple concepts of dendrimer synthesis from dendrons are illustrated in scheme 1.10. Dendrimers normally are organized using dendrons as building blocks.

Scheme 1.10. Scheme of dendrimer synthesis from dendrons

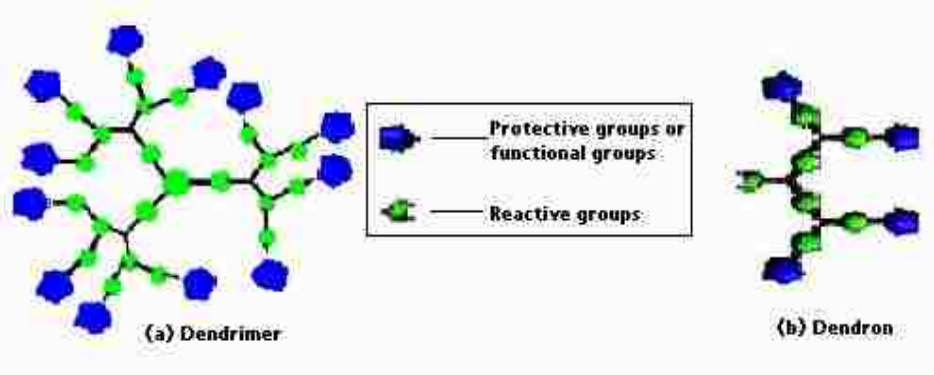

Two general approaches have been used to synthesize dendrimers: the convergent approach and the divergent approach.[36] In the divergent approach, the dendritic growth starts from the core. The peripheral function groups of the core react with the complementary reactive group of the building block monomer with latent branch points. After activation, the latent branching points can continue growth by reacting with new added building block monomer (Scheme 1.11). In the convergent approach, different generations of dendrons are first synthesized inward by repeated activation of focal points and coupling of the activated focal points with the complementary functional groups of monomers with latent focal points. The last step is the coupling of the same generation dendrons to a designed core (Scheme 1.12). Both approaches require repeated coupling and activation. Other approaches include (1) the macromonomer approach where monomers with substituted dentrons polymerize,[36, 48] (2) the coupling approach where dendrons are coupled to the backbone of polymers[49] or a plane surface,[50] and (3) the dendritic cores self-assembly approach where dendrons assembly around cores by hydrogen bonding[51] or around transitional metal ions by ligand bonding.[52]

Scheme 1.11. Divergent approach of dendrimer synthesis [4]

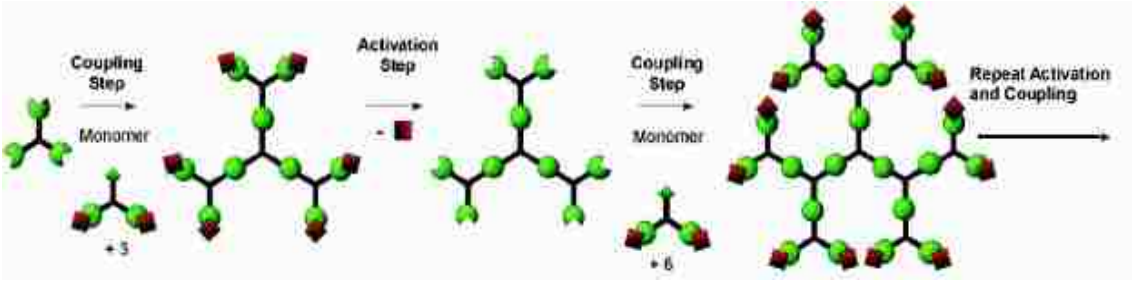

Scheme 1.12. Convergent approach of dendrimer synthesis: (a) synthesis of dendron; (b) coupling of dendrons to the core

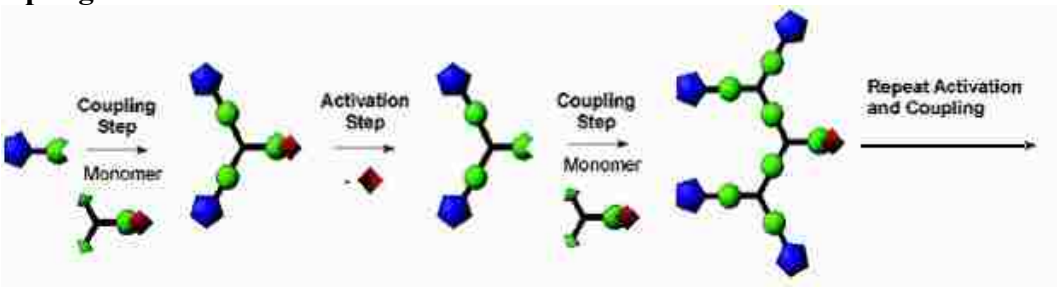

(a) Synthesis of dendron[4]

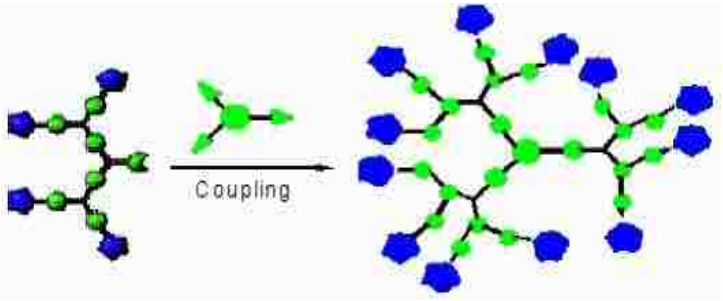

(b) Coupling of dendrons onto the core

Although it was almost immediately recognized as an important alternative structure,[53, 54] dendronized polymers or side chain dendritic polymers have not received enough attention.[55-57] Recently, a fourth generation dendronized polystyrene with unique properties attributed to the high concentration of dentritic substituents was reported.[57] The interest in the potential applications of these new materials is increasing.[58] Jahromi etc prepared dendronized polymers by reacting diisocyanoester with dendron through an additional polymerization and investigated

its rheology; they showed its elastic modulus G′ decreased with the generation number while its loss modulus G″ almost did not change. The intermolecular entanglement was not observed from its G′, G″ versus angular frequency.[59] Michael A. Zhuravel synthesized dendronized protein by conjugating peptide with hydrophobic dendron;[60] Hitoshi Sashiwa attached PAMAM dendron and PAMAM dendron onto a chitosan backbone[61, 62]; Malcolm Driffield synthesized dendritic branches based on L-lysine.[63] Sarah L. Goh and J. M. J. Frechet conjugated polyester dendron onto DNA.[64]

1.5 Dendronization of Cellulose

1.5.1 Proposed Advantages of Dendronized Cellulose Derivatives

As the most abundant biodegradable polymer in nature, the dendronization of cellulose can provide a series of affordable platforms for carrying different functional groups in one molecule. This mechanism with biodegradable biocompatible features may have potential applications as potent drugs, drug delivery matrices, delivery vehicles for hydrophobic active components, antimicrobial coatings, etc. Incorporation of dentritic structures is an effective means for amplifying the number of functional groups along the cellulose backbone as the polyfunctionality of dendrimers increases geometrically with each generation. Dendronized cellulose derivatives (DendronCell) can be synthesized with both hydrophilic and hydrophobic structures, which allow diversity in potential applications in pharmaceutical science.[65] It is reasonable to imagine that dendrimers of cellulose would be biocompatible and they may have important applications in human health. In addition, one dendronized cellulose molecule can carry many functional groups similar to the number of functional groups that a higher generation dendrimer can carry but without the need of synthesizing the higher generation dendron. This may achieve a similar effect which high generation expensive dendrimer can reach but with

much low cost. The dendronization of cellulose has not received enough attention in the scientific society.

1.5.2 Newkome's AB3 Monomer Dendron

Di-*tert*-butyl 4-[2-(ter-butoxycarbonyl)ethyl]-4-aminoheptanedicarboxylate, BA, was synthesized[66] and used (Scheme 1.13) as a building block for polyamidoamine dendrimers by Newkome *et al*.[67] We have showed that BA building blocks can also be elaborated to the backbone of cellulose as side chains. New cellulose derivatives can be formed by further elaborating polyamidoamine dendrons with hydrophilic functional groups on the cellulose backbone.

Scheme 1.13. One polyamidoamine dendrimer developed in Newkome group[67]

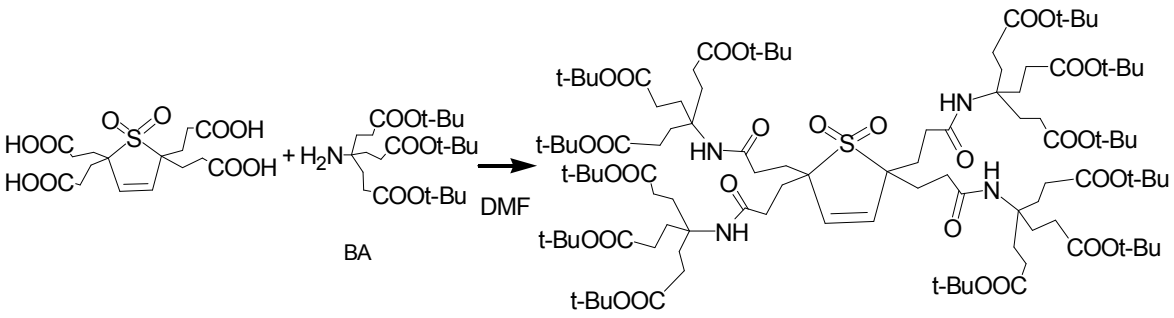

1.5.3 Our Design of Dendronized Cellulose Derivatives: Dendrigraft-polyamino and Dendrigraft-polyquat

We envisioned a series of dendronized cellulose derivatives with a new architecture: a cellulose comb copolymer with radial hydrophilic brushes where biodegradable cellulose was the backbone and amphiphillic teeth were elaborated as the side chains (Scheme 1.14). Hydrophobic dendrons, BAs, were elaborated directly on the cellulose backbone as the stem of amphiphilic teeth. Many hydrophilic groups were further elaborated to the hydrophobic dendron sections of the side chains forming a radiant hydrophilic brush structure. Currently, we use amino groups as

the periphery hydrophilic groups. These unique dendrimerized cellulose derivatives (Dedrigraft-polyamino) are expected to have favorable water solubility with potential applications in drug delivery.

Scheme 1.14. Illustration of a water soluble dendronized cellulose: dendrigraft polyamino

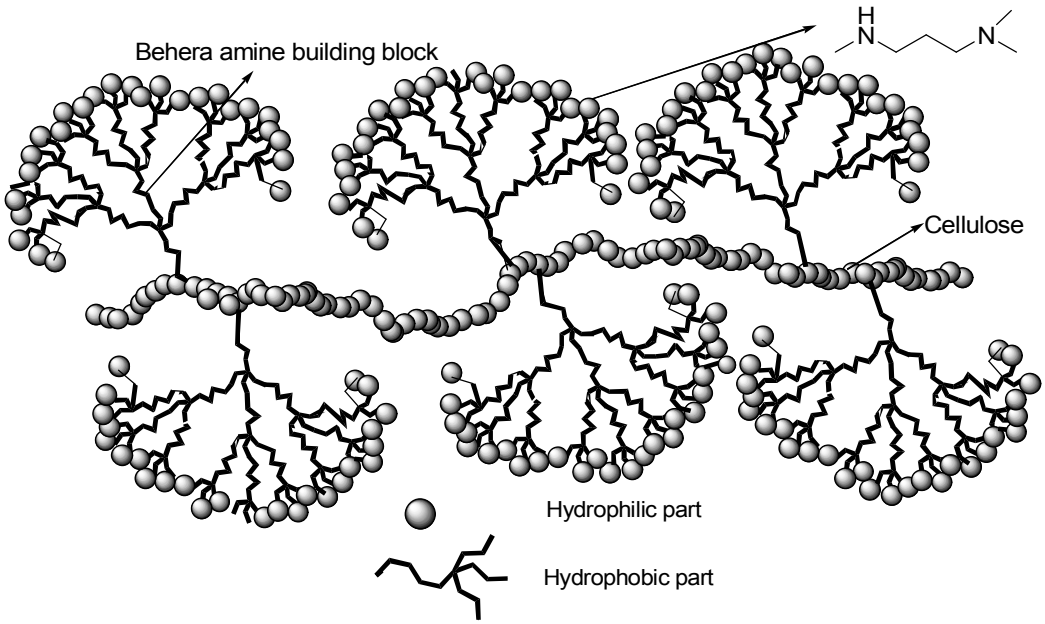

Many biologically active compounds have quaternary nitrogen functionality. Quaternized chitosan modified with quate188 has proven to demonstrate antimicrobial activity in our group; but it was not clear if the antimicrobial activity came from the quaternary nitrogen created with quat-188 or came from the unique structure of chitosan. In 1999, C. Z. Chen et al. reported the synthesis and antimicrobial activities of quaternized PI dendrimer.[68] In their paper, 2-chloroethyl isocyanate was used to react with the amine surface group of PI dendrimer and dimethyl alkyl amines (C8, C10, C12, C14, and C16) were used to conduct nucleophilic attack on the carbon with chloride on new formed PI dendrimer. The quaternized PI generation 4 dendrimer with C12 (carbon chain length of twelve) exhibited high antimicrobial activity against *E. Coli* and *S. Aureus.*[47] Based on the above reports, we designed our dendronized cellulose with two categories of quaternary nitrogen periphery groups: very hydrophilic di-quaternary nitrogen

(Scheme 1.15, Dendrigraft-polydiquat) and mono-quaternary nitrogen with hydrophobic alkyl chains (Scheme 1.16, Dendrigraft-polyquat).

Scheme 1.15. Illustration of a water soluble dendronized cellulose with hydrophilic di-quaternary nitrogen: dendrigraft polydiquat

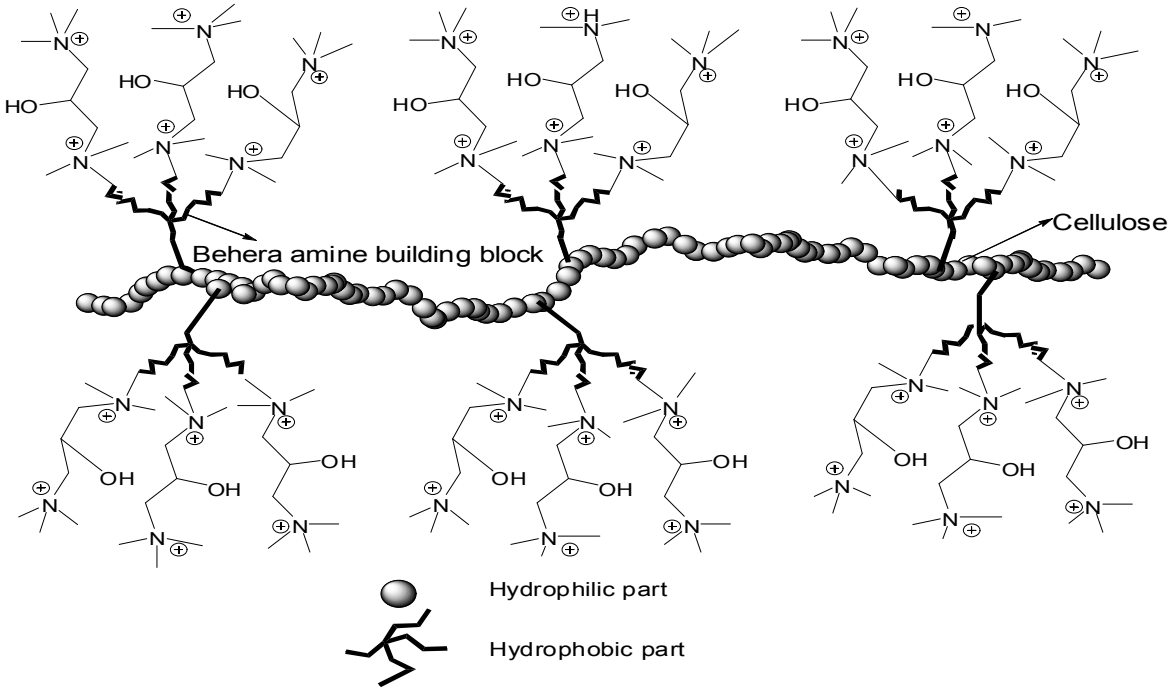

Scheme 1.16. Illustration of a water soluble dendronized cellulose with quaternary nitrogen with hydrophobic alkyl chains: dendrigraft polyquat

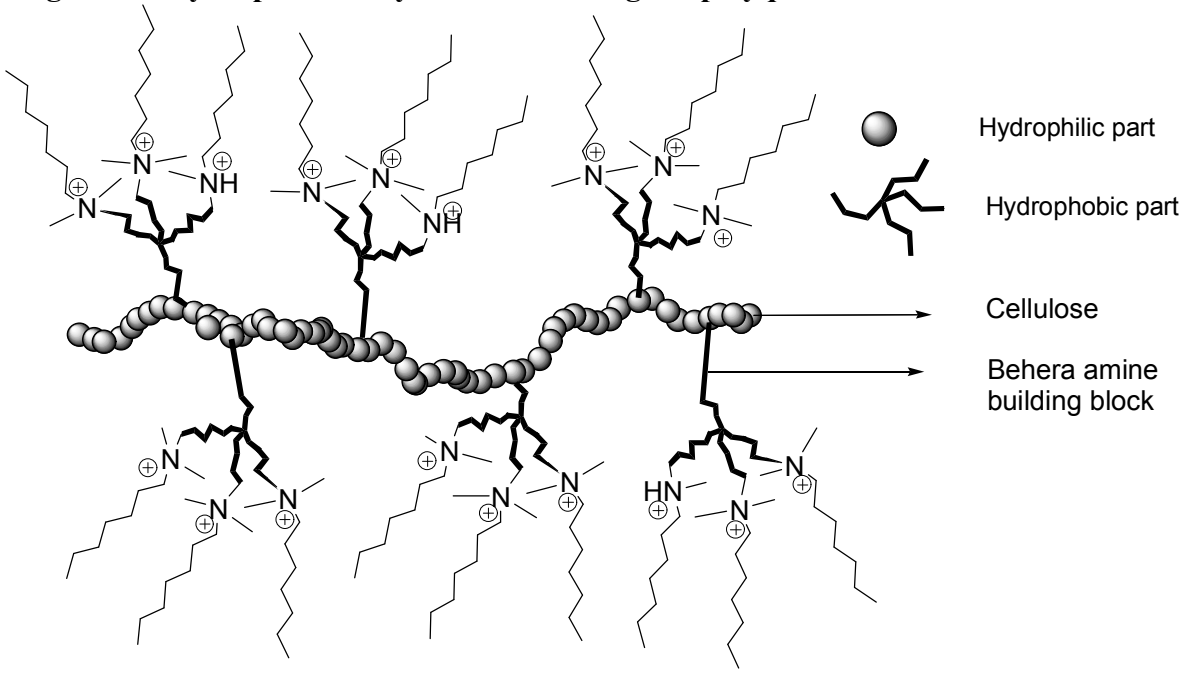

By elaborating quaternary nitrogen onto the tip of BA dendrons of the dendrimerized cellulose derivatives, we can create novel dendronized cellulose derivatives with very dense concentrations of quaternary nitrogen groups in local microenvironment aqueous media. The cellulose derivatives of dendrigraft-polyquats are expected to give the copolymer better water solubility and form molecules of quaternary nitrogen cation clusters. Highly dense concentrations of quaternary nitrogen microenvironment can be formed even in very dilute solutions of the dendrigraft-polyquat. The quaternary ammonium dendronized cellulose derivatives are expected to have favorable antimicrobial properties.

1.6 Present Project

The proposed dendrigraft-polyamino cellulose derivatives are expected be capable of carrying hydrophobic active components or hydrophobic molecules. The proposed dendri-polyquat and cellulose derivatives are expected to be potential potent antimicrobial agents.

My dissertation project focused on the following contents:

(1) Synthesis of dendronized cellulose derivatives with amino groups and hydrophobicity study of their microenvironment in aqueous solution.

(2) Synthesis of dendronized cellulose derivatives with hydrophilic di-quaternary nitrogen and that with mono-quaternary nitrogen with hydrophobic alkyl chains as periphery functional groups.

(3) Antimicrobial activity evaluation of novel quaternary ammonium dendronized cellulose derivatives.

CHAPTER 2. SYNTHESIS AND CHARACTERIZATION OF NEWKOME'S DENDRON

2.1 Introduction

Dendronized polymers may be synthesized in both divergent approach and convergent approach. In the end of 1970's, Newkome and Tomolia etc. started to synthesize dendrimers by using the divergent approach, in which dendrimers were built from the core outward to periphery.[35] Later Frechet[40] *etc.* began synthesizing dendrimer using the convergent approach by first synthesizing different generation dendrons and then coupling dendrons onto the central cores. Different kinds of dendrons have been synthesized and appeared in the literatures: PAMAM dendrimer by Tomali's group,[33] polyaryl ether dendron by Frechet's group, polyamide dendron developed by Newkome's group, and polylysine dendron,[69] etc. Among them, the function groups in Newkome's polyamide dendron can be amplified in 1→3 C-branched dendron in each generation, which is amplified more rapidly compared to the 1→2 ratio in other dendrons. Fewer generations are required to achieve the same number of functional groups in one dendrimer molecule utilizing Newkome's dendron. This advantage attracted us to use Newkome's dendron to dendronize cellulose backbone. To synthesize dendronized cellulose derivatives, two generations of Newkome's dendron were synthesized first.

Behera's amine (BA) can be considered as the 1st generation Newkome's dendron. In 1991, Newkome, G. R. and Behera, R. K. etc.[70] reported their synthesis of BA by conducting a Michael addition of nitromethane with *tert*-butyl acrylate to produce nitrotriester and then reduce it into the aminotriester, BA. Later in 1996, Newkome and C. D. Weis improved the procedure (Scheme 2.1) which could produce Behera amine in large scale (5L).[71]

They also elaborated BA to different cores layer by layer divergently by using dicyclohexylcarbodiimide (DCC) chemistry in DMF solution. In 2000, C. M. Cardona etc.

published the synthesis of the 2nd generation Newkome's dendron (G-2-amino) by first preparing the 2nd generation Newkome's predendron (G-2-nitro) using DCC chemistry in THF solution by reacting Behera's amine with acidic groups of the nitrotriacid prepared by hydrolyzing Newkome's predendron nitrotriester and then reducing it into G-2-amino (Scheme 2.2) in absolute alcohol with hydrogen [72, 73]

Scheme 2.1. Synthesis of BA

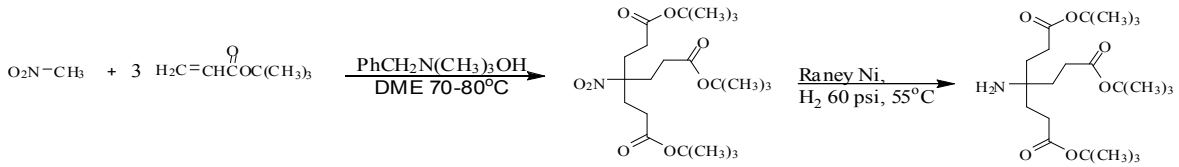

Scheme 2.2. Synthesis of the 2nd generation Newkome's dendron using DCC chemistry[72]

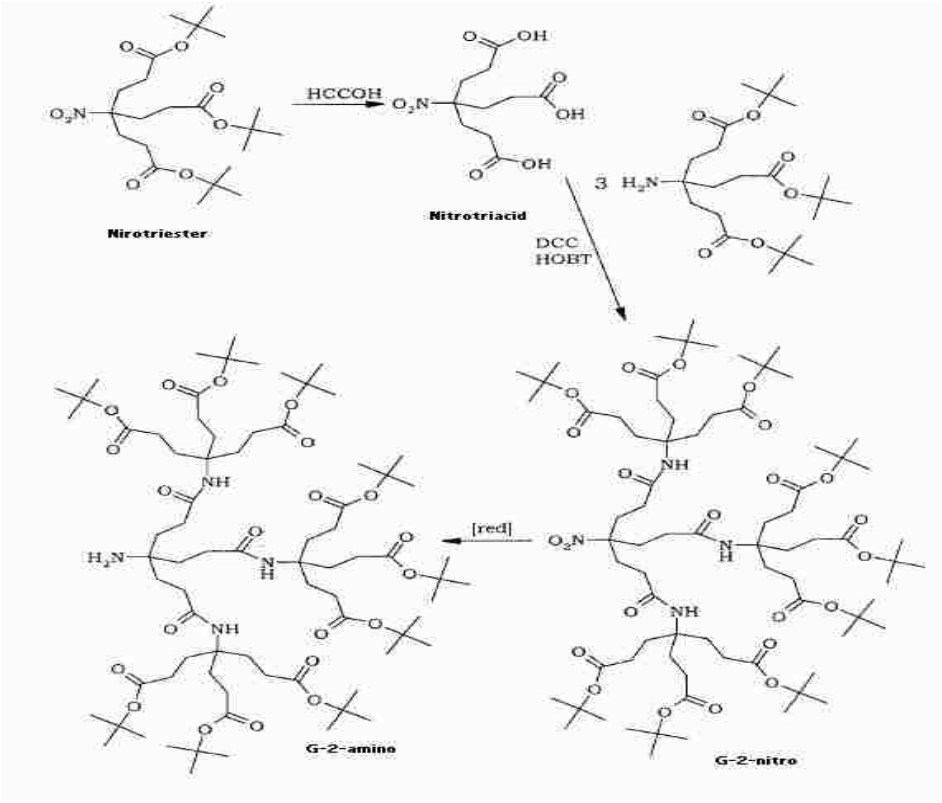

In 2002, Newkome *etc.* published their synthesis of G-2-nitro using DCC chemistry in DMF solution and the reduction of G-2-nitro into G-2-amino. They also transformed G-2-amino into

its isocyanate form , which is quite active, and attached it to silica surface.[74] In 2005, Newkome's group published a new way of making G-2-nitro using Michael addition reaction as a JOC note.[75] (Scheme 2.3)

Scheme 2.3. Synthesis of the 2nd generation Newkome's dendron using Michael addition

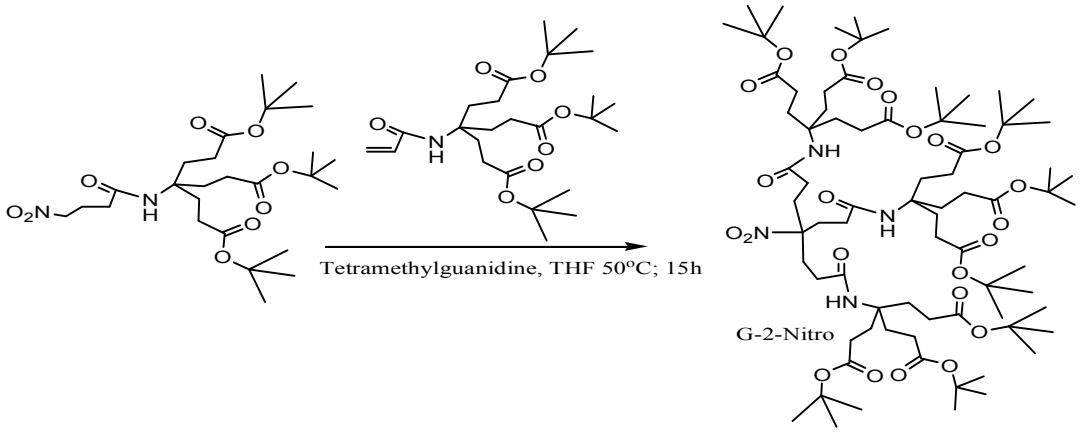

I first tried to prepare G-2-nitro by using Michael addition following the procedure published by Newkome's group because this route does not require using expensive chemicals. The Michael addition did not succeed. DCC chemistry was then used to prepare the G-2-nitro in both DMF solution and THF solution. Higher yield of G-2-nitro was obtained in the DMF solution than in the THF solution. The further reduction of G-2-nitro with hydrogen produced G-2-amino, the 2nd generation Newkome's dendron.

2.2 Experimental

2.2.1 Synthesis of Behera's Amine

2.2.1.1 Synthesis of Di-*tert*-butyl 4-[2-(ter-butoxycarbonyl) ethyl]-4-nitro heptanedicarboxylate (Nitrotriester)

The nitritriester was synthesized following the procedures[71] published by Newkome' group in a smaller scale. Nitromethane (6.1g, 5.4mL, and 0.103 mol) and *tert*- butyl acrylate (39.7 g, 45.37 mL, 0.310 mol) were used to conduct Michael addition in 1, 2-dimethyoxyethane (DME,

20 mL) solvent. Triton B was used as the catalyst. The nitrotriester (25 g, 0.056 mol, yield 55%) was obtained as a white powder. ^{1}H NMR (250 MHz, $CDCl_3$) (Figure 2.1): δ 1.41 (CH_3, 27H), 2.17(CH_2, 12H); ^{13}C NMR (62.9MHz, $CDCl_3$) (Figure 2.2): δ 27.9 (CH_3), 29.7(CH_2CO), 30.3(CH_2CNO_2), 81.1(CCH_3), 92.1 (CNO_2), 171.0 (CO_2).

2.2.1.2 Synthesis of Di-tert-butyl 4-[2-(ter-butoxycarbonyl) ethyl]-4-amino heptanedicarboxylate (BA)

BA was synthesized by following the procedure published in the literature[71] in a smaller scale. Raney nickel catalyst Al-Ni (3.0 g; 26 mmol Ni) was first activated with aqueous sodium hydroxide solution (75 mL; 10%; 0.188 mol)) for one hour. Vigorous hydrogen was released immediately. The liquid was then washed with water (40 mL ×3) and absolute ethanol (20 mL×3). The nitrotriester (5 g; 11.2 mmol) proceeded hydrogenization under the catalysis of fresh activated nickel in absolute ethanol (50 mL) at the hydrogen pressure of 55 psi and at the temperature of 50-55°C overnight. After filtration through a celite cake, the filtrate was evaporated to dryness. BA (4.56 g, 11.0 mmol, yield 98%) was obtained as a white powder. ^{1}H NMR (250MHz, $CDCl_3$) (Figure 2.3): δ 1.40 (CH_3, 27H), 1.58 (t, CH_2, 6H), 2.20 (t, CH_2, 6H); 7.24(NH_2); ^{13}C NMR (250MHz, $CDCl_3$) (Figure 2.4): δ 27.8 (CH_3), 30.3 (CH_2CO), 34.7 (CH_2CNH_2), 52.2 (CNH_2), 80.7 (CCH_3), 171.0 (CO_2). FTIR (KBr, pellet): 3365, 2977, 2936, 1728, 1678 cm^{-1}.

2.2.2 Synthesis of 2nd Generation Newkome's Dendron

2.2.2.1 Synthesis of Nitrotriacid

The nitrotriester (12 g, 28.9 mmol) was hydrolyzed by stirring in formic acid (60 mL, 96%) overnight. The mixture was diluted with toluene (15 mL) and evaporated to dryness. The white

nitrotriacid powder (7.1 g, 28.7 mmol, and yield 99.4%) was obtained. ^{1}H NMR (250MHz, $CDCl_3$): δ 2.25 (t, CH_2, 6H), 2.20 (t, CH_2, 6H).

2.2.2.2 Synthesis of the 2nd Generation Newkome's Nitrodendron (G-2-Nitro) Using DCC Chemistry

The nitrotriacid (0.55 g, 1.99 mmol) was then dissolved in dry DMF (5 mL). 1-Hydroxybenzotriazole (HOBT, 0.82 g, 5.95 mmol) in DMF (2 mL) solution was added to the above solution and stirred for 15min. DCC (1.25 g, 5.97 mmol) in DMF (3 mL) solution was then added to the reaction system. After 5 minutes, the mixture became cloudy. BA (2.89 g, 14.2 mmol) in DMF (5 mL) solution was added. The mixture was stirred for four days at room temperature. A white precipitate formed during the stirring process. The mixture was filtered. The filtrate was evaporated to a viscous oil and then dissolved in DCM (5 mL) and washed sequentially with aqueous HCl (50 mL × 3, 10%), H_2O (50 mL × 3), and brine solution (20 mL). Dried $MgSO_4$ (2.5g) was added to the organic layer. After staying overnight, the organic layer was filtered, and concentrated with a rotovap to get viscous yellow oil. The residue was purified using a silica gel column (1:1 CH_2Cl_2/EtOAc). The white powder G-2-nitro (1.5 g, 1.02 mmol, 51%) was obtained after the solvent was evaporated. FT-IR (KBr pellet): 1728, 1677 cm^{-1}. ^{1}H NMR ($CDCl_3$): 1.44 (s, CH_3, 81H); 2.23 (gen 1: CH_2CH_2, 12H; gen2: CH_2CH_2, 18H); 1.98(gen2: CH_2CH_2, 18H); 6.28 (N*H*, 3H). ^{13}C NMR: 27.53 (*C*H_3); 29.25, 29.37 (gen 2: *C*H_2*C*H_2); 31.57 (gen 1: *C*H_2*C*H_2); 57.06 (gen 2: *C*(CH_2-CH_2)); 92.34(gen 1: *C*(CH_3)$_3$); 170.71 (*C*ONH); 172.24 (*C*OOtBu). MALDI-TOF MS (dithranol matrix): 1489.66, 1490.65 (M + Na+), 1491.65 (MH). Calculated 1491.92 [M+Na^+]

2.2.2.3 Second-generation Amine Dendron (G-2-amino)

The fresh activated Raney Ni (2.0 g, mmol) was transferred to a Parr hydrogenation bottle with absolute ethanol (50 mL) and G-2-nitro (2.54 g, 1.73 mmol). The hydrogenation was conducted at the hydrogen pressure of 55 psi and at a temperature of 50-55°C for 24 hours. Nickel was removed by suction filtration through a celite cake. The filtrate was cooled in ice for four hours and a solid precipitated. After recovered by suction filtration, it was dried in vacuo to give pure G-2-amino dendron (2.14 g, 1.49 mmol, yield 86%). ^{1}H NMR ($CDCl_3$): 1.43 (CH_3, 81 H, s,), 1.95 (gen2: CH_2CH_2, 18H), 2.20 (gen 1: CH_2CH_2, 12H; gen2: CH_2CH_2, 18H), 6.10 (NH, 3H). ^{13}C NMR ($CDCl_3$): 27.83(CH_3), 28.37, 30.10(gen 2: CH_2CH_2), 32.26(gen 1: CH_2CH_2), 57.75(gen 2: $C(CH_2\text{-}CH_2)$), 173.06(COOtBu). FTIR (KBr pellet) 1728(C=O, ester), 1678 cm^{-1}(C=O, amide); MALDI-TOS MS *m/z* 1438.89 [M +], 1439.89, 1440.93, 1441.95, 1443.08. Calculated 1438.95 [M].

2.3 Results and Discussions

2.3.1 Synthesis of Behera's Amine

2.3.1.1 Synthesis of Nitro-triester

Triton B was used to produce anions of $NO_2CH_2^-$, NO_2CHR^-, and $NO_2CR_2^-$, which were used to conduct a triple Michael addition reaction with *t*-butyl acrylate. The 1st Michael addition reaction proceeded easily at 65 °C. The 2nd and 3rd Michael addition reaction required a little higher temperature in the range of 75-80 °C. The reaction temperature in the whole process was controlled below 85 °C. Higher temperature will lead to side reactions and low yield of product. The nitrotriester was obtained as a white powder in a yield 55%, somelower than that published by Newkome's group. C-CH_2CH_2 showed the same chemical shift at 2.17 (Figure 2.1). The

protons of C=C double bond disappeared in its proton NMR spectrum, and the chemical shift of tertiary carbon at 92.18 (Figure 2.2) confirmed the chemical structure of nitroester.

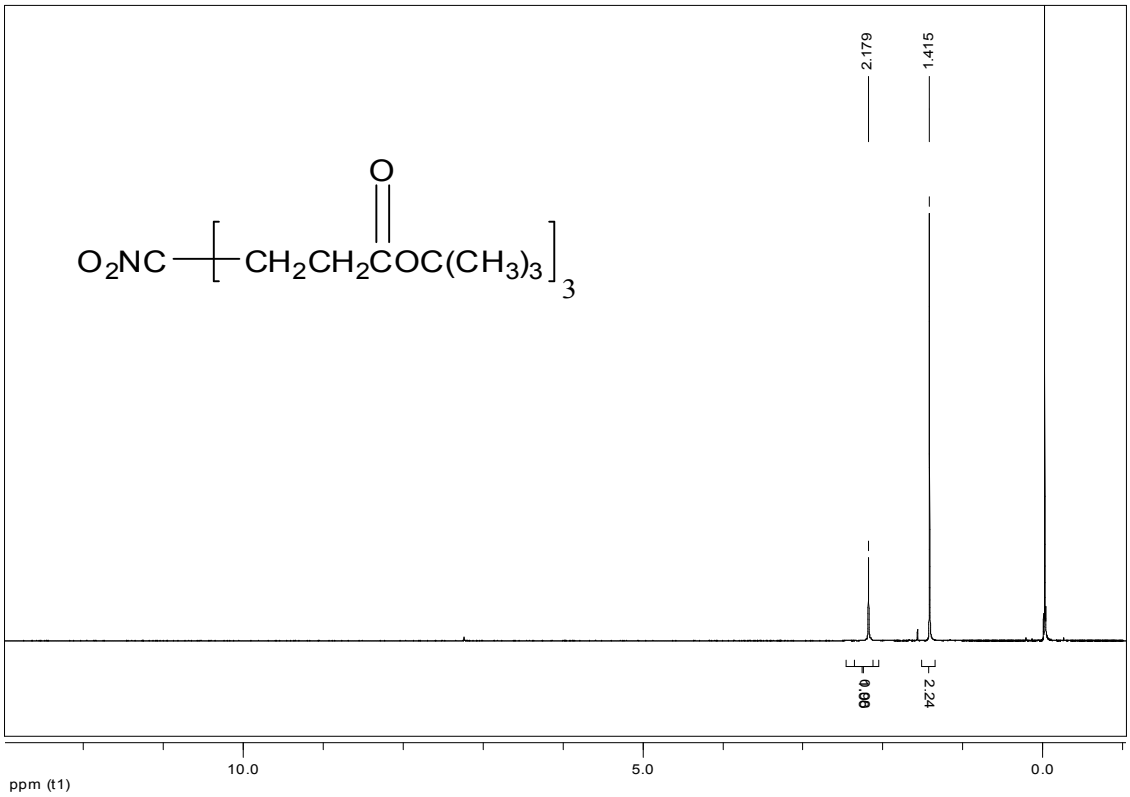

Figure 2.1. ^{1}H NMR spectrum of nitrotriester.

2.3.1.2 Synthesis of Behera's amine

In the whole hydrogenization reaction and purifying process, temperature was controlled below 55 °C to prevent BA from conducting the potential intra-molecular amidation reaction. BA showed melting point at 51 °C. The chemical shift of C-CH_2CH_2 at 2.25 in the nitrotriester was separated into two peaks at 1.58 (t, CH_2, 6H) and 2.20 (t, CH_2, 6H) in BA (Figure 2.3). The ratio chemical shifts of CH_3, C-CH_2CH_2, and C-CH_2CH_2 was at 4.5:1.0:1.0. The change of the chemical shift of tertiary carbon from 92.2 in nitrotriester to 52.2 in BA (Figure 2.4) was consistent with the chemical structure of BA and confirmed that the nitro group in nitrotriester was reduced to amino group in the hydrogenization process.

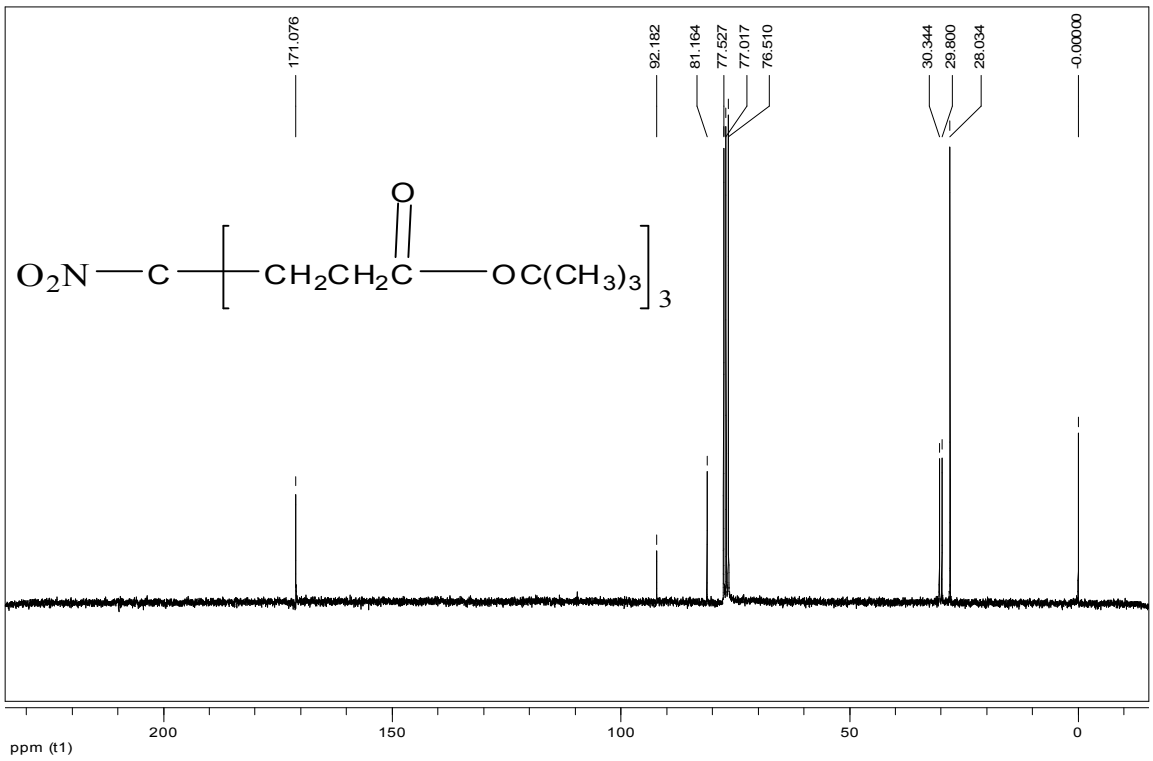

Figure 2.2. ^{13}C NMR spectrum of nitrotriester.

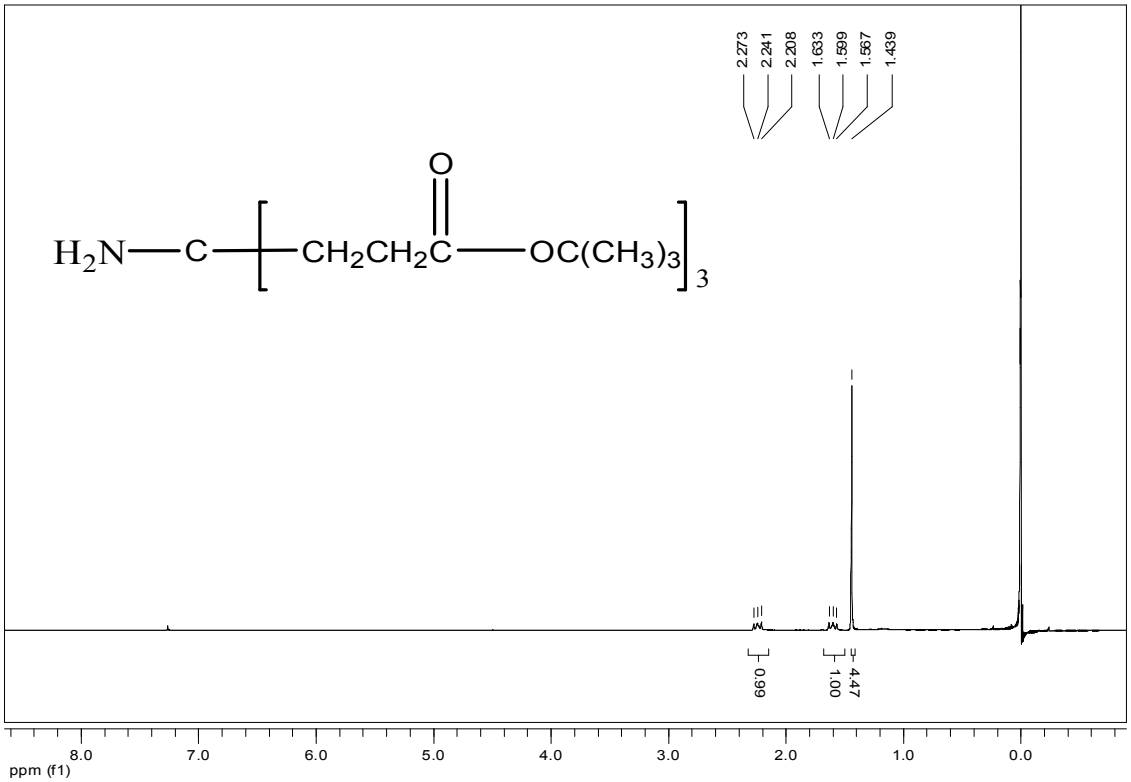

Figure 2.3. ^{1}H NMR spectrum of Behera amine.

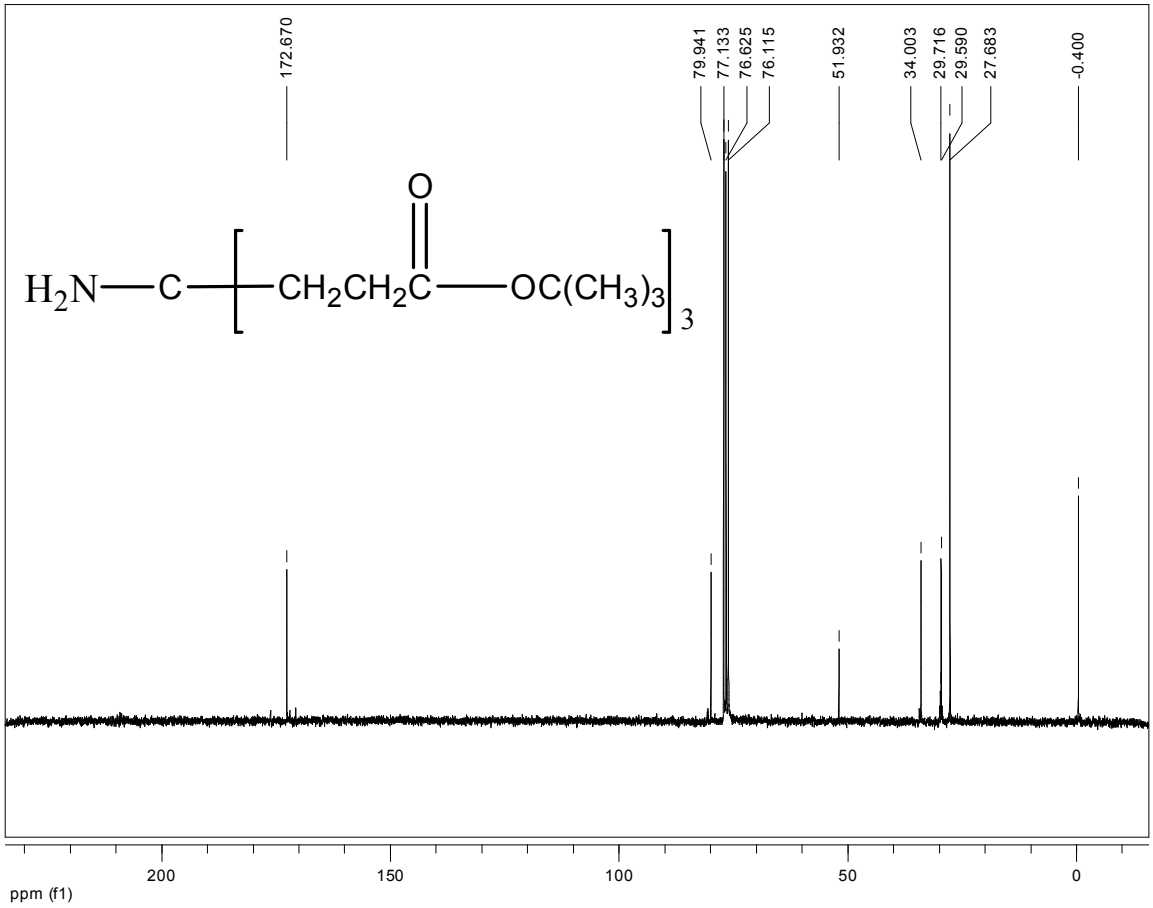

Figure 2.4. ^{13}C NMR spectrum of Behera amine.

2.3.2 Synthesis of 2nd Generation Newkome's Dendron

2.3.2.1 Synthesis of G-2-Nitro Dendron Using DCC Chemistry

Dicyclohexylcarbodiimide (DCC) is frequently used to conjugate or crosslink enzymes and antibodies.[76] Scheme 2.4 illuatrated the mechanism of the reaction. I synthesized G-2-nitro following the procedure published by G. R. Newkome et al[74] in both THF and DMF solvents. G-2-nitro was obtained in both solvents; however, a higher yield of the product was obtained in the DMF solvent system. The coupling reaction proceeded with a higher efficiency in the DMF solvent. After passing through a silica gel column using a mobile phase of CH_2Cl_2/EtOAc (1:1), G-2-nitro was obtained. Dry solvent and inert atmosphere/Schlenk line techniques were used to

maximize yield. The chemical shift of 1st generation NO_2C-$C\underline{H}_2C\underline{H}_2$ overlapped with 2nd generation NHC-$C\underline{H}_2CH_2$ at 2.2 (Figure 2.5). The chemical shift of tertiary carbon of NO_2C (92.34) is different from that of tertiary carbon of NHC (57.06) (Figure 2.6). G-2-nitro showed 1489, 1490, and 1491 MALDI peak (Figure 2.7), which are the mass of one molecule of G-2-nitro plus one sodium ion. These confirmed the formation of G-2-nitro.

Scheme 2.4. Synthesis of G-2-Nitro by DCC chemistry

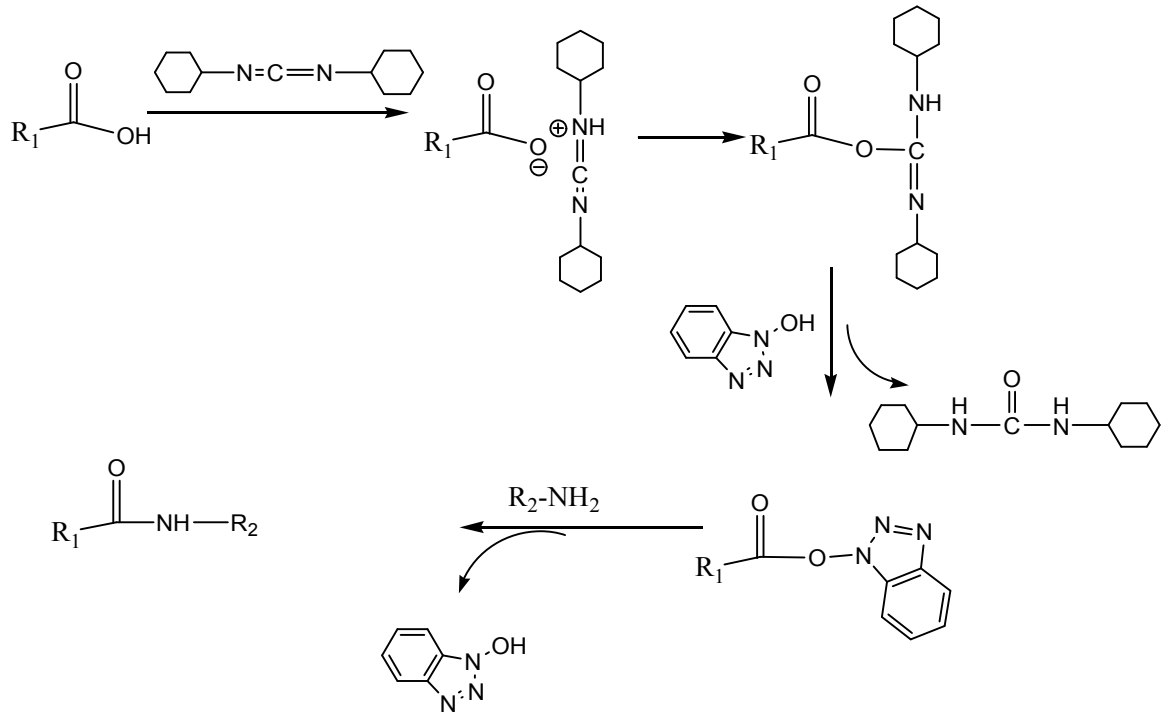

2.3.2.2 Synthesis of G-2-amine Dendron

The reduction of nitro group of the 2nd generation dendron was more difficult than that for preparing BA. In its NMR spectra, the change of N*H* peaks to 6.1 from 6.27 (Figure 2.8) and the disappearing of 92.2 peak of NO_2C (Figure 2.9) indicated that the nitro group was reduced into the amino group. MALDI peaks of 1438, 1439, 1440, 1441, and 1443 (Figure 2.10) were the mass of one G-2-amine molecule plus one positive proton charge. All NMR spectra and MALDI

confirmed the chemical structure of G-2-amine. The white powder product is more stable than BA because the intra-molecular amidation reaction is more inhibited in G-2-amine.

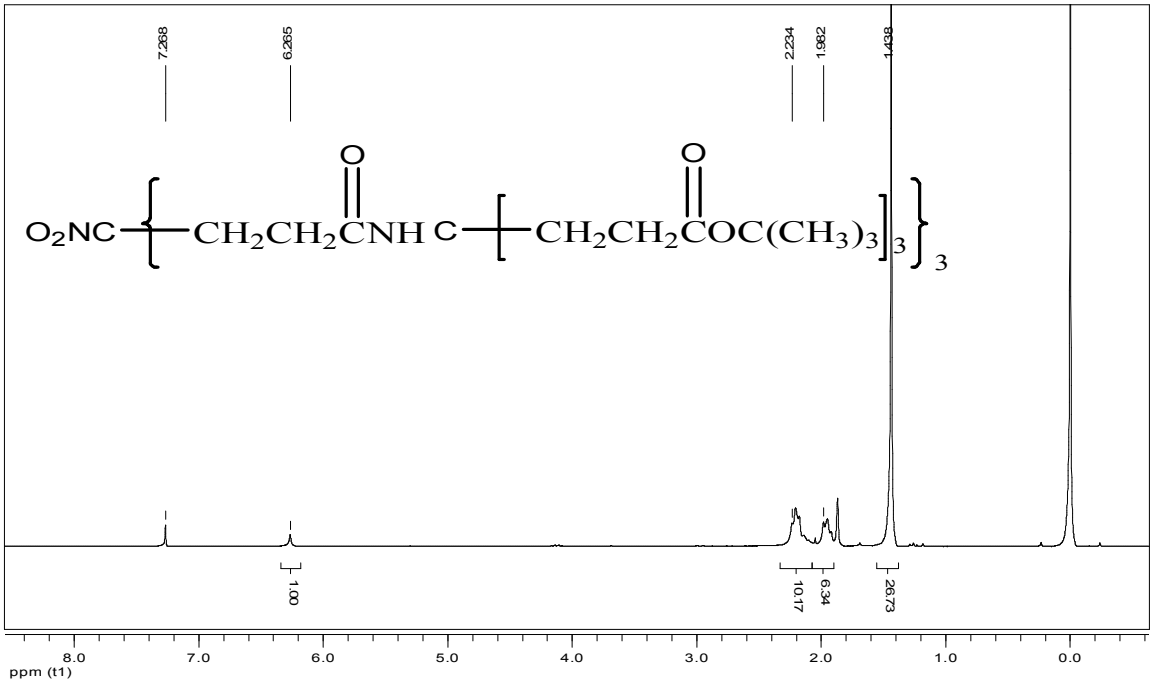

Figure 2.5. ^{1}H NMR spectrum of G-2-nitro.

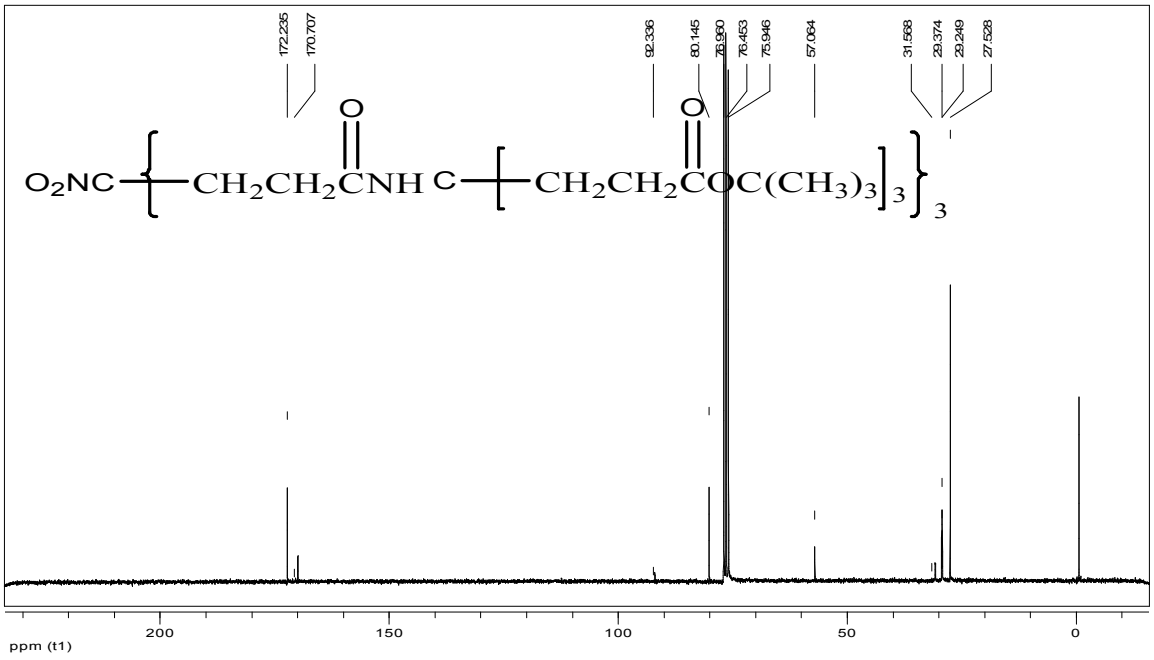

Figure 2.6. ^{13}C NMR spectrum of G-2-nitro.

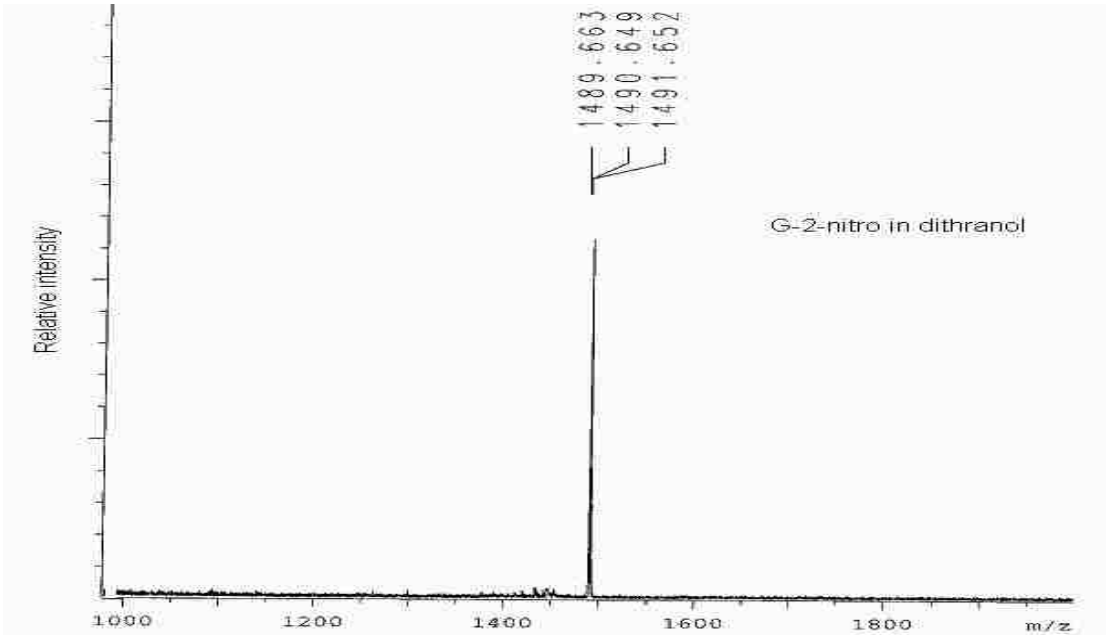

Figure 2.7. MALDI-TOF mass spectra of G-2-nitro.

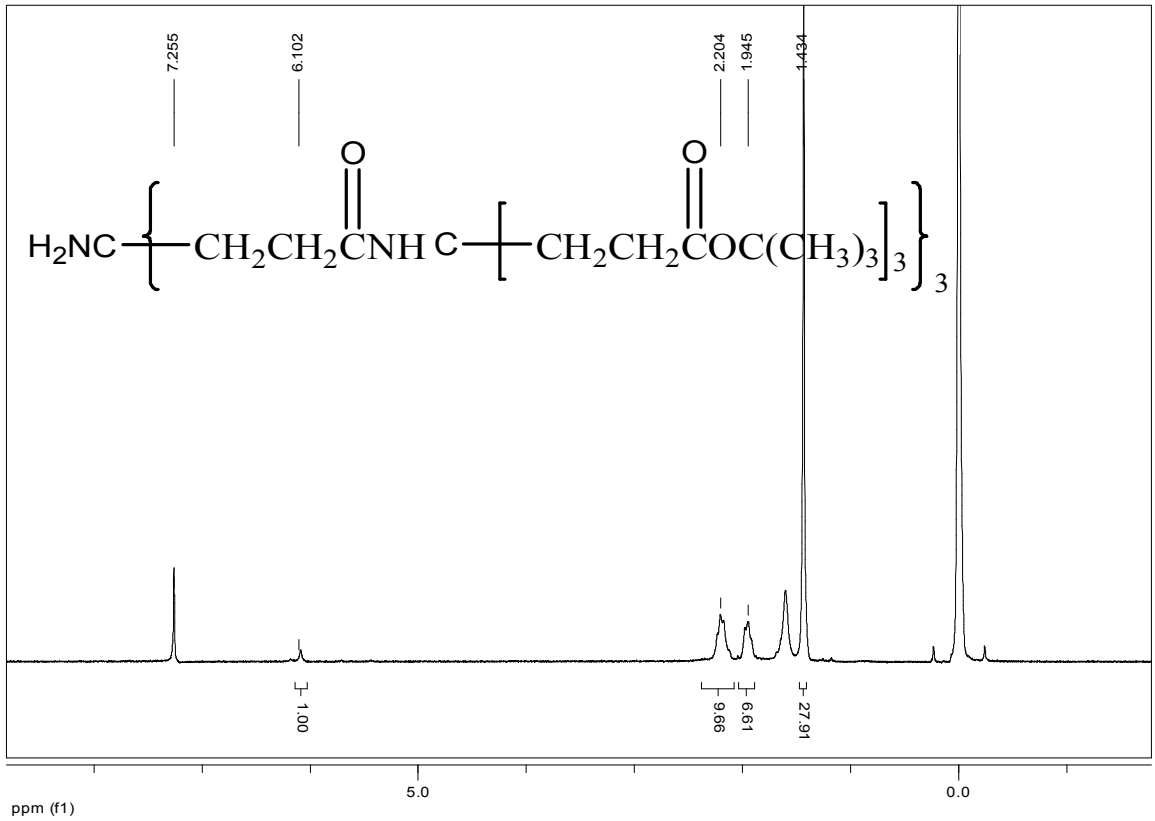

Figure 2.8. ^{1}H NMR spectrum of G-2-amine.

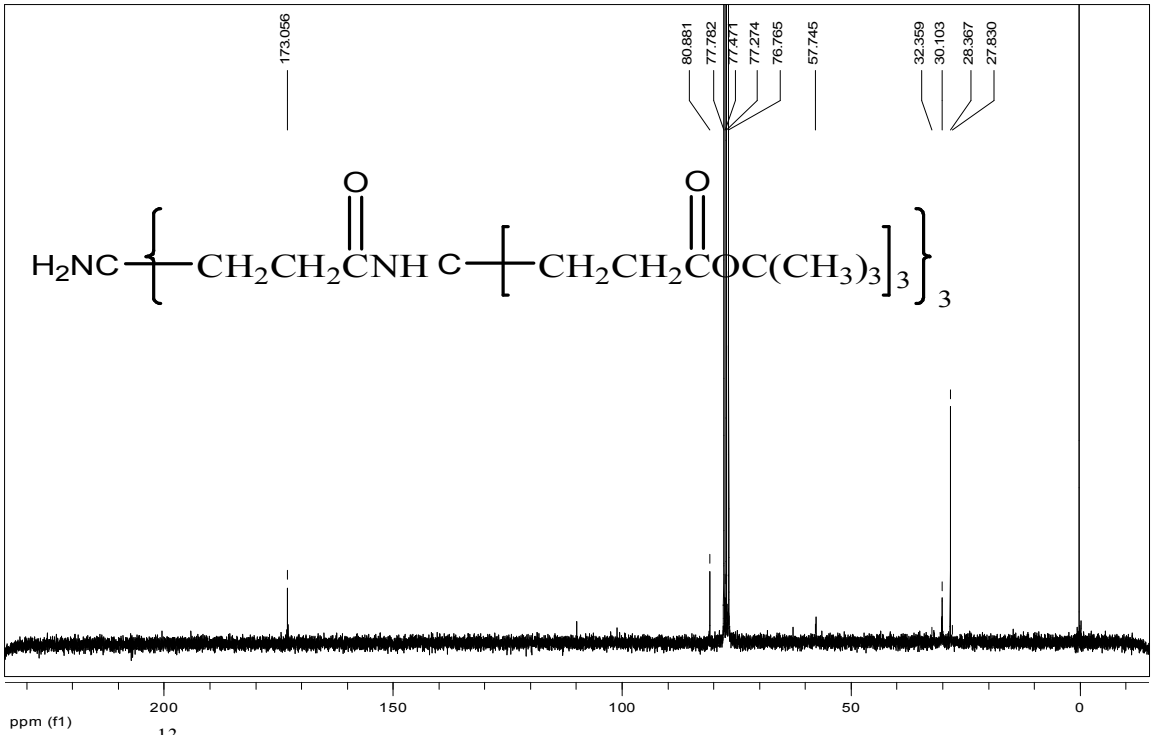

Figure 2.9. ^{13}C NMR spectrum of G-2-amine.

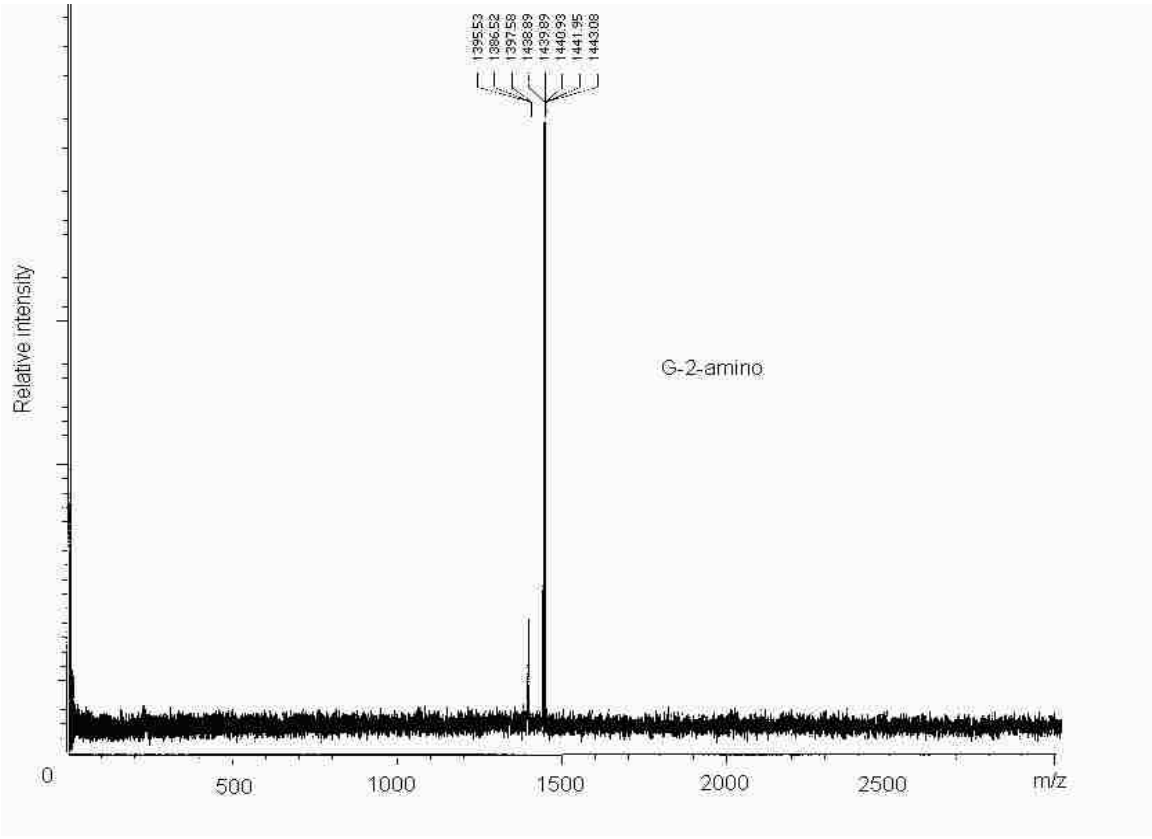

Figure 2.10. MALDI-TOF mass spectra of G-2-amine.

2.3.3 FTIR Characterization

Nitrotriester showed (Figure 2.11) very strong ester carbonyl stretch vibration at 1727.40 cm^{-1} and C-O stretch at 1152 cm^{-1}. In addition to the above two peaks, BA also showed strong hydrogen-bond absorption at 3315, 3371, and 3420 cm^{-1}. Both G-2-nitro and G-2-amine showed strong absorptions of amide I at 1656 cm^{-1} and amide II at 1539 cm^{-1}plus the ester carbonyl stretch and C-O stretch.

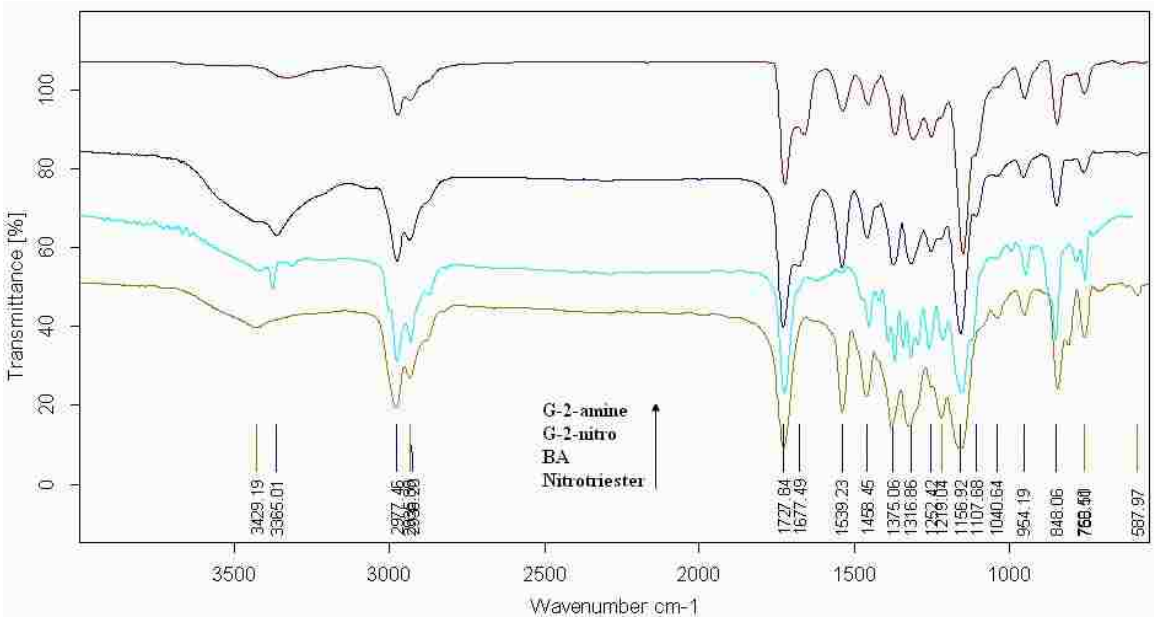

Figure 2.11. FTIR spectra of nitrotriester, BA, G-2-nitro, and G-2-amine.

2.3.4 Thermo-analysis Characterization

Figure 2.12 and table 2.1 showed the TGA and DSC thermograms of BA. The endothermic peak at 53.37-66.02ºC without weight loss is the melting point of BA. The small endothermic peak at 219.55ºC corresponded with the intra-molecular amidation reaction releasing one *t*-butyl group; the big endothermic peak at 224.40 –234.77 ºC of BA corresponded with releasing two *t*-

butyl groups due to decomposition. Scheme 2.5 showed the proposed mechanism of thermo-decomposition of BA at different temperatures.

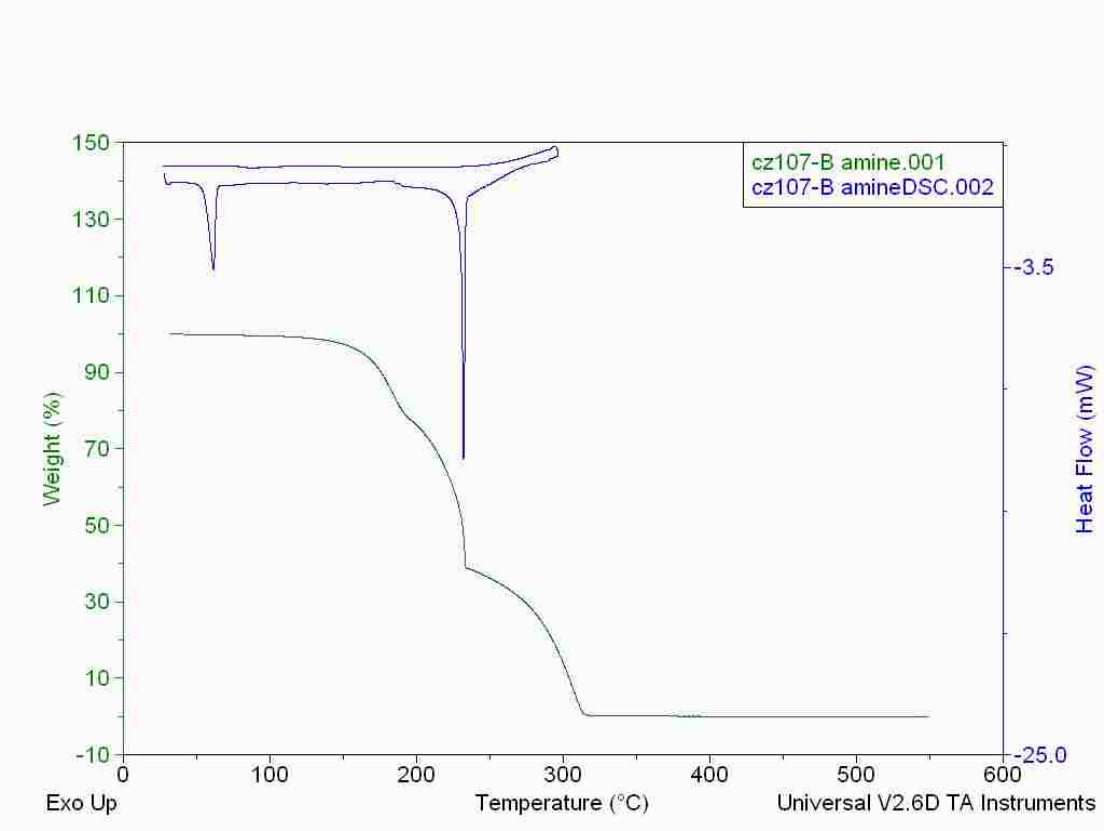

Figure 2.12. TGA and DSC spectra of BA.

Scheme 2.5. Mechanism of decomposition of BA under heating

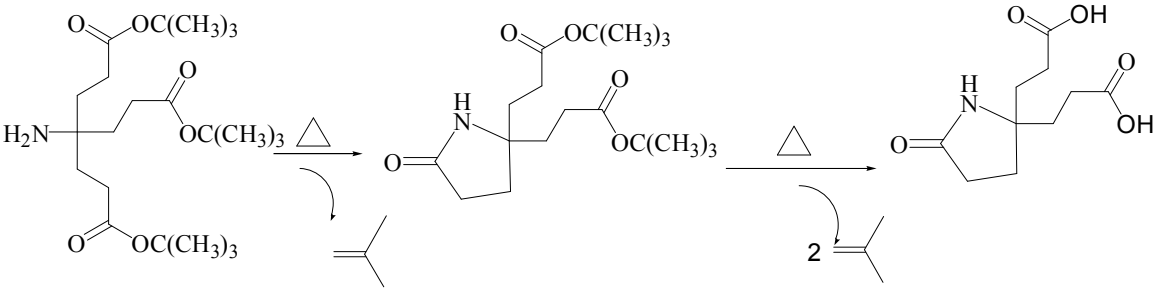

Figure 2.13 showed the TGA thermograms of nitrotriester, BA, and G-2-amine. The weight loss was calculated by integrating the corresponding peaks of weight derivative curves. Nitrotriester exhibited a significant weight loss (39.18%) at 189.40-232.07 ^{o}C from losing three *t*-butyl groups each molecule (theoretically 37.75%). BA lost one *t*-butyl group with each

molecule at 150.87-197.50 ^{o}C due to an intra-molecular cyclization reaction and lost two *t*-butyl groups with each molecule at 197.5-238.5 ^{o}C due to decomposition releasing two isobutene. These two peaks overlapped somewhat. The weight loss for the 2nd peak was 28.5% which was close to the theoretical weight loss of 26.99% due to losing two isobutene. G-2-amine began losing one *t*-butyl group with each molecule from 185.44 ^{o}C due to intermolecular amidation reaction and continued losing all *t*-butyl groups up to 223.47 ^{o}C. The weight loss from 185.44 ^{o}C to 223.47 ^{o}C is about 35.13%, close to 35% of the theoretical weight loss due to losing nine *t*-butyl groups. Based on the TGA weight loss result of these model compounds, the weight loss of the peak of 197.5-238.5 ^{o}C was used to estimate the DS of BA of CMCBA in chapter 3. There was no residue above 500 ^{o}C for nitrotriester, BA, and G-2-amine.

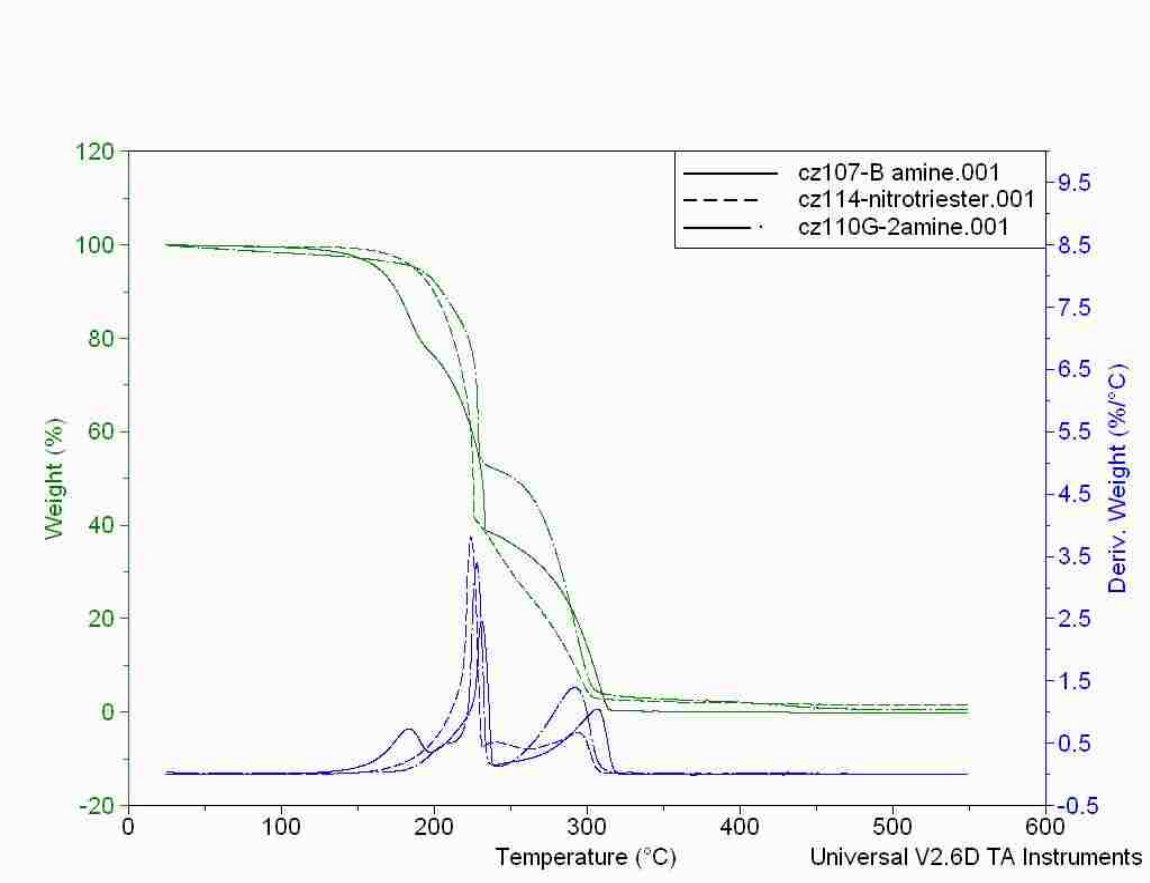

Figure 2.13. TGA spectra of nitrotriester, BA, and G-2-amine.

Table 2.1. TGA peaks of nitrotriester, BA, and G-2-amine

Samples	Temperature range	Weight loss	Theoretical weight loss	Residue at 500 °C
Nitrotriester	T_{d1}: 188.90-230.07 ºC	39.18%	37.75% (loss 3 isobutene)	0 %
	T_{d2}: 230.07-310.00 ºC			
BA	T_{d1}: 163.72-197.09 ºC	8.36%	13.49% (loss 1 isobutene)	0%
	T_{d2}: 197.09-239.55 ºC	28.5%	26.99% (loss 2 isobutene)	
	T_{d3}: 239.53-313.81 ºC			
G-2-amine	T_{d1}: 186.08-235.01 ºC	35.13%	35.00% (loss 9 isobutene)	0%
	T_{d2}: 235.66-315.71 ºC			

2.4 Conclusions

(1) NMR spectra and FTIR spectra confirmed the molecular structure of nitrotriester, BA, G-nitro, and G-2-amine.

(2) TGA thermograms showed that nitrotriester, BA, and G-2-amine lose their *t*-butyl group due to thermo-decomposition. Nitrotriester showed a significant weight loss (40.25%) at 189.40-232.07 °C from losing three *t*-butyl groups. BA began to lose one *t*-butyl group with each molecule from 150.87 °C due to intramolecular cyclization reaction and continued to lose two *t*-butyl groups with each molecule from 197.5 to 238.5 °C due to decomposition releasing isobutylene. G-2-amine lost nine *t*-butyl groups from 185.44 °C to 223.47 °C.

(3) The large endothermic peak around 224.40–234.77 ºC of BA in its DSC thermogram corresponded with its weight loss peak attributed to losing two *t*-butyl groups with each molecule.

CHAPTER 3. SYNTHESIS AND CHARACTERIZATION OF WATER SOLUBLE AMIDOAMINE DENDRONIZED CELLULOSE DERIVATIVES*

3.1 Introduction

Previously, Doris Culberson discovered that N,N-dimethylaminopropylcarbomoylmethyl cellulose (CMCDMPDA) formed by elaborating a methyl ester of CMC-M[5] with N,N-dimethylpropanenenamine produced a water soluble derivative. This is due to the breaking of intermolecular hydrogen bonds in cellulose. The formation of these amidoamide derivatives is an effective procedure for producing non-ionic water soluble cellulose derivatives. In 2000, R. Barbucci *et al* used 1,3-propanediamine in an analogous fashion to react with activated cellulose, [2-(N-methyl pyridium) carboxymethyl cellulose] iodide (MPCMCI), to prepare cross-linked cellulose gel (Scheme 3.1).[77]

Scheme 3.1. Synthesis of cross-linked cellulose gel by R. Barbucci

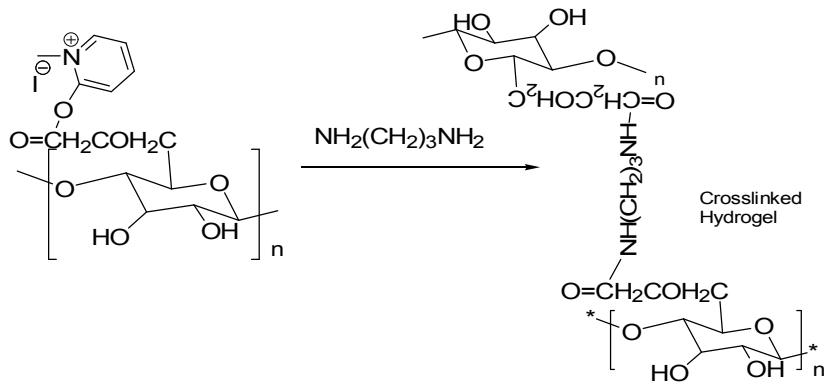

From 2000, Loren M. Price explored the attachment of BA onto cellulose backbone[78] based on similar synthesis methodology for preparing cross-linked cellulose by R. Barbucci; however, he used BA with a monoamino functional group to react with MPCMCI. In his research, only limited quantities of dendonized cellulose derivatives were obtained due to the difficulty of the synthesis. The molecular size, conformation, molecular weight and molecular weight

* Portions of this chapter were reproduced by permission from *Biomacromolecules* **2006,** 7, (1), 139-145. Copyright 2006 American Chemical Society.

distribution of the dendronized cellulose derivatives have not been characterized. Its potential applications have not been evaluated. The synthesis methodology needs to be improved.

By elaborating cellulose backbone with BA, we can create dendronized cellulose either the 1st generation derivatives CMCBA or the 2nd generation derivative CMCBABA. Both CMCBA and CMCBABA are hydrophobic and water insoluble because BA is hydrophobic. As I mentioned in chapter one, by elaborating CMCBA and CMABABA with DMPDA, new dendrigraft-polyamino derivatives CMCBADMPDA and CMCBABADMPDA (Scheme 3.2), which may carry lots of hydrophilic amino periphery functional groups, are formed. They are expected to be water-soluble so it is possible to characterize their molecular structure and molecular weight using solution techniques including NMR, gel-permeation chromatography (GPC), and light scattering.

Scheme 3.2. Illustration of a water soluble dendronized cellulose with potential drug delivery function

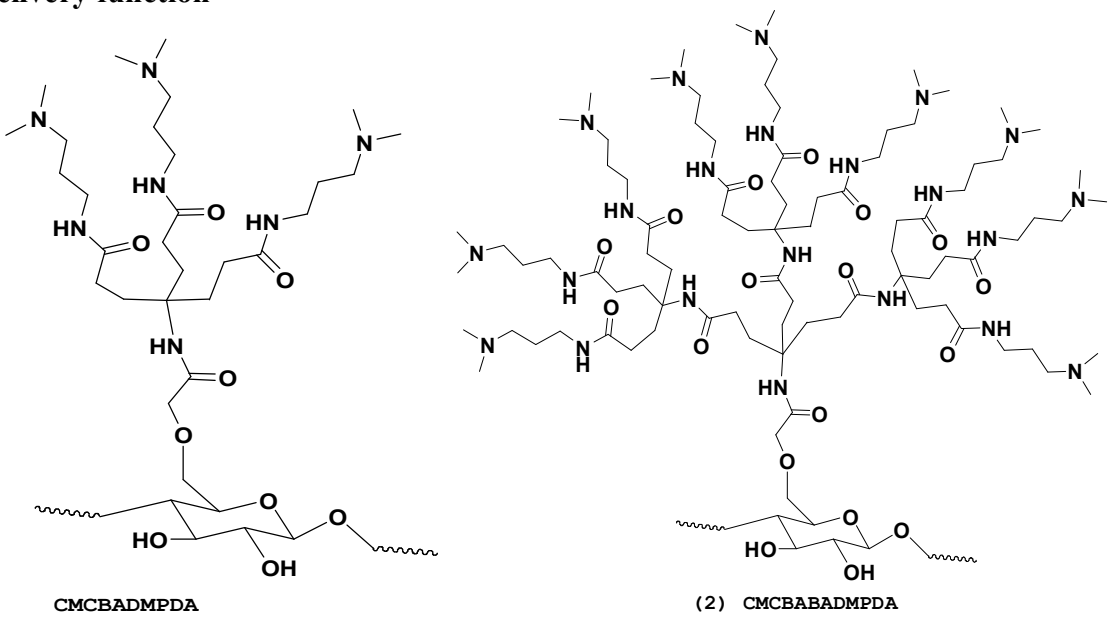

Due to their unique structure with a hydrophobic interior and an exterior made up of hydrophilic amino groups, CMCBADMPDA and CMCBABADMPDA are expected to be unimolecular micelles. They are expected to have certain capacities to hold hydrophobic

molecules of active components, which is a useful application in the human health and personal care industry. In this chapter, the synthesis of CMCBADMPDA and CMCBABADMPDA are reported. Their FTIR, NMR spectra confirmed their chemical structure. Their molecular weight, molecular weight distribution, molecular size and conformation were characterized by using GPC-LS.[79, 80]

The degrees of substitution (DS) of functional groups on polymers are important in determining the properties of modified polymers. Polymer derivatives prepared from the same polymer with the same functional group could have completely different properties and different applications depending on their specific DS. For example, when the DS of CMC is less than 0.3, CMC is water insoluble; however, CMC becomes water soluble when its DS is greater than 0.4.[81] In this chapter, the control of the DS of BA in CMCBA was investigated by adjusting the DS and the molecular weight of the starting polymer CMC, and the relative concentration of 2-chloro-*N*-methylpyridinium iodide (CMPI) in preparing activated ester MPCMCI.[82] A TGA technique was used to estimate the DS of CMCBA.

3.2 Experimental

Materials. Sodium carboxymethylcellulose (CMC), hydrochloric acid, methanol, tetrabutylammoniumhydroxide (TBAH, 40% in water), *N*,*N*-dimethylformamide (DMF), 2-chloro-*N*-methylpyridinium iodide (CMPI), triethylamine, formic acid, nitromethane, *tert*-butyl acrylate, sodium bicarbonate, magnesiumsulfate, celite, ethyl alcohol, ether, Raney nickel, pyrene, and *N*,*N*-dimethyl-1,3-propanediammine (DMPDA) were purchased from the Aldrich Chemical Co. Dialysis membranes [molecular weight cutoff (MWCO) 6000-8000] were purchased from Spectrum Laboratories, Inc.

Instrumentation. Fourier transform infrared (FT-IR) spectra were obtained on a Perkin-Elmer 1760X FT-IR spectrometer using KBr/sample disks. ^{1}H NMR and ^{13}C NMR spectra of the polymers were obtained on a Bruker DPX250 MHz spectrometer. Deuterium oxide (D_2O) was used as the solvent. Weight loss and derivative weight loss curves were obtained on a high-resolution modulated TGA 2950 thermogravimetric analyzer from TA Instruments. All runs were performed under a nitrogen atmosphere and through a ramp starting from room temperature and increasing up to 500 °C at 5 °C/min. Intrinsic viscosity measurements were performed with aqueous solutions of CMC and its derivatives with concentrations ranging from 0.03 to 0.40 g/dL at 25 °C. A Z107 Ubbelohde viscometer from Cannon Instrument Co. with a solvent flow time of 77.26 seconds was used to measure the intrinsic viscosities. All measurements were made in 0.1 N NaCl to minimize any Donnan effects. A gel-permeation chromatography (GPC) system equipped with a differential refractometer combined with a DAWN DSP laser photometer from Wyatt Technology Corporation (GPC-LS) was used to determine molecular sizes, molecular weights, and molecular weight distributions (MWD), Mw/Mn, of polymers. ASTRA software was employed for data collection and analysis. The samples were eluted with aqueous 0.4 N ammonium acetate-0.01 N NaOH through two PL Aquagel-OH 8 μm columns at a flow rate of 1.0 mL/min. The differential refractive indexes (dn/dc) of the polymers in the same solution were measured on a Brice-Phoenix differential refractometer, model BP-2000-V, from Phoenix Precision Instrument Co.

3.2.1 Synthesis of CMCDMPDA

NaCMC (1.00 g, 4.59 mmol, MW=250k, DS=0.7) was activated with 2-chloro-*N*-methylpyridinium iodide as described by Barbucci *et al*. The resultant active ester, 2-oxy-*N*-methylpyridinium iodide cellulose methylcarboxylate (MPICMC), was not isolated. DMPDA

(20 mL) and three drops of triethylamine were added to the solution of MPICMC, and the mixture was allowed to stir for one day. The solution was diluted with 50 mL of water and the low molecular weight byproducts were removed by dialysis. After 1 week, when no further salts were detected in the dialysate, the solution in the dialysis tube was concentrated by the use of a rotovaporator. The concentrated solution of the product was dried under a vacuum and afforded CMCDMPDA (0.91 g, 3.43 mmol, 75% yield). ^{1}H NMR (D_2O), δ (ppm): 1.44($CH_2CH_2CH_2$), 2.02([$N(CH_3)_2$], 2.18($CONHCH_2$-CH_2), 2.47[$CH_2N(CH_3)_2$], 3.25-4.5 (broad peaks of anhydroglucose ring). ^{13}C NMR (62.9 MHz, D_2O): 46.16 [$N(CH_3)_3$], 58.22 [$CH_2N(CH_3)_2$], 31.80 ($CH_2CH_2CH_2$), 40.83 ($NHCH_2$), 105.35 (C1), 77.51, 76.04, 74.07, and 72.63.40 (C2_C5), 60.56 (C6), 83.40 (C7), 180.23 (OCH2*C*NHC). FT-IR (cm^{-1}), KBr pellets: 3423 (s, O-H stretch), 2934 (w, C-H stretch), 1649 (s, amide I shoulder), 1595 (amide II band), 1109 and 1059 (s, C-O-C stretch).

3.2.2 Synthesis of CMCBADMPDA

3.2.2.1 Synthesis of CMCBA

Sodium CMC (2.00 g, 9.17 mmol, MW=250k, DS=0.7) was dissolved in water (100 mL). The pH of the above solution was adjusted to 4 with acetic acid and 5 mL of 10% HCl to produce protonated CMC, which was then precipitated in methanol (200 mL). After the resultant precipitate was dried by freeze-drying, it was dissolved with the aqueous 40% TBAH solution (4.32 mL, 6.59 mmol) and 20 mL of water. The corresponding tetrabutylammonium (carboxymethyl) cellulose (TBACMC) was recovered by lyophilization. The dry TBACMC was dissolved in DMF (200 mL). A solution of CMPI (2.55 g, 10.00 mmol) in DMF (25 mL) was added, and the mixture was stirred for 12 hours. Up to 600 mL of DMF was added to maintain the system in a homogeneous state. A BA (4.19 g, 10.1 mmol) solution in 20 mL of DMF was

then added, and the reaction was stirred for 24 h. To isolate the CMCBA, the mixture was dialyzed in deionized water for one week. The contents of the dialysis tube were reduced to about 25 mL using a Büchi rotavapor R-200, and then solvent evaporation was continued to dryness in a vacuum oven at room temperature. The insoluble residue, CMCBA (3.02 g, 8.43 mmol, 92%) was characterized by FT-IR and TGA. FT-IR (cm^{-1}), KBr pellets: 3440 (O-H stretch), 2978 and 2933 (w, C-H stretch), 1728(C=O ester), 1670 (s, amide I shoulder), 1539 (amide II band), 1109 and 1063 (s, C-O-C stretch).

3.2.2.2 Synthesis of CMCBADMPDA

CMCBA (1.24 g, 3.46 mmol, MW=250k, DS=0.7) was stirred with formic acid (20 mL) and water (4 mL) for 24 hours. After the liquid was evaporated to dryness, the solid was washed with water (3 × 10 mL). The resultant "polyacid" was dissolved in aqueous TBAH (5.15 mL, 7.86 mmoL) and water (10 mL). After the mixture was stirred for 24 hours, the TBA salt was again dried by freeze-drying under vacuum. The TBA salt was dissolved in 100 mL of DMF, and a solution of CMPI (2.5 g, 9.78 mmol) in 25 mL of DMF was added. After the mixture was stirred for 24 hour, an excess of DMPDA (25 mL, 198.5 mmol) was added and the mixture was stirred for another 24 hour. The product was isolated by dialysis/evaporation as described above. The residue of CMCBADMPDA (0.46 g, 1.18 mmol, 34% yield) was characterized by FT-IR, TGA, and GPC-LS. ^{1}H NMR (250 MHz, D_2O): δ (ppm) 2.19 [$N(CH_3)_3$], 2.61 (CH_2N), 1.62 ($CH_2CH_2CH_2$), 1.75 (CH_2CH_2CONH), 2.35 (d, $CONHCH_2$), 2.35(CCH_2CH_2CONH), 3.25-4.5 (broad peaks of anhydroglucose ring). ^{13}C NMR (62.9 MHz, D_2O): 44.19 [$N(CH_3)_3$], 56.44 [$CH_2N(CH_3)_2$], 29.83 ($CH_2CH_2CH_2$), 39.23 ($NHCH_2$), 39.21 (CCH_2CH_2), 29.80 (CH_2CONH), 178.46 ((CH_2CH_2CONH), 102.55 (C1), 77.60, 75.36, 71.40, and 70.64 (C2_C5), 60.56 (C6),

83.40 (C7). FT-IR (cm^{-1}), KBr pellets: 3429 (O-H stretch), 2924 (w, C-H stretch), 1639 (s, amide, I shoulder), 1603 (amide II band), 1112 and 1062 (s, C-O-C stretch).

3.2.3 Synthesis of CMCBABADMPDA

3.2.3.1 Synthesis and Characterization of CMCBABA

CMCBA (4.0 g, 7.6 mmol) was stirred with formic acid (40 mL, 826 mmol) and water (4 mL; 220 mmol) for 12 hours. Formic acid was then removed under a vacuum. Water (20 mL) was used to wash the solid three times. The solid was dissolved in TBAH (10.7 mL; 16.3 mmol). After 24 hours, it was freeze dried in a vacuum. Then the solid was dissolved in DMF (100 mL) and 2-chloro-N-methylpyridinium iodide (4.28 g, 16.7 mmol) was added. More DMF (1000 mL) was added to keep the mixture in solution. After 24 hours of stirring, BA (6.5 g, 15.7 mmol) and triethylamine (0.5 mL) was added and stirring continued for another 24 hours. The product CMCBABA was formed immediately. After dialysis for one week, the solvent was evaporated and the residue was dried in a vacuum to give CMCBABA (4.6 g, 3.8 mmol, yield 50%). The product was characterized by using TGA. FT-IR (cm^{-1}), KBr pellets: 3426 (O-H stretch), 2978 and 2932(w, C-H stretch), 1728(C=O ester), 1660 (s, amide I shoulder), 1546 (amide II band), 1156 and 1063 (s, C-O-C stretch).

3.2.3.2 Synthesis of CMCBABADMPDA

CMCBABA (2.0 g; 1.7 mmol) was stirred with formic acid (40 mL; 826 mmol) overnight. Then, the formic acid was removed under a vacuum. Water (20 mL) was used to wash the solid three times. Next, it was dissolved in TBAH (11 g; 17 mmol). After 24 hours, it was freeze dried. The solid was dissolved in DMF (100 mL) and 2-chloro-N-methylpyridinium iodide (5.28 g, 20.7 mmol) was added. More DMF (1500 mL) was added to keep the mixture in solution.

After 24 hours of stirring, DMPDA (30 mL, 238 mmol) and triethylamine (0.5 mL) was added and stirring continued for another 24 hours. The product CMCBABADMPDA was formed immediately. After one week dialysis, the solvent was evaporated and the residue was dried in a vacuum to give CMCBABADMPDA (1.5 g; 1.11 mmol, yield 65%). ^{1}H NMR (250MHz, D_2O): δ (ppm) 2.46 ($N(CH_3)_2$), 2.93 (CH_2CH_2N), 1.89 ($CH_2CH_2CH_2$), 2.66($CONHCH_2$), 1.89(CCH_2CH_2CO, gen1 and gen2); 2.66 (CCH_2CH_2, gen1 and gen2), 3.25-4.5 (broad peaks of anhydroglucose ring). ^{13}C NMR (62.9MHz, D_2O): 46.74 [$N(CH_3)_2$], 58.12 [$CH_2N(CH_3)_2$], 38.08 ($NHCH_2$), 25.08 ($CH_2CH_2CH_2$), 28.37 (CCH_2CH_2, gen2), 15.66 (CCH_2CH_2, gen2), 20.15 (CCH_2CH_2, gen1), 180.50 (CH_2CH_2CONH, gen2), 104.76 (C1), (70-85) (C2~C5, C7), 60.60 (C6). FT-IR (cm^{-1}), KBr pellets: 3426 (O-H stretch), 2937 (w, C-H stretch), 1643 (s, amide, I shoulder), 1597 (amide II band), 1112 and 1062 (s, C-O-C stretch).

3.3 Results and Discussion

3.3.1 Synthesis of CMCDMPDA

(Carboxymethyl)cellulose (CMC) is activated for nucleophilic modification by forming an active ester with 2-chloro-*N*-methylpyridinium chloride (CMPI) as described by Barbucci et al.[77] After conversion of the sodium salt of CMC (CMCNa) to the tetrabutylammonium salt (TBACMC), the salt became soluble in DMF and all of the subsequent transformations could be conducted in homogeneous solutions. The ratio of TBACMC to CMPI can be adjusted to selectively activate a given percentage of carboxyl groups. We have used an excess of CMPI in the conversions to maximize the DS of BA achieved except in the experiments where controlling DS of BA on CMC through adjusting the relative concentration of CMPI in the reaction. All carboxylic acid functionalities were activated by the use of the reaction sequence.

Once activated, the MPICMC underwent a nucleophilic attack by an amine, which eliminates *N*-methyl-2-pyridone. A small amount of triethylamine was added to the reaction mixture to act as a hydrogen iodide scavenger. The reaction is effectively irreversible and the *N*-methyl-2-pyridone is a cosolvent for the reagents and products. The impact of the CMC-Na activation steps was evaluated by converting it to the corresponding 3-(*N*, *N*-dimethylamino) propanecarboxamide derivative (CMCDMPDA) (Scheme 3.3).

Scheme 3.3. Synthesis of CMCDMPDA

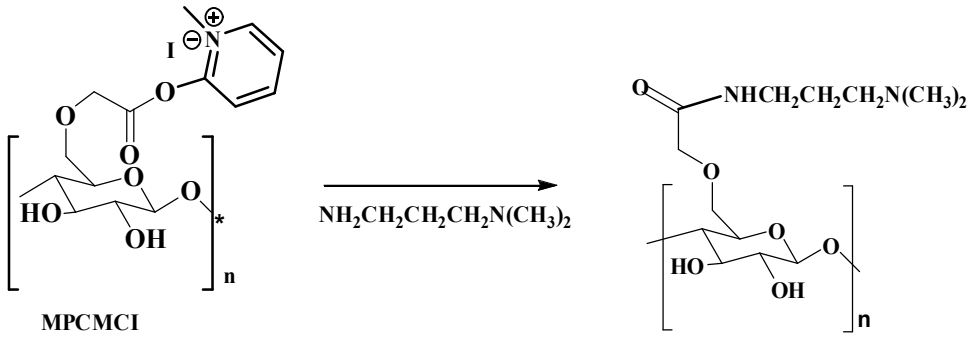

The ^{1}H NMR and ^{13}C NMR spectra of this model compound were consistent with the proposed structure as shown in Figure 3.1 and Figure 3.2. The protons at δ = 2.02 ppm and carbon at δ = 46.16 of *N*, *N*-dimethyl resonance are the identifying features for multifunctional aminoamide derivatives described in this project. The triplets at δ = 2.18 and 2.47 ppm are assigned to the methylene groups adjacent to the amino and amide functions, respectively. The multiplet at δ = 1.44 is assigned to the central methylene group of the propyl substitute. The anhydroglucose appear as broad resonances between δ = 3.25 and 4.5 ppm of their protons and the carbon peaks of δ = 102.55 (C1), 77.50, 76.04, 74.07, and 72.63 (C2-C5), 60.56 (C6), 83.40 (C7).[83] The intrinsic viscosity of this derivative was 3.5 dL/g, suggesting that backbone degradation accompanying NaCMC activation is minimal. The reduction in viscosity could be attributed to the replacement of ionic substituents with neutral aminoamide substituents.

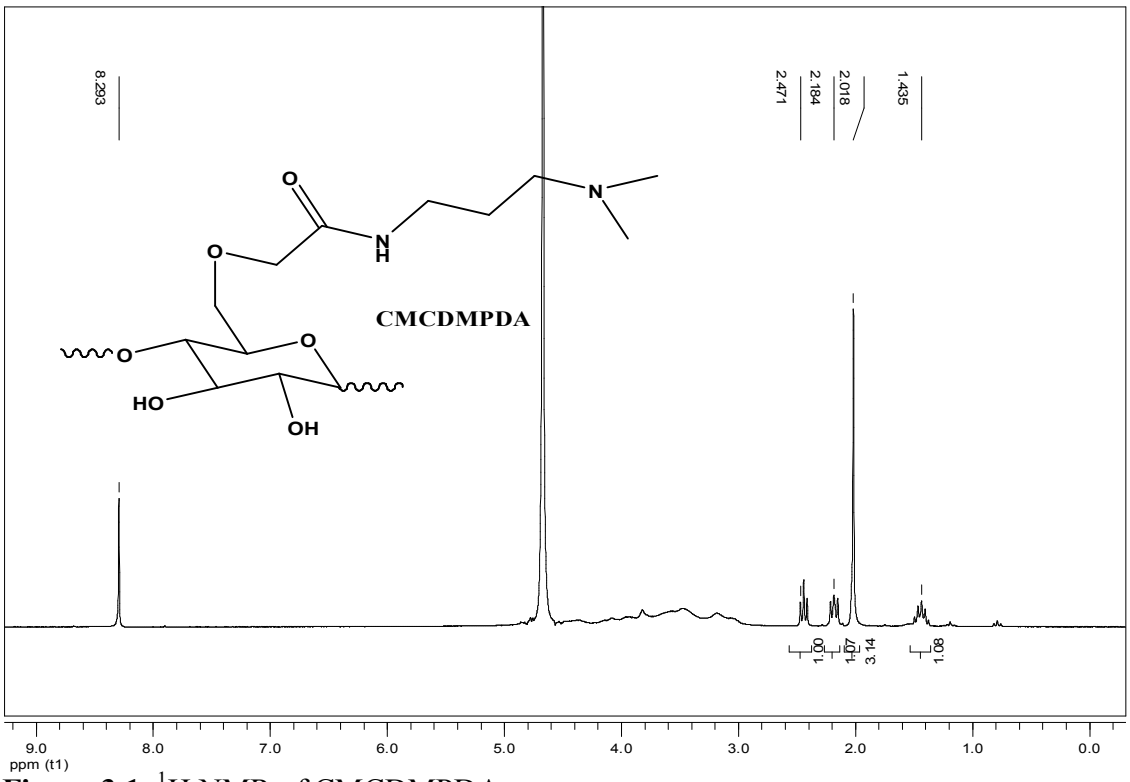

Figure 3.1. [1]H NMR of CMCDMPDA.

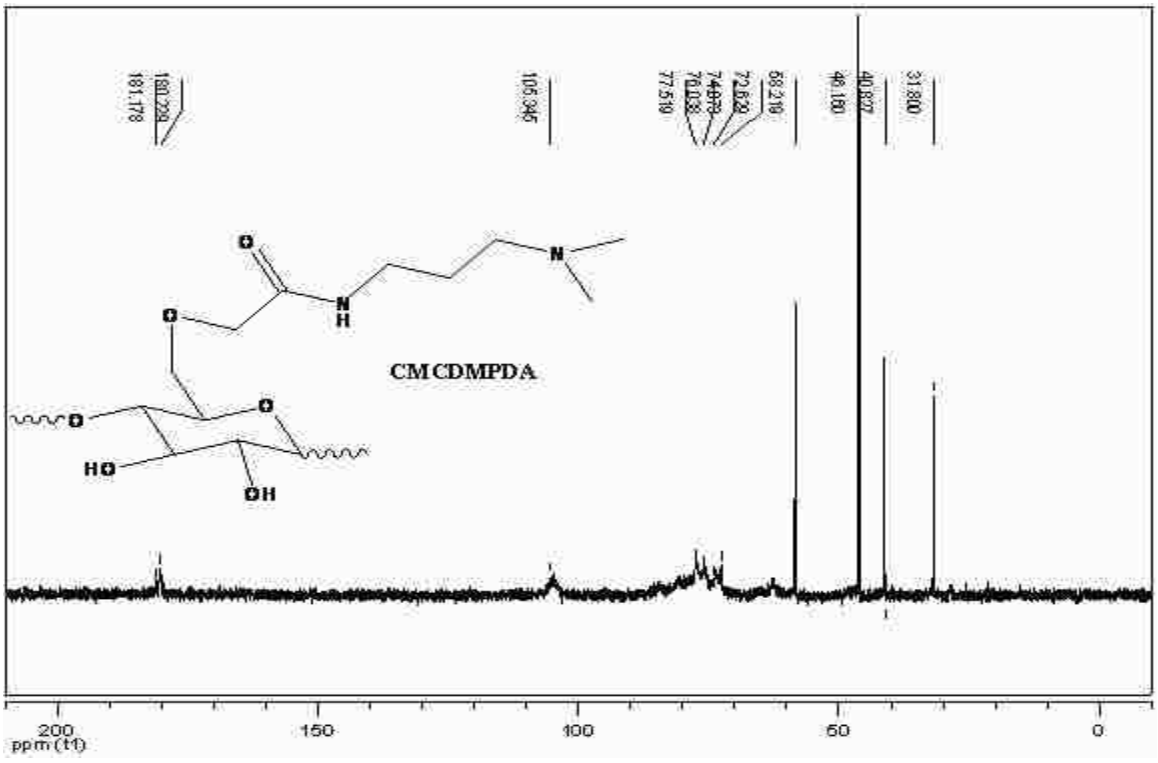

Figure 3.2. [13]C NMR of CMCDMPDA.

3.3.2 Synthesis of CMCBA

To produce a series of tris-substituted derivatives, the DMPDA was replaced by the macromonomer Behera's amine (BA). Behera's amine is an AB3 macromonomer with one reactive amine functionality and three *tert*-butyl ester functionalities. Behera's amine features a chemically stable sp3 carbon branching center, three preformed branches, an amino moiety with high nucleophilicity, and the eventual quantitative hydrolysis of the *tert*-butyl esters to unveil the carboxylic acid groups. Behera's amine facilitates the synthesis of a multigeneration side-chain dendritic polymer with a minimum of coupling and deprotection steps. The formation and elaboration of the first-generation dendronized cellulose is illustrated in Scheme 3.4. FTIR spectra of CMCBA showed the strong ester peak at 1728 cm^{-1}, amide I at 1640 cm^{-1}, amide II at 1545 cm^{-1},[84] and a strong hydrogen bond absorption at 3431 cm^{-1}. The FTIR was consistent with proposed chemical structure of CMCBA (Figure 3.12). CMCBA obtained was insoluble in water, DMF, and DMSO.

Scheme 3.4. Synthesis of CMCBA

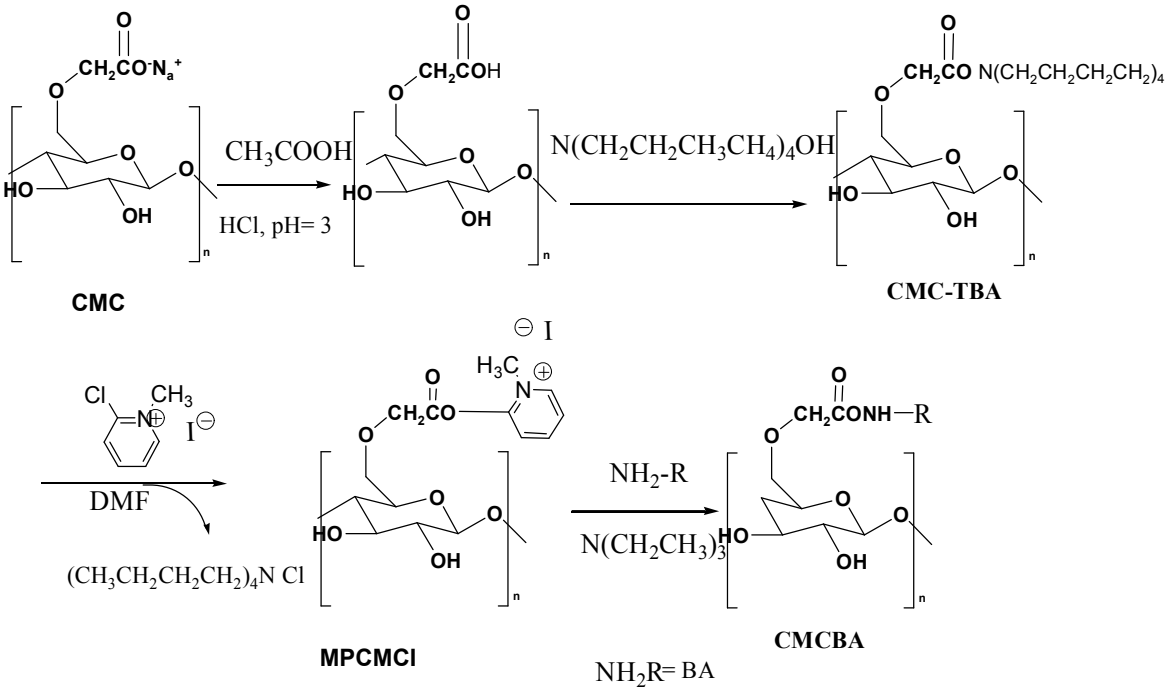

3.3.2.1 Characterization of Degree of Substitution (DS) of CMCBA

Although the dendronization of cellulose is conducted in solution, once the derivative is isolated it can not be re-dissolved. The poor solubility of CMCBA limited the options for estimating the degree of substitution achieved. One unique property of tert-butyl esters, i.e. their thermal decomposition to isobutylene, could be exploited to estimate the number of BA residues introduced. (Scheme 3.5) We observed that the weight loss of CMCBA of the 1st peak from 196˚C (Figure 3.3) was related to the degradation of *tert*-butyl moieties of CMCBA to isobutylene. In chapter two, we proved that the weight loss of this peak of the weigh derivative curves in nitrotriester, BA, and G-2-amine all agreed with their theoretical weight losses. The DSC spectra of CMCBA (Figure 3.4) also proved this observation. The strong endothermic character of the 1st peak of CMCBA in figure 3.4 corresponding to the 1st TGA weight loss derivative peak in figure 3.3 is responsible for the decomposition of t-butyl ester releasing butane. The weight loss of the 1st peak of CMCBA could be correlated with the DS of BA on CMCBA in equation 3.1. The DS of BA on CMCBA could be evaluated based on the weight loss of the 1st peak using equation 3.2 transformed from equation 3.1.

Scheme 3.5. The thermo decomposition of *tert*-butyl ester releasing isobutene[85]

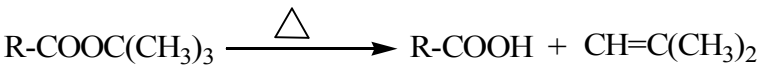

Weight calculation equation 3.1:

$$WL = \frac{3CH_2 = C(CH_3)_2 \times DS_2}{C_6H_7O_3 + OH \times (3 - DS_1) + OCH_2COOH \times (DS_1 - DS_2) + OCH_2CONHC[CH_2CH_2COOC(CH_3)_3]_3 \times DS_2}$$

Where WL is the weight loss from 196˚C

---------- Equation 3.1

DS calculation equation 3.2:

$$DS_2 = \frac{WL \times [C_6H_7O_3] + OH \times (3 - DS1) + WL \times OCH_2COOH}{WL \div 3 \times (CH_2 = C(CH_3)_2 + WL \times OCH2COOH - WL \times OH_2CONHC(CH_2CH_2COOC(CH_3)_3]_3}$$

----------Equation 3.2

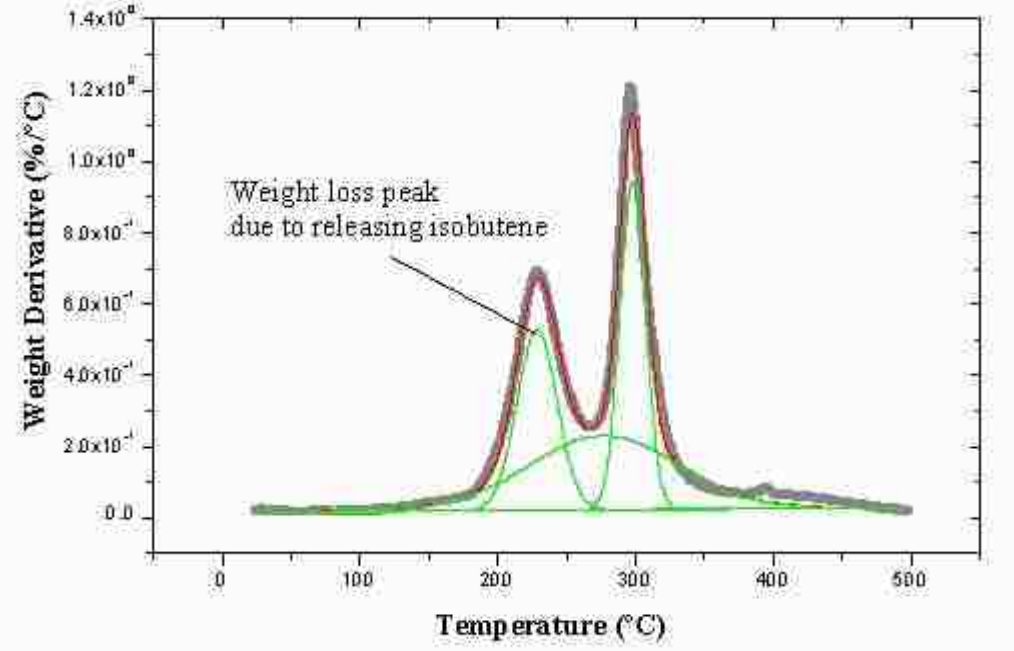

Figure 3.3. Deconvoluted TGA weight derivative curves of CMCBA for DS calculation of CBCBA based on the weight loss.

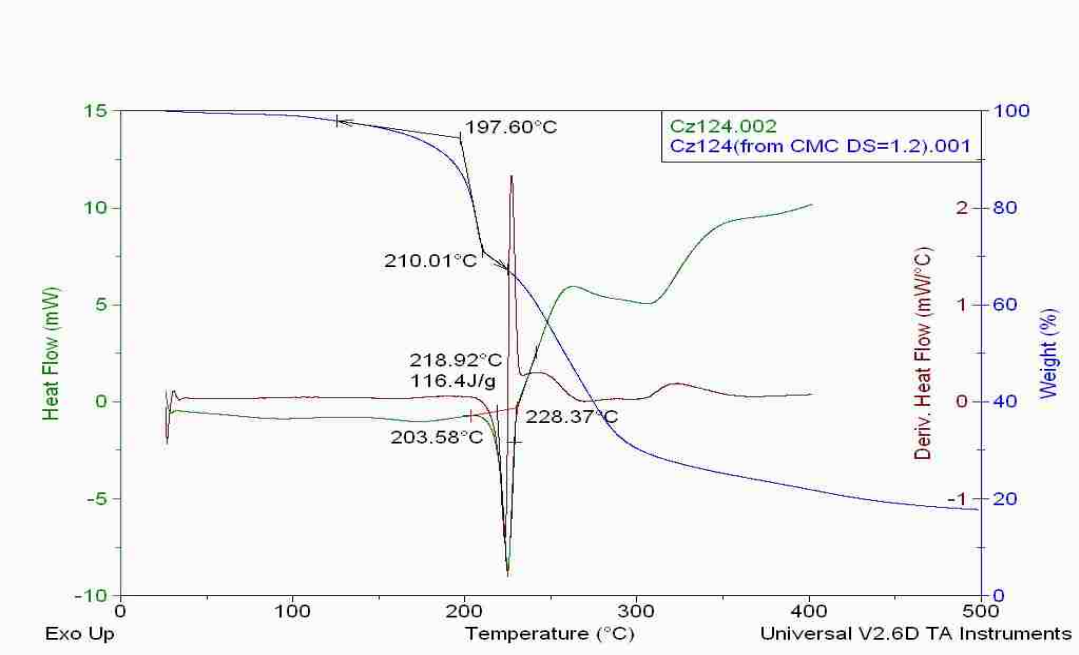

Figure 3.4. The corresponding peaks of the DSC curve and TGA curve of CMCBA.

3.3.3 Control of DS of CMCBA

Several factors may have influence on the DS of BA on CMCBA in the synthesis. Among them, the important factors are the DS and molecular weight of CMC, the relative concentration of CMPI added in reaction system which controls the activation of CMCTBA, etc. In this section, the influences of the above factors on the DS of CMCBA were investigated.

3.3.3.1 Influence of DS of CMC on DS of CMCBA

The influence of DS of CMC on DS of CMCBA was examined by using starting material CMC (MW=250k) with different DS (Table 3.1 and Figure 3.5). To minimize interferance of incomplete activation, the reactions were conducted using excess amounts of both CMPI and BA in the reaction systems. Table 3.1 showed that the higher the DS of CMC of the starting material was used, the higher the DS of BA on CMCBA was obtained. The DS of CMCBA obtained was normally lower compared to that of the corresponding CMC. The limitation of DS obtained using CMC with DS=1.2 was around 0.78. This phenomenon was expected because there was limited space on the CMC backbone for the access of bulky dendron which limited the nucleophilic grafting reaction.

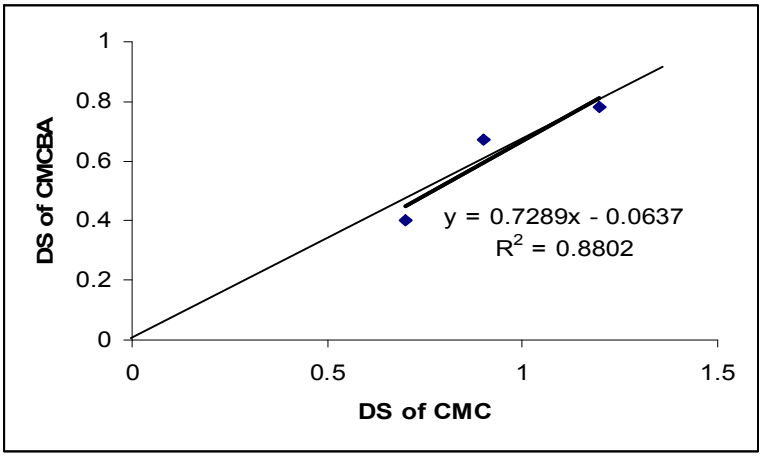

Figure 3.5. Influence of DS of CMC on DS of CMCBA.

Table 3.1. Influence of DS of CMC on DS of CMCBA [a]

	CZ-122	CZ-123	CZ-124
DS of source CMC	0.7	0.9	1.2
DS of CMCBA	0.40	0.67	0.78
CMC (g)	2.50	2.51	2.51
Yield (g)	1.38	2.87	2.13
Yield (%)	34%	54.3%	41%

[a] Excess CMPI; CMC (DS=0.7, MW=250k)

3.3.3.2 Influence of MW of CMC on DS of CMCBA

The effect of MW of CMC on the DS of CMCBA was studied by using starting CMC with two different MW for each DS under excess CMPI and excess BA to exclude the interference of incomplete activation (Table 3.2).

Table 3.2. Influence of MW of CMC on DS of CMCBA [a]

MW of source CMC	250k	700k	90k	250k
DS of CMC	0.9	0.9	0.7	0.7
DS of CMCBA	0.67	0.67	0.48	0.40
CMC (g)	2.51	2.51	2.51	2.51
Yield (g)	2.87	3.57	0.37	1.38
Yield (%)	54.3%	67%	9%	41%

[a] Excess CMPI

Two DSs (0.7 and 0.9) of CMC were used. For CMC with DS of 0.9, the DS of CMCBA did not change significantly from MW of 250k to 700k. This indicated that as soon as the activated CMC-MPI swelled in the DMF solvent, the nucleophilic addition-elimination of BA with

CMCMPI would take place. The DS of CMCBA obtained using CMC (DS=0.7) with MW of 90k was 0.48, which was slightly higher than 0.40, that of CMCBA obtained using CMC (DS=0.7) with high MW of 250k.

3.3.3.3 Influence of relative concentration of CMPI on DS of CMCBA

The effect of relative concentration of CMPI on DS of CMCBA was studied by partly activating CMC through controlling the relative concentration of CMPI (Table 3.3 and Figure 3.6). CMC (DS=0.7; MW=90k) was used as the starting material.

Table 3.3. Influence of relative concentration of CMPI on DS of CMCBA

Targeted DS of CMCBA	Excess	0.7	0.42	0.25	0.105
DS of CMCBA	0.48	0.35	0.29	0.21	0.087
CMC (g)	2.67	2.67	2.67	2.67	2.67
Yield (g)	2.40	2.22	2.82	2.83	1.70
Yield (%)	51%	57%	73%	80%	56%

Table 3.3 showed that the higher relative concentration of CMPI in the reaction resulted in the higher DS of CMCBA. When the relative concentration of CMPI or target DS of CMCBA was low, the DS of CMC could increased with the concentration of CMPI linearly; when the concentration of CMPI or target DS was relatively high, the DS of CMC increased slowly corresponding with the increasing concentration of CMPI. The steric factor of dendron began to play an important role when the target DS of CMCBA was above 0.25. The DS of CMCBA produced from CMC (DS=0.7; MW=90k) was limited to 0.48 due to the steric barrier encountered by bulky dendron attacking CMCMPI. The DS of CMCBA from starting CMC (DS=0.6, MW=90k) was limited to 0.48 due to the steric barrier effect of bulky dendron attacking CMCMPI.

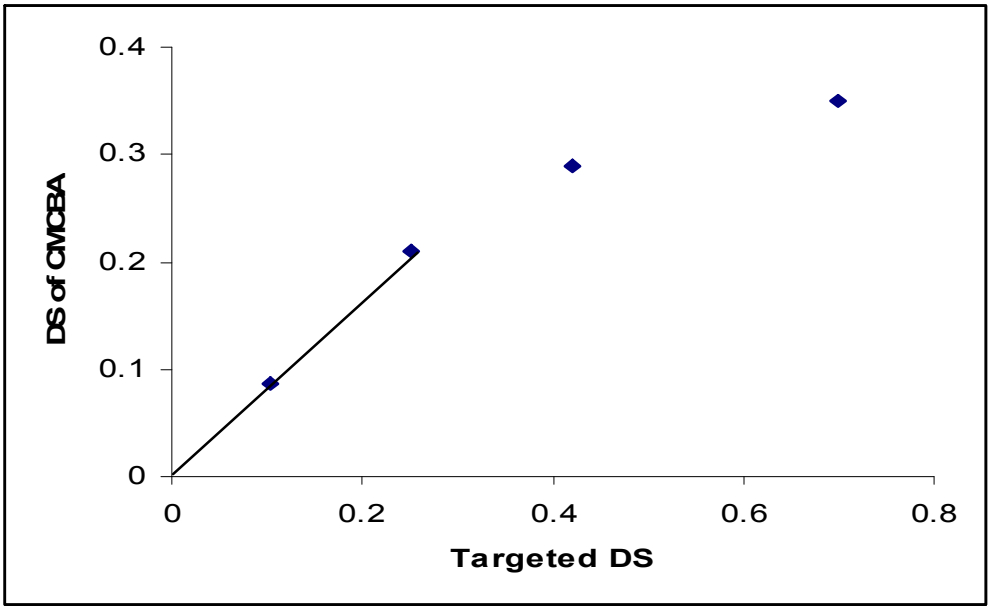

Figure 3.6. CMCBA with different DS produced using different concentration CMPI.

3.3.4 Synthesis of CMCBABA

The synthesis of CMCBABA started from the hydrolysis of CMCBA with formic acid (Scheme 3.6) followed by transforming it into DMF soluble tetrabutylammonium salt TBA^{+} $^{-}$CMCBA by using TBAH. The activation with CMPI transformed TBA^{+} $^{-}$CMCBA into activated MPCMCBAI. Finally the amino group of BA effects a displacement with MPCMCBAI, which produced the 2nd generation dendronized cellulose derivative, CMCBABA. This procedure is similar to that we used to prepare CMCBA but differs because we use BA instead of DMPDA to conduct the addition elimination reaction with a different activated ester, the 1st generation activated dendronized cellulose derivative MPCMCBAI. Similar to CMCBA, the corresponding 2nd dendronized CMCBABA is not soluble in water. The chemical structure of CMCBABA could not be easily characterized by using the solution NMR. Its FTIR spectrum showed strong ester peak at 1728 cm^{-1}, amide I at 1640 cm^{-1}, amide II at 1545 cm^{-1}, and strong hydrogen bond absorption at 3431 cm^{-1}(Figure 3.12). However, the ratio between the intensity of ester peak at

1728 cm^{-1} and hydrogen-bonding absorption at 3431 cm^{-1} is higher for CMCBABA than that for CMCBA. This was consistent with its chemical structure.

Scheme 3.6. Synthesis of CMCBABA

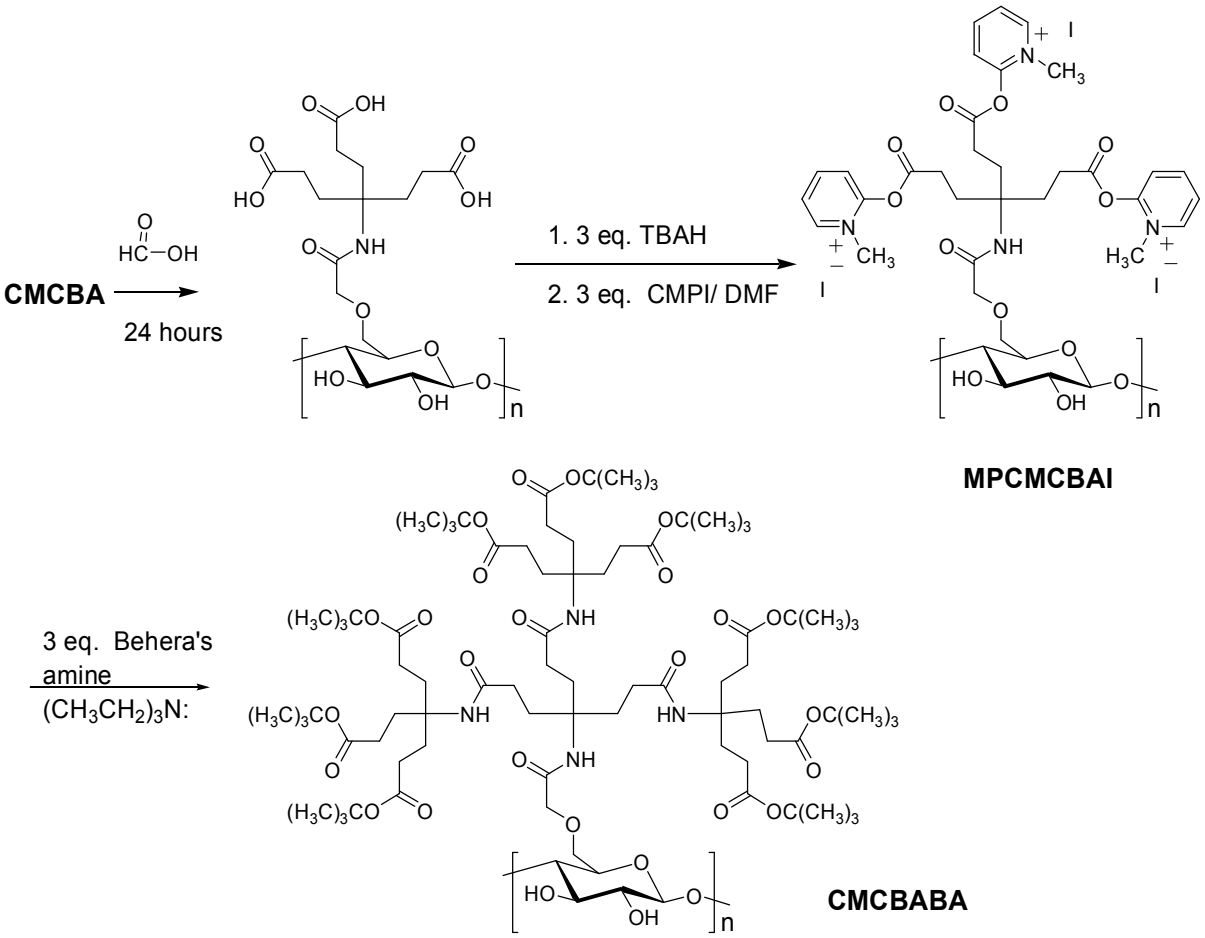

Similar to the characterization of DS of CMCBA, the extended DS of CMCBABA for the 2nd generation was also estimated by measuring the weight loss of CMCBABA decomposition of releasing isobutene by TGA technique. The derivative weight loss curve of CMCBABA showed one extended peak releasing isobutene compared to that of CMCBA (Figure 3.7). This indicated that CMCBABA has two layers of BA on its cellulose backbone. The weight loss derivative peak of BA in CMCBABA is apparently much bigger than that of cellulose backbone in CMCBA and it became the major weight loss in TGA spectra of CMCBABA. The weight loss of

CMCBABA from 196˚C to 275˚C was expressed in equation 3.3 and the extended DS of BA (DS_3) on the 2nd generation CMCBABA was calculated using equation 3.4, which is derived from equation 3.3.

Weight loss equation 3.3:

$$\text{Weight Loss} = \frac{9CH_2{=}C(CH_3)_2 \cdot DS_3 + 3CH_2{=}C(CH_3)_2 \cdot (DS_2\text{-}DS_3)}{C_6H_7O_3 + OH \cdot (3 - DS_1) + OCH_2COOH \cdot (DS_1 - DS_2) + OCH_2CO\text{-}NHC\{CH_2CH_2COOC(CH_3)_3\}_3 \cdot (DS_2\text{-}DS_3) + OCH_2CO\text{-}NH\{CH_2CH_2CONHC[CH_2CH_2COOC(CH_3)_3]_3 \cdot DS_3\}}$$

---------- Equation 3.3

DS calculation Equation 3.4:

$$DS_3 = \frac{WL*\{C_6H_7O_3+OH*(3\text{-}DS_1)+OCH_2COOH(DS_1\text{-}DS_2)^+OCH_2CONHC[CH_2CH_2COOC(CH_3)_3]_3\}*DS_2\text{-}3CH_2{=}C(CH_3)_2DS_2}{9CH_2{=}C(CH_3)_2 - 3CH_2{=}C(CH_3)_2 + WL*OCH_2CONHC[CH_2CH_2COOC(CH_3)_3]_3\text{-}WL*OCH_2CONHNHC\{CH_2CH_2CONHC[CH_2CH_2COOC(CH_3)_3]_3}$$

---------- Equation 3.4

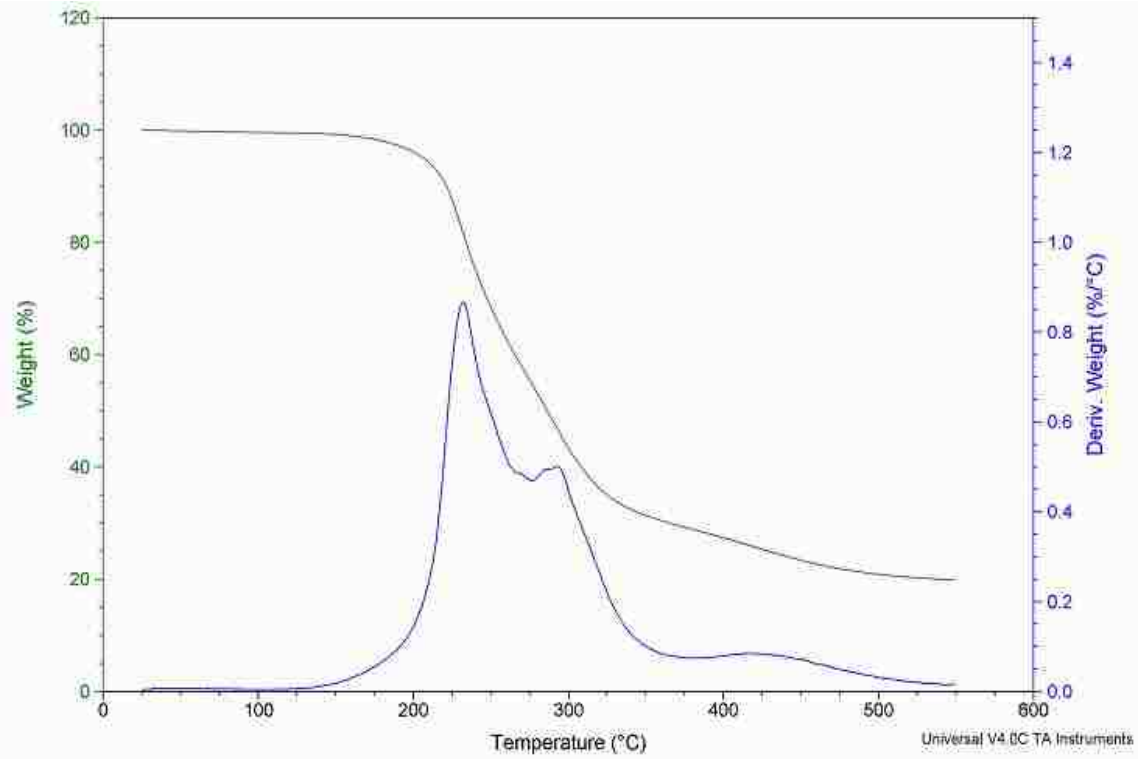

Figure 3.7. TGA of CMCBABA.

3.3.5 Synthesis of CMCBADMPDA

The elaboration reaction principle of CMCBADMPDA is similar to that in synthesizing CMCBABA but different in using DMPDA to conduct the nucleophilic addition-elimination reaction with the activated 1st generation dendronized cellulose ester MPCMCBAI (Scheme 3.7).

Scheme 3.7. Synthesis of CMCBADMPDA

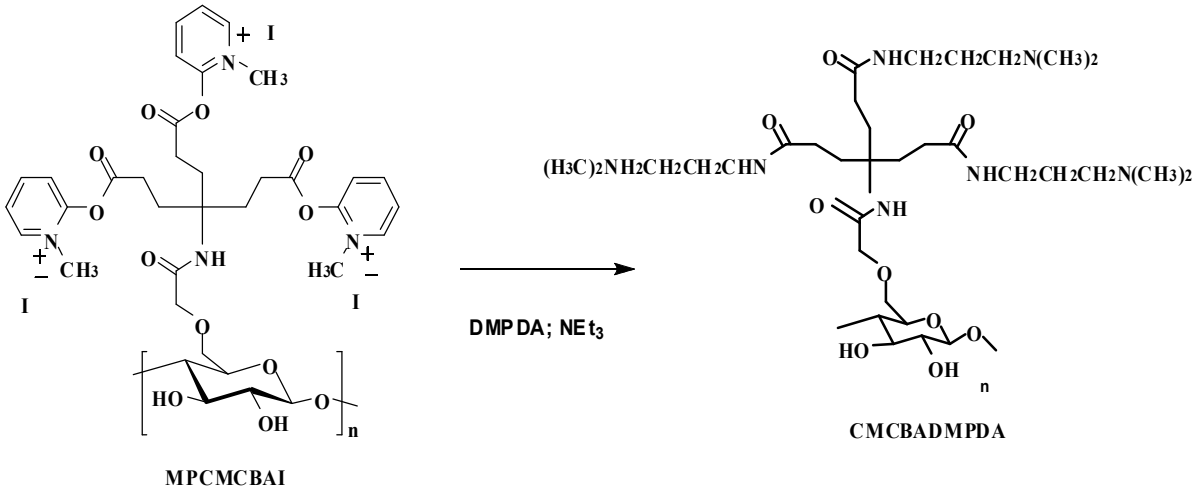

The conversion of the *tert*-butyl ester functions to the more hydrophilic aminoamide groups with *N*, *N*-dimethyl-1, and 3-propanediamine yielded a water-soluble derivative suitable for solution NMR characterization. Its ^{1}H NMR (Figure 3.8) and ^{13}C NMR spectra (Figure 3.9) were consistent with the proposed structure. The chemical shifts of amide carbon (171.46 ppm) in CMCBADMPDA are close to those corresponding chemical shifts of amide carbon (177.4 ppm) in 1-[[*N*-[3-(*tert*- butoxycarbonyl)- 1,1-bis[2-(*tert*-butoxycarbonyl)ethyl]propyl]amino]-arbonyl]adamantane made by Newkome et al. The extremely strong 44.19 [N (CH_3)$_2$] and 2.19 [N(CH_3)$_2$] ppm shifts associated with the strong 29.83 ($CH_2CH_2CH_2N$) and 1.44 ($CH_2CH_2CH_2N$) ppm shifts are assigned to the (*N*, *N*-dimethylamino)-propyl subtituent of CMCBADMPDA. The chemical shifts of protons on anhydroglucose rings (3.25-4.5) are broad and overlapping, but the strong resonances confirm the presence of the cellulose backbone. It was impossible to calculate

the degree of substitution based on such extensively overlapped proton NMR peaks of CMCBADMPDA. Table 3.4 showed the synthesis of several batches of CMCBADMPDA.

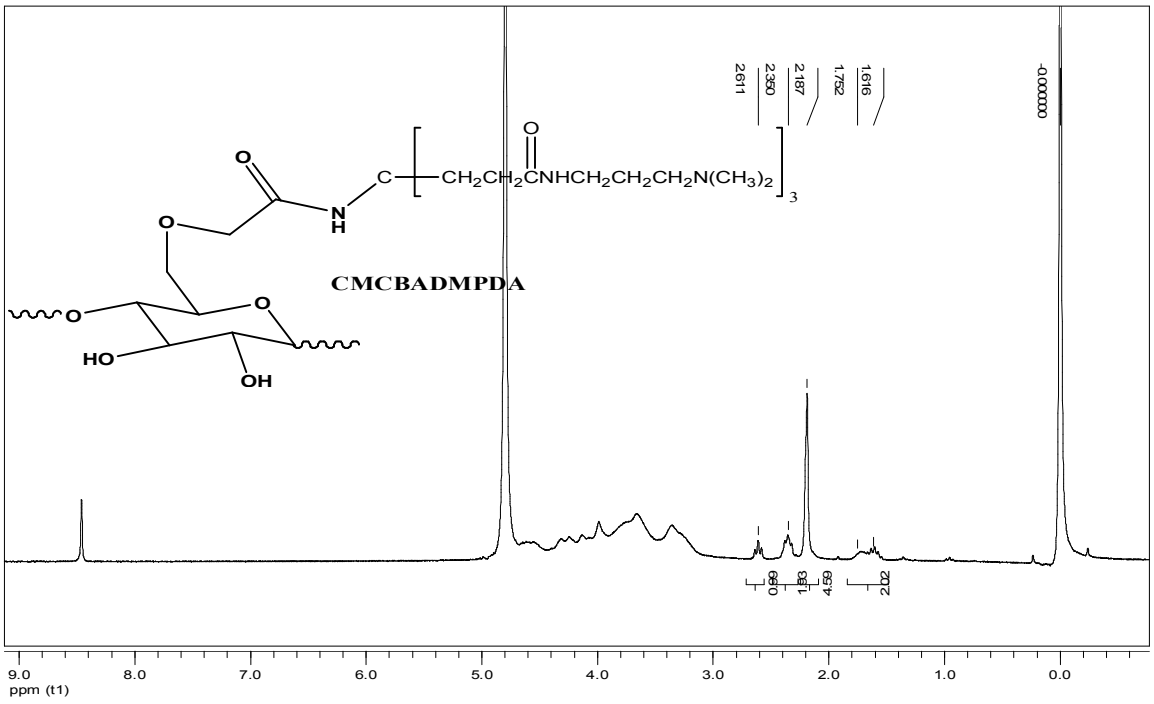

Figure 3.8. [1]H NMR Spectrum of CMCBADMPDA.

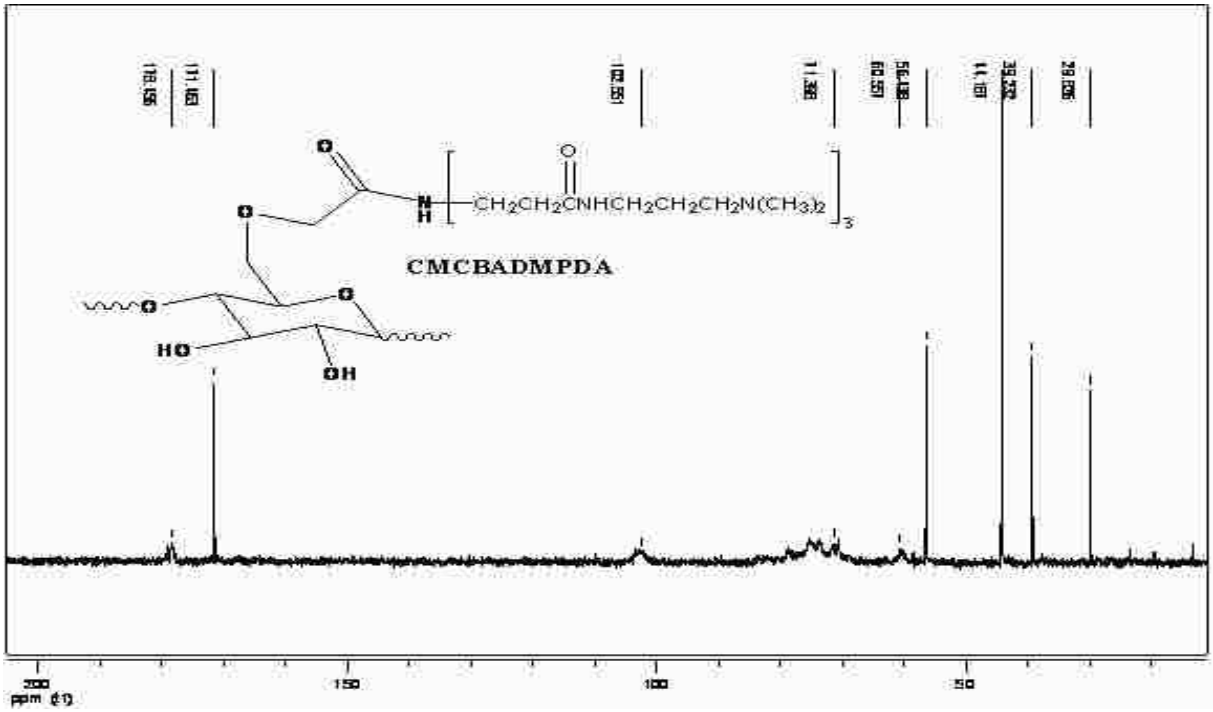

Figure 3.9. [13]C NMR Spectrum of CMCBADMPDA.

Table 3.4. Synthesis of CMCBADMPDA

CMCBA (g)	1.35	2.91	2.14	3.00	0.38
DS2 of CMCBA	0.40	0.67	0.78	0.67	0.48
Yield (g)	1.15	2.81	2.06	2.63	0.55
Yield (%)	84%	86%	86%	78%	130%
Source CMC (MW)	250k	250k	250k	700k	90k
Source CMC (DS)	0.7	0.9	1.2	0.9	0.7

3.3.6 Synthesis of CMCBABADMPDA

The synthesis of CMCBABADMPDA (Scheme 3.8) is also similar to that of CMCBADMPDA but using DMPDA to react with a different activated ester, the activated 2nd generation ester of CMC (MPCMCBABAI). The conversion of the tert-butyl ester groups of the 2nd generation CMCBABA to the more hydrophilic aminoamide groups with N,N-dimethyl-1,3-propanediamine yielded a water-soluble derivative with much better water solubility. ^{1}H NMR (Figure 3.10) and ^{13}C NMR spectra (Figure 3.11) were consistent with the proposed structure. The chemical shifts of amide carbon (180.5, 173.7 and 167.3 ppm) in CMCBABADMPDA corresponded to its three carbons of three amide groups. The extremely strong 46.74 [N(CH$_3$)$_2$] and 2.46 [N(CH_3)$_2$] ppm shifts are assigned to the (*N*,*N*-dimethylamino)-propyl subtituent of CMCBABADMPDA. The stronger chemical shifts around 1.89 of protons are associated with the CH_2CH$_2$ from the 2nd generation dendron. The broad 3.25-4.5 shifts of protons on anhydroglucose rings confirmed the presence of the cellulose backbone. It was also impossible to calculate the degree of substitution based on such extensively overlapped proton NMR peaks of CMCBABADMPDA.

Scheme 3.8. Synthesis of CMCBABADMPDA

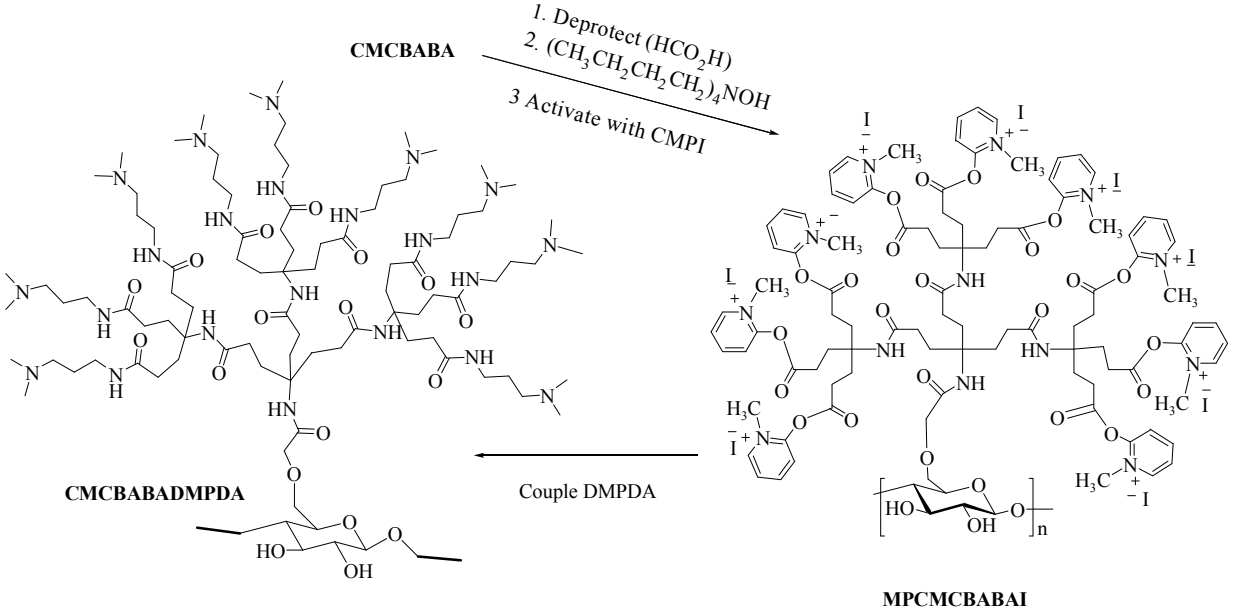

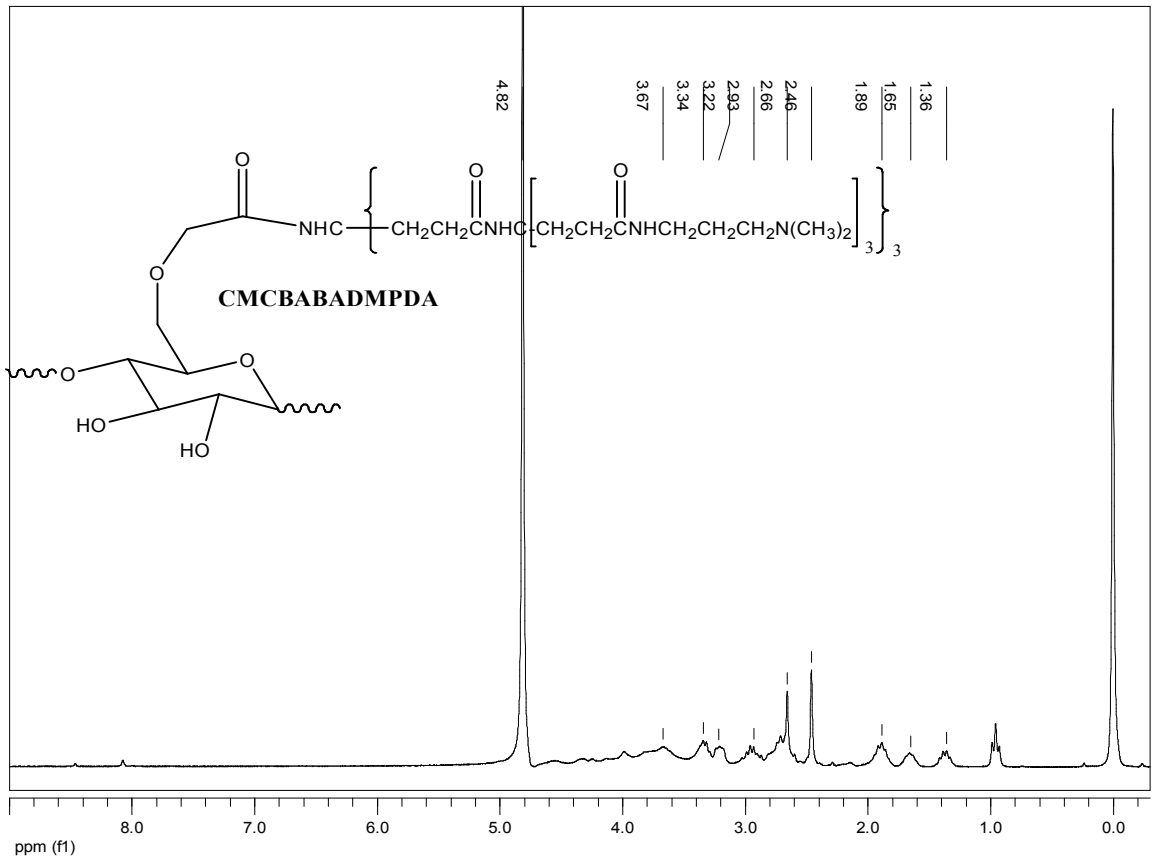

Figure 3.10. ^{1}H NMR Spectrum of CMCBABADMPDA.

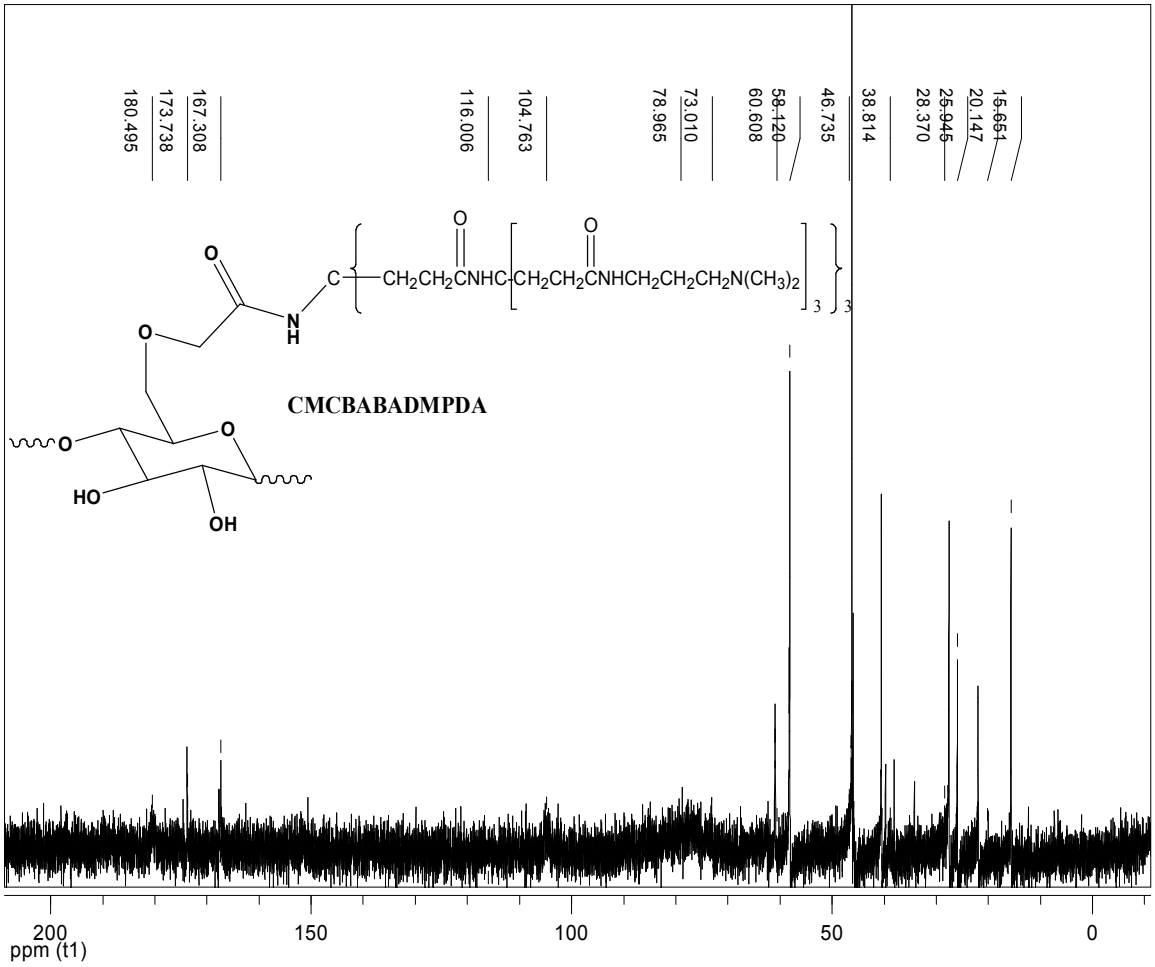

Figure 3.11. ^{13}C NMR Spectrum of CMCBABADMPDA by divergent approach.

3.3.7 FTIR Characterization of CMC, CMCBA, CMCBABA, CMCBADMPDA, and CMCBABADMPDA

Figure 3.12 showed the FTIR spectra of CMC, CMCBA, CMCBABA, CMCBADMPDA, and CMCBABADMPDA. CMC showed strong 1600 cm^{-1} of C=O of COONa. Both of CMCBA and CMCBABA showed strong 1728 cm^{-1} of C=O of ester, 1640 cm^{-1} of amide I, and 1546 cm^{-1} of amide II. CMCBADMPDA and CMCBABADMPDA both showed strong 1640 cm^{-1} of amide I and 1546 cm^{-1} of amide II. Neither of them demonstrated 1728 cm^{-1} of C=O of ester. Their FTIR spectra were also consistent with their proposed structure.

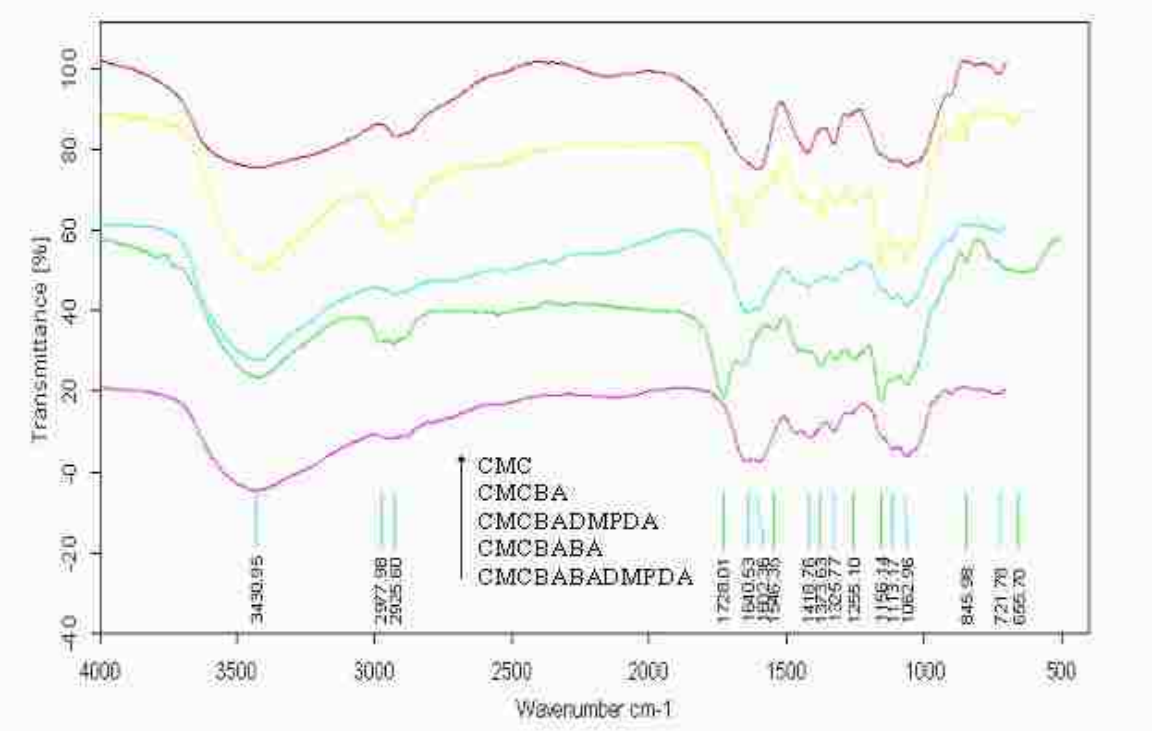

Figure 3.12. FTIR Spectrum of CMC, CMCBA, CMCBABA, CMCBADMPDA, and CMCBABADMPDA.

3.3.8 TGA Characterization of CMC, CMCBA, CMCBADMPDA, and CMCBABADMPDA

Figure 3.13 shows the weight loss curves of CMC, CMCBA, and CMCBABA and Figure 3.14 shows the weight loss curves of CMC, CMCBADMPDA, and CMCBABADMPDA. Their weigh loss at 100 ºC, residue at 100 ºC, and temperature of weight loss peak are listed in Table 3.5. CMC has one big weight loss from 259.22 ºC to 284.78ºC, which associated with the thermal decomposition of cellulose backbone of CMCBA. CMCBA has two major weight losses: one from 197.74 ºC to 209.77ºC, which corresponded with degradation of *tert*-butyl moieties releasing isobutene, and one from 236.25 ºC to 289.95ºC, which is related with degradation of cellulose backbone. The weight loss of CMCBABA consisted of one decomposition of cellulose backbone from 251.66 ºC to 315.02ºC and one broad range decomposition from 212.64 ºC to 242.46 ºC which is the result of the decomposition of two

layers of *tert*-butyl groups. Both CMCBADMPDA and CMCBABADMPDA showed one major weight loss temperature range; but temperature range for the major weight loss of CMCBABADMPDA is much broader. This agreed with that CMCBABADMPDA has one more layer dendritic structure than CMCBADMPDA.

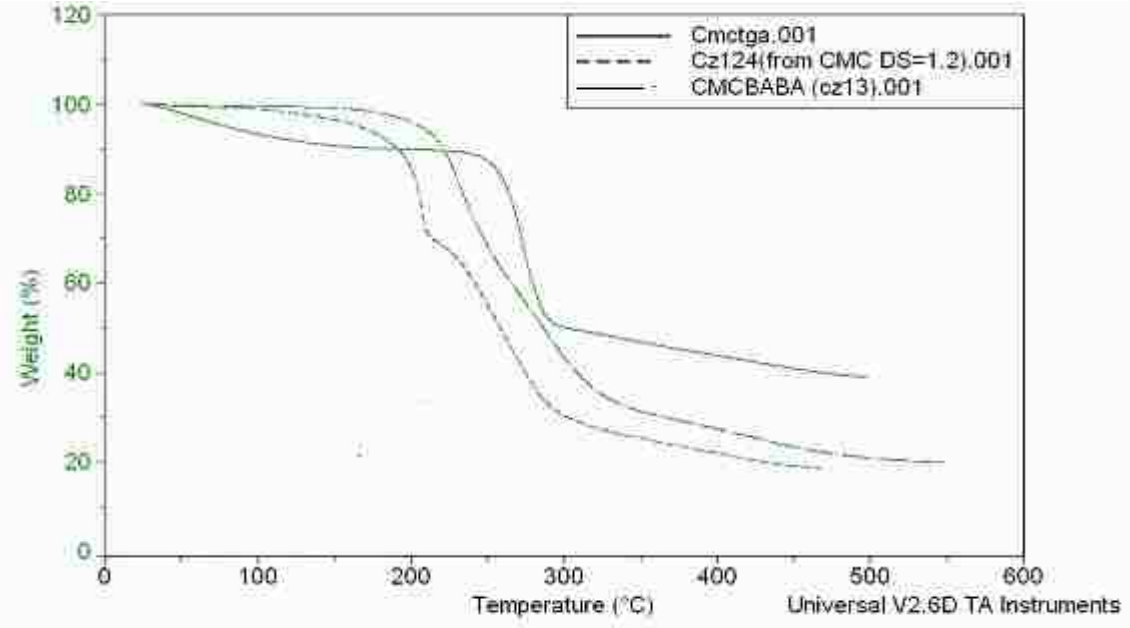

Figure 3.13. Thermo analysis plots of CMCBA and CMCBABA.

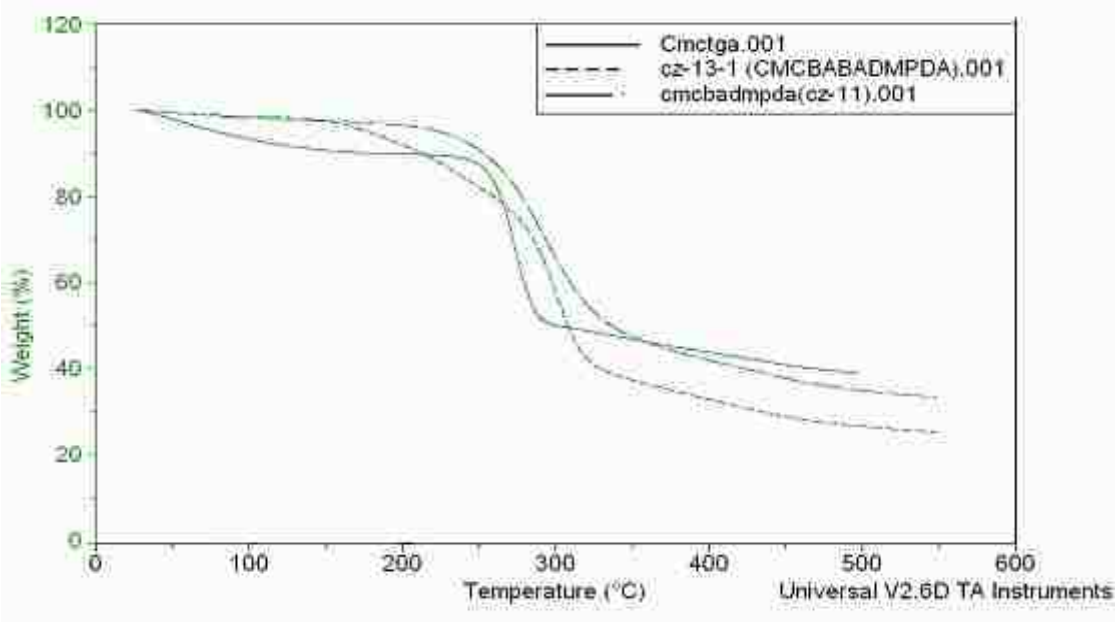

Figure 3.14. Thermo analysis plots of CMC, CMCBADMPDA, and CMCBABADMPDA.

Table 3.5. Weight loss, residue of CMC, CMCBA, CMCBABA, CMCBADMPDA, and CMCBABADMPDA

Samples	Weight loss RT-100ºC	Peak 1	Peak 2	Residue at 500ºC
CMC	6.60%	259.22-284.78ºC		39%
CMCBA	0.43%	197.74-209.77ºC	236.25-289.95ºC	17.77%
CMCBABA	0.43%	212.64-242.46ºC	251.66-315.02ºC	20.84%
CMCBADMPDA	1.7%	255.77-326.61ºC		34.92%
CMCBABADMPDA	1.70%	267.72-317.81ºC		26.54%

The weight loss RT-100ºC corresponded to the water absorption. CMCBA, and CMCBABA have lowest water adsorption of 0.43%; CMCBADMPDA, and CMCBABADMPDA have water adsorption of 1.70%, which is lower than 6.4% of CMC. The residues at 500ºC of CMCBA and CMCBABA are both smaller than that of CMCBADMPDA, CMCBABADMPDA, and CMC probably because the side chain dendron with t-butyl groups on CMCBA and CMCBABA could easily decompose.

3.3.9 Intrinsic Viscosity Characterization of CMCBADMPDA and CMCBABADMPDA

Introduction of a single generation dendron and 2nd generation dendron led to a significant reduction in the solution viscosity of their derivatives compared to that of CMC. The intrinsic viscosity of CMCBADMPDA, 0.39dL/g, is an order of magnitude less than that of CMC, 5.62dL/g. The intrinsic viscosity of CMCBABADMPDA, 0.66dL/g, is also close to one eighth of the intrinsic viscosity of CMC. All measurements were made in 0.1N NaCl to minimize any Donnan effects. Introduction of the dendrimer structure appears to lead to a collapse of the extended coil conformation normally exhibited by CMC.

In addition to the change in polarity and charge density, the dendritic structure increases the density by introducing multiple branching sites along the chain; however, the possibility that the cellulose backbone has degraded after being subjected to exposure to such a diverse collection of reagents must be considered. The impact of the CMC-Na activation steps was evaluated by converting it to the corresponding 3-(N,N-dimethylamino)propane carboxamide derivative (CMC-DMPDA). The intrinsic viscosity of this derivative was 3.5 dL/g, suggesting that backbone degradation accompanying NaCMC activation was minimal. The reduction in viscosity could be attributed to the replacement of ionic substituents with neutral aminoamide substituents.

The intrinsic viscosity is an important parameter for polymers with drug and drug delivery applications. Figure 3.15 shows the curves for measuring the intrinsic viscosity values of CMC, CMCDMPDA, CMCBADMPDA, and CMCBABADMPDA. Table 3.5 shows the intrinsic viscosity data of CMC, CMCDMPDA, CMCBADMPDA and CMCBABADMPDA. 0.1N NaCl was used as the solvent for all samples. The intrinsic viscosity of CMCBADMPDA and CMCBABADMPDA decreased significantly compared to those of CMC and CMCDMPDA. This is good for drug or drug delivery applications. The decreasing of intrinsic viscosity of CMCBADMPDA and CMCBABADMPDA compared to that of CMCDMPDA may result from two factors. One factor is that the dendronized cellulose may show a more compacted conformation compared with the cellulose without grafting. The other factor is that the cellulose backbone of CMCBADMPDA may degrade after repeated time consuming treatments using acid in its preparation process. CMC may show larger molecular size than CMCDMPDA, CMCBADMPDA and CMCBABADMPDA in aqueous state due to the negative charge on CMC molecules.

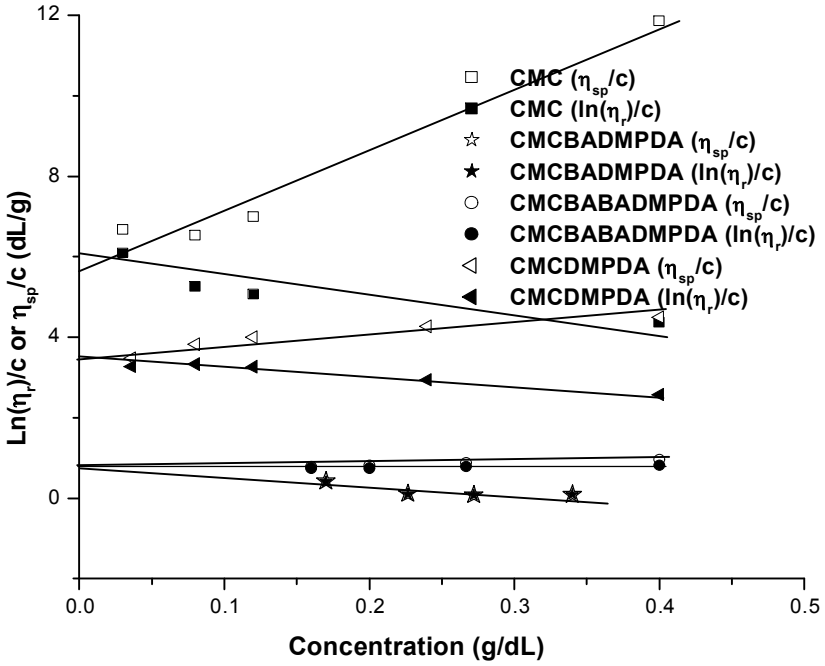

Figure 3.15. Intrinsic viscosity of CMCBABADMPDA and CMCBADMPDA.

Table 3.6. Intrinsic viscosity of CMC, CMCDMPDA, CMCBADMPDA

Polymer	CMC	CMCDMPDA	CMCBADMPDA	CMCBABADMPDA
Intrinsic viscosity(dL/g)	5.62	3.57	0.39	0.66

3.3.10 Molecular Weight and Molecular Size Characterization of CMC, CMCDMPDA, CMCBADMPDA, and CMCBABADMPDA by GPC-LS

The large reduction in the intrinsic viscosity of CMCBADMPDA could have resulted from the degradation of cellulose backbone during the deblocking of the tert-butyl esters in formic acid. The actual molecular weight of the derivative was determined using a GPC-LS system based on Zimm approach: $\frac{Kc}{R_\theta} = \frac{1}{Mw}(1 + \frac{q^2 R_g{}^2}{3}) + 2A_2 c$ where $K = \frac{4\pi^2 n^2 (dn/dc)^2}{\lambda_0{}^4 N_a}$ is the optical constant, q is the scattering vector, R_θ is the Rayleigh ratio, R_g is the radius of gyration of polymer molecules, A_2 is the 2nd virial coefficient, c is the concentration of polymer, n is the

solution refractive index, λ_0 is the wave number of laser light, and N_a is the Avogadro's number. The *dn/dc* of CMCBADMPDA was measured to be 0.1473 for red light at 632 nm based on $\Delta n = c \cdot \frac{dn}{dc}$, where Δn is the refractive index of polymer solution, in a diluted 0.4N ammonium acetate-0.01N NaOH solution.

Figure 3.16 showed both the laser scattering peaks as well as their corresponding DRI peaks. Table 3.6 confirmed that both the Mn and Mw molecular weights of CMCBADMPDA and CMCDMPDA decreased significantly compared to those of CMC due to acid treatment in its synthesis process. Further, the M_w/M_n or molecular weight distribution (MWD) of CMCBADMPDA decreased to 1.656 from 3.17, that of CMC. The narrowing of the MWD after our acid treatment suggests that either selective hydrolysis of the longer chains or fractionation of the sample during the multiple dissolution and precipitation steps required to complete the modification. Figure 3.17 showed the relationship between z-average RMS radius R_z and molecular weights in logarithmic scale measured by GPC-LS.

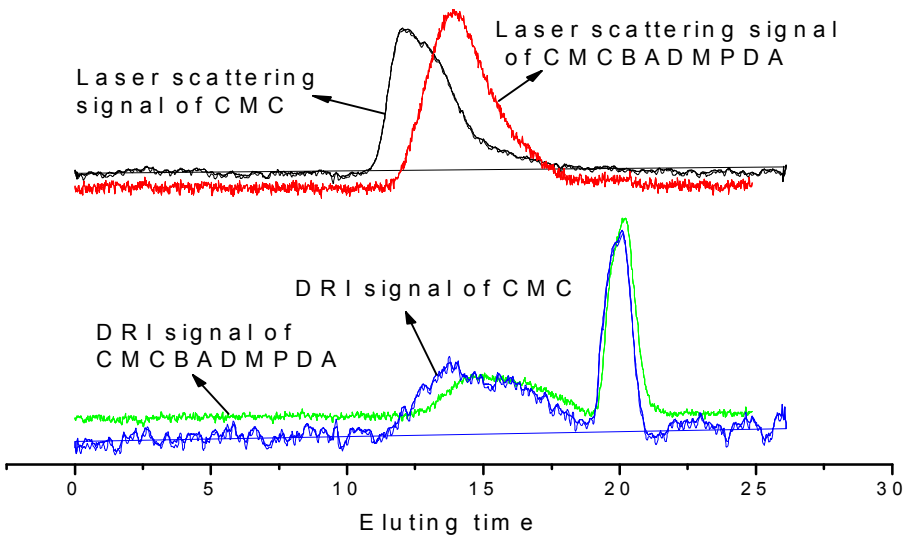

Figure 3.16. GPC-LS traces of CMC and CMCBADMPDA.

Table 3.7. The molecular size, molecular weight, and distribution of CMC, CMADMPDA, and CMCBADMPDA from GPC-LS

Polymer	Mn	Mw	Mz	MWD	DP	RMS R_n (nm)
CMC	72400	229500	542900	3.17	332.11	24.0
CMCDMPDA	61410	108000	189900	1.76	234.9	19
CMCBADMPDA	59130	97940	177400	1.656	109.64	17.4

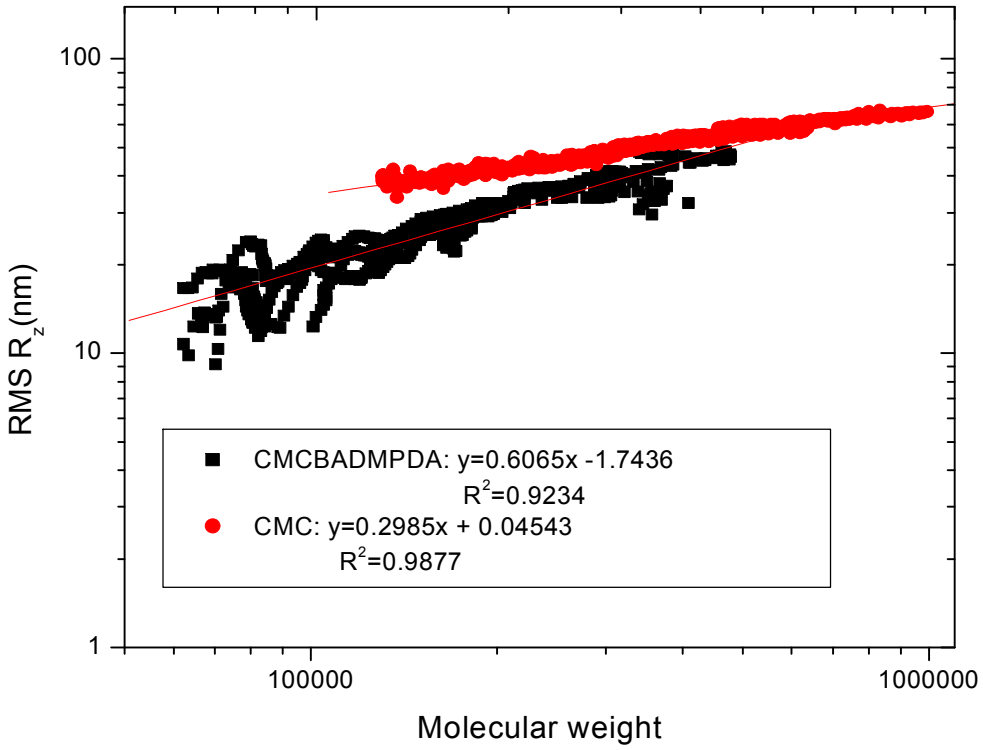

Figure 3.17. Relationship between RMS R_zs and molecular weights of CMCBADMPDA and CMC.

The slope for CMCBADMPDA was 0.6065, which was larger than 0.2985 for CMC. For polymers in solutions of good solvents, their radius of gyration (*Rg*) is proportional to $M^{0.6}$. This data suggests that CMC was not well dissolved in the aqueous solution and CMCBADMPDA

showed stiff conformation. Another factor, the compact conformation of the tris-aminoamide molecular structure, may also contribute to the higher power index of 0.6. Based on the linear fit curves in Figure 3.17, the RMS R_z of CMC molecules with M_W of 97,000 should be around 33.09 nm while that of CMCBADMPDA with the same M_W was around 19.8 nm. The CMCBADMPDA molecules show a more compact conformation compared with CMC molecules in aqueous solution.

3.4 Conclusions

(1) A side chain composed of both a hydrophobic BA and a hydrophilic DMPDA was elaborated to a CMC backbone, leading to 1st generation and 2nd generation aminoamide cellulose derivatives with a hydrophilic backbone and amphiphilic side chains. The chemical structures of the derivatives were confirmed by their FT-IR spectra and NMR spectra.

(2) The DS of CMC has important influence on the DS of CMCBA. The DS of CMCBA could be adjusted by controlling the relative concentration of CMPI. The DS of CMCBA could increase while increasing both the DS of CMC and the relative concentration of CMPI. The MW of CMC did not show significant influence on the DS of CMCBA.

(3) CMCBADMPDA and CMCBABADMPDA showed single weight loss peak which moved to higher temperature compared to that of CMC. CMCBA and CMCBABA have lowest water absorption of 0.43%; CMCBADMPDA, and CMCBABADMPDA have water absorption of 1.70%, which is lower than 6.4% of CMC.

(4) CMCBADMPDA and CMCBABADMPDA showed lower residue percentages at 500 ^oC than CMC but showed higher residue percentages at 500^oC than their corresponding CMCBA and CMCBABA.

(5) The d*n*/d*c* of CMCBADMPDA was measured to be 0.1473 at 632.8 nm.

(6) The weight average molecular weight of CMCBADMPDA was measured to be 97940 by GPC-LS while that of CMCDMPDA was 108000.

(7) The intrinsic viscosity of CMCBADMPDA and CMCBABADMPDA are 0.39 dL/g and 0.66 dL/g respectively, which are much smaller than the intrinsic viscosity (5.62 dL/g) of CMC and the intrinsic viscosity (0.66 dL/g) of CMCDMPDA.

(8) CMCBADMPDA and CMCBABADMPDA showed much lower intrinsic viscosity than CMCDMPDA due to their dendritic structure. CMCBADMPDA showed a more compacted conformation in aqueous solution than CMC.

CHAPTER 4. HYDROPHOBICITY/HYDROPHILICITY STUDY OF WATER SOLUBLE AMIDOAMINE DENDRONIZED CELLULOSE DERIVATIVES

4.1 Introduction

Many hydrophobic chemicals have been proved to be effective on some tough diseases; but they can not be used as efficient drugs because they can not be dissolved in human blood and can not be easily transferred to the target pathogen cells to kill the disease. For example, the anticancer drugs taxol, tamoxifen, and m-porphyrin have very low solubility in water.[86] Scheme 4.1 shows the molecular structure of taxol, tamoxifen, and m-porphyrin. Using overdose of the insoluble drugs brings serious side effects on human bodies. The water soluble CMCBADMPDA and CMCBABADMPDA have inner hydrophobic zones composed of CH_2 and amide groups. Numerous hydrophilic periphery amino groups are in the outer zones of their molecular conformations. Their inner hydrophobic zones are expected to be able to absorb hydrophobic molecules with active components. They are expected to be potential hydrophobic active component carriers.

Scheme 4.1. The molecular structure of several hydrophobic drugs

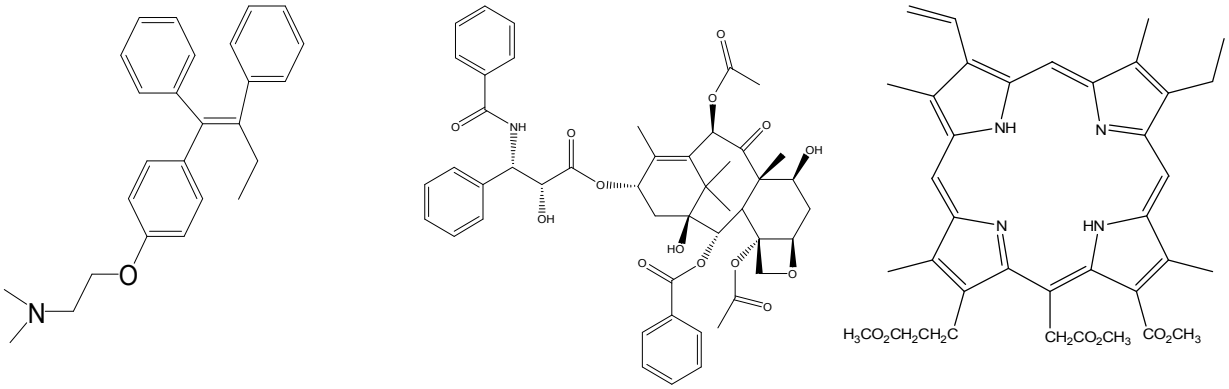

(a)Tamoxifen (b)Taxol (c) m-Porphyrin

The fluorescence of pyrene has been used to investigate the hydrophobicity of microenvironment by several research groups.[87-89] Pyrene is a colorless solid. Its fluorescence spectra in solution phase showed significant fine structure (vibronic bands). The fluorescence

spectra of dilute pyrene solution showed five dominant peaks (Figure 4.1) which corresponded to sixteen different vibration bands. The intensities of these five peaks in its spectra underwent significant perturbations in different solvents with different polarities due to complex solute-solvent dipole-dipole coupling.[90] Polar solvents significantly enhanced the intensity of peak 1. The ratio I_1/ I_3, where I_1 and I_3 are the intensities of peak 1 at 372 nm and peak 3 at 383 nm respectively, was very sensitive to the polarity variation of local environments. Pyrene has been used as the molecular probe to describe the hydrophobic domain in local microenvironments and has been used as a model compound to display the drug loading ability of drug carriers.

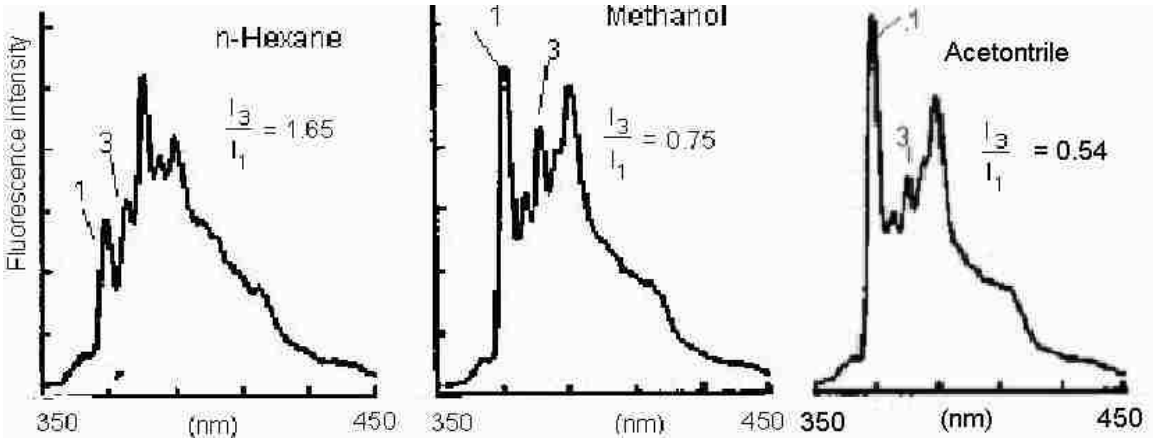

Figure 4.1. Solvent dependence of Vibronic band intensities in pyrene monomer fluorescence: [pyrene] = 2μM; λ_{excit} = 310nm.[90]

In Dr. Daly's group, M. A. Manuszak used the ratio of I_1/ I_3 to qualitatively describe the local hydrophobicity in a polyquaterium DQNNED solution.[91] More polar solvents often had higher values of I_1/ I_3. Lower value of I_1/ I_3 often indicated that more pyrene molecules were located in the hydrophobic domain of the media. In this project, pyrene molecules were used as molecular probes to study the local hydrophobicity/hydrophilicity properties of the inner layer of dendronized cellulose derivative molecules and to determine the local positioning of hydrophobic molecules in aqueous CMCBADMPDA solution and aqueous CMCBABADMPDA solution.[92]

4.2 Experimental

4.2.1 Solution Preparation

Pyrene was first dissolved in hexane to prepare its solution. Pyrene solution (2×10^{-4} g/L) was then injected into a small bottle. The solvent was evaporated at 50 ºC in a water bath. After that, an aqueous polymer solution with known concentration was injected into the bottle. The mixture was equilibrated in a water bath at 50 ºC overnight. All pyrene solutions were kept from light by aluminum foil.

4.2.2 Fluorescence Measurement

The fluorescence spectra of pyrene (2 μM) in the aqueous solution were recorded on a Perkin-Elmer luminescence spectrometer, model LS50B, while the sample was excited at 335 nm. Both the excitation bandwidth and emission bandwidth were 2.5 nm.

4.3 Results and Discussions

The fluorescence spectra of pyrene in different generations, different concentrations of dendronized cellulose derivatives, and different saline conditions were measured at 2 μM pyrene. Their ratios of I_{373}/I_{384} under the different conditions are listed in table 4.1.

4.3.1 The Hydrophobicity of CMCBADMPDA in Its Aqueous Solutions with Different Concentrations

The interaction of pyrene with two different concentrations (0.125% and 0.2%) of CMCBADMPDA was evaluated in 0.1 N NaCl solutions (Figure 4.2 and Table 4.1). An average I_{373}/I_{384} ratio of 1.77 was observed. This ratio was slightly lower than that of pyrene in water. Pyrene in the dendronized cellulose solution remained in a hydrophilic environment. The first

generation dendrimer did not introduce a hydrophobic microenvironment large enough to hold pyrene molecules.

Table 4.1. The ratio of I_{373}/I_{384} of pyrene (2μM) in aqueous solutions

Media	Dendrimer Concentration (g/l)	NaCl (N)	I_{373}/I_{384}
H_2O			1.85
H_2O		0.1N	1.85
CMCBADMPDA	1.25		1.77
CMCBADMPDA	1.25	0.1N	1.77
CMCBADMPDA	2.0		1.75
CMCBADMPDA	2.0	0.1N	1.77
CMCBABADMPDA	0.5		1.80
CMCBABADMPDA	0.5	0.1N	1.80
CMCBABADMPDA	5.0		1.63
CMCBADMPDA	5.0	0.1N	1.62

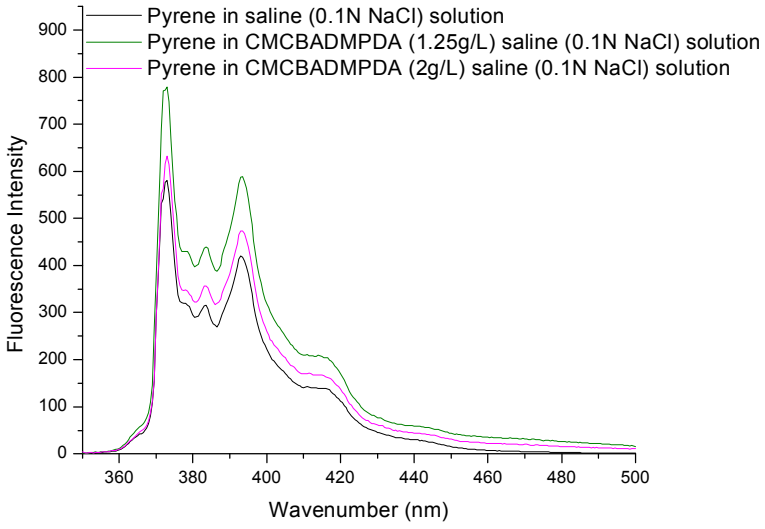

Figure 4.2. Fluorescence emission of pyrene in different concentration of CMCBADMPDA.

4.3.2 The Hydrophobicity of CMCBABADMPDA in Its Aqueous Solutions with Different Concentrations

The interaction of pyrene with two different concentrations (0.05% and 0.5%) of CMCBABADMPDA was evaluated in 0.1 N NaCl solutions (Figure 4.3 and Table 4.1). The I_{373}/I_{384} ratio of pyrene was 1.8 in 0.05% CMCBABADMPDA aqueous solution, which was close to that of pyrene in water. However, the I_{373}/I_{384} ratio of pyrene was 1.62 in 0.5% CMCBABADMPDA solution, which is slightly lower than that of pyrene in water. This indicated that most pyrene molecules stayed outside the molecules of CMCBABADMPDA in a low concentration aqueous CMCBABADMPDA solution; but more pyrene molecules could stayed inside hydrophobic zones of CMCBABADMPDA at a higher CMCBABADMPDA aqueous concentration. This was the feature of unimolecular micelles. CMCBABADMPDA showed a slight hydrophobic microenvironment and its molecules could carry hydrophobic molecules in its aqueous solution.

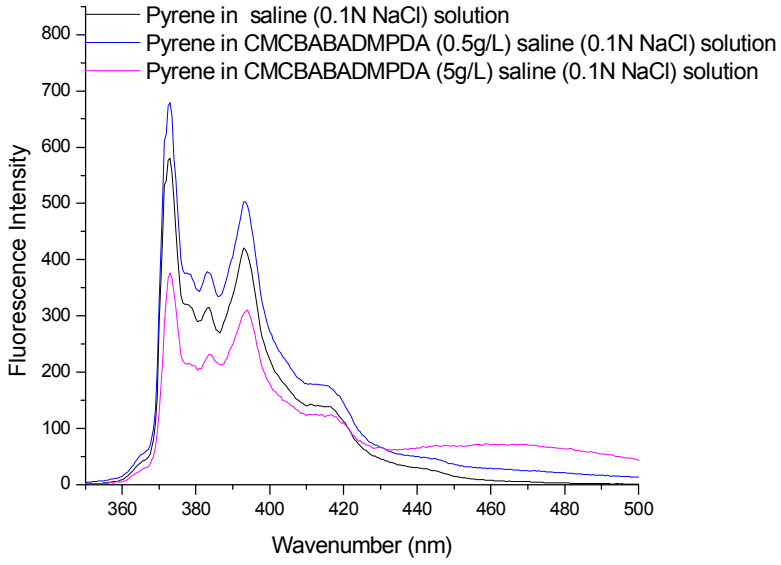

Figure 4.3. Fluorescence emission of pyrene in different concentration of CMCBABADMPDA.

4.3.3 Effect of Saline Condition on the Hydrophobicity of the Microenviroments in Aqueous CMCBADMPDA and CMCBABADMPDA Solution

Figure 4.4 and Figure 4.5 shows the fluorescence emission spectra of pyrene in both CMCBADMPDA and CMCBABADMPDA. Both of the two figures shows that 0.1 N NaCl could change the fluorescence emission intensity of pyrene dramatically; but table 4.1 showed that the I_{373}/I_{384} ratio changed little in both of CMCBADMPDA and CMCBABADMPDA under both 0.1N NaCl and nonsaline conditions. The hydrophobicity of the microenvironment of aqueous dendronized cellulose solution did not change due to the change in the saline condition.

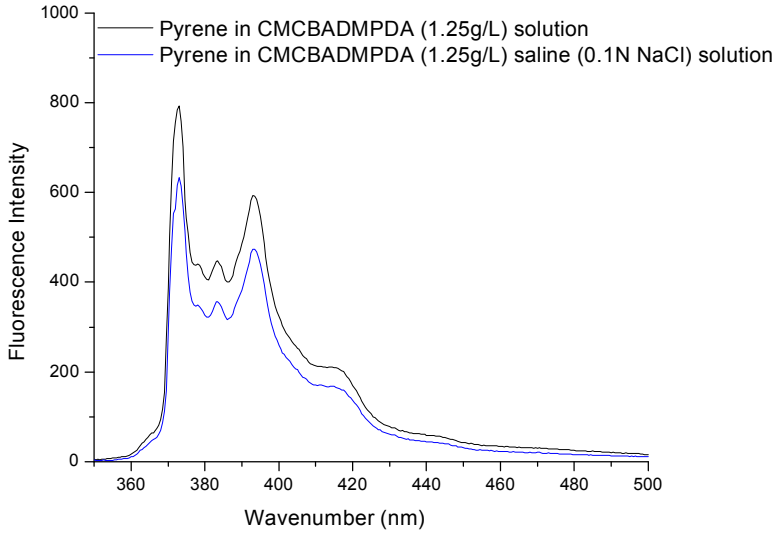

Figure 4.4. Influence of saline condition on fluorescence emission of pyrene in aqueous CMCBADMPDA solution.

4.4 Conclusions

(1) I_1/ I_3 of pyrene in both CMCBADMPDA and CMCBABADMPDA solutions with 0.1 N NaCl did not change compared to that of their corresponding solutions in pure water. Saline did not have a significant influence on the hydrophobicity of the microenvironment in neither of the two dendronized derivatives.

(2) I_1/ I_3 of pyrene of CMCBADMPDA did not change significantly compared to that in pure water. CMCBADMPDA showed a very hydrophilic microenvironment in its aqueous solution.

(3) CMCBABADMPDA showed a more expressive hydrophobic microenvironment than CMCBADMPDA. CMCBABADMPDA may carry more pyrene molecules than CMCBADMPDA.

(4) A higher concentration of CMCBABADMPDA solution showed lower I_1/ I_3 of pyrene and more hydrophobic microenvironment. It could carry more hydrophobic molecules than the CMCBABADMPDA solution with a lower concentration.

(5) The saline condition could dramatically change the fluorescence intensity of pyrene in both CMCBADMPDA and CMCBABADMPDA solutions. However, it changed little in the I_1/ I_3 of pyrene in these solutions.

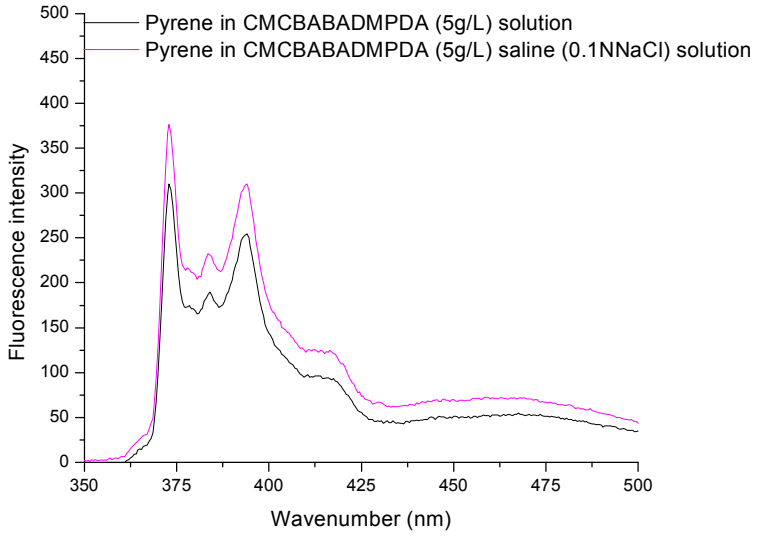

Figure 4.5. Influence of saline condition on fluorescence emission of pyrene in aqueous CMCBABADMPDA solution.

CHAPTER 5. SYNTHESIS OF DENDRONIZED CELLULOSE DERIVATIVES WITH QUATERNARY AMMONIUM FUNCTIONAL GROUPS

5.1 Introduction

As I mentioned in chapter one, small organic molecules with quaternary nitrogen such as cetyl trimethylammonium chloride, dicetyl dimethylammonium chloride *etc.* have been used as disinfectants and cleaning agents in personal care[93] and agriculture biocides. They are normally synthesized through the nucleophilic substitution of tertiary amine with alkyl halide. In Dr. Daly's group, iodomethane has been frequently used to conduct methylation reaction with tertiary amino groups of several polysaccharide derivatives to prepare their corresponding quaternary ammonium salts. D. A. Culberson obtained quaternary ammonium salt of cellulose with low DS by using aminoamide cellulosics which directly reacted with iodomethane at room temperature.[5] D. Logan prepared monoquat alkyl carbomoyl chitosan by directly substituting iodomethane with aminoalkyl carbamoyl chitosan at room temperature.[27]

Two methods have been used to elaborate hydrophilic quaternary nitrogen onto cellulose or chitosan derivatives by using quat-188 in Dr. Daly's group. (Scheme 5.1) One method is to use 2,3-epoxypropyltrimethylammoniumchloride, an epoxidized quat188. The other is to use quat-188, 65% aqueous solution of 3-chloro-2-hydroxypropyl trimethyl chloride, as quaternizing agent to react with aminoamide cellusics or chitosan, where the epoxidized quat188 is believed to be formed in-situ upon the addition of NaOH. D. A. Culbserson prepared hydrophilic diquaternary ammonium salt of cellulose by using both of the two options elaborated above. D. Logan and M. R. Thatte used the amine groups of chitosan derivatives to react with quat-188. They obtained water soluble quaternary ammonium chitosan derivatives with different hydrophobicity and that with different anion function groups. Some of their quaternary

ammonium chitosan derivatives have been found to exhibit good antimicrobial properties toward E. coli and S. aureus.

Scheme 5.1. Synthesis of quaternary ammonium polysaccharide derivatives by D. A. Culbserson, D. Logan, and M. R. Thatte [5, 27, 28]

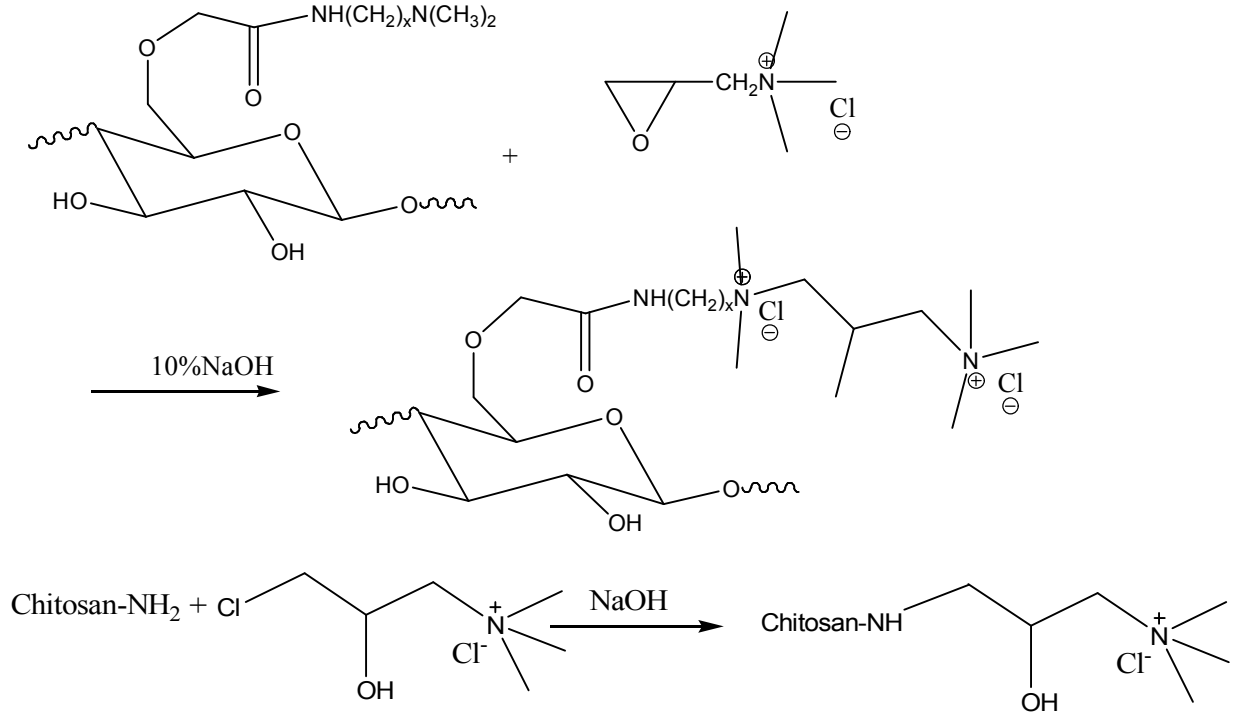

It is well known that quaternized nitrogen groups was able to endow polymer derivatives with certain antibacterial properties.[28, 46, 94] Low molecular weight dendrimeric quats (Scheme 5.2) are recently demonstrating excellent antibiotic properties in S. L. Cooper's group.[45]

As I proposed in chapter one, concentrated quaternary nitrogen atoms in one dendronized polymer molecule have the potential to endow the dendronized polymer with more potent antibacterial properties and to provide an alternative affordable route for synthesizing novel materials that carry many functional groups in one molecule rather than using expensive spherical dendrimers. The cylinder-like structure of dendronized cellulose derivative may have a different mechanism in the interaction with bio-cells from that of spherical dendrimers.

Scheme 5.2. The quaternary ammonium dendrimer developed by Stuart L. Cooper[45]

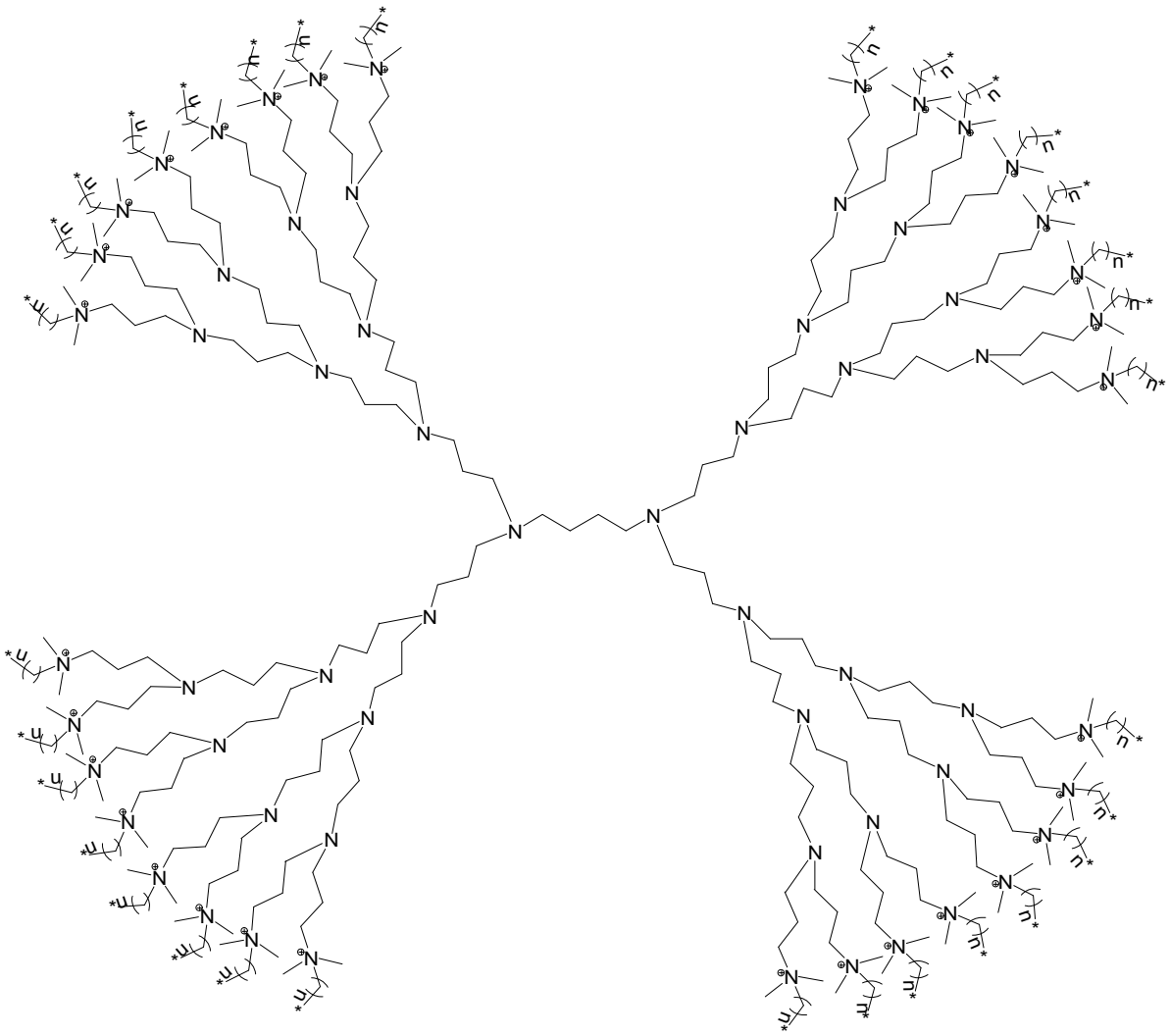

We propose to elaborate quaternary nitrogen onto the tip of BA dendrons of the dendronized cellulose derivatives which can form a comb copolymer with very dense concentrations of quaternary nitrogen groups in local microenvironment in an aqueous media. (Scheme 1.15 and Scheme 1.16) This should give the copolymer certain water solubility and form molecules of quaternary nitrogen cation clusters. I expect that high dense concentrations of quaternary nitrogen microenvironment can be formed even in extremely diluted solutions of the modified dendronized cellulose derivatives with a natural polymer backbone. The dendronized cellulose

derivatives with quaternary nitrogen tips are expected to have potential qualities that enable them to act as polymeric drug candidates for some tough diseases and also as antimicrobial coating for medical devices and public facilities.

In this chapter, we propose to synthesize dendronized cellulose derivatives with hydrophilic diquaternary nitrogen functional groups that can be prepared by using quat-188 (CMCBADMPDA-Quat188) and that with monoquaternary nitrogen with hydrophobic alkyl chains prepared by using alkyl halide. Since the chain length of alkyl substituents on quaternary nitrogen has been reported to have significant influence on the antimicrobial properties of their quaternary ammonium salt, I also proposed to synthesize quaternary ammonium dendronized cellulose derivatives with different chain lengths on their quaternary nitrogen (CMCBADMPDA-R). Their representative molecular structures are shown in Scheme 5.3. Their antimicrobial performances will be evaluated in chapter 6. The derivatives of CMCBADMPDA-R with different carbon chain length of one, four, six, eight, ten, twelve, and eighteen were abbreviated as CMCBADMPDA-C1, CMCBADMPDA-C4, CMCBADMPDA-C6, CMCBADMPDA-C8, CMCBADMPDA-C10, CMCBADMPDA-C12, and CMCBADMPDA-C18 respectively.

In the antibacterial property test, we discovered that CMCBADMPDA-C10 had higher antimicrobial activity than CMCBADMPDA-R with other chain lengths. Because the DS of the functional groups is an essential structure parameter of polymer in determining its properties and applications, the control of extended DS of alkyl chain length of ten on CMCBADMPDA-C10 (extended DS of C10) was explored by adjusting the relative concentration of decylbromide in the reaction system. CMCBADMPDA-C10s with high extended DS of C10 were found water insoluble; they were proposed to be modified by using propylene oxide and quat-188 to improve

their water solubility. The new derivatives, CMCBADMPDA-C10 modified with propylene oxide (CMCBADMPDA-C10-PO) and CMCBADMPDA-C10 modified with quat-188(CMCBADMPDA-C10-quat188) (Scheme 5.4), were found to exhibit excellent water solubility.

Scheme 5.3. The water soluble dendrimerized cellulose derivatives with quaterary nitrogen tips on their side chains for potential drug

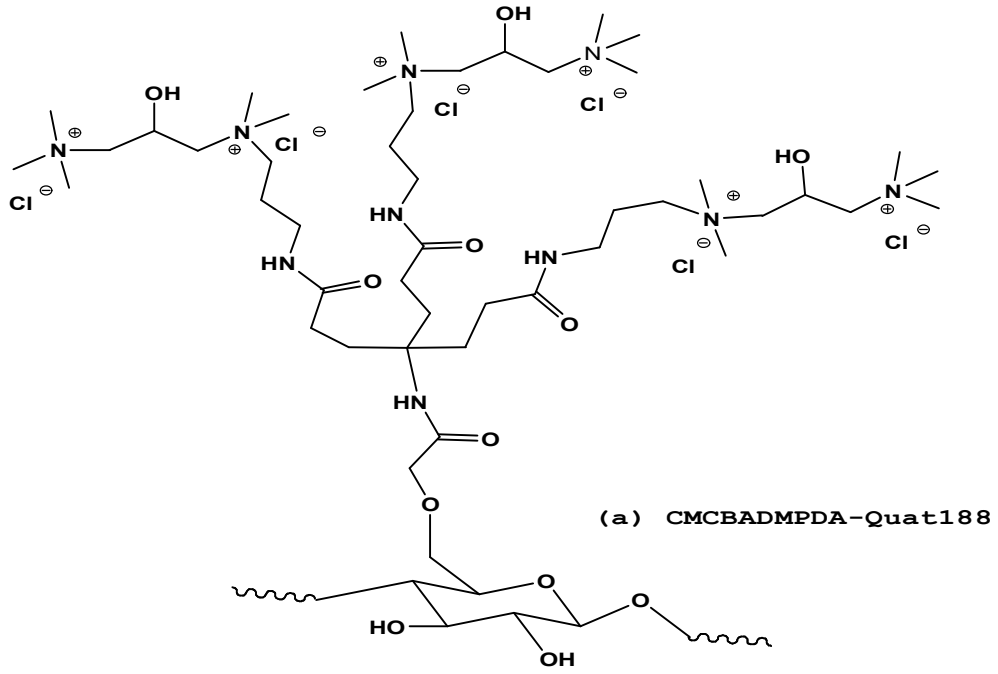

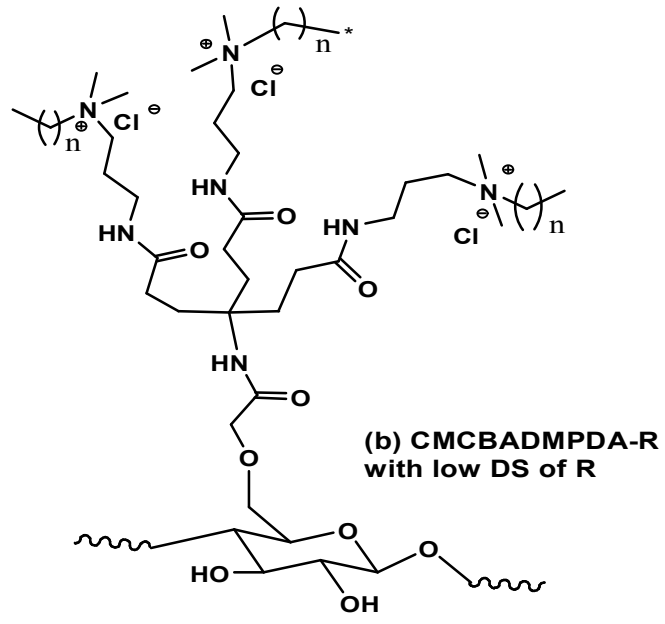

Scheme 5.4. The water soluble dendrimerized cellulose derivatives with high DS of C10

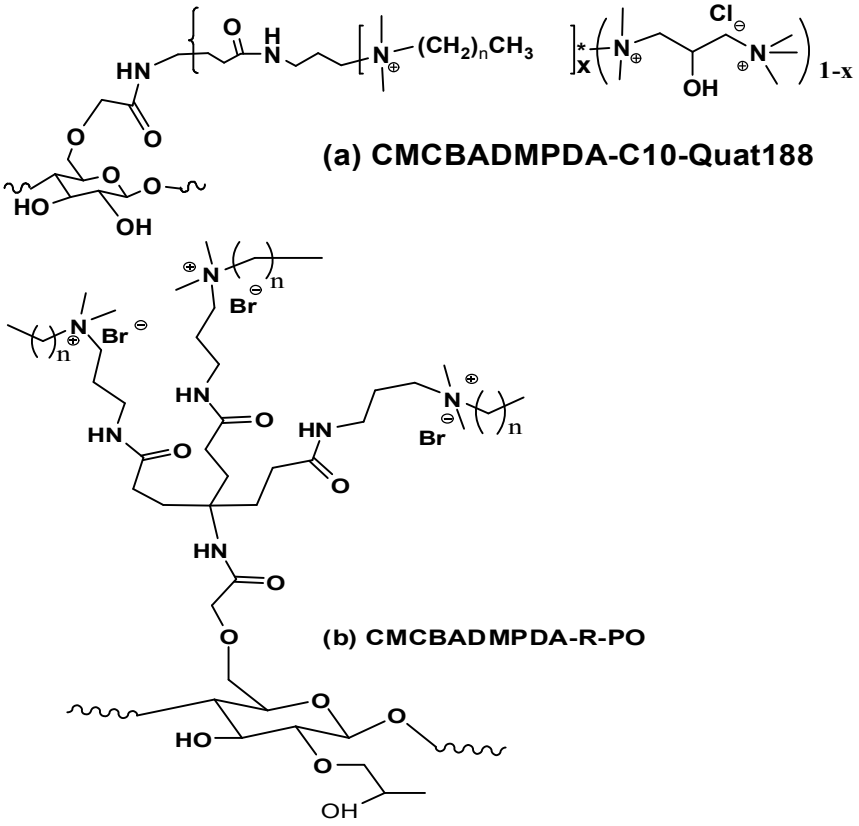

5.2 Experimental

5.2.1 Synthesis of CMCDMPDA-Quat188

CMCDMPDA-Quat188 was synthesized by following the procedure published in D. A. Culberson's dissertation[5] for comparison with CMCBADMPDA-Quat188.

5.2.2 Synthesis of CMCBADMPDA-Quat188

CMCBADMPDA (0.19 g, 0.31 mmol) in water (5 mL) mixed with a 65% aqueous Quat-188 (1mL, 5.3 mmol). Sodium hydroxide (0.75 g, 18.8 mmol) was added. The mixture was kept at 50 °C under stirring for 2 hours and then was dialyzed against water for one week. After dialysis, the solution was freeze dried in a vacuum. CMCBADMPDA-Quat188 (0.16 g, 0.155

mmol, yield: 50%) was obtained. ^{1}H NMR (250MHz, D_2O, 60 ºC) (Figure 5.1): δ (ppm) 3.24 and 3.26($^{+}$N(CH_3)$_3$), 2.14 (CCH_2CH$_2$), 1.95 (CH$_2$CH_2CH$_2$), 2.72 (CCH$_2$CH_2), 3.3-5.0 (HOCHCH_2N^{+}, $^{+}$NHCH$_2$CHOH, CH_2^{+}NH, broad peaks of anhydroglucose ring). ^{13}C NMR (62.9MHz, D_2O) (Figure 5.2): 54.60 (CH$_2$*C*HOHCH$_2$CH), 56.76 [$^{+}$N(*C*H$_3$)$_2$, $^{+}$N(*C*H$_3$)$_3$], 64.62 [*C*H$_2$N^{+}(CH$_3$)$_2$], 25.00 (CH$_2$*C*H$_2$CH$_2$), 16.00 (C*C*H$_2$CH$_2$), 31.82 (CH$_2$*C*H$_2$CO), 38.71 (CONH*C*H$_2$CH$_2$), 66.32 [CH$_2$CH$_2$*C*H$_2^{+}$N(CH$_3$)$_2$], 68.24 [CH$_2^{+}$N(CH$_3$)$_2$*C*H$_2$CHOH], 70.07 [CHOH*C*H$_2^{+}$N(*C*H$_3$)$_3$], 180.04(*C*ONH), 104.77(C1), (60-80)(C2~C6), 83.40(C7), 185.80(C8).

5.2.3 Synthesis of CMCBADMPDA-C1

CMCBADMPDA (0.07 g, 0.11 mmol) was dissolved in water (1 mL). Ethanol (1 mL) and iodomethane (1 mL; 2.28 g, 16 mmol) was added. Stirring was continued for 2 hours. Then, the mixture was dried in a vacuum. CMCBADMPDA-Quat-N (0.08 g, 0.085 mmol, yield 77%) was obtained. ^{1}H NMR (250MHz, D_2O): δ (ppm) 3.26($^{+}$N(CH_3)$_3$), 3.24(CH_2N^{+}), 1.95(CH$_2$CH_2CH$_2$), 2.72(CONHCH_2), 2.14(C*C*H$_2$C*H*$_2$), 3.25-4.5 (broad peaks of anhydroglucose ring); ^{13}C NMR (62.9MHz, D_2O) (Figure 5.3): 53.64 [$^{+}$N(*C*H$_3$)$_3$], 61.92 [*C*H$_2$N^{+}(CH$_3$)$_2$], 24.5(C*C*H$_2$CH$_2$), 28.79 (CH$_2$*C*H$_2$CH$_2$), 34.42 (*C*H$_2$CONH), 37.25 (CONH*C*H$_2$), 175.99(CH$_2$CH$_2$*C*ONH), 102.70(C1), (65-80)(C2~C5, C7), 60.63(C6).

5.2.4 Synthesis of CMCBADMPDA-R

Six CMCBADMPDA (0.20 g; 0.33 mmol) samples were dissolved in six small flasks each containing DMSO (5 mL) separately. Each solution was diluted with tetrahydrofuran (THF, 2 mL) and an excess of alkyl bromide (10.2 mmol) was added, i. e. 1-C_4H_9Br, 1-C_6H_{13}Br, 1-C_8H_{17}Br, 1-$C_{10}H_{23}$Br, 1-$C_{12}H_{25}$Br, and 1-$C_{18}H_{37}$Br. The reactions were kept at 25 ^{o}C for 24 hours. The mixtures were dialyzed against distilled water for one week. The solutions retained

by the membrane were first lyophilized and then the residues were dried in the *vacuo* at 100°C overnight. White solid products were obtained. For CMCBADMPDA-C18, the crude water layer needed to be extracted with chloroform (20 mL) three times to remove the excess alkyl halide and then was dried in *vacuo* at 100°C overnight. CMCBADMPDA-C4 ^{1}H NMR (250MHz, D_2O) (Figure 5.4): δ (ppm) 2.76 [$^+$N(CH_3)$_3$], 2.96 (CH_2N$^+$), 0.82 (CH_2CH_3), 1.23 (CH_2CH$_3$), 1.53 (CH_2CH$_2$CH$_3$), 1.86($CH_2CH_2CH_2$), 2.56(CONHCH_2), 2.10(CCH_2CH$_2$), 2.02(CCH_2CH_2), 3.25-4.5 (broad peaks of anhydroglucose ring); CMCBADMPDA-C6 ^{1}H NMR (250MHz, D_2O) (Figure 5.4): δ (ppm) 2.76 [$^+$N(CH_3)$_3$], 2.97(CH_2N$^+$CH_2), 0.82 (CH_2CH_3), 1.20 [(CH_2)$_4$CH$_3$], 1.63 ($CH_2CH_2CH_2$), 2.60 (CONHCH_2), 2.00 (CCH_2CH$_2$), 1.95 (CCH_2CH_2), 3.25-4.5 (broad peaks of anhydroglucose ring); CMCBADMPDA-C8 ^{1}H NMR (250MHz, D_2O) (Figure 5.4): δ (ppm) 2.78 [$^+$N(CH_3)$_3$], 3,24 (CH_2N$^+$CH_2), 0.80(CH_2CH_3), 1.20-1.33[(CH_2)$_6$CH$_3$], 1.73 ($CH_2CH_2CH_2$), 2.60 (CONHCH_2), 2.00(CCH_2CH$_2$), 1.95 (CCH_2CH_2), 3.25-4.5 (broad peaks of anhydroglucose ring); CMCBADMPDA-C10 ^{1}H NMR (250MHz, D_2O) (Figure 5.4): δ (ppm) 2.80 [$^+$N(CH_3)$_3$], 2.96 (CH_2N$^+$CH_2), 0.80 (CH_2CH_3), 1.10-1.30 [(CH_2)$_8$CH$_3$], 1.73 ($CH_2CH_2CH_2$), 2.60(CONHCH_2), 2.00 (CCH_2CH$_2$), 1.95 (CCH_2CH_2), 3.25-4.5 (broad peaks of anhydroglucose ring); CMCBADMPDA-C12 ^{1}H NMR (250MHz, D_2O) (Figure 5.4): δ (ppm) 2.78 [$^+$N(CH_3)$_3$], 3.22 (CH_2N$^+$CH_2), 0.78 (CH_2CH_3), 1.10-1.40 [(CH_2)$_{10}$CH$_3$], 1.73 ($CH_2CH_2CH_2$), 2.60 (CONHCH_2), 2.00 (CCH_2CH$_2$), 1.86 (CCH_2CH_2), 3.25-4.5 (broad peaks of anhydroglucose ring); CMCBADMPDA-C18 ^{1}H NMR (250MHz, D_2O): δ (ppm) 2.76 ($^+$N(CH_3)$_3$), 2.96 (CH_2N$^+$CH_2), 0.78 (CH_2CH_3), 1.10-1.40 [(CH_2)$_{10}$CH$_3$], 1.73 ($CH_2CH_2CH_2$), 2.60 (CONHCH_2), 2.00 (CCH_2CH$_2$), 1.85 (CCH_2CH_2), 3.25-4.5 (broad peaks of anhydroglucose ring).

5.2.5 Synthesis of CMCDMPDA-R

The quanternary un-dendronized cellulose derivatives with corresponding alkyl chains on monoquanternary nitrogen derivatives (CMCDMPDA-R) were synthesized for the purpose to compare their antimicrobial activities with the corresponding CMCBADMPDA-R. The derivatives of CMCDMPDA-R with different carbon chain length of one, four, six, eight, ten, twelve, and eighteen were abbreviated as CMCDMPDA-C1, CMCDMPDA-C4, CMCDMPDA-C6, CMCDMPDA-C8, CMCDMPDA-C10, CMCDMPDA-C12, and CMCDMPDA-C18 respectively, similar to the abbreviation of CMBACDMPDA-R with different carbon chain lengths.

Six CMCDMPDA (0.24 g; 0.79 mmol) samples were dissolved in six small flasks each containing DMSO (5 mL) separately. Each solution was diluted with THF (2 mL) and an excess of alkyl bromide (10.2 mmol) was added, i. e. 1-C_4H_9Br, 1-$C_6H_{13}Br$, 1-$C_8H_{17}Br$, 1-$C_{10}H_{23}Br$, 1-$C_{12}H_{25}Br$, and 1-$C_{18}H_{37}Br$. The reactions were kept at 25 ^{o}C for 24 hours. The mixtures were dialyzed against distilled water for one week. The solutions retained by the membrane were first lyophilized and then the residues were dried in a *vacuo* at 100^{o}C overnight. White solid products were obtained. For CMCDMPDA-C18, the crude water layer needed to be extracted with chloroform (20 mL) three times to remove the excess alkyl halide; then, it was dried in a *vacuo* at 100^{o}C overnight. White solid products were obtained. CMCDMPDA-C8 ^{1}H NMR (250MHz, D_2O): δ (ppm) 2.78 [$^{+}N(CH_3)_3$], 3,24 ($CH_2N^{+}CH_2$), 0.80(CH_2CH_3), 1.20-1.33[$(CH_2)_6CH_3$], 1.73 ($CH_2CH_2CH_2$), 2.60 ($CONHCH_2$), 3.25-4.5 (broad peaks of anhydroglucose ring); CMCDMPDA-C10 ^{1}H NMR (250MHz, D_2O): δ (ppm) 2.80 [$^{+}N(CH_3)_3$], 2.96 ($CH_2N^{+}CH_2$), 0.80 (CH_2CH_3), 1.10-1.30 [$(CH_2)_8CH_3$], 1.73 ($CH_2CH_2CH_2$), 2.60($CONHCH_2$), 3.25-4.5 (broad peaks of anhydroglucose ring); CMCDMPDA-C12 ^{1}H NMR

(250MHz, D_2O): δ (ppm) 2.78 [$^{+}N(CH_3)_3$], 3.22 ($CH_2N^{+}CH_2$), 0.78 (CH_2CH_3), 1.10-1.40 [$(CH_2)_{10}CH_3$], 1.73 ($CH_2CH_2CH_2$), 2.60 ($CONHCH_2$), 3.25-4.5 (broad peaks of anhydroglucose ring).

5.2.6 Synthesis of CMCBADMPDA-C10 with Different DS of C10

Five samples of CMCBADMPDA (0.10 g; 0.16 mmol) were dissolved in DMSO (5 mL) in five vials. Dioxane (0.5 mL) was added as the co-solvent to each solution. Then, different amounts of 1-Bromodecane (0.05 g, 0.22 mmol; 0.071 g, 0.32 mmol; 0.089g, 0.40 mmol; 0.107g, 0.48 mmol; 0.125g, 0.56 mmol) and corresponding amounts of sodium bicarbonate (0.023g, 0.27 mmol; 0.031g, 0.37mmol; 0.038g, 0.45mmol; 0.043g, 0.51mmol; 0.051g, 0.60 mmol) were added to each solution. The reactions were kept at 90 ^{o}C for 24 hours. The mixtures were dialyzed against deionized water for one week. The solution retained by the membrane was first lyophilized and then the residue was dried overnight in a *vacuo* at 100^{o}C. White cotton-like solid products were obtained.

5.2.7 Synthesis of CMCBADMPDA-C10-quat188

Partly substituted CMCBADMPDA-C10 (0.04 g, 0.04 mmol) was added to aqueous sodium hydroxide solution (10%, 5mL) with Quat-188 (0.4mL, 2.12 mmol). The system was kept at 60 ^{o}C for 12 hours. The mixtures were then dialyzed against distilled water for one week. The solution retained by the membrane was first lyophilized and then the resulting residue was dried in a *vacuo* at 100^{o}C overnight. White cotton-like products were obtained. CMCBADMPDA-C10-Quat188 ^{1}H NMR (250MHz, D_2O): δ (ppm) 3.24 [$CHOHCH_2^{+}N(CH_3)_3$ and $CHOHCH_2^{+}N(CH_3)_2CH_2$], 2.89 [$CH_2CH_2CH_2^{+}N(CH_3)_3$]], 3.47 ($^{+}NCH_2CHOH$), 3.37

($CH_2N^+CH_2$), 0.80 (CH_2CH_3), 1.10-1.30 [$(CH_2)_8CH_3$], 1.73 ($CH_2CH_2CH_2$), 2.60 ($CONHCH_2$), 2.14 (CCH_2CH_2), 1.95 (CCH_2CH_2), 3.25-4.5 (broad peaks of anhydroglucose ring).

5.2.8 Synthesis of CMCBADMPDA-C10-PO

CMCBADMPDA-C10 (0.10 g, 0.09 mmol) gradually swelled in isopropanol (5 mL) for 2 hours. Aqueous sodium hydroxide (20%, 2 mL) was added. The mixture was stirred for 10 minutes. Propylene oxide (1 mL) was added into the system. The mixture was refluxed at 60 ^oC for 3 hours. The mixtures were then dialyzed against distilled water for one week. The solution retained by the membrane was first lyophilized and then the resulting residue was dried overnight in a *vacuo* at 100^oC. White cotton-like solid was obtained. CMCBADMPDA-C10 ^1H NMR (250MHz, D_2O) (Figure 5.8): δ (ppm) 3.07($^+N(CH_3)_3$), 3.30($CH_2N^+CH_2$), 0.89 (CH_2CH_3), 1.00-1.78[$(CH_2)_8CH_3$, $CH_2CH_2CH_2$, ($CH_2CHOHCH_3$,) 2.19(CCH_2CH_2), 2.01(CCH_2CH_2), 3.25-4.5 (broad peaks of anhydroglucose ring).

5.2.9 Determination of Quat Content of Quaternary Ammonium Dendronized Cellulose Derivatives

CMCBADMPDA-R (10~20 mg) gradually swelled up in deionized water (1 mL) overnight. Ethanol (5 mL) was added. The mixture was titrated with $AgNO_3$ solution (2 mM) under stirring. The conductivity of the mixture in a titration process was measured using a YSI Model 32 conductance meter from YSI Inc. The dramatic increasing of conductivity of the system indicated the end point of titration. The degree of quaternization (DQ) was calculated based on the concentration of anion in the dendronized cellulose derivatives and was expressed as the weight percentage of quaternary nitrogen in the sample.

5.3 Results and Discussions

5.3.1 Synthesis and Characterization of CMCBADMPDA-Quat188

The synthesis reaction equation of CMCBADMPDA is shown in scheme 5.5. The dimethyl amino end groups on the tips of side branches of CMCBADMPDA served as the nucleophiles to react with 3-chloro-2-hydroxypropyl trimethylammonium chloride (Quat-188). This nucleophilic attack may be facilitated by the *in situ* formation of an epoxide intermediate. The reaction was conducted at 50 ^{o}C for 2 hours. A longer reaction time and higher temperature were avoided because cellulose backbone may be decomposed at high temperatures and strong base environments. After dialysis, the residual aqueous solution was clear, viscous, and sticky. After lyophilizing, the white cotton-like solid of CMCBADPMDA-Quat188 could be easily dissolved in water. Its proton NMR spectrum (Figure 5.1) in D_2O had both the strong peak of 3.24 (a, e, $^{+}N(C\underline{H}_3)$), shifted from 2.5 of proton of methyl group on tertiary amine, and the broad peak from 3.2 to 4.8 from the cellulose backbone. Its ^{13}C NMR spectrum (Figure 5.2) showed strong carbon peak on quaternary nitrogen at 54.60 (a, e, $^{+}N(\underline{C}H_3)$),[5] which is different from carbon's peak on tertiary amine at 46.16. The NMR spectra confirmed the proposed structure.

Scheme 5.5. Synthesis of CMCBADMPDA-Quat188

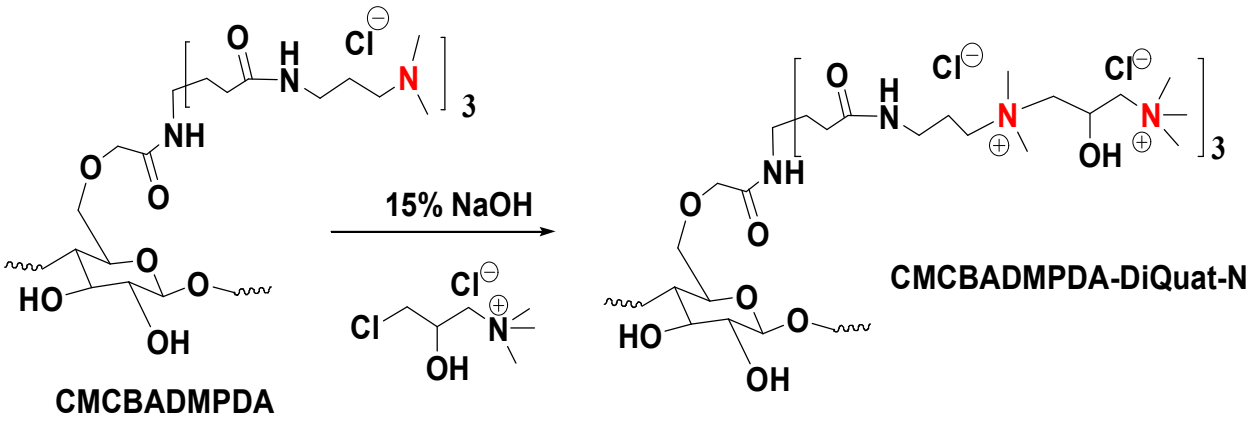

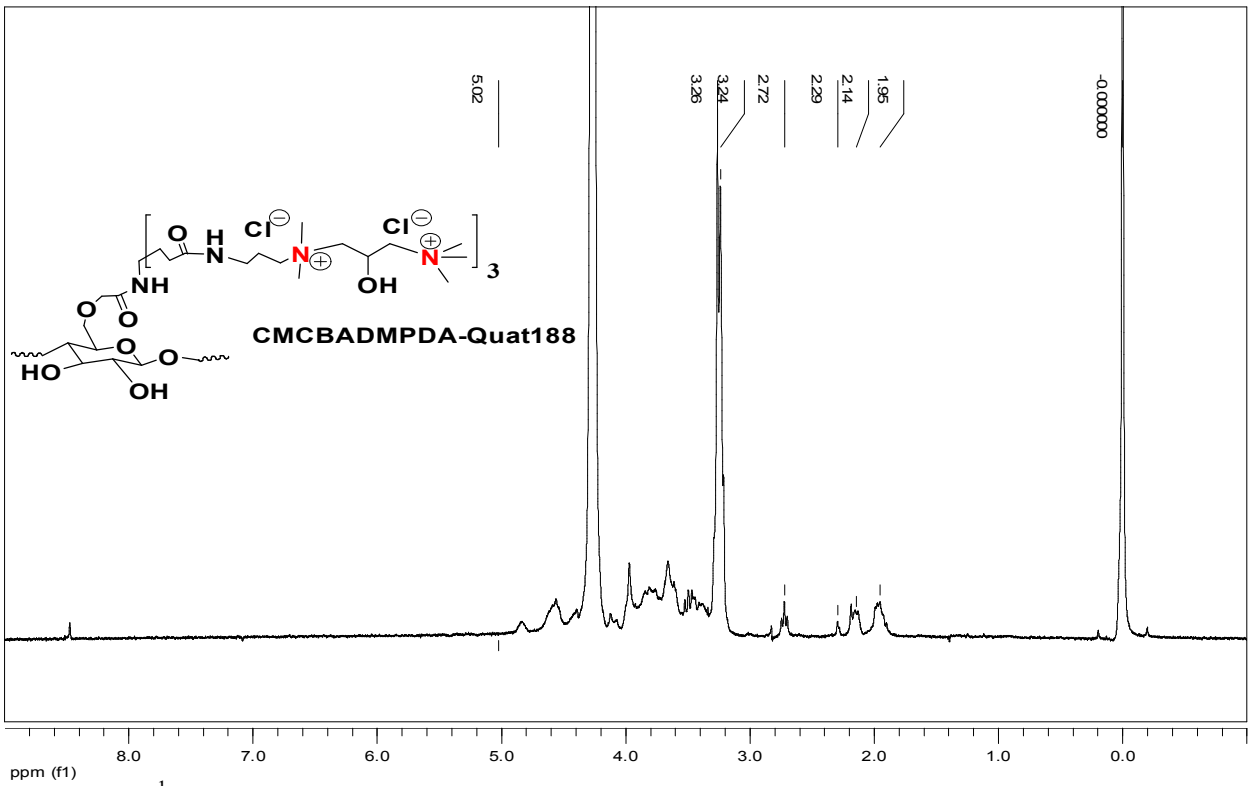

Figure 5.1. [1]H NMR Spectrum of CMCBADMPDA-quat188.

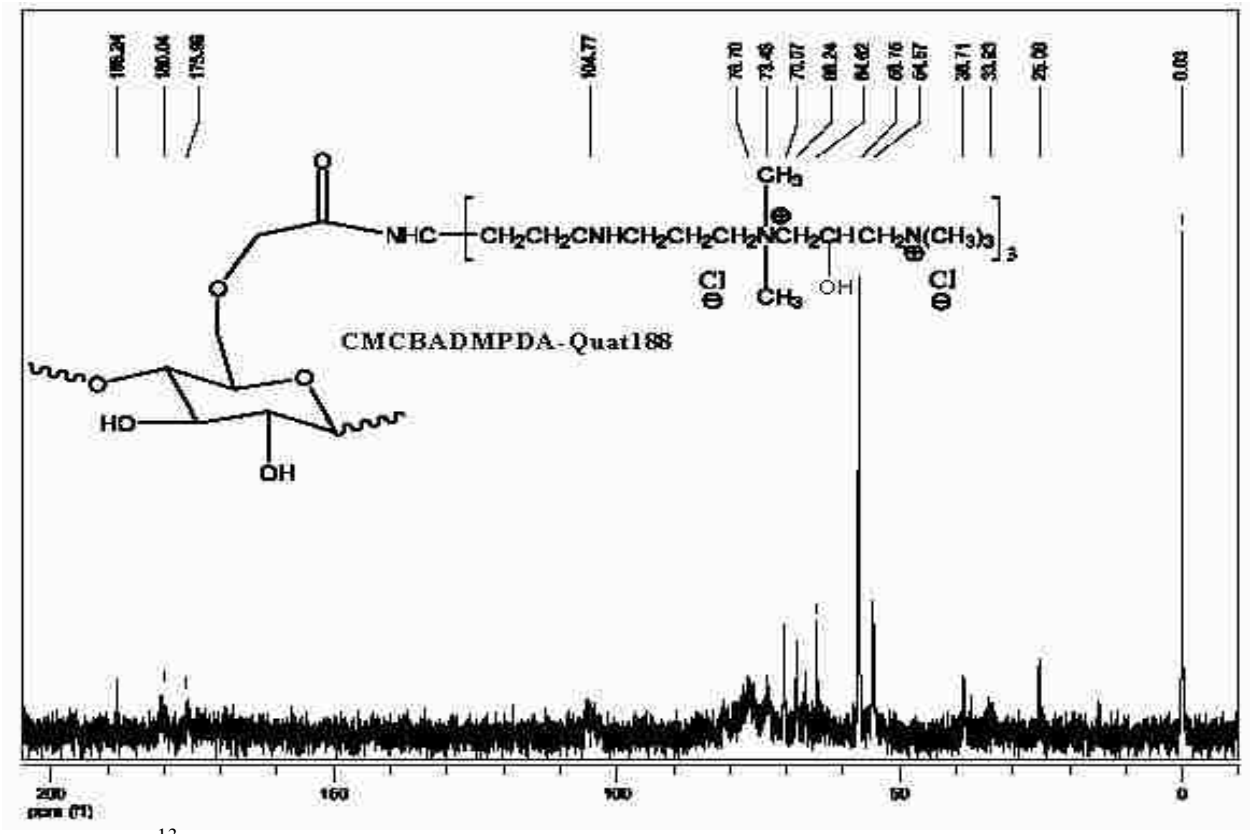

Figure 5.2. [13]C NMR Spectrum of CMCBADMPDA-Quat188.

5.3.2 Synthesis and Characterization of CMCBADMPDA-R

The synthesis of CMCBADMPDA-R was first explored in preparing CMCBADMPDA-C1 as a model compound by using iodomethane to react with CMCBADMPDA. CMCBADMPDA was first dissolved in water and ethanol was used as the co-solvent with water. The nucleophilic substitution reaction was conducted at room temperature. After reaction, ethanol and iodomethane could be easily evaporated out of the mixture by using a rotovapor at 60 ^{o}C. After lyophilizing the concentrated residue aqueous solution, white CMCBADMPDA-C1 was obtained as a white solid. The 3.02($^{+}$N(CH_3)$_3$), 3.10(b, CH_2N^{+}) of its proton chemical shifts and 53.64 [$^{+}$N(CH_3)$_3$] of its carbon chemical shift in its spectra (Figure 5.3) are associated with quaternary nitrogen and confirmed that the tertiary nitrogen in CMCBADMPDA was transformed into the quaternary nitrogen in CMCBADMPDA-C1. The quaternization was first tried by adding iodomethane into aqueous CMCBADMPDA solution. Because iodomethane is insoluble in water, the reaction could only be conducted in the interface of water and iodomethane. The quaternization reaction seldom occurred as the result of the reaction. After adding ethanol as co-solvent, CMCBADMPDA-C1 could be easily obtained.

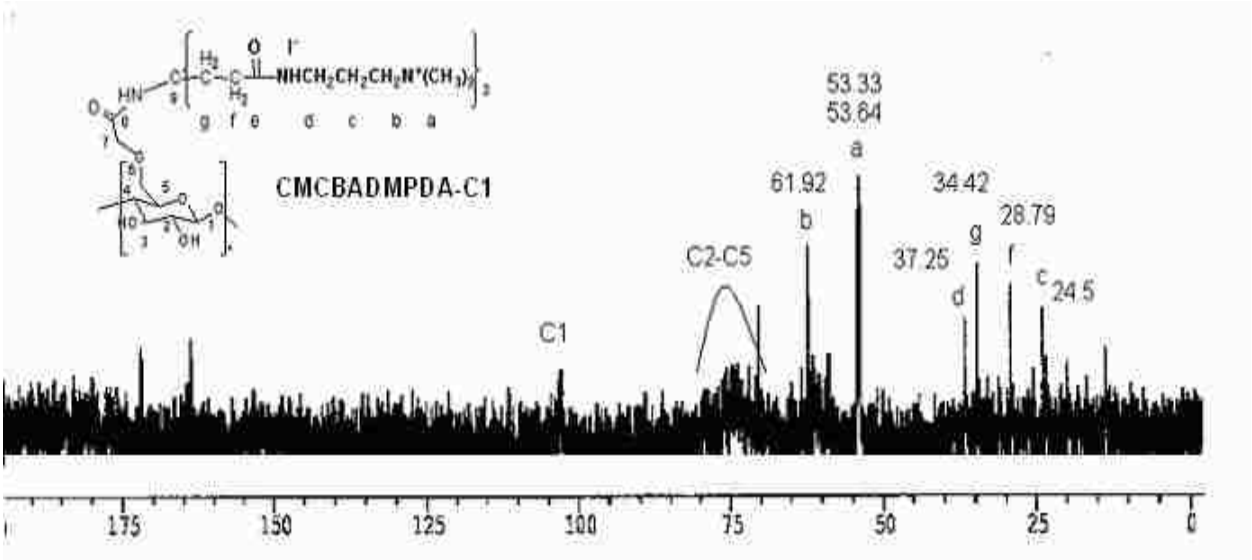

Figure 5.3. ^{13}C NMR of CMCBADMPDA-C1.

The synthesis of CMCBADMPDA-R was then tried by using 1-bromooctane to react with CMCBADMPDA using two-component solvent systems of H_2O/THF, DMSO/THF, and DMSO/dioxane at room temperature following the reaction showed in scheme 5.6. CMCBADMPDA-C8 was obtained in all three solvent systems. CMCBADMPDA was soluble in a hot DMSO solution. Since the DMSO/dioxane solvent system permitted the reaction to be conducted in a broad range of temperature, it was chosen as the solvent system for preparing CMCBADMPDA-R with different carbon chain lengths from four carbons to eighteen carbons.

Scheme 5.6. Synthesis of CMCBADMPDA-R with different chain length of R

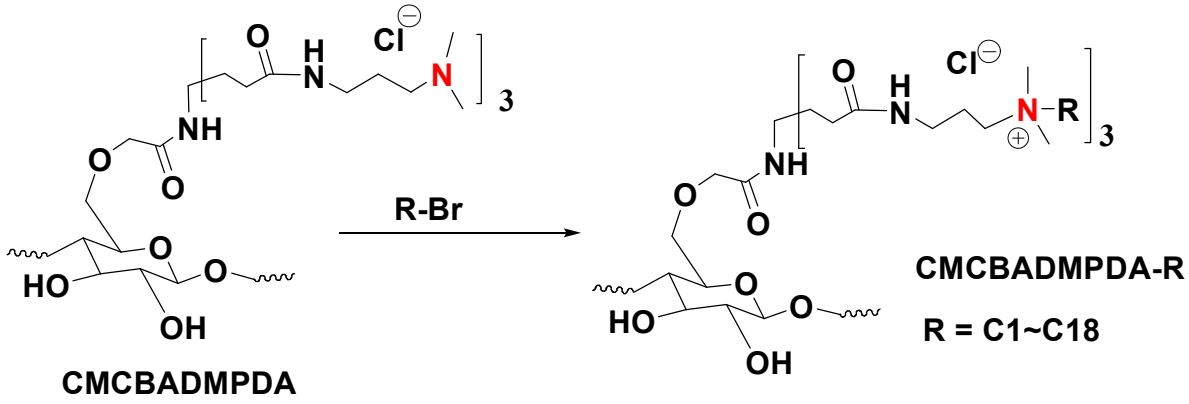

Figure 5.4 showed all the proton NMR spectra of CMCBADMPDA-R with different carbon chain lengths. The derivatives of CMCBADMPDA-R listed in figure 5.4 were all obtained by reacting CMCBADMPDA with their corresponding alkyl bromide at room temperature. CMCBADMPDA-R derivatives all have proton chemical shifts around 2.91 [$^{+}$N(CH_3)$_2$], 0.9 (CH_3), and 1.15-1.43 (CH_2). Their NMR spectra were consistent with their proposed chemical structures. Table 5.1 showed the product yield for each preparation. All of their FTIR (Figure 5.5) showed strong C-H stretch absorption around 2925 cm^{-1} and 2864 cm^{-1}. With the increasing length of R on CMCBADMPDA-R, the ratio between the absorption of hydrogen bonds at 3425cm^{-1} and that of C-H stretches around 2925 cm^{-1}and 2864 cm^{-1} decreased.

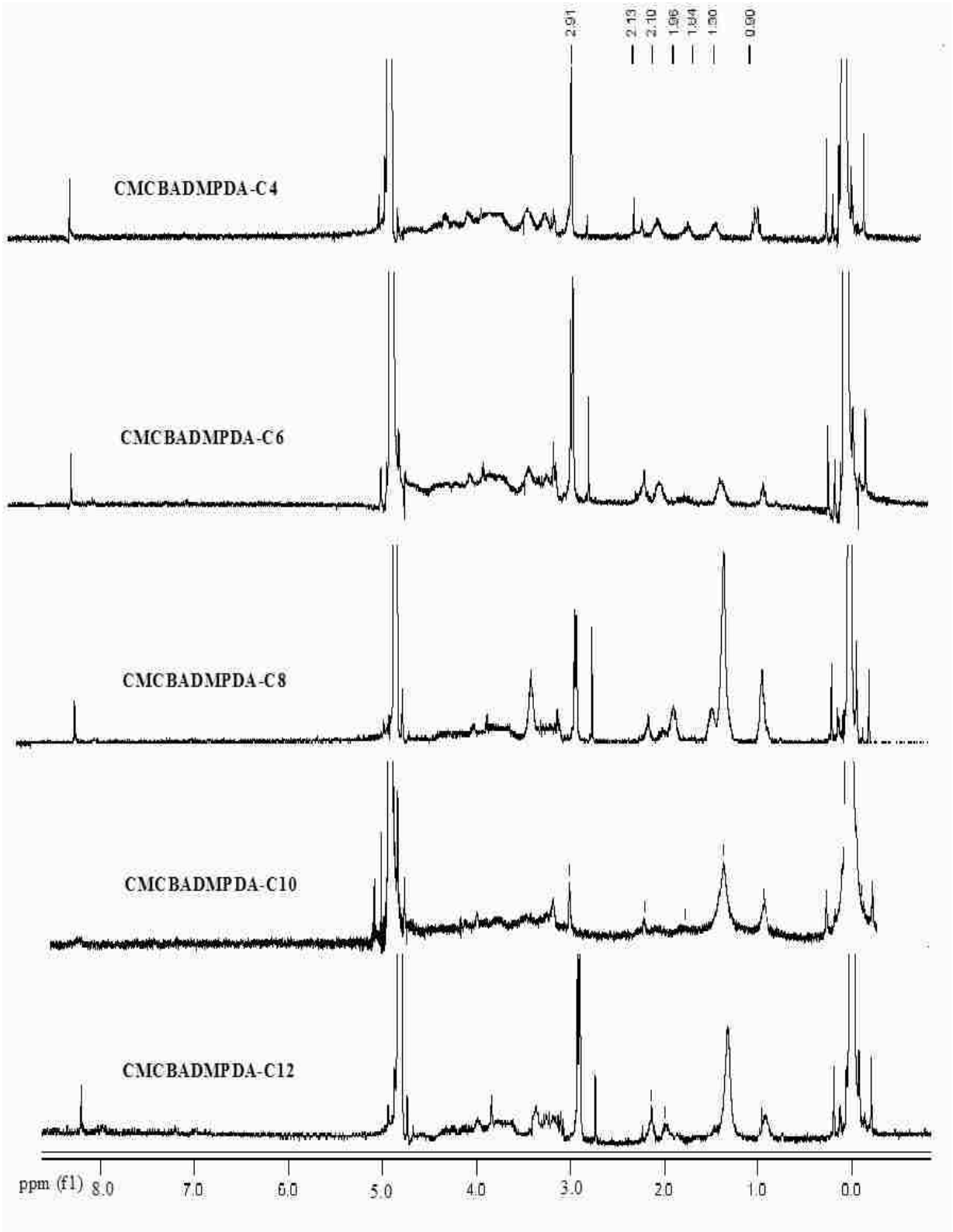

Figure 5.4. ^{1}H NMR of CMCBADMPDA-R with R=C4~C12.

Table 5.1. Preparation of CMCBADMPDA-R

CMCBADMPDA-R	Alkyl chain length	CMCBADMPDA (g)	Yield (g)
CMCBADMPDA-C4	C4	0.20	0.17
CMCBADMPDA-C6	C6	0.20	0.15
CMCBADMPDA-C8	C8	0.20	0.30
CMCBADMPDA-C10	C10	0.20	0.36
CMCBADMPDA-C12	C12	0.20	0.40
CMCBADMPDA-C18	C18	0.20	0.20

----Room temperature and over amount alkyl bromide

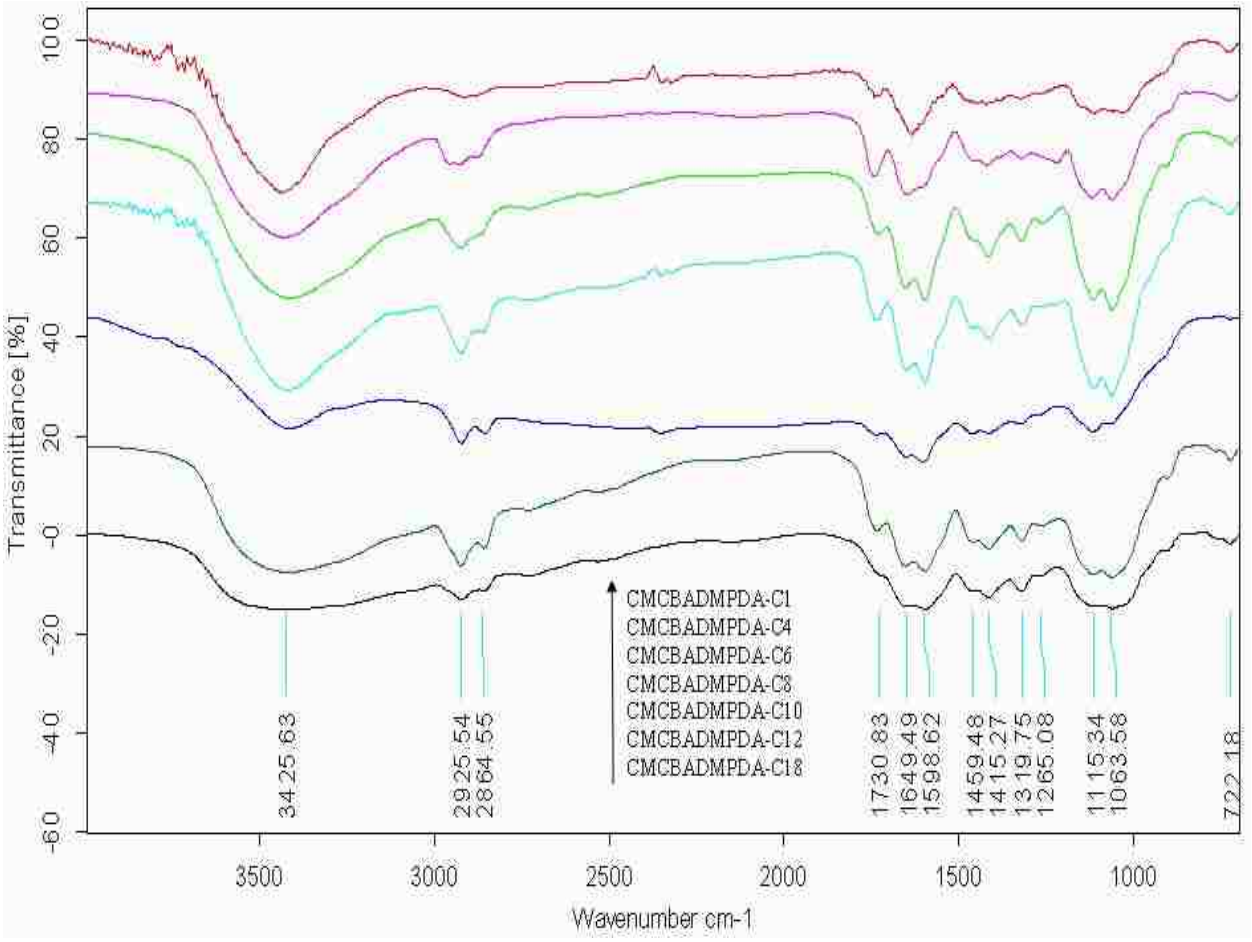

Figure 5.5. FTIR of CMCBADMPDA-R.

I was surprised to have found that all the spectra of CMCBADMPDA-R showed the significant peak of 1731 cm^{-1}, which is normally the absorption of stretch vibration of carbonyl C=O double bond of ester. This indicated that CMCBADMPDA-R may contain some ester

groups of –COOR. I proposed that the esterification reaction (Scheme 5.7) might take place in the quaternization process if there were some

Scheme 5.7. The catalysis mechanism of CMCBADMPDA-R for esterification reaction in the quaternization process

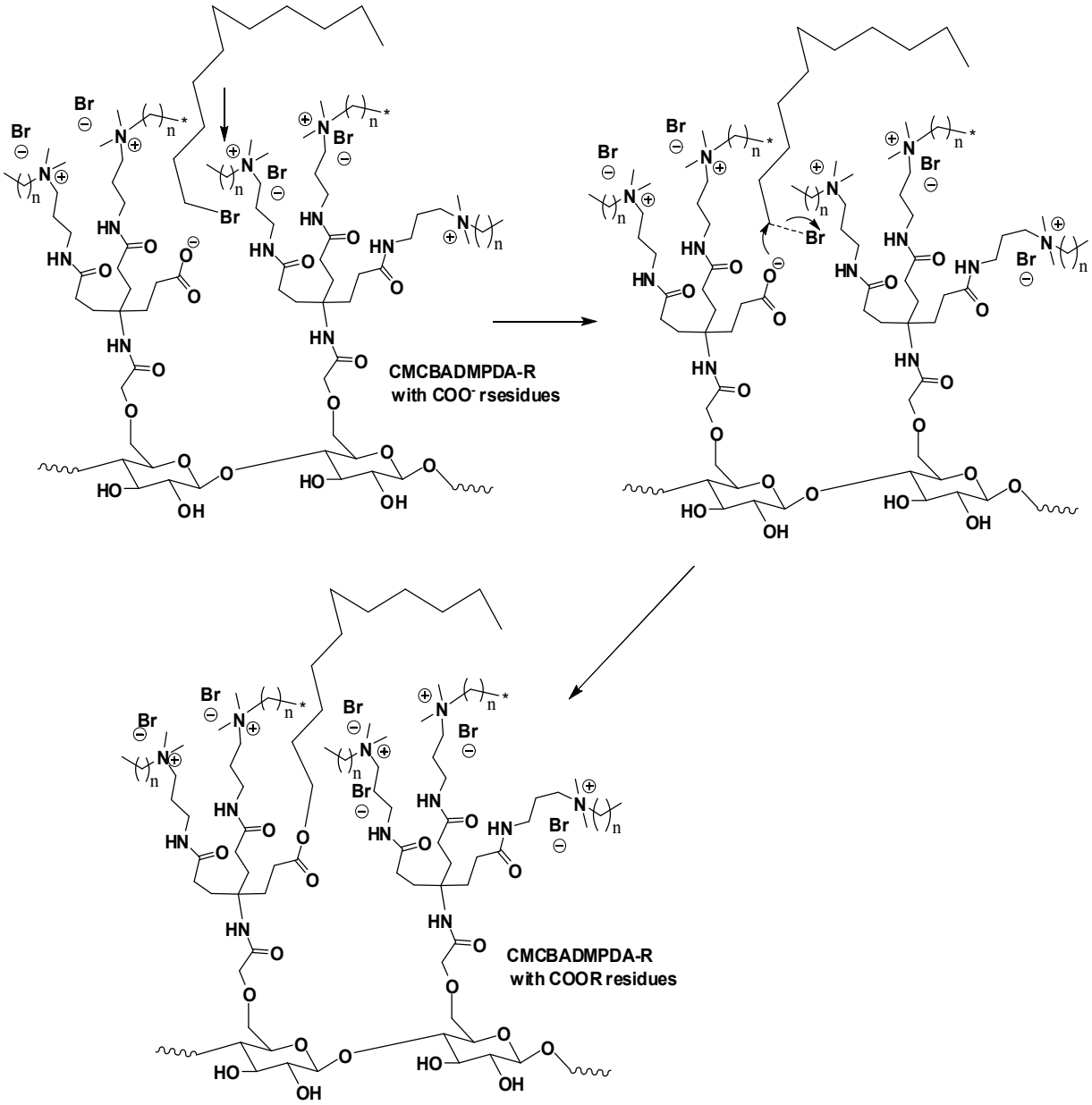

residues of carboxylic acid anions -COO^- in the dendronized CMCBADMPDA. The on-site quaternary nitrogen with alkyl groups in CMCBADMPDA-R were extremely efficient in catalyzing the esterification reaction of -COO^- groups with alkyl bromide although the -COO^-

group is a weak nucleophile.[84, 95] This nucleophilic reaction even occurred at room temperature while the quaternization reaction proceeded.

5.3.3 Control of the Degree Quaternization (DQ) of CMCBADMPDA-C10

The MIC test of CMCBADMPDA-R derivatives showed that CMCBADMPDA-C10 had better antimicrobial property than CMCBADMPDA-R with other carbon chain lengths. DS of functional groups is acknowledged to be extremely important in determining the properties of modified polymers. The degree quaternization (DQ) is defined as the weight percentage of quaternary nitrogen in the sample in this project. DQ is more important in comparing the antimicrobial activities of quaternized polymer derivative. The DQ would reflect the extended DS of C10 if the esterification process did not occur in synthesizing CMCBADMPDA-C10. We choose to synthesize CMCBADMPDA-C10 with different DQ by adjusting the relative concentration of 1-bromodecane added into the reaction system. To improve the reaction efficiency, the experiment was conducted at a higher temperature of 90 ^{o}C. Table 5.2 showed the DQ and targeted extended DS of C10 in CMCBADMPDA-C10. Because the CMCBADMPDA that we obtained contained a small amount of ester which is consisted of small portions of alkyl chain of C10, the extended DS of C10 in CMCBADMPDA-C10 included two parts: the DQ resulted from quaternization and the substitution resulted from the esterification.

Previously, Dr. Culberson measured the DQ of the cellulose derivatives that she synthesized by titrating them with sodium dodecyl sulphate (SDS) and anionic polymer potassium polyvinylsulfate.[5] The titration process was very tedious due to the slow response of macromolecular interaction. Recently, Jie Wu *etc*. measured the DQ of the quaternized chitosan derivatives by titrating the concentration of chloride ion in the samples with silver nitrate in aqueous solution.[96] My first trial of titration of my aqueous dendronized derivatives by using

silver nitrate failed because my samples contained HCO_3^- anion in the preparation process and therefore, the extremely low concentration of $AgHCO_3$ could not precipitate out of the aqueous titration system. Then I titrated the mixture solution of $(C_2H_5)_4NBr$ and $NaHCO_3$ in an ethanol/ H_2O (5:1) cosolvent system with the concentration of anion close to that of my polymer derivatives. The conductivity of the mixture was measured in the titration process. The dramatic changes in its conductivity indicated the end point of the titration. The titration of the model compound gave us a result that agreed to its real anion concentration. We estimated the DQ of our dendronized cellulose derivatives by measuring its conductivity signal in the co-solvent system of EtOH/H_2O (5:1) titrated with silver nitrate solution. The DQ was calculated based on the following equation.

$$DQ(\%) = \frac{14 \times V_{AgNO3} C_{AgNO3}}{W_{sample}} \times 100(\%)$$

V_{AgNO3} and C_{AgNO3} were the volume, and concentration of $AgNO_3$ used in the titration respectively. W_{sample} is the weight of the cellulose derivative sample used in the titration.

Table 5.2. The DQ of CMCBADMPDA-C10 measured by titration

	Cz 215-1	Cz215-2	Cz215-3	CZ 213-2
Targeted DS of C10	15%	20%	25%	30%
Targeted DQ (%)	2.22	2.73	3.05	3.16
N^+% (Corrected)	1.44	2.03	1.49	2.968
CMCBADMPDA (g)	0.10	0.10	0.10	0.10
CMCBADMPDA-C10 Yield (g)	0.10	0.13	0.15	0.14

The titration results were showed in table 5.2. Increasing the relative concentration of $C_{10}H_{25}Br$ initially could result in higher DQ. When the relative concentration of $C_{10}H_{25}Br$ reached 25% target extended DS, the DQ obtained started decreasing. The DQ obtained was

always lower than the target DQ. When the concentration of $C_{10}H_{25}Br$ in the reaction system is above a critical value, increasing its concentration could increase the percentage of $C_{10}H_{25}$- ester in the derivative which would result in CMCBADMPDA-C10 with higher extended DS of C10 but lower DQ.

Figure 5.6 shows the FTIR of CMCBADMPDA-C10 with target extended DS of C10 of 35% and 100%. Increasing the relative concentration of 1-bromodecane resulted in a higher ratio of the intensity of C-H stretch at 2925 cm^{-1} and 2864 cm^{-1} to that of hydrogen bond at 3420 cm^{-1}. This indicated that there was more alkyl chain in CMCBADMPDA-C10 with high target extended DS of C10. I also discovered that adding an excess amount of 1-bromodecane can increase the ester residue in CMCBADMPDA-C10 dramatically. The ratio between ester absorption at 1731 cm^{-1} and amide I adsorption at 1679 cm^{-1} in CMCBADMPDA-C10 with target extended DS of C10 at 100% was significantly higher that that of CMCBADMPDA-C10 with target extended DS of C10 at 35%.

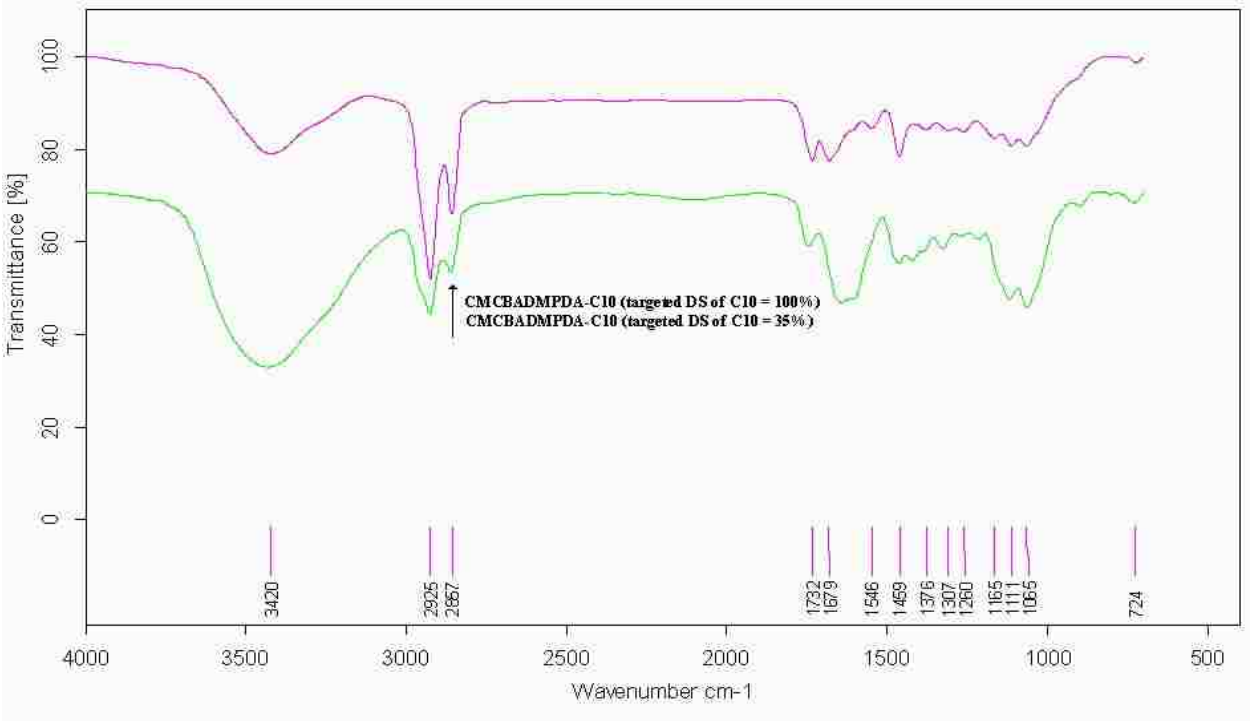

Figure 5.6. FTIR of CMCBADMPDA-C10 with different DS of C10.

5.3.4 Synthesis and Characterization of CMCBADMPDA-C10-quat188

The derivatives of CMCBADMPDA-C10 with high target extended DS of C10 became water insoluble. To improve its water solubility, they were modified with quat-188. Their residue amino groups were elaborated with di-quaternay nitrogen periphery groups in the newly formed derivative CMCBADMPDA-C10-Quat188. Scheme 5.8 shows the reaction. The reaction mechanism is similar to that of the reaction for synthesizing CMCBADMPDA-Quat188. Water insoluble CMCBADMPDA-C10 with high DS of C10 could be penetrated with aqueous hydroxide solution and quat-188. With further quaternization by quat-188, water-insoluble CMCBADMPDA-C10 derivatives gradually became swollen and finally dissolved in the aqueous solution. Dialysis of the mixture produced viscous CMCBADMPDA-C10-quat188 solution in the dialysis tube. After being concentrated by a rotovapor and further lyophilized, white cotton-like solids were obtained as the products.

Scheme 5.8. The synthesis of CMCBADMPDA-C10-Quat188

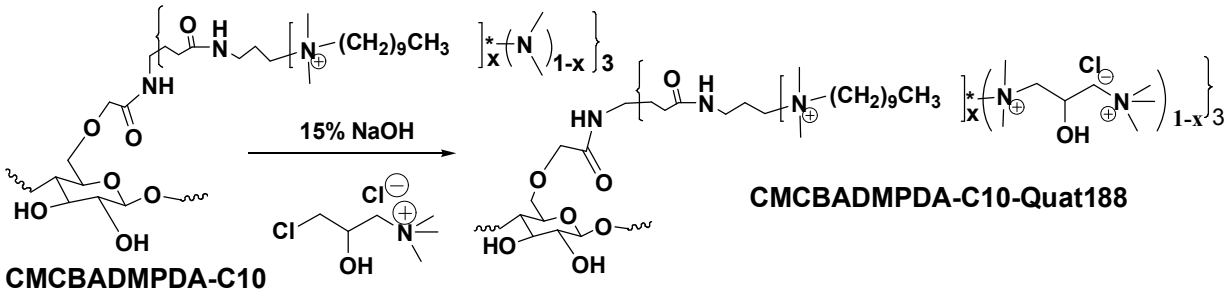

The proton NMR spectrum (Figure 5.7) of CMCBADMPDA-C10-quat188 showed both typical proton peak of methyl group on mono-quaternary nitrogen with alkyl chain C10 in hydrophobic micro-environment at 2.89 and typical proton peak of methyl group on di-quaternary nitrogen proximate to hydroxyl groups in hydrophilic micro-environment at 3.24. Table 5.3 shows the yields of the synthesis.

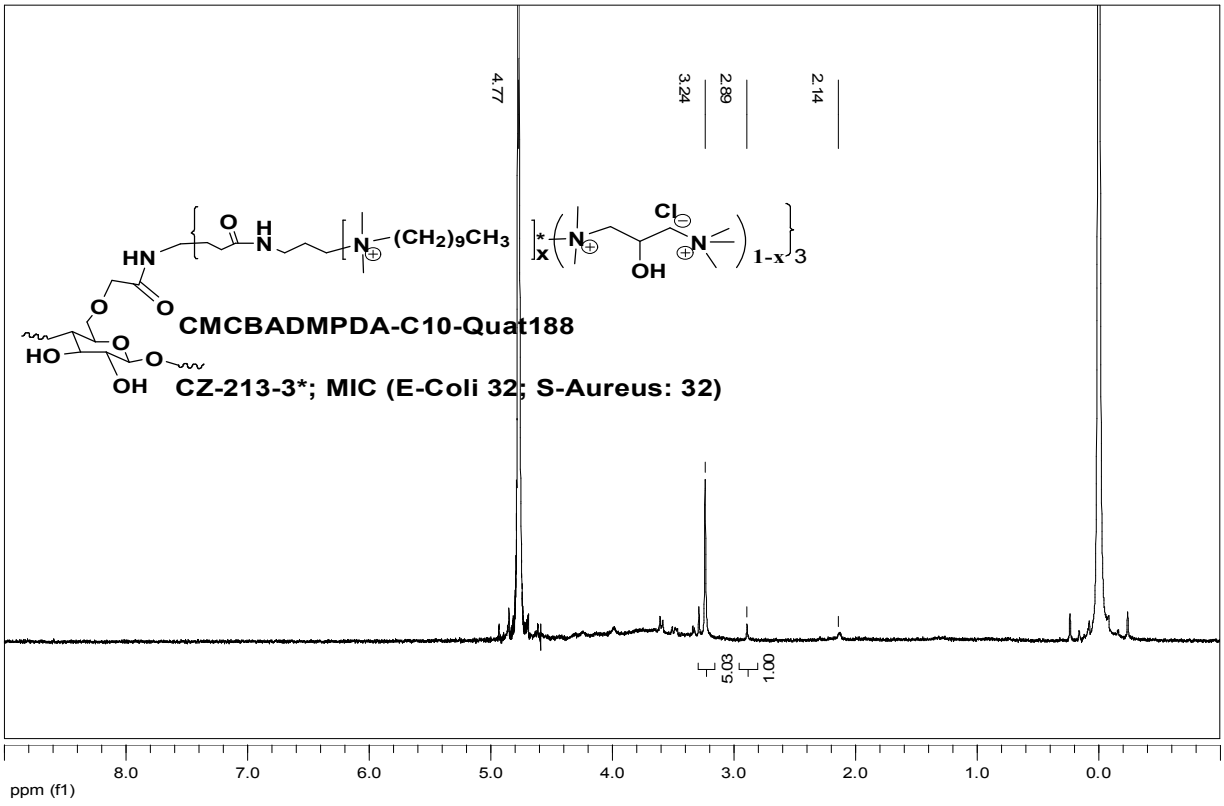

Figure 5.7. ^{1}H NMR of CMCBADMPDA-R-Quat188.

Table 5.3. The synthesis of CMCBADMPDA-C10-Quat188

Run	1	2	3	4	5	6	7
Targeted DS of C10	15%	20%	25%	30%	40%	50%	60%
CMCBADMPDA-C10 (g)	0.04	0.04	0.04	0.04	0.05	0.05	0.04
CMCBADMPDA-C10-Quat188 Yield (g)	0.01	0.02	0.03	0.03	0.04	0.02	0.05

5.3.5 Synthesis and Characterization of CMCBADMPDA-R-PO

To understand the origin of the antimicrobial property of CMCBADMPDA-C10, CMCBADMPDA-C10 was synthesized with the highest possible extended DS of C10 by using an excess of 1-bromodecane in its preparation. Then, it was modified with propylene oxide and

was transformed into water soluble CMCBADMPDA-C10-PO. Scheme 5.9 shows the reaction equation. The derivatives CMCBADMPDA-C10 were first swellen with isopropanol. They were then treated with sodium hydroxide to prepare alkalized CMCBADMPDA-C10, which could open the epoxide ring of propylene oxide to form hydroxypropyl cellulose with hydrophobic quaternary nitrogen (CMCBADMPDA-C10-PO). After dialysis and freeze drying, the derivatives CMCBADMPDA-C10-PO were produced as white cotton-like solids. They were water soluble.

Scheme 5.9. The synthesis of CMCBADMPDA-R-PO

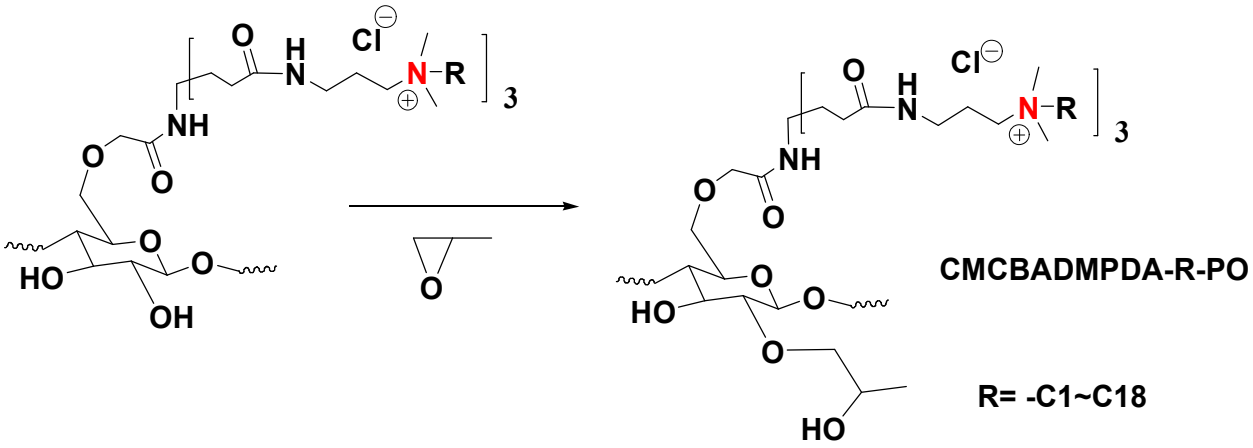

The proton NMR spectrum (Figure 5.8) of CMCBADMPDA-C10-PO showed that the chemical shift of proton on methyl groups on mono-quaternary nitrogen with hydrophobic C10 alkyl chain was shifted a little bit downfield to 3.07 from 2.91, that of CMCBADMPDA-C10. I attributed this phenomenon to the much more polar local microenvironment where methyl groups on mono-quanternary nitrogen are located in CMCBADMPDA-C10-PO than that in CMCBADMPDA-C10. CMCBADMPDA-C10-PO also showed a strong peak of proton of methyl from hydroxypropyl groups at 1.29. This indicated that hydroxypropyl groups may exist as polypropylene oxide oligomers connected with a cellulose backbone in CMCBADMPDA-C10-PO. Table 5.4 shows the yields for the synthesis of CMCBADMPDA-C10-PO.

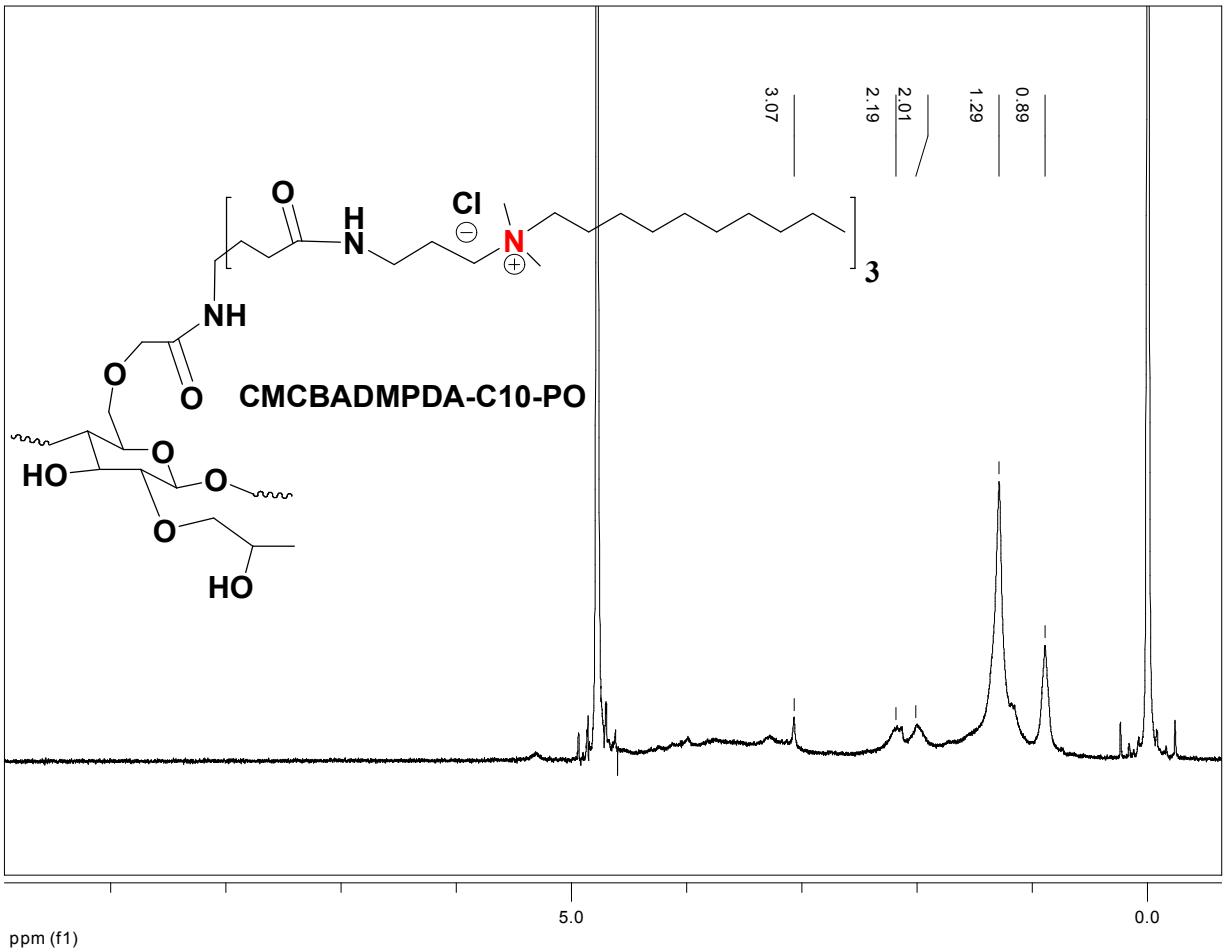

Figure 5.8. ^{1}H NMR of CMCBADMPDA-R-PO.

Table 5.4. The synthesis of CMCBADMPDA-C10-PO

Run	1	2
CMCBADMPDA-C10 (g)	0.17	0.16
CMCBADMPDA-C10-PO Yield (g)	0.03	0.06
Source CMC	MW=250k; DS=1.2	MW=700k; DS-0.9

5.3.6 FTIR Characterization

Figure 5.9 shows the FTIR spectra of CMCBADMPDA-C10, CMCBADMPDA-C10-PO, CMCBADMPDA-C10-quat188, and CMCBADMPDA-quat188. The CMCBADMPDA-C10

with target extended DS of C10 at 100% had significant ester absorption around 1732 cm^{-1}. Neither CMCBADMPDA-C10-PO nor CMCBADMPDA-C10-quat188 had absorption at 1732 cm^{-1}. This indicated that the strong basic condition in preparing CMCBADMPDA-C10-PO and CMCBADMPDA-C10-quat188 hydrolyzed the ester residue in CMCBADMPDA-C10. All the FTIR spectra of CMCBADMPDA-C10, CMCBADMPDA-C10-PO, and CMCBADMPDA-C10-quat188 showed stronger C-H stretch around 2924 cm^{-1} than that of CMCBADMPDA-quat188.

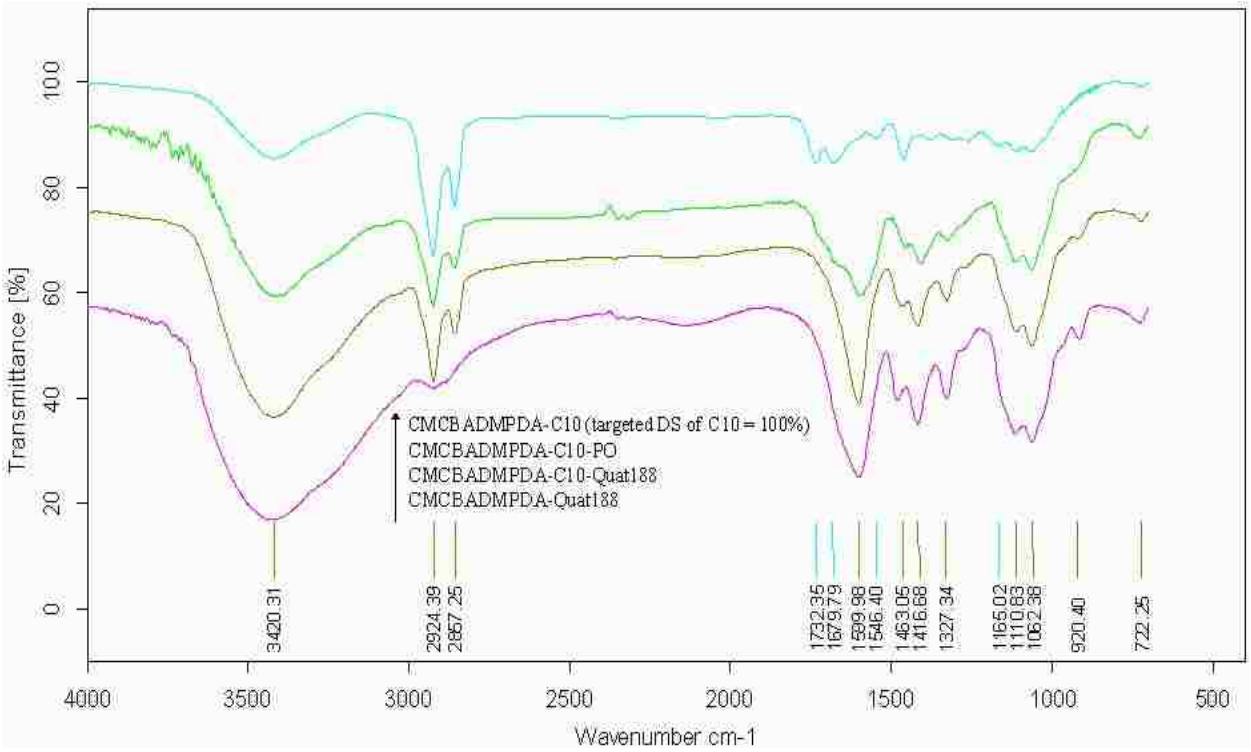

Figure 5.9. FTIR of quaternary ammonium dendronized cellulose derivatives with different functional groups.

5.3.7 Thermo Analysis Characterization

TGA thermogram of CMCBADMPDA-C10, CMCBADMPDA-C10-PO, CMCBADMPDA-C10-Quat188, and CMCBADMPDA-Quat188 were compared with that of CMCBADMPDA in figure 5.10 and figure 5.11. The comparison results are listed in Table 5.5. CMCBADMPDA-

C10 showed the lowest weight loss at 100 ºC. The hydrophobic C10 alkyl chain on CMCBADMPDA-C10 made it difficult to absorb water moisture. The increasing amount of hydroxyl groups on CMCBADMPDA-C10-PO, CMCBADMPDA-C10-Quat188, and CMCBADMPDA-Quat188 promoted the water retention of these derivatives. The derivatives with more C10 alkyl chains showed lower residues at 500 ºC. This indicated that C10 alkyl chain could be released away in the heating process. It seems that both CMCBADMPDA and CMCBADMPDA-Quat188 showed one broad peak in their weight derivative curves which were the significant overlaps of thermal decomposition of side chains with that of cellulose backbones. CMCBADMPDA-C10, CMCBADMPDA-C10-PO, and CMCBADMPDA-C10-quat188 showed two broad peaks in their weight derivatives curves. The following Hofmann elimination reaction was proposed to be mainly responsible for their first broad peaks (Scheme 5.10).[84]

Scheme 5.10. Thermal decomposition of CMCBADMPDA-C10 through Hofmann elimination

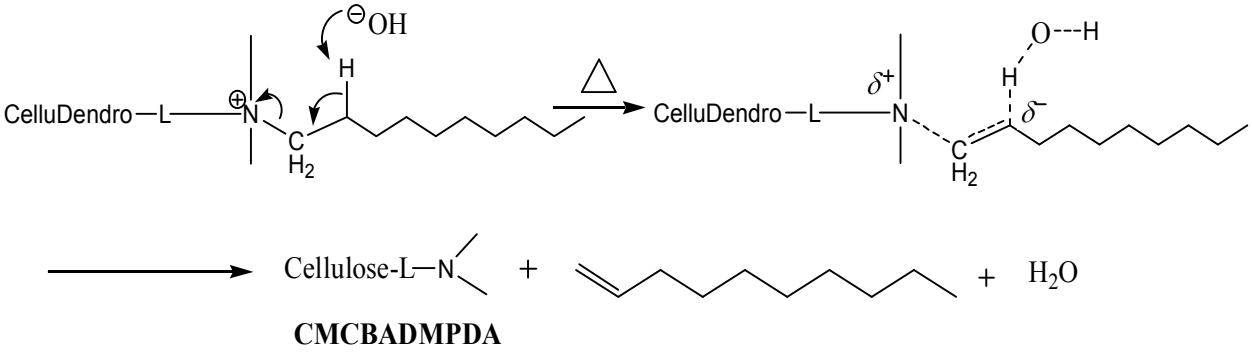

As I mentioned before, the FTIR spectrum of CMCBADMPDA-C10 had significant ester absorption at 1732 cm^{-1}. CMCBADMPDA-C10 we prepared actually had a significant amount of ester of C10 in its molecular structure. The decomposition of ester residue in CMCBADMPDA-C10 also contributed to the first peak in its TGA weight derivative spectrum. The decomposition mechanism (Scheme 5.11) of ester in CMCBADMPDA-C10 was proposed to be similar to that kicking out of t-butyl groups in the thermal decomposition of CMCBA

producing alkene. There was little possibility of forming 1-decanol in its decomposition because the boiling point of 1-decanol is 246.9 °C and the big endothermic peak for this ester decomposition is from 233 °C to 244 °C. The weight loss of the first peaks of CMCBADMPDA-C10-PO, CMCBADMPDA-C10-quat188 was significantly smaller than that of CMCBADMPDA-C10. In the process of synthesizing CMCBADMPDA-C10-PO, CMCBADMPDA-C10-quat188, 10-15% sodium hydroxide solutions were used to treat CMCBADMPDA-C10 in the temperature range from 55 ºC to 60 ºC. This should hydrolyze the ester of C10 alkyl chain in CMCBADMPDA-C10. Both CMCBADMPDA-C10-PO and CMCBADMPDA-C10-quat188 were proposed to contain no significant amount of C10 alkyl chain esters in their structures. This agreed with the relative smaller first peaks in their TGA thermogram of CMCBADMPDA-C10-PO and CMCBADMPDA-C10-quat188.

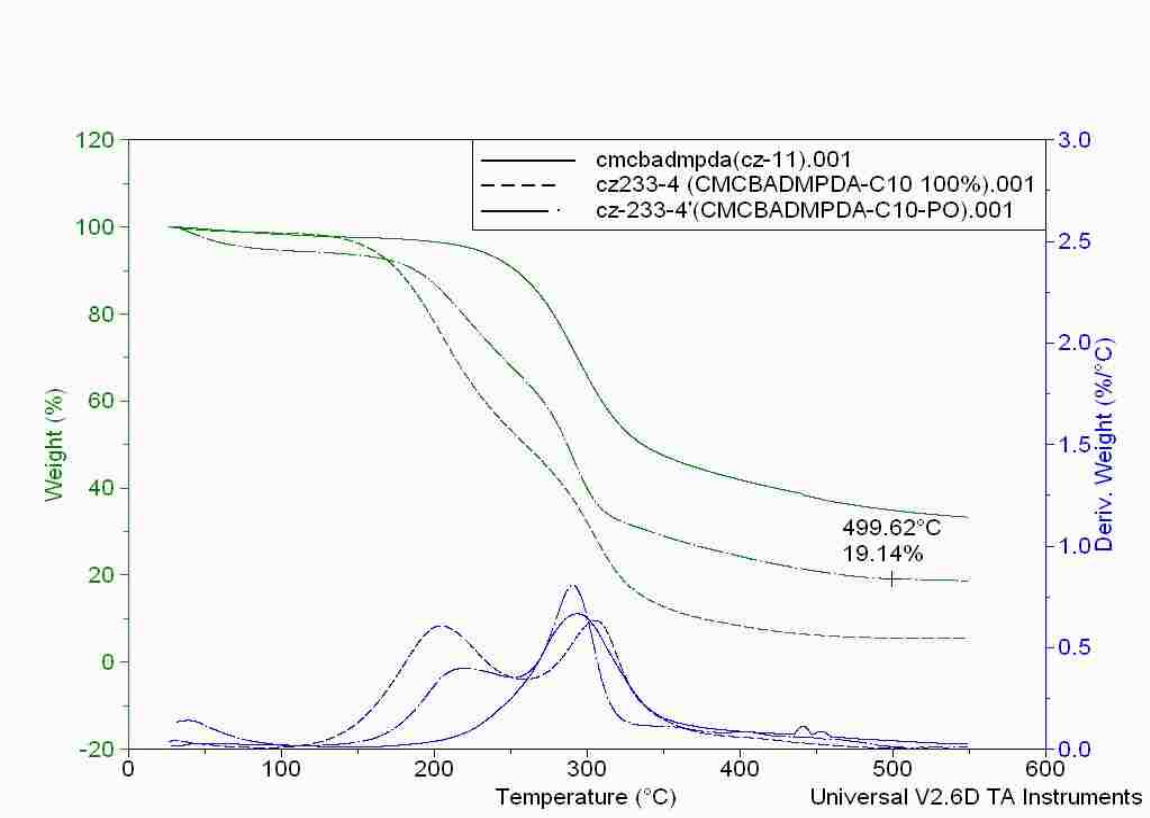

Figure 5.10. TGA curves of CMCBADMPDA, CMCBADMPDA-C10, and CMCBADMPDA-C10-PO.

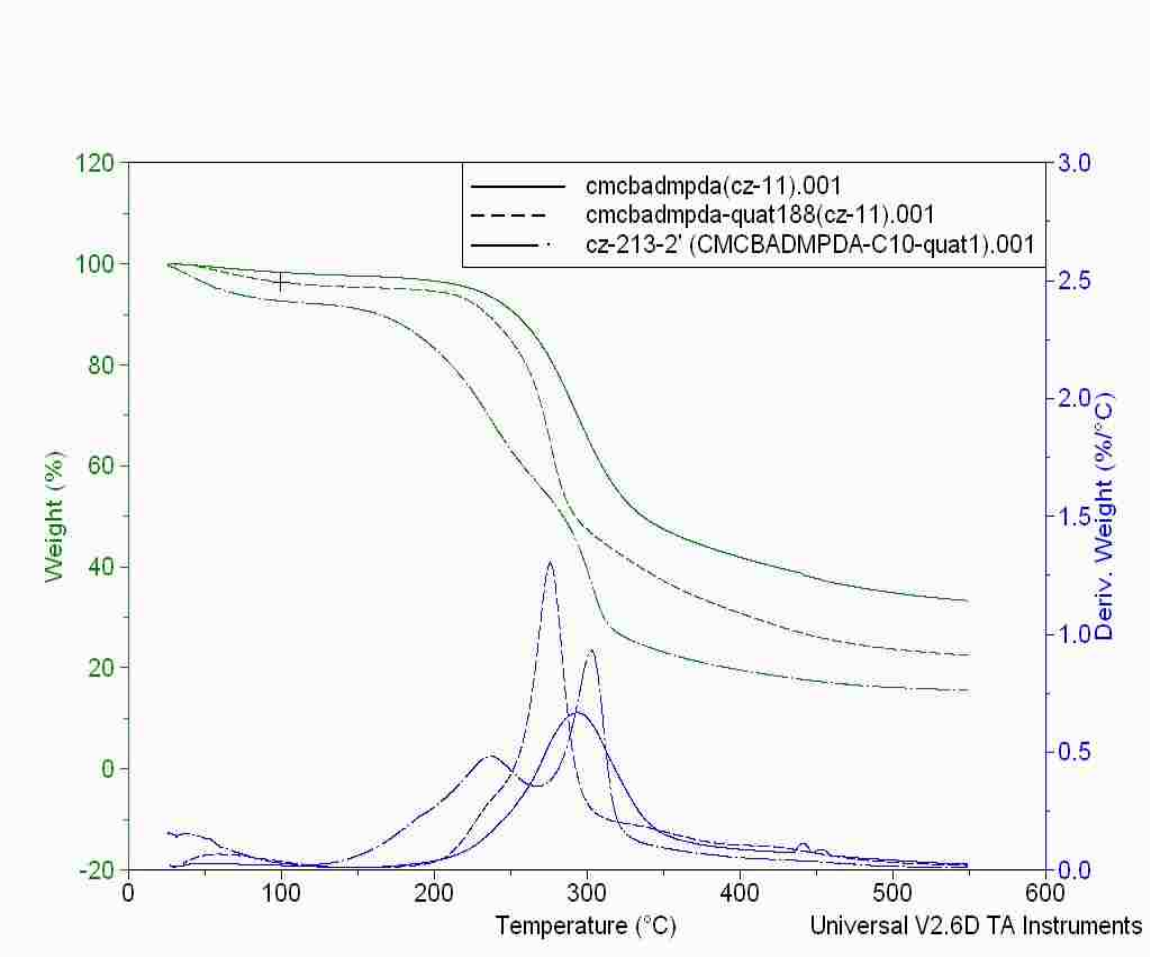

Figure 5.11. TGA curves of CMCBADMPDA, CMCBADMPDA-quat188, and CMCBADMPDA-C10-quat188.

Table 5.5. The TGA analysis result of quaternary ammonium dendronized cellulose derivatives

Samples	Weight loss RT-100ºC	Peak 1	Peak 2	Residue at 500ºC
CMCBADMPDA	1.7%	255.77-326.61ºC (36.94%)		34.92%
CMCBADMPDA-Quat188	3.569%		254.22-293.44 (33.48%)	22.54%
CMCBADMPDA-C10 (100%)	1.374%	168.01-226.69 (29.56%)	288-334.5 (35.21%)	5.42%
CMCBADMPDA-C10(100%)-PO	5.133%	186.03-232.89 (16.14%)	277.73-311.89 (20.93%)	18.72%
CMCBADMPDA-C10-quat188 (cz213-2′)	6.948%	194.03-247.59 (20.43%)	291.75-315.73 (17.87%)	15.61%

Scheme 5.11. Thermal decomposition of the ester groups on CMCBADMPDA-C10

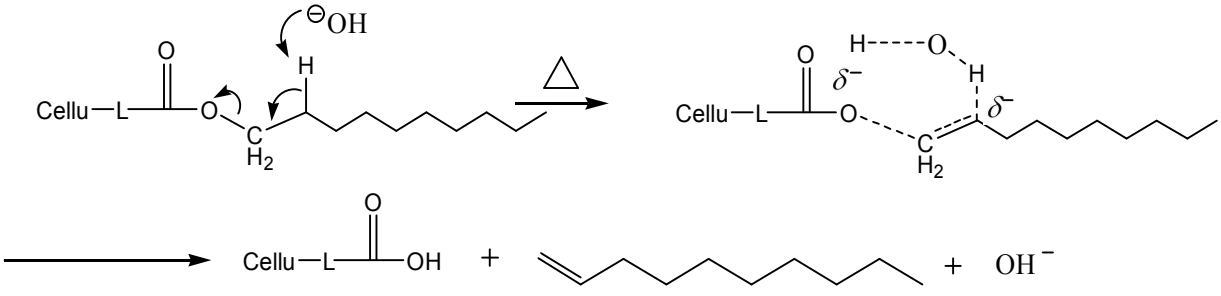

DSC thermogram of CMCBADMPDA-quat188 (Figure 5.12) showed a broad glass transition and molecular adjustment from 119ºC to 154 ºC. From 160 ºC, a stable heating process with a Cp of 0.1437J/g took place until 201 ºC without weight loss. From 201.92 ºC, an endothermic process began with no significant weight loss. The molecular chains of CMCBADMPDA-Quat188 might begin to melt at this point. From 209.23 ºC, the 1st thermo decomposition process became significant and released a colossal amount of heat quickly (27.17 J/g). The 2nd thermo decomposition became dominate from 249 ºC with fast but modest endothermic enthalpy to 263.29 ºC. From 270 ºC, the 3rd exothermic thermo decomposition predominated which was proposed from the decomposition of cellulose backbone. The deconvoluted weight derivative TGA curves of CMCBADMPDA-quat188 (Figure 5.12) showed that there were three major thermo decomposition chemical reaction processes that are responsible for the weight loss during the degradation of CMCBADMPDA-quat188, which corresponded to the three major thermo changing processes shown in its DSC thermogram.

DSC spectrum of CMCBADMPDA-C10 (Figure 5.13) showed that a glass transition around 43 ºC followed by a similar broad glass transition but in reverse direction from 71 ºC to 98 ºC. From 131 ºC, the C10 alkyl chain began melting. The small amount of impurities entrapped in its crystal structure was evaporated in this temperature range with very small weight loss, the 1st weight loss process. From 171 ºC to 221 ºC, the 2nd process began with a quick weight loss and

modest endothermic enthalpy, which is the process of Holfmann elimination. Decylene gas was proposed to be released. From 233 ºC, the ester elimination reaction became dominant with big endothermic enthalpy producing a strong endothermic peak of 43.2 J/g. The 3rd weight loss occurred at this temperature with the 2nd big weight loss, which was proposed to be the degradation of ester releasing decylene gas. After reaching 244 ºC, a 4th different chemical decomposition began with small endothermic enthalpy. From 285 ºC, another strong exothermic chemical decomposition process started, which is the 5th weight loss process. Significant weight loss occurred in the four chemical decomposition processes from the 2nd process to the 5th process. The deconvoluted weight derivative TGA curves of CMCBADMPDA-C10 (Figure 5.13) also showed that there are four major processes that are responsible for the weight loss of thermo degradation of CMCBADMPDA-C10. These processes are also overlapped together. Its DSC thermogram agreed with its deconvoluted TGA curve.

DSC spectrum of CMCBADMPDA-C10-Quat188 (Figure 5.14) showed a broad glass transition of local segments from 72 ºC to 113 ºC with little weight loss and an endothermic enthalpy. A stable physical molecular chain adjustment occurred up to 145 ºC. Then small amounts of impurity solvent began evaporated with a little weight loss, the 1st weight loss process. From 170 ºC, an endothermic thermal decomposition process took place with significant weight loss, which was proposed due to the Hofmann elimination, the 2nd weight loss process. From 199 ºC, this process overlapped with the exothermic thermal degradation which resulted from the quat-188 part, the 3rd weight loss process. A small endothermic peak rose from 220 ºC to 238 ºC, which was proposed to be caused from the possible melting of polymer molecules. From 238 ºC to 250 ºC, an endothermic process dominated due to the decomposition of the CMCBADMPDA-quat188 part of CMCBADMPDA-C10-Quat188, the 4th weight loss

process. The 5th process took place after reaching 250 ºC in which a strong exothermic degradation process dominated from the degradation of cellulose. The deconvoluted TGA weight derivative curve (Figure 5.14) showed five major weight loss processes from 130 ºC to 300 ºC, which were consistent with that showed in its DSC thermogram.

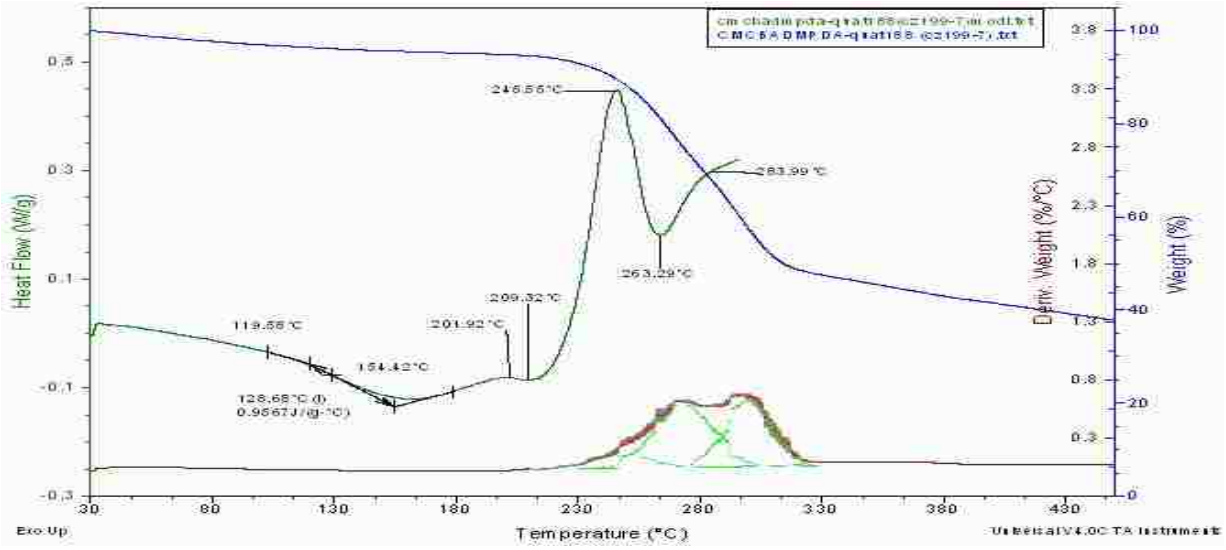

Figure 5.12. DSC curve, weight loss curve, and deconvoluted TGA weight derivative curve of CMCBADMPDA-quat188.

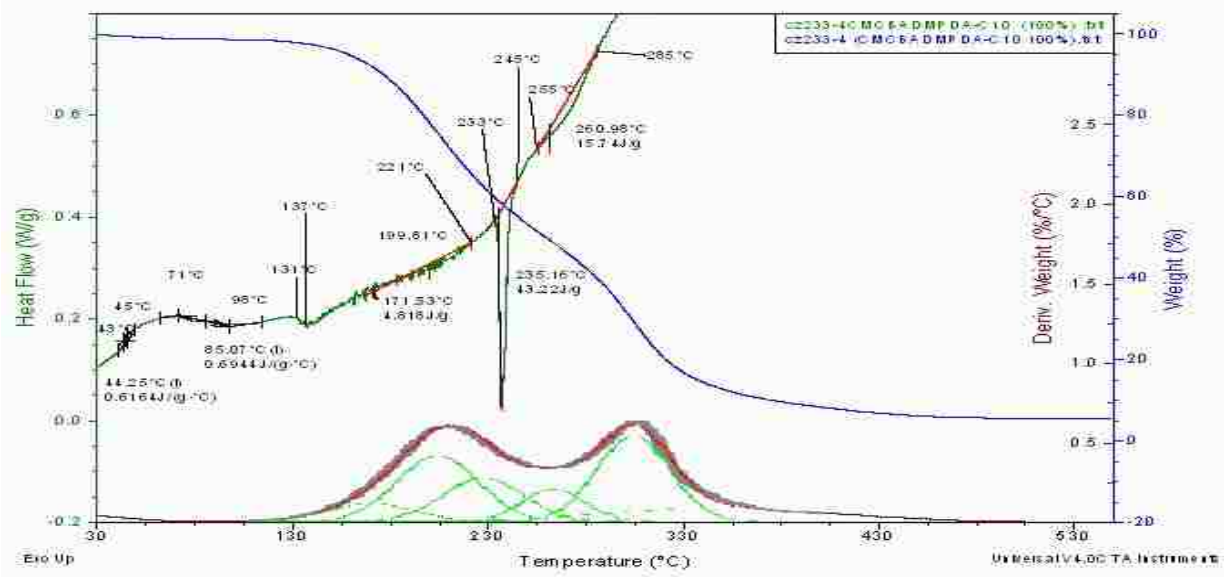

Figure 5.13. DSC curve, weight loss curve, and deconvoluted TGA weight derivative curve of CMCBADMPDA-C10 with targeted DS of C10 of 100%.

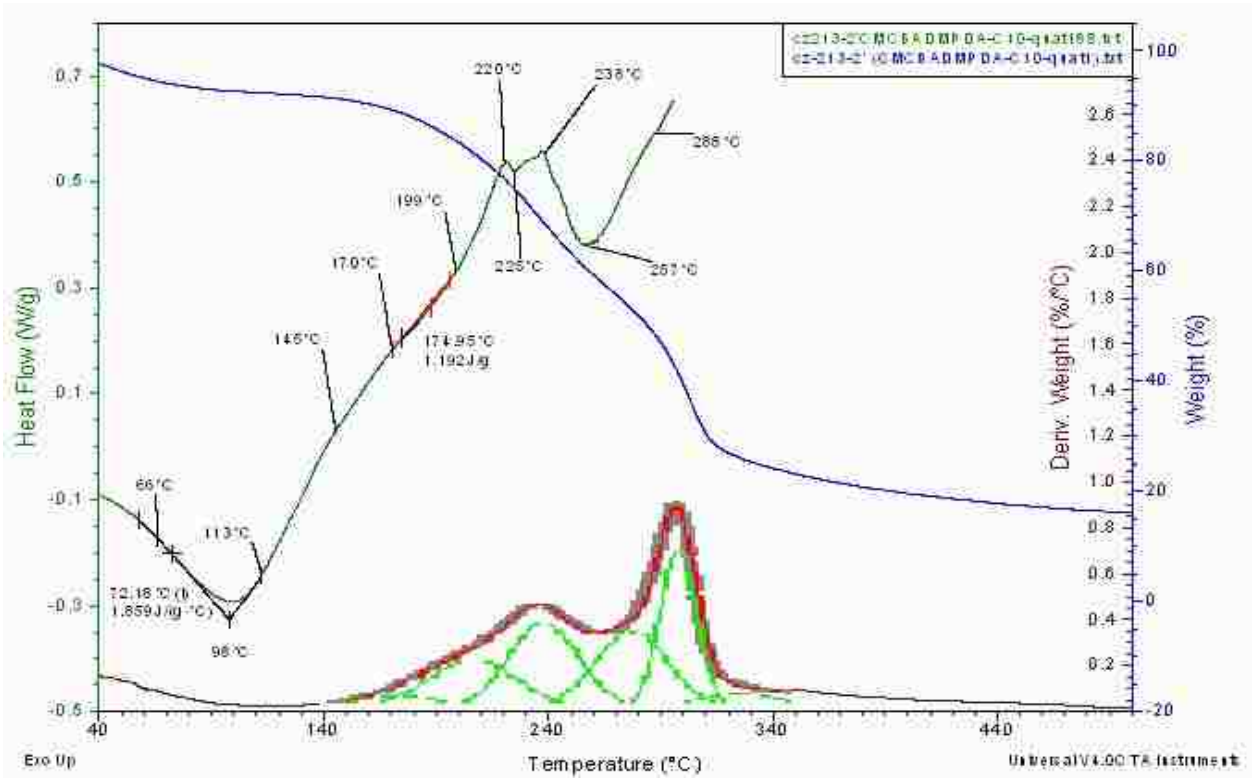

Figure 5.14. DSC curve, weight loss curve, and deconvoluted TGA weight derivative curve of CMCBADMPDA-C10-Quat188.

DSC spectrum of CMCBADMPDA-C10-PO (Figure 5.15) showed a long range molecular adjustment endothermic glass transition from 67 ºC to 117 ºC with minimal weight loss. Then it went through fine molecular adjustment around 154 ºC. From 158ºC to 224 ºC, the 1st endothermic thermo degradation process with small endothermic enthalpy gradually became a predominate process producing a big weight loss, which was related to the Hofmann elimination. Then an exothermic degrading process dominated for during 3 ºC, another process with endothermic enthalpy prevailed the thermal degradation from 226 ºC to 244 ºC, which was proposed to be the result of the melting of polymer molecules. The 2nd exothermic thermal degradation process controlled to 273 ºC, which was probably due to the degradation of proxylene oxide oligomer side chain. The 3rd exothermic degradation became dominating afterwards, which was related to the cellulose backbone degradation. The deconvoluted TGA

weight derivative curve of CMCBADMPDA-C10-PO (Figure 5.15) confirmed the three major thermal chemical degradation processes.

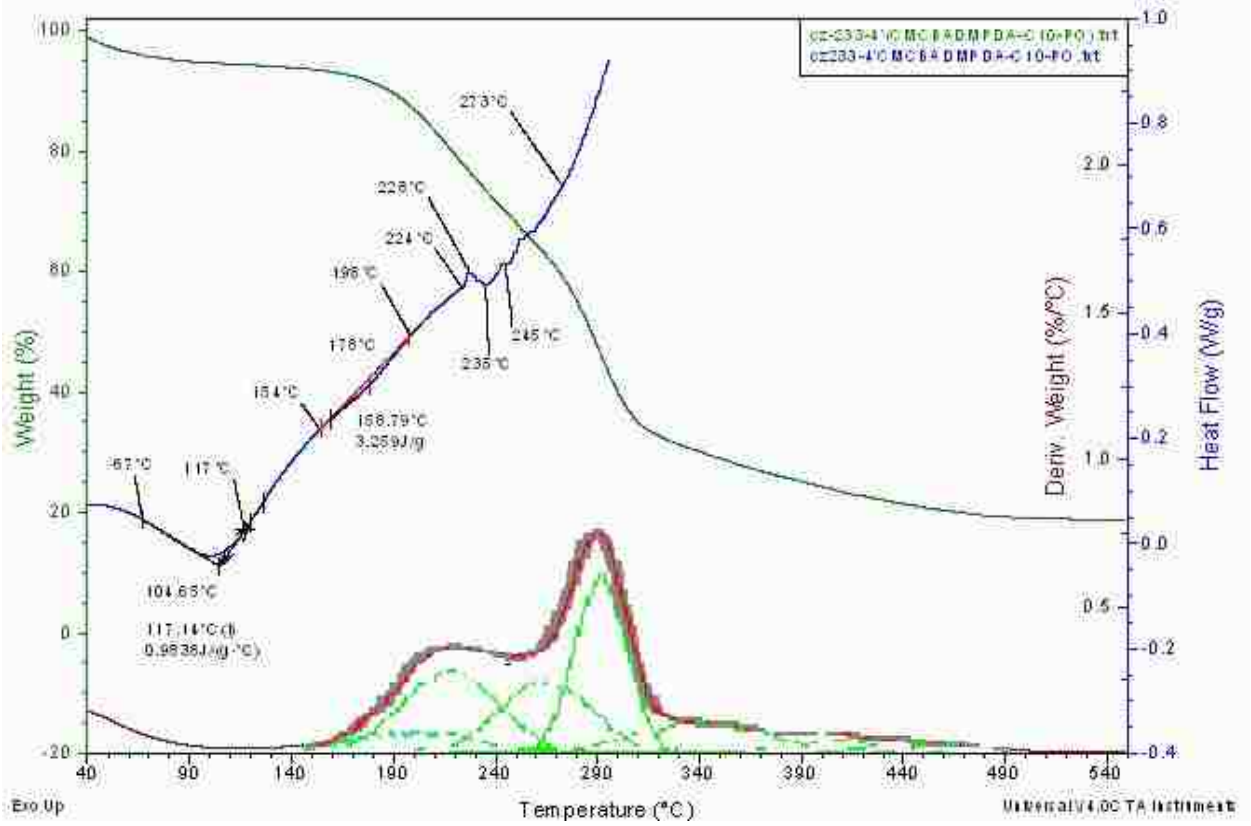

Figure 5.15. DSC curve, weight loss curve, and deconvoluted TGA weight derivative curve of CMCBADMPDA-C10-PO.

5.4 Conclusions

(1). CMCBADMPDA-R with R=C1~C18, CMCBADMPDA-C10-Quat188, CMCBADMPDA-C10-PO, and CMCBADMPDA-Quat188 were obtained. Their chemical structures were confirmed using NMR, FTIR. CMCBADMPDA-R with R=C1~C18 may contain a small amount of ester of COOR in its structure.

(2). The DS of C10 on CMCBADMPDA-C10-Quat188 and CMCBADMPDA-C10 were controlled by adjusting the relative concentration of $C_{10}H_{25}Br$ in the reaction system. Higher DQ derivatives could be obtained by increasing the relative concentration of $C_{10}H_{25}B$ in the reaction

system at a low concentration of $C_{10}H_{25}Br$. Increasing the relative concentration of $C_{10}H_{25}Br$ resulted in lower DQ when the concentration of C10-Br is above its critical concentration.

(3). CMCBADMPDA-C10 was an excellent catalyst for the esterification of alkyl bromide with carboxylic acid. This may be useful for making ester directly through salt of carboxylic acid with alkyl bromide path in industry.[97]

(4). The DQ of cellulose derivatives were measured using conductivity titration. The thermo properties of products synthesized were analyzed by TGA and DSC combined with their FTIR spectra. The titration results agreed with corresponding their FTIR spectra and their thermograms of TGA and DSC.

CHAPTER 6. ANTIMICROBIAL ASSESSMENT OF WATER SOLUBLE DENDRONIZED CELLULOSE DERIVATIVES WITH QUATERNARY AMMONIUM FUNCTIONAL GROUPS

6.1 Introduction

Biocidal polymers have numerous applications including its use as surgical gloves, condoms, ointments for medical devices, disinfectants, and preservatives in paints, waxes, oils, cosmetics, gels. As I have discussed in chapter 1, cellulose's advantage as an inexpensive abundant natural polymer have made itself a component in a variety of products. Several research groups have been interested in endowing cellulose with antibacterial properties to expand its application into new fields.

Cellulose polyquats, polyquaternium 10 and polyquaternium 4, have been used in shampoos, conditioners, gels, mousses, lotions, moisturizers, and cleansers as personal care products. Controlled free radical polymerization was recently used to graft cellulose with controlled lengths of vinyl polymers to modify the surface of cellulose. The grafted cellulose derivatives were elaborated for bearing quaternary nitrogen groups.[11, 14] Cellulose was chemically modified with dimethylol-5,5-dimethylhydantion and 2-amino-4-chloro-6-hydroxy-s-triazine for preparing antimicrobial textiles.[16-20, 98]

Recently, poly(propylene imine) dendrimer was quaternized with alkyl periphery groups in S. L. Cooper's group. The quaternized dendrimer exhibited high antimicrobial properties against *E. Coli* and *S. Aureus*.[47] The quaternization of chitosan, which was intensively investigated in Dr. Daly's group, provided a viable path for preparing quaternized cellulose derivatives.[5, 27, 28] The dendronization of cellulose supplied new possibilities for endowing cellulose with higher antimicrobial activities. Dendronized cellulose derivatives have the potential to carry more antibacterial functional groups with one molecule because of its compacted conformation in

aqueous solutions. The mechanism of the interaction of dendronized cellulose with bacteria cells may be different from that of polymeric antibacterial agents with random coil conformations in aqueous solutions. The rigid structures of dendronized cellulose derivatives with strong interaction with cells produce the potential to change the conformation of cell walls and to denature bacterial cells more efficiently. Therefore they have the potential to kill bacteria cells more effectively. Due to the degradable feature of natural cellulose backbones, dendronized cellulose antibiotics may also be degraded into small units with no harmful effects to the human body. In addition, they have the potential to be affordable and environmental benign antibiotics for many industrial applications.

In chapter 5, I synthesized dendronized cellulose derivatives CMCBADMPDA-Quat188 with hydrophilic di-quaternary nitrogen periphery groups and CMCBADMPDA-R with quaternary nitrogen with hydrophobic alkyl chain periphery groups. I also modified water insoluble CMCBADMPDA-C10 with propylene oxide and quat-188 into its water soluble forms of CMCBADMPDA-C10-PO and CMCBADMPDA-C10-Quat188.

In this chapter, I report their antimicrobial properties as determined by measuring their minimum inhibitory concentration (MIC) against two representative bacteria: gram negative bacterium *E-coli* and gram positive bacterium *S. aureus*. The influences of the dendritic structure, hydrophobicity/hydrophobicity of quaternary nitrogen, and the alkyl chain length of R on mono-quaternary nitrogen of CMCBADMPDA-R on the antimicrobial property were investigated.[99, 100] The effect of the degree of quaternization (DQ) of CMCBADMPDA-C10 on the antimicrobial activity was also studied.

Bacterial cells usually have five essential structural components: chromosomes, ribosomes, cytoplasmic membranes, and cell walls. Cell walls are the cell covering outside the cytoplasmic

membranes, which act as permeable barriers that regulate the passage of substances into and out of the cell, keep the chemical composition of the interior environment of the cell from changing, and to maintain the normal function of every component of bacteria cells. Phospholipid bilayers are important compositions of cell walls and cytoplasmic membranes that show their hydrophilic head groups in exterior surface and interior surface. Cytoplasmic membranes often consists of significant amount of phospholipids such as phosphatidylglycerol (PG) and phosphatidylethanolamine (PE).[101, 102] Water soluble fluorescence dyes encapsulated in phospholipid vesicles are frequently used[103, 104] as biomarkers for simulating the membrane breaking processes of cell walls and cytoplastic membranes. In this chapter, the influences of CMCBADMPDA-10 and CMCBADMPDA-10-quate188 on the permeability of bacterial cells are investigated by studying the dye release profile of calcein encapsulated in phospholipid vesicles self-assembled using PG and PE. The molecular structure and mechanism of the antimicrobial action of the dendronized cellulose derivatives are discussed.

6.2 Experimental

6.2.1 Materials

E. coli (ATCC 25922) and *S. aureus* (ATCC 29213) were the two microorganisms used for the MIC test. They were stored at -80 °C before the experiment. Potassium phosphate monobasic and potassium phosphate dibasic were from EMD Chemicals Inc. Sterile 96-well cell culture cluster plates were Costar® 3596 from Corning Inc. Polystyrene sterile tubes (5 mL capacity) were BD Falcon® from BD Biosciences. Difco™ Nutrient Broth (NB) was bought from Becton, Dickinson and Company. UV-VIS Spectrophotometer was a Cary 50 from Varian Inc. Acrylic disposable cuvettes were from Cutin Matheson Scientific, Inc. Syringe filters (0.2 μm) were from Nalge Company. Autoclave AMSCO Sterilizer 3021 was from AMSCO / STERIS.

Rolordrum™ and Shaker Model G-33 were from New Brunswick scientific Co, Inc. Eight channel pippettor was a Costar® 8-Pette multichannel pipettor from Corning Inc. Troughs were sterilizing polypropylene trays from Bel-Art Products.

Calcein used for dye release study was from Acros Organics. The PG used to form phospholipids was 1-palmitoyl-2-oleoyl-*sn*-glycero-3-[phospho-*rac*-(1-glycerol)] (POPG). Both POPG and PE were from Avanti Polar Lipids, Inc. Sephadex G-25 columns were from the PD-10 from Amersham Biosciences.

6.2.2 Evaluation of Antimicrobial Activity

The antimicrobial activities of dendronized cellulose derivatives were evaluated using their MIC values against two representative bacteria: gram negative bacterium *E-coli* and gram positive bacterium *S. aureus*. The assessments were conducted in transparent 96-well plates[28] by recording the lowest concentration of polymer which could keep the well clear after being incubated with bacteria cells.

6.2.2.1 Preparation of Solutions, Glassware, and Other Accessories

Phosphate buffer (PBS; pH=7): Aqueous KH_2PO_4 (0.1 M) solution was prepared by dissolving KH_2PO_4 (10.88 g, 0.080 mol) in distilled water (800 mL). Aqueous K_2HPO_4 (0.1 M) solution was prepared by dissolving K_2HPO_4 (13.92 g, 0.080 mol) in distilled water (800 mL). PBS (pH=7, 600 mL) solution was prepared by mixing KH_2PO_4 solution (0.1 M, 78 mL), K_2HPO_4 solution (0.1 M, 122 mL), and distilled water (400 mL) together.[28]

NB (0.8%) solution in PBS: NB (3.2 g) was dissolved in PBS (400 mL) to prepare NB broth (400 mL, 0.8%).

Glassware and other accessories: All glassware, solutions, water, micropipette tips, and troughs et al were autoclaved in an AMSCO Sterilizer 3021 at 120°C using steam (15 PSI) for 20 minutes on the day before the test.

6.2.2.2 Evaluation Procedures

Preparation of cell suspension: Cell suspensions had to be fresh and were prepared on the day of the test. *E-coli* and *S. aureus* taken directly from the refrigerator were separately inoculated into two culture test tubes with NB (5 mL). The test tube was then put on a Rolordrum™ from New Brunswick Scientific Co. and incubated at 37°C for 14 hours while rotating. Each of the above cell suspension (1 mL) was then transferred into a flask with sterile NB (25 mL). Each of the NB with bacteria cells was incubated at 37°C on a shaker (Shaker Model G-33) for *another* 3.5 hours in order to reach its mid-log phase.

The above suspensions (1 mL) were then diluted with sterile NB until the optical densities (OD) of the diluted suspensions were 0.200 for *E. coli.* and 0.400 for *S. aureus* respectively. Their ODs were measured using 600 nm wave number light on a Cary 50 UV-Vis spectrometer; absorbencies were autozeroed with the sterile NB. The diluted suspensions were further diluted with sterile NB with a dilution factor of 5. The clear cell suspensions prepared were immediately stored at 0°C for the MIC test. The dilution should be conducted in a clean sterile hood.

Sterilization of the working hood: The bench in the hood was sprayed with ethanol and burned to kill bacteria before the test. Two flames of ethanol were maintained in the hood while preparing 96-well plates for the test.

Preparation of 96-well plates: The test plates were prepared in a sterile working hood. The 96-well plates were divided into three different columns (zones) for three purposes: cell control,

agent control, and agent test (Scheme 6.1). Table 6.1 showed the compositions of the wells for each zone on 96-well plates. One kind of cellulose derivative was only permitted in each agent control column and each agent test column. Different concentrations of one cellulose derivative (50 μL) were added to the wells in one agent control column and one agent test column from a range of high concentration to low concentration with a dilution factor of two corresponding to the wells from A to H. PBS (50 μL) was then added to each well on the plate. Distilled water (100 μL) was added to each well of cell control. Next, NB (50 μL) was added to each well of agent control. Finally, cell suspension (50 μL) was added to each well of cell control and agent test column. The plate was then enclosed with the cover. Each well on the plate should be clear after all compositions were added to the wells.

Scheme 6.1. Schematic representation of a 96-well plate for antimicrobial activity evaluation[28]

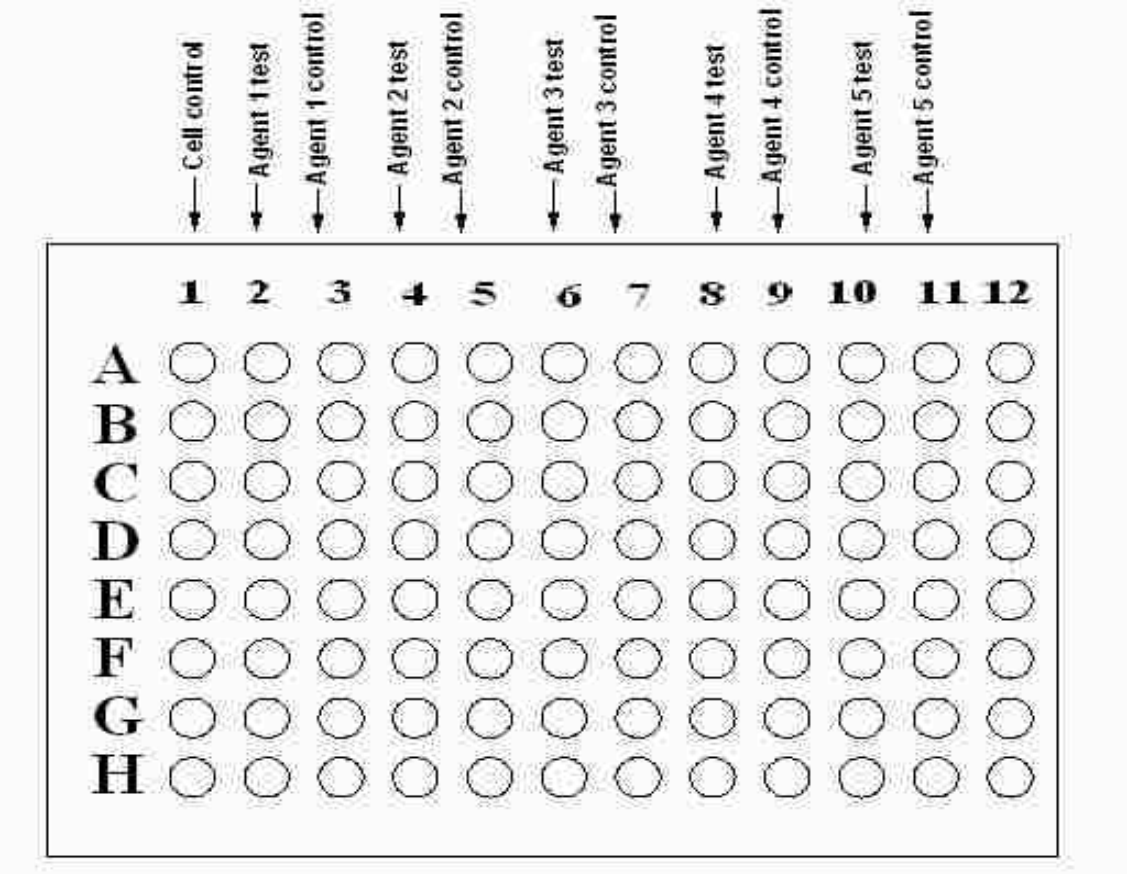

Table 6.1. The compositions in the wells in the three zones on 96-well plates

	Cell Control	Agent Control	Test Well
PBS	50μL	50μL	50μL
Distilled water	100μL		
Antibacterial agent		100μL	100μL
NB		50μL	
Cell suspension	50μL		50μL

Evaluation of MIC values and antimicrobial activities: The finished plate was incubated at 37°C for 14 hours. Each well was then analyzed based on its clarity. The clear well in agent test column indicated that the cellulose derivative could inhibit the growth of the microorganism at its concentration in this well. The turbid well in agent test column indicated that the cellulose derivative could not inhibit the microorganism growth at its concentration in this well. The lowest concentration of the cellulose derivative in the well, which was clear after incubation with bacteria cells, was defined as its MIC value. After incubation, the wells of cell control should be turbid but the wells of agent control should be clear.

6.2.3 Dye Release in Encapsulated Phospholipid Vesicles

POPG (12.5 μmol, 0.96 mL) and PE (12.5 μmol, 0.90 mL) were mixed in a small vial. Nitrogen gas was used to evaporate the solvent. The vial was then roto-vaporated to completely remove the solvents. Calcein (2.5mL, 40 mM) in PBS buffer (10mM, pH=7) was added to the vial. The solution was then warmed in water and frozen in acetone/liquid nitrogen for three cycles. After sonication for 15 minutes, it was sequentially frozen, warmed, sonicated, frozen, and warmed. The suspension was then run through a Sephadex G-25 column to remove the

excess calcein.[103] A FP-6300 JASCO fluorescence spectrometer was used to monitor the fluorescence intensity change at 494 nm excitation light and 512 nm excitation light after adding quaternary dendronized cellulose derivative solution into the phospholipid vesicle suspension with calcein entrapped inside. The bandwidths for both excitation and emission were kept at 2.5 nm.

6.3 Results and Discussion

6.3.1 Dendritic Effect on the Antibacterial Properties of Dendronized Cellulose

In this project, the first question we wanted to answer was if the dendritic structures of cellulose derivatives could improve their antimicrobial performance. I synthesized the quaternary ammonium dendronized cellulose derivatives with alkyl chains of C8 and C12 (CMCBADMPDA-C8 and CMCBADMPDA-C12) and their corresponding cellulose derivatives without dendritic structure (CMCDMPDA-C8 and CMCDMPDA-C12) at room temperature. The MIC test result were listed in Table 6.2.

Table 6.2. Effect of dendritic structure on the antimicrobial activity of cellulose derivatives

	MIC (μg/mL) against *E-coli*	MIC (μg/mL) against *S-aureus*
CMCDMPDA-C8	>512[a]	>512[a]
CMCBADMPDA-C8	512[a]	512[a]
CMCDMPDA-C12	>256[b]	>256[b]
CMCBADMPDA-C12	256[b]	256[b]

a---- In 1.5% Et-OH
b----in H2O

Table 6.2 showed that CMCBADMPDA-C8 had MIC values of 512 μg/mL against E-Coli and 512 μg/mL against S-aureus, which were both lower than that of CMCDMPDA-C8. CMCBADMPDA-C12 showed MIC values of 256 μg/mL against *E-coli* and 256 μg/mL against *S-aureus*, which were also both lower than that of CMCDMPDA-C12. Both CMCBADMPDA-C8 and CMCBADMPDA-C12 with dendritic structure demonstrated better antimicrobial

performance compared to their corresponding derivative CMCDMPDA-R without dendritic structure. The dendritic structures of cellulose derivatives could improve their antimicrobial performance.

6.3.2 Effect of Di-quaternary Nitrogen and Chain Lengths on the Antibacterial Properties of Dendronized Cellulose

Antimicrobial activities were found in some quaternized chitosan derivatives that were synthesized by modifying chitosan with quat-188 by D. Logan and Mrunal R. Thatte in our group; but it was not clear where these antimicrobial activities came from. The question was "Did the quaternary nitrogen produced with qaut188 or the hydrophobic structure of chitosan lead to the antibacterial properties of polymers modified with quat-188?" To design better polysaccharide derivative antibiotics, it is critical to understand the source of these antimicrobial properties. I synthesized CMCBADMPDA-Quat188 with highly concentrated hydrophilic periphery di-quaternary nitrogen and CMCBADMPDA-R with different hydrophobic alkyl chains, different alkyl chain length, on monoquaternary nitrogen as periphery groups. The MIC test results (Table 6.3) showed that the MIC values of CMCBADMPDA-Quat188 against *E-coli* and against *S-aureus* were both higher than 512 μg/mL. The low antimicrobial activity of CMCBADMPDA-Quat188 proved that the antibacterial properties of quaternized polymers prepared with quat-188 did not result from the hydrophilic quaternary nitrogen produced with quat188.

The hydrophobicity of the alkyl chain on periphery monoquaternary nitrogen of dendronized cellulose derivatives showed important influences on their antimicrobial activities (Table 6.3). All derivatives CMCBADMPDA-R with carbon chain length of eight, ten, and twelve demonstrated antimicrobial activity. CMCBADMPDA-C10 showed better antimicrobial

performance than CMCBADMPDA-R with other chain lengths. The hydrophobic alkyl chain on periphery quaternary nitrogen could endow dendronized cellulose derivatives with antimicrobial properties. Our quaternized dendronized cellulose derivatives showed similar chain length effects on the antimicrobial behavior to that of quaternized poly(propyleneimine) dendrimers developed in Stuart L. Cooper's group.[47]

Table 6.3. Effect of chain lengths and diquat on the antibacterial properties of dendronized cellulose

		MIC (μg/mL) against *E-coli*	MIC (μg/mL) against *S-aureus*
Diquat	CMCBADMPDA-Quat188	>512 [b]	>512 [b]
Chain length effect	CMCBADMPDA-C4	>512 [a]	>512 [a]
	CMCBADMPDA-C6	>512 [a]	>512 [a]
	CMCBADMPDA-C8	512 [a]	512 [a]
	CMCBADMPDA-C10	32 [b]	16 [b]
	CMCBADMPDA-C12	512 [a]	128 [a]
	CMCBADMPDA-C18	>512 [a]	>512 [a]

a---- In 1.5% Et-OH
b----in H2O

6.3.3 Effects of Degree of Quaternization on the Antibacterial Properties of CMCBADMPDA-C10

The DS of functional groups is important in determining the property of modified polymer. We chose to use CMCBADMPDA-C10 to study the influence of their DQ on their antimicrobial performance. In this project, the extended DS of C10 was defined as the weight percentage of C10 in the sample. Since there was esterification reaction accompanied with quaternization, the extended DS of C10 on CMCBADMPDA-C10 included two parts: the C10 alkyl chain on quaternary nitrogen and that on the ester. The DQ is the weight percentage of quaternary nitrogen in the dendronized cellulose derivative, which truly reflects the degree of quaternization and the weight percentage of C10 on quaternary nitrogen.

The MIC test of CMCBADMPDA-10 (Table 6.4) showed that CMCBADMPDA-10 with DQ of 2.03% 1.49%, 1.44% had MIC values of 32, 128, and that higher than 128 µg/mL against *E-coli* respectively. In comparison, they showed MIC values of 16, 128, and the value higher than 128 µg/mL against *S-aureus* respectively. CMCBADMPDA-10 with higher DQ exhibited lower MIC values against both of *E-Coli* and *S-aureus* and higher antimicrobial activities.

Table 6.4. Effect of DQ on the antibacterial properties of dendronized cellulose CMCBADMPDA-C10

Samples	Cz 215-1	Cz215-2	Cz215-3
Target extended DS (%)	15%	20%	25%
Targeted DQ (N^+%)	2.22	2.73	3.05
DQ (N^+%)	1.44	2.03	1.49
MIC (µg/mL) against *E-Coli*	>128	32	128
MIC (µg/mL) against *S-aureus*	>128	16	128

The extended DS of C10 on CMCBADMPDA-C10 (Table 6.4) showed complex effects on their antimicrobial performance. CMCBADMPDA-C10 reached the lowest MIC values, 32 µg/mL against *E-coli* and 16 µg/mL against *S-aureus*, and the best antimicrobial performance at target extended DS of 20%. CMCBADMPDA-C10 with target extended DS of C10 higher than 20% or target extended DS of C10 lower than 20% showed weaker antimicrobial performances. The reason was that initially increasing the relative concentration of $C_{10}H_{25}Br$ in reaction system could increase the DQ of CMCBADMPDA-C10. When the relative concentration of $C_{10}H_{25}Br$ in reaction system was above a critical concentration, more amounts of $C_{10}H_{25}Br$ were transformed into the C10 ester residue groups but not the C10 on periphery quaternary nitrogen

of CMCBADMPDA-C10. A high extended DS, CMCBADMPDA-C10 became water insoluble and exhibited higher MIC value and lower antimicrobial activity in the MIC test.

6.3.4 Effect of Degree of Quaternization of C10 on the Antibacterial Properties of CMCBADMPDA-C10-Quat188

CMCBADMPDA-C10 became water insoluble when its target extended DS of C10 was above 25%. By modifying CMCBADMPDA-C10 with quat188, water insoluble derivatives CMCBADMPDA-C10 with high target extended DS were transformed into the derivatives CMCBADMPDA-C10-quat188, which were water soluble. Table 6.5 shows that CMCBADMPDA-C10-quat188 with DQ of C10 1.44%, 1.49%, and 2.03% exhibited MIC values of 256, 128, and 64 µg/mL against both *E-coli* and *S-aureus* respectively. The CMCBADMPDA-C10-quat188 with higher DQ of C10 demonstrated lower MIC values and higher antimicrobial activity.

Table 6.5. Effect of DQ of C10 on the antibacterial properties of CMCBADMPDA-C10-Quat188

Target extended DS of C10	DQ (N^+%)	Samples	MIC (µg/mL) against *E-Coli*	MIC (µg/mL) against *S-aureus*
15%	1.44	CMCBADMPDA-C10-Quat188	256	256
20%	2.03	CMCBADMPDA-C10-Quat188	64	64
25%	1.49	CMCBADMPDA-C10-Quat188	128	128
40%	1.48	CMCBADMPDA-C10-Quat188	128	128
50%	1.49	CMCBADMPDA-C10-Quat188	128	128

Table 6.5 also shows that CMCBADMPDA-C10-quat188 expressed the highest antimicrobial activity, 64µg/mL against both of *E-coli* and *S-aureus*, when the target extended DS of the starting reactant CMCBADMPDA-C10 was at 20%. This result agreed with the MIC test result of CMCBADMPDA-C10 with different target extended DS of C10. This proved that the antimicrobial property of dendronized cellulose derivatives came from their hydrophobic C10 alkyl chain. The DQ of CMCBADMPDA-C10 determined the DS of C10 in CMCBADMPDA-

C10-quat188 because the C10 ester in CMCBADMPDA-C10 was hydrolyzed in preparing CMCBADMPDA-C10-quat188. When the target extended DS of C10 was above 20%, the DQ of mono-quaternary nitrogen with C10 of CMCBADMPDA-C10-quat188 were kept at similar levels. This lead to the result that the MIC values of corresponding CMCBADMPDA-C10-quat188 were maintained at 128 ppm against both *E-coli* and *S-aureus*. Table 6.5 clearly shows that CMCBADMPDA-C10-quat188 with higher DQ exhibited higher antimicrobial activity. Their antimicrobial activity resulted from the hydrophobic periphery alkyl chain C10.

6.3.5 The Antimicrobial Property of CMCBADMPDA-C10-PO

If the assumption that the antimicrobial property of quaternized polymers came from the hydrophobic alkyl chain was correct, CMCBADMPDA-C10-PO was expected to show certain degrees of antimicrobial activity. I synthesized CMCBADMPDA-C10 using extra amount of $C_{10}H_{25}Br$ and then I transformed it into CMCBADMPDA-C10-PO, which was water soluble. The MIC test (Table 6.6) shows that CMCBADMPDA-C10-PO demonstrated limited antimicrobial activity. It is well known that neither cellulose nor polypropylene oxide exhibits antimicrobial activity. The antimicrobial activity of CMCBADMPDA-C10-PO must come from the hydrophobic part C10 on quaternary nitrogen in the dendronized cellulose derivatives.

Table 6.6. The antimicrobial properties of dendronized cellulose CMCBADMPDA-C10-PO

Sample	MIC (μg/mL) against *E-coli*	MIC (μg/mL) against *S-aureus*
CMCBADMPDA-C10-PO	256	256

----CMC (700k, DS=0.9)

6.3.6 The Mode of Antimicrobial Action of Dendronized Cellulose Derivatives

Trimethyl decanyl ammonium bromide usually shows MIC value against *S-aureus* to be around 79.4 μg/mL.[105] Our dendronized cellulose derivatives CMCBADMPDA-C10 could show MIC values of 32 μg/mL against *E-coli* and 16 μg/mL against *S-aureus*. The

antimicrobial activity of CMCBADMPDA-C10 was improved significantly compared to that of trimethyl decanyl ammonium bromide and that of CMCDMPDA-C10. It is broadly accepted that ordinary polymeric agent molecules with random coil conformation first absorb or bind with bacteria cell membranes that have negative charges through electrostatic attractions.[106] Then polymeric agents affect the membrane permeability which leads to the leakage of proteinaceous material and other intracellular constituents of microbial cells. This can cause the death of cells because of the loss of essential fluids.

We proposed that the action mode of our dendronized CMCBADMPDA-R (Scheme 6.2) may be similar to that of ordinary quaternized polymeric agents that bind with the negative charged cell membranes due to their electrostatic attractions. However, they are probably more efficient in breaking the cell membranes due to the many hydrophobic alkyl chains on their rigid and compacted molecular structures. The positive charges of periphery quaternary nitrogen on CMCBADMPDA-R are believed to be helpful in binding CMCBADMPDA-R molecules on the negative cell membranes.

The processes of CMCBADMPDA-R killing microorganism are proposed as the following:

(1) Numerous periphery positive charges of dendronized structure attach on the membrane surface of microbial cells primarily due to the strong electrostatic attractions with the negative charged cell membranes.

(2) Several hydrophobic alkyl chain needles can insert into the membranes of bacterial cells.

(3) The molecular motions of the rigid structure of CMCBADMPDA-R join the segment motions of hydrophobic alkyl chain needles that are inserted into the membranes of microbial cells.

(4) The motions of alkyl chain needles on cell membranes break the membranes.

(5) The cytoplasmic liquids leak out of the cells from the broken membranes.

(6) The microorganism cells die due to the leaking of their cytoplasmic liquids

Scheme 6.2. The action mode of our dendronized CMCBADMPDA-R killing bacteria cell[a]

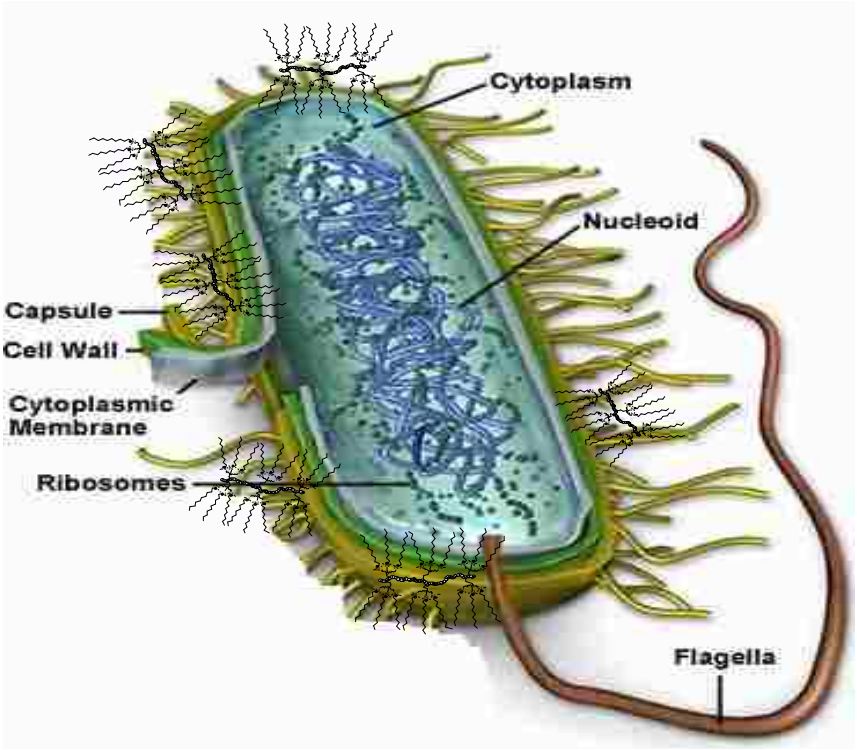

[a]This scheme is the modification of the prokaryotic cell image from http://micro.magnet.fsu.edu/cells/procaryotes/images/procaryote.jpg.

6.3.7 Phospholipid Vesicle Leakage Releasing Encapsulated Dye

To understand how our quaternary dendronized cellulose derivatives kill bacteria or inhibit the growth of bacteria, I used POPG and PE, two common compositions in the lipid bilayer of bacteria cell, to self-assemble into phospholipid vesicles in a PBS water solution in pH=7. Water soluble dye calcein was entrapped inside the phospholipid vesicles in the self assembly process. After removing the excess dye, the suspensions of POPG/PE vesicles (Figure 6.1) showed increased fluorescence signal of emission light around 512 nm with the increasing of their exposing time to dilute CMCBADMPDA-C10 and CMCBADMPDA-C10-quat188. After

adding small quantities of CMCBADMPDA-C10 and CMCBADMPDA-C10-quat188, the phospholipid vesicles showed defects in their bilayer structure which separated the dye inside and the water outside the vesicles. The quenched calcein molecules inside the vesicles passed through these defects of bilayer walls of phospholipid vesicles. The increased concentration of calcein in PBS water media outside the vesicles produced the increasing fluorescence signal in figure 6.1 with the increasing time of exposure of these vesicles to both CMCBADMPDA-C10 and CMCBADMPDA-C10-quat188. This suggested that both CMCBADMPDA-C10 and CMCBADMPDA-C10-quat188 probably could break the membranes of bacterial cells, leading to leaking of cytoplasmic liquid inside bacteria, and produce the death of bacteria.

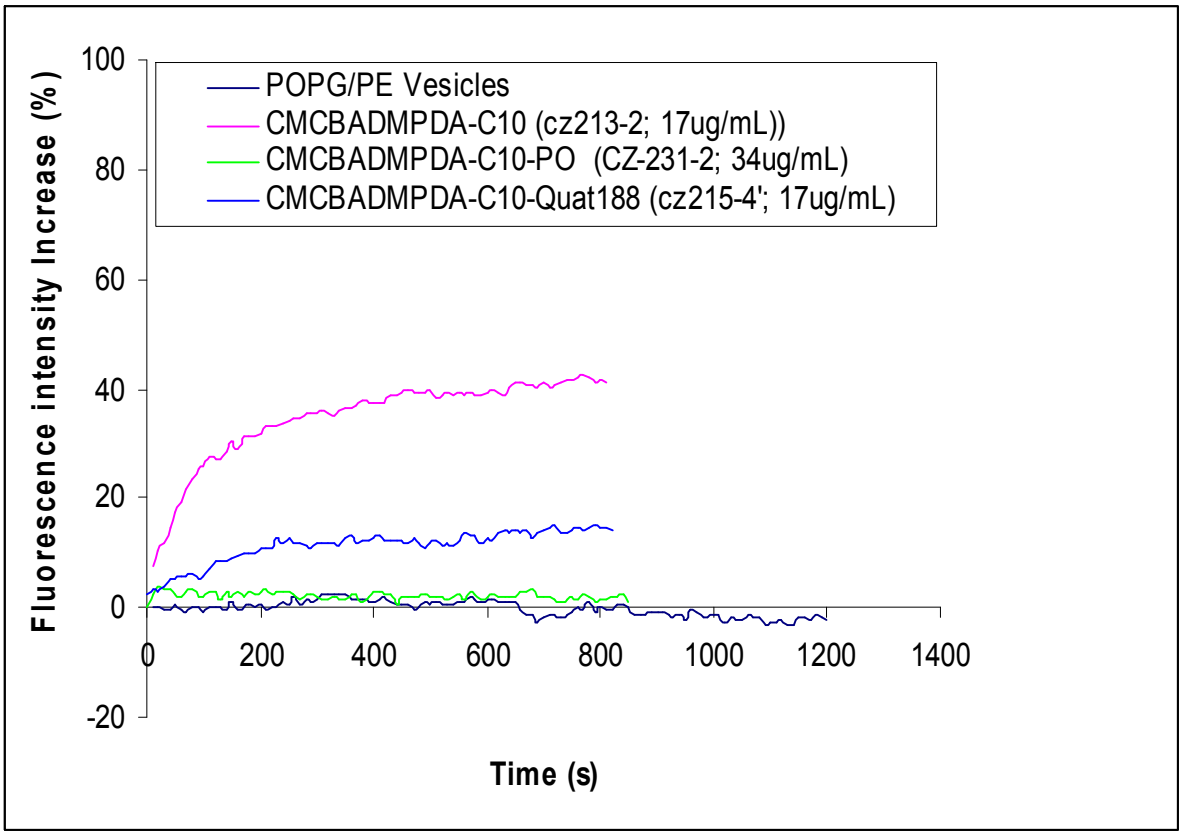

Figure 6.1. Dye release profile from PG/PE vesicles encapsulated with calcein after adding CMCBADMPDA-C10 (17 μg/mL; MIC: 32 μg/mL against *E-Coli*), CMCBADMPDA-C10-Qaut188 (17 μg/mL; MIC: 256 μg/mL), and CMCBADMPDA-C10-PO (34 μg/mL, MIC>512 μg/mL).

6.4 Conclusions

(1) Dendronized cellulose derivatives CMCBADMPDA-R with hydrophobic alkyl chains showed better antimicrobial performance compared to their counterparts without a dendritic structure, CMCDMPDA-R.

(2) All CMCBADMPDA-C8, CMCBADMPDA-C10, and CMCBADMPDA-C12 demonstrated antimicrobial activities.

(3) CMCBADMPDA-C10 exhibited higher antimicrobial activity than derivatives CMCBADMPDA-R with other alkyl chain lengths.

(4) CMCBADMPDA-C10 at DQ of 2.03% showed the best antimicrobial properties at 32 μg/mL against *E-coli* and 16 μg/mL against *S-aureus*.

(5) The best MIC values for CMCBADMPDA-C10-quat188 we obtained were 64 μg/mL against *E-coli* and 64 μg/mL against *S-aureus*.

(6) CMCBADMPDA-C10-PO demonstrated limited antimicrobial activity.

(7) CMCBADMPDA-Quat188 did not show potent antibacterial activity. The antimicrobial activity of quaternized polymer did not come from the hydrophilic quaternary nitrogen groups produced with quat-188.

(8) Hydrophobic alkyl chains on quaternary nitrogen conferred the dendronized cellulose derivatives antimicrobial activity.

CHAPTER 7. SYNTHESIS OF DENDRONIZED CELLULOSE DERIVATIVES BY NUCLEOPHILIC SUBSTITUTION OF TOSYLATED CELLULOSE OR BROMOPROPYLCELLULOSE

7.1 Introduction

In the previous six chapters, I have discussed the synthesis and biological properties of dendronized cellulose derivatives prepared from sodium carboxylmethyl cellulose. It would be appealing if we could synthesize dendronized cellulose derivatives directly from cellulose backbone. One possible way to achieve this goal is to start the synthesis of dendronized cellulose from cellulosics with good leaving groups for nucleophilic substitution. Two such derivatives would be tosylated celluslose (Scheme 7.1) and bromopropyl cellulose. (Scheme 7.2) Thomas Heinze *etc.* synthesized cellulose p-toluene sulfonic acid esters (tosylates) homogeneously in dimethylacetamide (DMAC)/ lithium chloride (LiCl), a good solvent system for cellulose.[107] Tim F. Liebert et al also reported the homogeneous synthesis of tosylcelluloses with DS from 0.4 up to 2.3 with different cellulosic materials using a co-solvent system of dimethyl sulfoxide (DMSO)/tetrabutyl ammonium fluoride (Bu_4NF).[108, 109] Recently, Klemm et al investigated the synthesis of cellulose tosylates with a diamino compound, 1,4-phenylenediamine, at 100 ºC.[110] U. Mais et al reported the synthesis of the functionalized cellulose derivative by reacting tosylated cellulose with dimethylamine at 50 ºC.[111]

Halides of cellulosics can be substituted by electro-rich amino groups. N. Aoki synthesized bromodeoxycellulose with DS around 0.8~0.9 using N-bromosuccinimide (NBS)-triphenyl phosphine to react with cellulose in LiBr-DMAC solution.[112, 113] Phosphorus trihalides have been traditionally used to transform hydroxyl groups into halides groups.[114] Hydroxyethylcellulose and hydroxypropyl cellulose (HPC) are commercially available. In this

project, bromopropyl cellulose (HP-Br) was synthesized using phosphorus tribromide to react HPC.

In this chapter, I describe the synthesis of tosylated cellulose in a DMAC/LiCl solution, and the synthesis of bromopropyl cellulose by reacting phosphorus tribromide with hydroxypropyl cellulose. Each of these substrates was allowed to react with Behara's amine (BA) in an effort to produce dendronized cellulose. A dendronized cellulose derivative with BA dendron (HPC-BA) was obtained though the nucleophilic substitution of bromopropylcellulose with the amino group of BA.(Scheme 7.2) However, no evidence for dendronized derivative formation was detected when cellulose tosylate was used as a substrate as proposed in Scheme 7.1.

Scheme 7.1. Proposed synthetic route of Cellulose-BA through tosylated cellulose

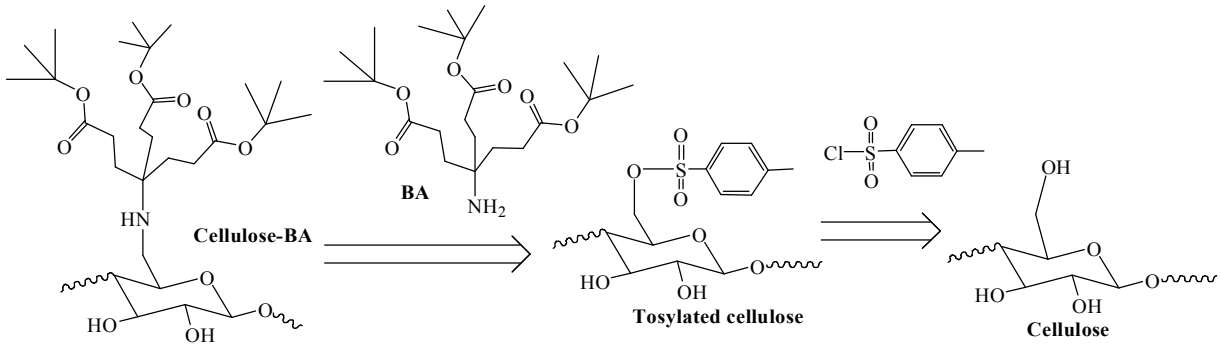

Scheme 7.2. Proposed synthetic route of HPC-BA through bromopropyl cellulose

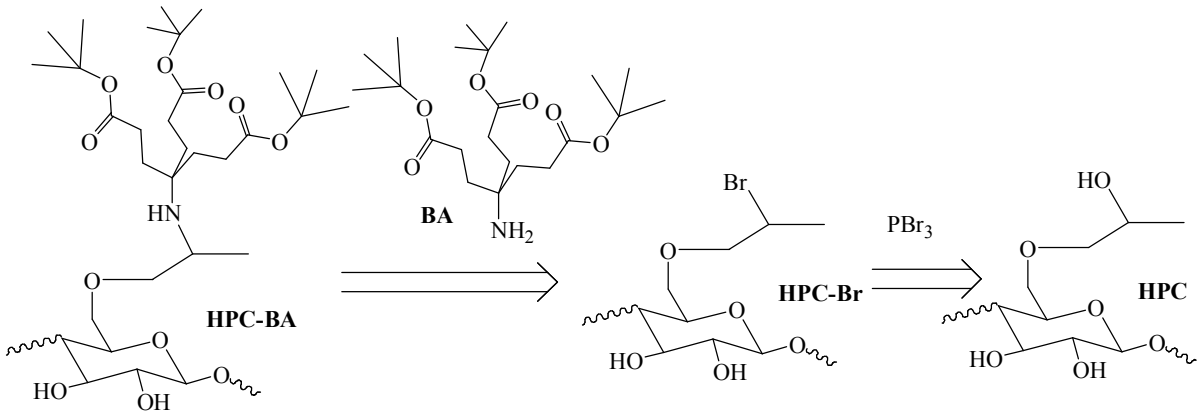

7.2 Experimental

7.2.1 Synthesis of Tosylated Cellulose

The synthesis of tosylated cellulose followed the procedure published by Thomas Heinze.[107] Cellulose (Avicel, 1.00 g, 8.77 mmol) was heated with DMAC (100 mL) at 140 ºC under stirring. Dried LiCl (2.00 g, 47.17 mmol) was added. The mixture was gradually cooled to room temperature under stirring and was kept overnight. The clear cellulose solution was then cooled to 8 ºC. Triethylamine (2 mL, 14.39 mmol) was added. Tosylchloride (2 g, 11.20 mmol) in DMAC (2 mL) was added to the above mixture. A slight pink colloid was formed immediately. The mixture was kept at 8 ºC and stirred for another 10 minutes. It was then added to ice-water (300 mL) in order to precipitate the product. After filtration, the crude product was suspended in ethanol (150mL) and filtered again. After filtration, the white crude product was re-suspended in acetone (150mL) and precipitated with water (200 mL). The solid recovered after the 2nd filtration was dried in an oven at 40ºC in vacuum. The product (0.96 g) was obtained as a white solid. ^{1}H NMR (DMSO-d_6) (Figure 7.1), δ (ppm): 1.22(C*H*$_3$), 7.48(C*H*CCH$_3$], 7.82[SCC*H,* aromatic H], 3.0-5.2 (broad peaks of anhydroglucose ring).

7.2.2 Synthesis of N,N-dimethylaminopropylcarbomoylmethyl Modified Cellulose (Cellulose-DMPDA) from Tosylated Cellulose

Tosylated cellulose (0.2 g) was dissolved in DMAC (50 mL). At 40 ºC, DMPDA (5 mL, 39.64 mmol) was added to the above solution. The reaction was maintained at 50 ºC for 24 hours. Then it was dialyzed with water for one week, and the solution in the tube was concentrated to approximately xx mL using a rotovap. The residual liquid was freeze dried. A white cotton-like product (0.15 g) was obtained. Cellulose-DMPDA ^{1}H NMR (D_2O), δ (ppm): 2.13(C*H*$_2$NHC*H*$_2$),

2.42 [$CH_2^+NH(CH_3)_2$], 1.87 ($CH_2CH_2CH_2$), 2.72[$CH_2^+NH(CH_3)_2$], 3.0-4.6 (broad peaks of anhydroglucose ring).

7.2.3 Synthesis of Bromopropylcellulose

Dried HPC (2.02 g, 11.73 mmol) was dissolved in dried THF (40 mL) and the reaction flask was immersed in an icewater bath to maintain the temperature at 5 ºC PBr_3 (0.25 g, 0.92 mmol) dispersed in dried THF (5 mL) was added to the solution of HPC drop by drop during a 10 minute interval. The reaction was stirred at 5 ºC for 2 hours. The mixture was then dialyzed against water. After dialysis, half of the suspension was freeze-dried and a white solid (0.60 g) was obtained. The remainder of the suspension was allowed to react with BA.

7.2.4 Synthesis of Cellulose-BA from Bromopropylcellulose

One half of HPC-Br (0.60g) suspension from dialysis was mixed with DMF (5 mL). The mixture was then concentrated in order to remove water and to form a HPC-Br/DMF suspension. Triethylamine (0.2 mL, 1.44 mmol) and BA (0.50 g, 11.23 mmol) dissolved in ethanol (25 mL) were added to the HPC-Br/DMF suspension. The reaction was kept at 50 ºC for 24 hours. The mixture was then concentrated by a rotovap until it became a wet oil. The wet oil was suspended in dichloromethane (DCM, 50 mL) and extracted with DCM (20 mL) three times. The precipitation was re-suspended in water (100 mL). After filtration, the slurry was freeze dried. A white product (0.50 g) was obtained; ^1H NMR (DMSO-d_6), δ (ppm): 1.05(CH_3CH), 1.39(CCH_3), 1.65(CCH_2CH_2), 2.19(CCH_2CH_2), 3.0-4.6 (broad peaks of anhydroglucose ring).

7.3 Results and Discussion

7.3.1 Attempted Synthesis of Cellulose-BA via Tosylated Cellulose

Cellulose needs to be heated with DMAC above 140 ºC prior to attempting to dissolve it. LiCl was added at a high temperature to form a complex with cellulose. The solution does not form immediately, but after overnight cooling, the cellulose suspension in DMAC/LiCl became a clear colorless solution. The tosylation process was very fast. Since the reaction is sensitive to water moisture, it is critical to assure that all reagents are dry before attempting the reaction. The tosylated cellulose was soluble in DMAC, DMSO, and pyridine. The proton NMR spectrum of tosylated cellulose (Figure 7.1) in DMSO showed both the chemical shifts of protons from aromatic ring at 7.48 and 7.82 and those of the anhydroglucose ring as a broad multiplet ranging from 3 to 5.3.

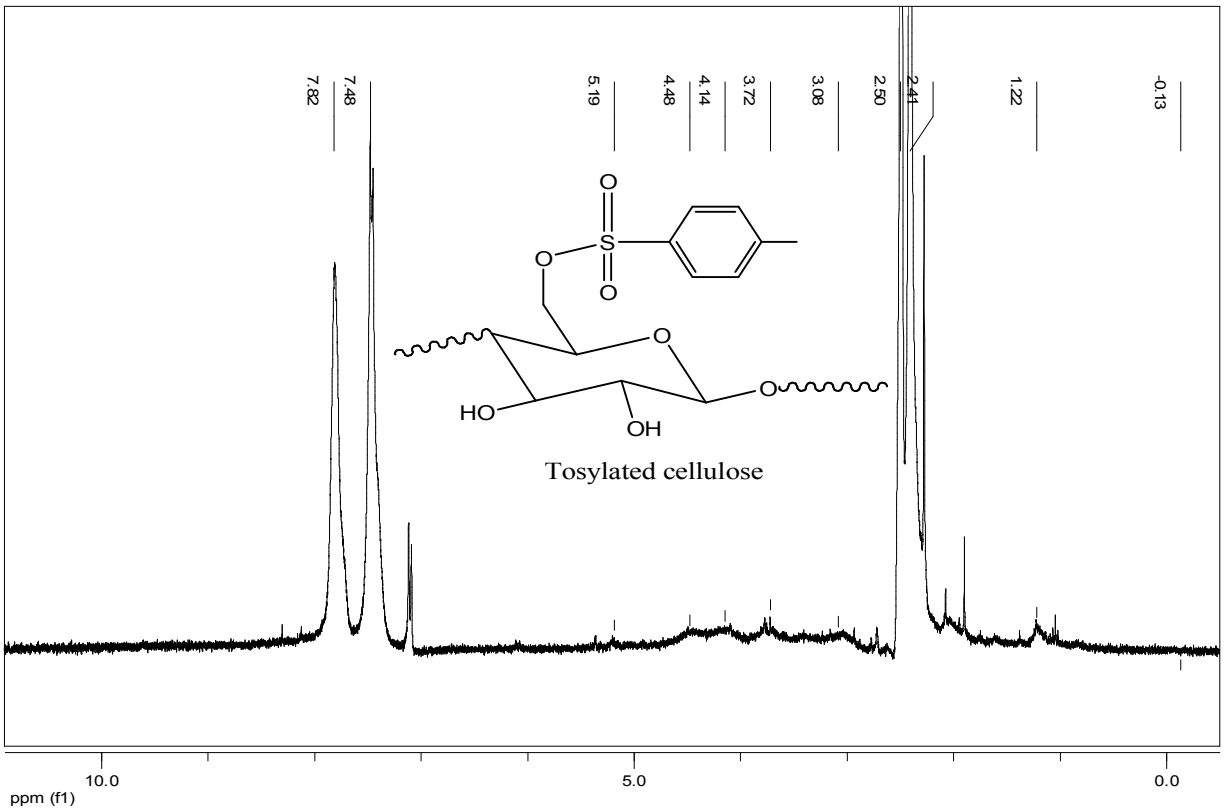

Figure 7.1. ^{1}H NMR spectra of tosylated cellulose.

Cellulose-DMPDA was first synthesized as a model compound for the synthesis of cellulose-BA (Scheme 7.3). The nucleophilic substitution was conducted at 50 ºC. After the reaction was finished, the cellulose-DMPDA obtained was soluble in both water and DMAC. Its proton NMR spectrum (Figure 7.2) in D_2O showed the chemical shift (3.21) of the proton of methyl group of (protonated tertiary nitrogen in highly hydrophilic microenvironment. It also displayed the chemical shift range of 3.00 to 4.8, the broad peaks of cellulose backbone, which is consistent with the proposed structure. The chemical shifts of 7.48 and 7.82 of aromatic ring disappeared in the proton NMR spectrum of Cellulose-DMPDA.

Scheme 7.3. Synthesis of Cellulose-DMPDA

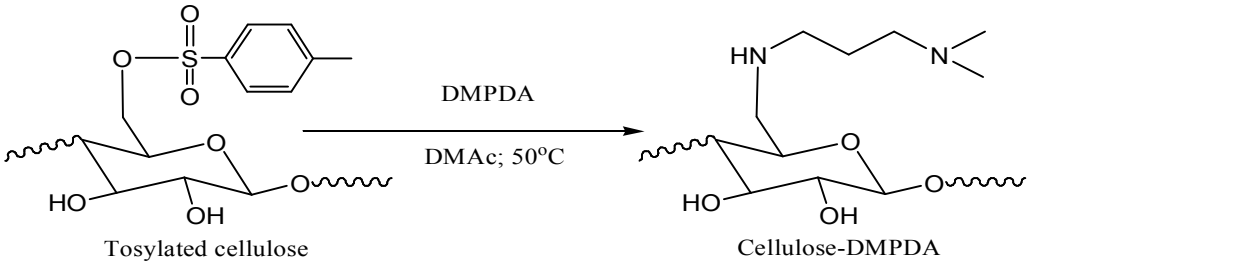

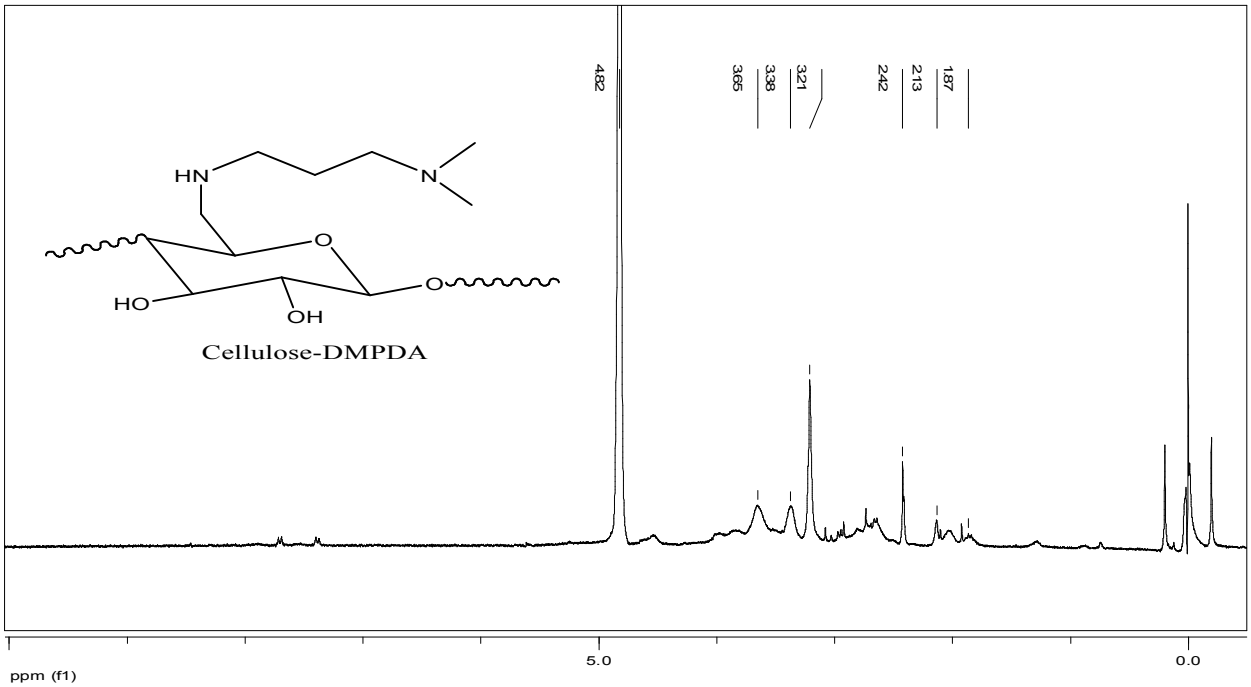

Figure 7.2. ^{1}H NMR spectrum of Cellulose-DMPDA.

However, no cellulose-BA was obtained when tosylated cellulose was reacted with BA at 50°C. This approach to synthesize cellulose-BA might require a higher temperature. However, BA can undergo an intra-molecular cyclization reaction when the reaction temperature is above 55°C. We did not try this synthesis at a higher temperature than 50°C.

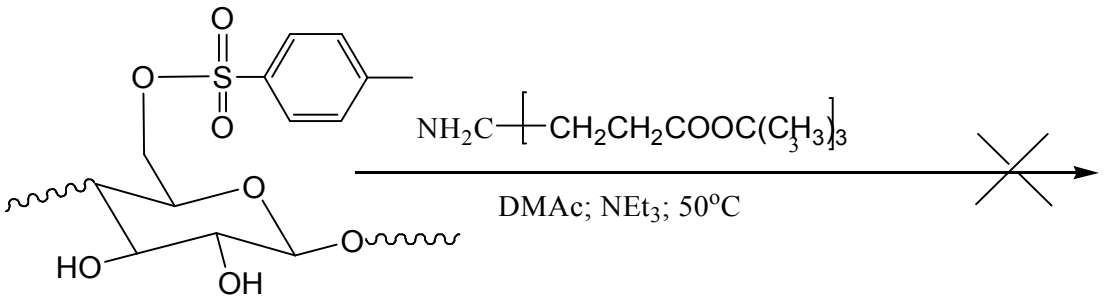

Tosylated cellulose

7.3.2 Synthesis of Dendronized Cellulose through Bromopropylcellulose

HPC has excellent solubility in many solvents. HPC also has hydroxyl groups on propyl substituents which protrude away from its cellulose backbone. By transforming HPC into HPC-Br, we created a new polymer with bromine functional groups protruding away from the cellulose backbone, which could be easily substituted with BA because the steric barrier from cellulose backbone was minimized in the molecular structures of HPC-Br. The bromination of HPC with PBr_3 was fast; but HPC-Br with high DS of bromine became insoluble in water, DMF, DMSO, and THF solvents. This greatly limited the further functionization.

We were able to control the DS of HPC-Br by controlling the relative concentration of PBr_3 added in the bromination reaction. HPC-Br with low DS obtained would swell in water, ethanol, and DMF. The swollen HPC-Br in a co-solvent mixture of DMF/ethanol reacted with BA at 50 °C. The nucleophilic substitution gave us dendronized cellulose HPC-BA. The proton NMR spectra (Figure 7.3) of the product showed strong chemical shifts of 1.30, 1.65, and 2.19 from BA dendron and the chemical shift range from 3.0 to 4.8, which is the broad peak of its cellulose

backbone. This confirmed the formation of cellulose-BA, a new dendronized cellulose derivative. Cellulose-BA was soluble in DMSO.

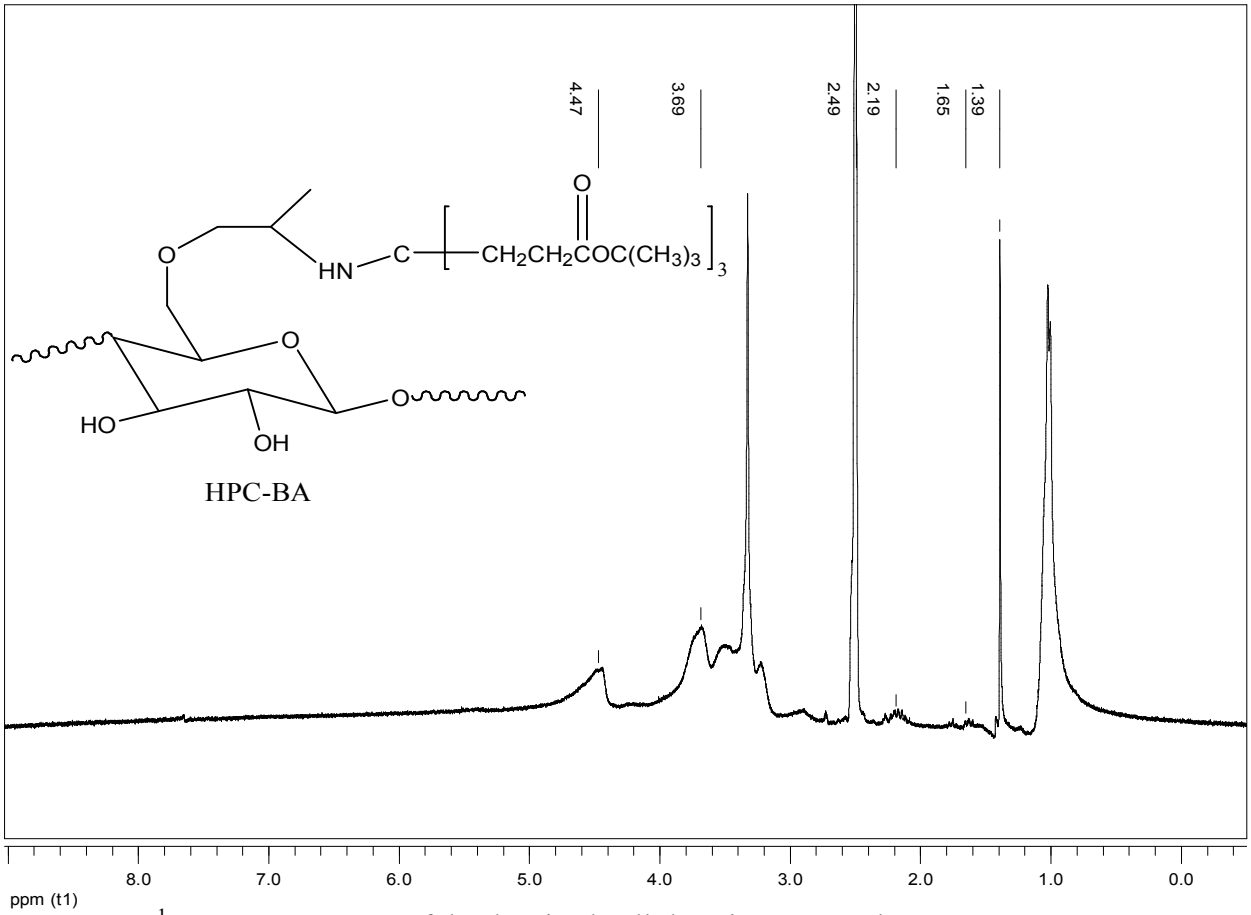

Figure 7.3. ^{1}H NMR spectrum of dendronized cellulose in DMDO-d_6.

7.4 Conclusions

(1) Dendronization of cellulose via HPC-Br is a viable way for making dendronized cellulose with Behera's amine.

(2) Dendronization of cellulose via tosylated cellulose with BA failed. The reaction must be conducted at a higher temperature than 50 °C, but the BA reagent begins to decompose at the higher temperatures required.

CHAPTER 8. SUMMARY AND FUTURE WORK

8.1 Conclusions

In this dissertation, two generations of Newkome's dendrons, BA and G-2-amine were synthesized following the procedures published by professor Newkome's group. A side chain composed of both a hydrophobic BA and a hydrophilic DMPDA was successfully elaborated to a CMC backbone, leading to 1st generation and 2nd generation aminoamide cellulose derivatives with a hydrophilic backbone and amphiphilic side chains. The 1st generation adduct CMCBA with different DS were obtained by adjusting the relative concentration of CMPI and the DS of CMC starting material. CMCBA with a higher DS could be synthesized through using high relative concentrations of CMPI and the CMC with a high DS.

The N,N-dimethylpropylenediamine derivatives of both two generations of dendronized cellulose derivatives, CMCBADMPDA and CMCBABADMPDA, showed much lower intrinsic viscosity than the model compound CMCDMPDA due to their dendritic structures. CMCBADMPDA showed a more compacted conformation in aqueous solution than CMC or CMCDMPDA. The relative intensity of I_1/ I_3 of pyrene fluorescence in both CMCBADMPDA and CMCBABADMPDA solutions showed that a saline condition did not have a significant influence on the hydrophobicity of the microenvironment in either of the two dendronized derivatives. CMCBADMPDA showed a very hydrophilic microenvironment in its aqueous solution while CMCBABADMPDA showed a more hydrophobic microenvironment than CMCBADMPDA. CMCBABADMPDA may carry more pyrene hydrophobic molecules than CMCBADMPDA. A higher concentration of CMCBABADMPDA solution could carry more hydrophobic molecules than that with a lower concentration.

A series of quaternary dendronized derivatives of CMCBADMPDA-R with R=C1~C18 were synthesized with different carbon chain lengths on the resultant quaternary nitrogen. The quaternary dendronized derivative CMCBADMPDA-C10-Quat188 was also synthesized with hydrophilic di-quaternary nitrogen as periphery functional groups. CMCBADMPDA-C10 derivatives with different degrees of quaternization (DQ) were obtained by adjusting the relative concentration of $C_{10}H_{25}Br$ in the reaction system. Higher DQ derivatives could be obtained by increasing the relative concentration of $C_{10}H_{25}Br$; but the reaction also produced decyl esters. CMCBADMPDA-C10s with high DSs of carbon chain length of ten were insoluble in water and further modification of CMCBADMPDA-C10s with high DS of C10 using propylene oxide and quat-188 produced water soluble CMCBADMPDA-C10-PO, and CMCBADMPDA-Quat188 derivatives. Dendronization of cellulose via HPC-Br provided an alternative way for making dendronized cellulose with Behera's amine dendron.

CMCBADMPDA-Quat188, the dendronized cellulose derivatives with hydrophilic diquaternary nitrogen periphery groups, did not show potent antibacterial activity. Enhanced antibacterial performance of cellulose derivatives was observed with hydrophobic alkyl chains on the quaternary nitrogens. CMCBADMPDA-R with R of alkyl carbon length of ten exhibited higher antimicrobial activity than that with other alkyl chain lengths. CMCBADMPDA-C10 at a DQ of 2.03% showed the best antimicrobial properties at 32 μg/mL against *E-coli* and 16 μg/mL against *S-aureus*. The hydrophobic alkyl chains on quaternary nitrogen conferred antimicrobial activity on the dendronized cellulose derivatives. Both of CMCBADMPDA-C10 and CMCBADMPDA-C10-quat188 with higher DQ demonstrated higher antibacterial performance. Dye release profiles of POPG/PE phospholipid vesicles with encapsulated calcein suggested that the antibacterial active CMCBADMPDA-C10 and CMCBADMPDA-C10-quat188 could break

the membranes of phospholipid vesicles and were likely to break the analogue structures of the cell walls and cytoplasmic membranes of bacteria. This could cause bacteria to loss necessary nutrients which quickened their extinction in antibacterial MIC test experiments.

8.2 Future Work

Future work on this project may be focused on the following several aspects:

(1) Synthesis of the 2nd generation dendronized cellulose derivative with hydrophobic alkyl chains on quaternary nitrogen as periphery groups and evaluation of their antibacterial properties.

(2) Synthesis of dendronized cellulose derivatives through bromopropyl cellulose.

(3) Grafting drug active peptide onto dendronized cellulose derivatives.

(4) The evaluation of CMCBADMPDA-quat188 as a gene delivery vector.

REFERENCES

1. Haigler, C. H. *Cellul. Chem. Its Appl.* **1985**, 30-83.

2. Nevell, T. P.; Zeronian, S. H. *Cellul. Chem. Its Appl.* **1985**, 15-29.

3. Kennedy, J. F.; White, C. A., *Bioactive Carbohydrates: In Chemistry, Biochemistry and Biology*. Ellis Horwood Ltd.: Chichester, UK, 1983; p 331 pp.

4 Nevell, T. P.; Zeronian, S. H., *Cellulose Chemistry and Its applications*. Ellis Horwood Limited: Chichester, England, 1985; p 21.

5. Culberson, D. A. Ph. D. Dissertation, Louisiana State University, Baton Rouge, LA, 1995.

6. Rowland, S. P.; Bertoniere, N. R. *Cellul. Chem. Its Appl.* **1985**, 112-37.

7. Wadsworth, L. C.; Daponte, D. *Cellul. Chem. Its Appl.* **1985**, 344-62.

8. Nicholson, M. D.; Merritt, F. M. *Cellul. Chem. Its Appl.* **1985**, 363-83.

9. Vail, S. L. *Cellul. Chem. Its Appl.* **1985**, 384-422.

10. Edwards, J. V.; Vigo, T. L., Biologically active fibers in health care. In *Bioactive Fibers and Polymers* Edwards, J. V.; Vigo, T. L., Eds. American Chemical Society: Washington, DC, 2001; pp 1-19.

11. Lee, S. B.; Koepsel, R. R.; Morley, S. W.; Matyjaszewski, K.; Sun, Y.; Russell, A. J. *Biomacromolecules* **2004,** 5, (3), 877-882.

12. Roy, D.; Guthrie, J. T.; Perrier, S. *Macromolecules* **2005,** 38, (25), 10363-10372.

13. Carlmark, A.; Malmstroem, E. E. *Biomacromolecules* **2003,** 4, (6), 1740-1745.

14. Parikh, D. V., Carboxymethylation-cotton for wound care management. In *Bioactive Fibers and Polymers*, Edwards, J. V.; Vigo, T. L., Eds. American Chemical Society: Washington, DC, 2001; pp 115-124.

15. Cen, L.; Neoh, K. G.; Kang, E. T. *Langmuir* **2003,** 19, (24), 10295-10303.

16. Sun, G., Durable and regenerable antimicrobial textiles. In *Bioactive Fibers and Polymers*, Edwards, J. V.; Vigo, T. L., Eds. American Chemical Society: Washington, DC, 2001; pp 243-252.

17. Sun, G.; Xu, X.; Bickett, J. R.; Williams, J. F. *Industrial & Engineering Chemistry Research* **2001,** 40, (4), 1016-1021.

18. Sun, Y.; Chen, Z.; Braun, M. *Industrial & Engineering Chemistry Research* **2005,** 44, (21), 7916-7920.

19. Williams, J.; Sun, G.; Xu, X.; Bickert, J., Antimicrobial properties of a novel N-halamine-based cellulose treatment process. In *Bioactive Fibers and Polymers*, Edwards, J. V.; Vigo, T. L., Eds. American Chemical Society: Washington, DC, 2001; pp 253-262.

20. Sun, G.; Xu, X. Durable and regenerable microbiocidal textiles. U. S. 9810648, 1998.

21. Bryskier, A. *Antimicrobial Agents* **2005**, 1-12.

22. Vigo, T. L., Antimicrobial polymers and fibers: retrospective and prospective. In *Bioactive Fibers and Polymers*, Edwards, J. V.; Vigo, T. L., Eds. American Chemical Society: Washinton, DC, 2001; pp 175-200.

23. Merianos, J. J., Quaternary Ammonium Antimicrobial Compounds. In *Disinfection, Sterilization and Preservation*, 4th ed.; Block, S. S., Ed. Lea and Febiger: Philadelphia, PA, 1990; pp 225-55.

24. May, O. W., Polymeric Antimicrobial Agents. In *Disinfection, Sterilization and Preservation*, 4th ed.; Block, S. S., Ed. Lea and Febiger: Philadelphia, PA, 1990; pp 322-33.

25. Guerrini, M. M.; Daly, W. H., Influence of cationic cellulose structure on interactions with sodium dodecyl sulfate. In *Polysaccharide Applications*, El-Nokaly, M. A.; Soini, H. A., Eds. American Chemical Society: Washington, DC, 1999; pp 214-233.

26. Manuszak-Guerrini, M. A.; Culberson, D. A.; Daly, W. H. Cationic cellulose derivatives with controlled charge density useful in cosmetic preparations. U. S. 5981737, 1999.

27. Logan, D. Ph. D. Dissertation, Louisiana State University, Baton Rouge, LA, 2001.

28. Thatte, M. R. Ph. D. Disstertation, Louisiana State University, Baton Rouge, LA, 2004.

29. Hiemenz, P. C., *Polymer Chemistry: The Basic Concepts*. Dekker New York, N. Y., 1984; p 738 pp.

30. Flory, P. J., *Principles of Polymer Chemistry*. Cornell Univ. Press: Ithaca, N.Y., 1953; p 672 pp.

31. Quirk, R. P.; Lee, Y.; Kim, J., Synthesis of branched polymers: an introduction. In *Star and Hyperbranched Polymers* Mishra, M. K.; Kobayashi, S., Eds. Marcel Dekker, Inc: New York, NY, 1999; pp 1-25.

32. Vogtle, F.; Stoddart, J. F.; Shibasaki, M.; Editors, *Stimulating Concepts in Chemistry*. Wiely-VCH: Weinheim, Germany, 2000; p 396 pp.

33. Tomalia, D. A. *Aldrichimica Acta* **2004,** 37, (2), 39-57.

34. Tomalia, D. A.; Naylor, A. M.; Goddard, W. A., III. *Angewandte Chemie* **1990,** 102, (2), 119-57.

35. Newkome, G. R.; Moorefield, C. N.; Vogtle, F., *Dendrimers, 2nd Edition*. Wiley Chichester, UK, 2001; p 330 pp.

36. Grayson, S. M.; Frechet, J. M. J. *Chemical Reviews (Washington, D. C.)* **2001,** 101, (12), 3819-3867.

37. Yeardley, D. J. P.; Ungar, G.; Percec, V.; Holerca, M. N.; Johansson, G. *Journal of the American Chemical Society* **2000,** 122, (8), 1684-1689.

38. Majoros, I. J.; Thomas, T. P.; Mehta, C. B.; Baker, J. R., Jr. *Journal of Medicinal Chemistry* **2005,** 48, (19), 5892-5899.

39. Kukowska-Latallo, J. F.; Candido, K. A.; Cao, Z.; Nigavekar, S. S.; Majoros, I. J.; Thomas, T. P.; Balogh, L. P.; Khan, M. K.; Baker, J. R., Jr. *Cancer Research* **2005,** 65, (12), 5317-5324.

40. Frechet, J. M. J. *Journal of Polymer Science, Part A: Polymer Chemistry* **2003,** 41, (23), 3713-3725.

41. Ambade, A. V.; Savariar, E. N.; Thayumanavan, S. *Molecular Pharmaceutics* **2005,** 2, (4), 264-272.

42. Kojima, C.; Kono, K.; Maruyama, K.; Takagishi, T. *Bioconjugate Chemistry* **2000,** 11, (6), 910-917.

43. Sideratou, Z.; Tsiourvas, D.; Paleos, C. M. *Langmuir* **2000,** 16, (4), 1766-1769.

44. Murugan, E.; Sherman, R. L., Jr.; Spivey, H. O.; Ford, W. T. *Langmuir* **2004,** 20, (19), 8307-8312.

45. Chen, C. Z.; Beck-Tan, N. C.; Dhurjati, P.; Van Dyk, T. K.; LaRossa, R. A.; Cooper, S. L. *Biomacromolecules* **2000,** 1, (3), 473-480.

46. Chen, C. Z.; Cooper, S. L. *Biomaterials* **2002,** 23, (16), 3359-3368.

47. Cooper, S. L.; Chen, C. Z. Quaternary ammonium-functionalized dendrimers and methods of use therefor. U. S. 6440405, 2002.

48. Kaneko, T.; Horie, T.; Asano, M.; Aoki, T.; Oikawa, E. *Macromolecules* **1997,** 30, (10), 3118-3121.

49. Desai, A.; Atkinson, N.; Rivera, F., Jr.; Devonport, W.; Rees, I.; Branz, S. E.; Hawker, C. J. *Journal of Polymer Science, Part A: Polymer Chemistry* **2000,** 38, (6), 1033-1044.

50. Pathak, S.; Singh, A. K.; McElhanon, J. R.; Dentinger, P. M. *Langmuir* **2004,** 20, (15), 6075-6079.

51. Elizarov Arkadij, M.; Chang, T.; Chiu, S.-H.; Stoddart, J. F. *Org Lett* **2002,** 4, (21), 3565-8.

52. Narayanan, V. V.; Wiener, E. C. *Macromolecules* **2000,** 33, (10), 3944-3946.

53. Hawker, C. J.; Frechet, J. M. J. *Polymer* **1992,** 33, (7), 1507-11.

54. Hawker, C.; Frechet, M. J. *Journal of the Chemical Society, Chemical Communications* **1990**, (15), 1010-13.

55. Ecker, C.; Severin, N.; Shu, L.; Schlueter, A. D.; Rabe, J. P. *Macromolecules* **2004,** 37, (7), 2484-2489.

56. Zhang, A.; Shu, L.; Bo, Z.; Schluter, A. D. *Macromolecular Chemistry and Physics* **2003,** 204, (2), 328-339.

57. Shu, L.; Schluter, A. D.; Ecker, C.; Severin, N.; Rabe, J. P. *Angewandte Chemie, International Edition* **2001,** 40, (24), 4666-4669.

58. Marsitzky, D.; Vestberg, R.; Blainey, P.; Tang, B. T.; Hawker, C. J.; Carter, K. R. *Journal of the American Chemical Society* **2001,** 123, (29), 6965-6972.

59. Schappacher, M.; Putaux, J. L.; Lefebvre, C.; Deffieux, A. *Journal of the American Chemical Society* **2005,** 127, (9), 2990-2998.

60. Zhuravel, M. A.; Davis, N. E.; Nguyen, S. T.; Koltover, I. *Journal of the American Chemical Society* **2004,** 126, (32), 9882-9883.

61. Sashiwa, H.; Shigemasa, Y.; Roy, R. *Macromolecules* **2001,** 34, (10), 3211-3214.

62. Sashiwa, H.; Yajima, H.; Aiba, S.-i. *Biomacromolecules* **2003,** 4, (5), 1244-1249.

63. Driffield, M.; Goodall, D. M.; Smith, D. K. *Organic & Biomolecular Chemistry* **2003,** 1, (14), 2612-2620.

64. Goh, S. L.; Francis, M. B.; Frechet, J. M. J. *Chemical Communications* **2002**, (24), 2954-2955.

65. Liu, M.; Frechet, J. M. J. *Pharmaceutical Science & Technology Today* **1999,** 2, (10), 393-401.

66. Newkome, G. R.; Weis, C. D. *Organic Preparations and Procedures International* **1996,** 28, (4), 495-498.

67. Newkome, G. R.; Weis, C. D.; Abourahma, H. *ARKIVOC* **2000,** 1, (3), 210-217.

68. Chen, C. Z.; Cooper, S. L. *Polymeric Materials Science and Engineering* **1999,** 81, 483-484.

69. Baigude, H.; Katsuraya, K.; Tokunaga, S.; Fujiwara, N.; Satoyama, M.; Magome, T.; Okuyama, K.; Borjihan, G.; Uryu, T. *Journal of Polymer Science, Part A: Polymer Chemistry* **2005,** 43, (11), 2195-2206.

70. Newkome, G. R.; Behera, R. K.; Moorefield, C. N.; Baker, G. R. *Journal of Organic Chemistry* **1991,** 56, (25), 7162-7.

71. Newkome, G. R.; Moorefield, C. N. Tertiary butyl cascade polymers. U.S. Pat. Appl. 2003097019, 2003.

72. Cardona, C. M.; McCarley, T. D.; Kaifer, A. E. *Journal of organic chemistry* **2000,** 65, (6), 1857-64.

73. Cardona, C. M.; Wilkes, T.; Ong, W.; Kaifer, A. E.; McCarley, T. D.; Pandey, S.; Baker, G. A.; Kane, M. N.; Baker, S. N.; Bright, F. V. *Journal of Physical Chemistry B* **2002,** 106, (34), 8649-8656.

74. Newkome, G. R.; Yoo, K. S.; Moorefield, C. N. *Designed Monomers and Polymers* **2002,** 5, (1), 67-77.

75. Newkome, G. R.; Kotta, K. K.; Moorefield, C. N. *Journal of Organic Chemistry* **2005,** 70, (12), 4893-4896.

76. Wong, S. S., *Chemistry of Protein Conjugation and Cross-linking*. CRS Press Inc.: Boca, Raton, Florida, 1991; p 340 pp.

77. Barbucci, R.; Magnani, A.; Consumi, M. *Macromolecules* **2000,** 33, (20), 7475-7480.

78. Price, L. M. Loisiana State University, Baton Rouge, LA, USA, 2001.

79. Zhang, C.; Price, L. M.; Daly, W. H. *Polymer Preprints (American Chemical Society, Division of Polymer Chemistry)* **2004,** 45, (2), 421-422.

80. Zhang, C.; Price, L. M.; Daly, W. H. *Biomacromolecules* **2006,** 7, (1), 139-145.

81. Feddersen, R. L.; Thorp, S. N., Sodium Carboxymethylcellulose. In *Industrial Gums, Polysaccharides and their Derivatives*, 3 ed.; Whistler, R. L.; BeMiller, J. N., Eds. Academic Press, Inc: New York, NY, 1993; pp 537-79.

82. Zhang, C.; Daly, W. H. *Polymer Preprints (American Chemical Society, Division of Polymer Chemistry)* **2006,** 47, (2), 35-36.

83. Yang, S.; Monsey, M. J.; Li, L.; Cholli, A. L.; Kumar, J., Structural aspects of low-molecular-weight azocellulose polymers: a solid-state 13C NMR study. In *NMR Spectroscopy of Polymers in Solution and in the Solid State*, Cheng, H. N.; English, A. D., Eds. American Chemical Society: Washington, DC, 2003; Vol. 834, pp 58-70.

84. Fessenden, R. J.; Fessenden, J. S., *Organic Chemistry*. Willard Grant Press: Boston, Massachusetts, 1979; p 607.

85. Newkome, G. R.; Weis, C. D.; Abourahma, H. *ARKIVOC [online computer file]* **2000,** 1, (3), 210-217.

86. Gao, Z.; Lukyanov, A. N.; Singhal, A.; Torchilin, V. P. *Nano Letters* **2002,** 2, (9), 979-982.

87. Wilhelm, M.; Zhao, C. L.; Wang, Y.; Xu, R.; Winnik, M. A.; Mura, J. L.; Riess, G.; Croucher, M. D. *Macromolecules* **1991,** 24, (5), 1033-40.

88. Winnik, F. M.; Regismond, S. T. A. *Colloids and Surfaces, A: Physicochemical and Engineering Aspects* **1996,** 118, (1/2), 1-39.

89. Winnik, F. M.; Winnik, M. A. *Polymer Journal (Tokyo, Japan)* **1990,** 22, (6), 482-8.

90. Kalyanasundaram, K.; Thomas, J. K. *Journal of the American Chemical Society* **1977,** 99, (7), 2039-44.

91. Guerrini, M. A. M. Ph. D. Dissertation. Louisiana State University, Baton Rouge, 1997.

92. Zhang, C.; Daly, W. H. *Polymer Preprints (American Chemical Society, Division of Polymer Chemistry)* **2005,** 46, (2), 707-708.

93. Williams, D. F.; Schmitt, W. H., *Chemistry and Technology of the Cosmetics and Toiletries Industry*. 1 ed.; Blackie Academic & Professional: London, UK, 1992; p 331 pp.

94. Merianos, J. J. *Disinfect., Steril., Preserv., 4nd Ed.* **1990**, 225-55.

95. Ebert, G. W.; Juda, W. L.; Kosakowski, R. H.; Ma, B.; Dong, L.; Cummings, K. E.; Phelps, M. V. B.; Mostafa, A. E.; Luo, J. *Journal of Organic Chemistry* **2005,** 70, (11), 4314-4317.

96. Wu, J.; Su, Z.-G.; Ma, G.-H. *International Journal of Pharmaceutics* **2006,** 315, (1-2), 1-11.

97. Hennis, H. E.; Easterly, J. P., Jr.; Collins, L. R.; Thompson, L. R. *Industrial & Engineering Chemistry Product Research and Development* **1967,** 6, (3), 193-5.

98. Sun, G.; Xu, X. *Textile Chemist and Colorist* **1998,** 30, (6), 26-30.

99. Daly, W. H.; Thatte, M.; Zhang, C.; Sajomsang, W. *Polymer Preprints (American Chemical Society, Division of Polymer Chemistry)* **2006,** 47, (2), 121-122.

100. Daly, W. H.; Zhang, C.; Sajomsang, W. *Abstracts, 62nd Southwest Regional Meeting of the American Chemical Society, Houston, TX, United States, October 19-22* **2006**, SRM-141.

101. Franklin, T. J., *Biochemistry and Molecular Biology of Antimicrobial Drug Action, 5th Edition*. 1998; p 17-8.

102. Karp, G., *Cell and Molecular Biology: Concepts and Experiments, 2nd Edition*. John Wiley & Sons, Inc.: New York, 1998; p 864 pp.

103. Arnt, L.; Rennie, J. R.; Linser, S.; Willumeit, R.; Tew, G. N. *Journal of Physical Chemistry B* **2006,** 110, (8), 3527-3532.

104. Trombetta, D.; Castelli, F.; Sarpietro, M. G.; Venuti, V.; Cristani, M.; Daniele, C.; Saija, A.; Mazzanti, G.; Bisignano, G. *Antimicrobial Agents and Chemotherapy* **2005,** 49, (6), 2474-2478.

105. Lambert, R. J. W.; Pearson, J. *Journal of Applied Microbiology* **2000,** 88, (5), 784-790.

106. Franklin, T. J., *Biochemistry and Molecular Biology of Antimicrobial Drug Action*. 5 ed.; Chapman & Hall: London, UK, 1998; p 224 pp.

107. Heinze, T.; Rahn, K.; Jaspers, M.; Berghmans, H. *Macromolecular Chemistry and Physics* **1996,** 197, (12), 4207-4224.

108. Lepoittevin, B.; Matmour, R.; Francis, R.; Taton, D.; Gnanou, Y. *Macromolecules* **2005,** 38, (8), 3120-3128.

109. Liebert, T. F.; Heinze, T. *Biomacromolecules* **2005,** 6, (1), 333-340.

110. Koschella, A.; Heinze, T. *Macromolecular Bioscience* **2001,** 1, (5), 178-184.

111. Mais, U.; Knaus, S.; Binder, W. H.; Gruber, H. *Lenzinger Berichte* **2000,** 79, 71-76.

112. Aoki, N.; Sakamoto, M.; Furuhata, K. *ACS Symposium Series* **1998,** 688, 83-93.

113. Aoki, N.; Furuhata, K.-i.; Saegusa, Y.; Nakamura, S.; Sakamoto, M. *Journal of Applied Polymer Science* **1996,** 61, (7), 1173-1185.

114. Majetich, G.; Hicks, R.; Zhang, Y.; Tian, X.; Feltman, T. L.; Fang, J.; Duncan, S., Jr. *Journal of Organic Chemistry* **1996,** 61, (23), 8169-8185.

APPENDIX: PERMISSION LETTER

ACS PUBLICATIONS DIVISION
APR 13 2007

Changde Zhang
375 W. Roosevelt St., Apt# 2228
Baton Rouge, LA70802
Tele: (225) 578-29851 (O)
Fax: (225)578-3458
e-mail: czhang9@lsu.edu

4/13/2007

Copyright Office
Publications Division
American Chemical Society
1155 16th Street, N.W.
Washington, DC 20036

To Whom It May Concern:

I am writing to obtain the permission for the use of an article published in the Biomacromolecules. I am a graduate student in the Department of Chemistry at Louisiana State University. I am the first author on the article and would like to include this article in my doctoral dissertation. The article is "Synthesis and characterization of an aminoamide dendronized cellulose derivative" , Zhang, C.; Price, L. M.; Daly, W. H. *Biomacromolecules* **2006**, 7, (1), 139-145.

Thanks for your consideration of my request!

Sincerely,

Changde Zhang 04/13/07

Changde Zhang
Department of Chemistry
Louisiana State University
Choppin Hall, Room 230
Baton Rouge, LA 70802
Tele: (225) 578-29851 (O)
Fax: (225)578-3458
e-mail: czhang9@lsu.edu

American Chemical Society

Publications Division
Copyright Office

1155 Sixteenth Street, NW
Washington, DC 20036
Phone: (1) 202-872-4368 or -4367
Fax: (1) 202-776-8112 E-mail: copyright@acs.org

VIA FAX: 225-578-3458 DATE: April 20, 2007

TO: Changde Zhang, Department of Chemistry, Louisiana State University
375 W. Roosevelt St., Apt. #2228, Baton Rouge, LA 70802

FROM: C. Arleen Courtney, Copyright Associate C. Arleen Courtney

Thank you for your request for permission to include **your** paper(s) or portions of text from **your** paper(s) in your thesis. Permission is now automatically granted; please pay special attention to the implications paragraph below. The Copyright Subcommittee of the Joint Board/Council Committees on Publications approved the following:

Copyright permission for published and submitted material from theses and dissertations
ACS extends blanket permission to students to include in their theses and dissertations their own articles, or portions thereof, that have been published in ACS journals or submitted to ACS journals for publication, provided that the ACS copyright credit line is noted on the appropriate page(s).

Publishing implications of electronic publication of theses and dissertation material
Students and their mentors should be aware that posting of theses and dissertation material on the Web prior to submission of material from that thesis or dissertation to an ACS journal may affect publication in that journal. Whether Web posting is considered prior publication may be evaluated on a case-by-case basis by the journal's editor. If an ACS journal editor considers Web posting to be "prior publication", the paper will not be accepted for publication in that journal. If you intend to submit your unpublished paper to ACS for publication, check with the appropriate editor prior to posting your manuscript electronically.

If your paper has **not** yet been published by ACS, we have no objection to your including the text or portions of the text in your thesis/dissertation in **print and microfilm formats**; please note, however, that electronic distribution or Web posting of the unpublished paper as part of your thesis in electronic formats might jeopardize publication of your paper by ACS. Please print the following credit line on the first page of your article: "Reproduced (or 'Reproduced in part') with permission from [JOURNAL NAME], in press (or 'submitted for publication'). Unpublished work copyright [CURRENT YEAR] American Chemical Society." Include appropriate information.

If your paper has already been published by ACS and you want to include the text or portions of the text in your thesis/dissertation in **print or microfilm formats**, please print the ACS copyright credit line on the first page of your article: "Reproduced (or 'Reproduced in part') with permission from [FULL REFERENCE CITATION.] Copyright [YEAR] American Chemical Society." Include appropriate information.

Submission to a Dissertation Distributor: If you plan to submit your thesis to UMI or to another dissertation distributor, you should not include the unpublished ACS paper in your thesis if the thesis will be disseminated electronically, until ACS has published your paper. After publication of the paper by ACS, you may release the entire thesis (**not the individual ACS article by itself**) for electronic dissemination through the distributor; ACS's copyright credit line should be printed on the first page of the ACS paper.

Use on an Intranet: The inclusion of your ACS unpublished or published manuscript is permitted in your thesis in print and microfilm formats. If ACS has published your paper you may include the manuscript in your thesis on an intranet that is not publicly available. Your ACS article cannot be posted electronically on a publicly available medium (i.e. one that is not password protected), such as but not limited to, electronic archives, Internet, library server, etc. The only material from your paper that can be posted on a public electronic medium is the article abstract, figures, and tables, and you may link to the article's DOI or post the article's author-directed URL link provided by ACS. This paragraph does not pertain to the dissertation distributor paragraph above. 06/07/06

VITA

Changde Zhang was the youngest child of Yueqin Zhang in Shandong Province of China. He obtained the Bachelor of Science in chemistry from Liaocheng Teacher College, Liaocheng, Shandong Province, China, in July 1986. Then, he entered the graduate school of Xi′an Jiaotong University and received his master degree of engineering in polymer material science in 1989. Afterwards he joined Beijing Petrochemical College as an instructor in polymer science and engineering and was promoted to associate professor in 1998. In January 2000, he was granted a BP (British Petroleum) fellowship and a Case Prime fellowship from Case Western Reserve University in Cleveland, Ohio, and came to study in America. He received a master degree of engineering in macromolecular science and engineering at Case Western Reserve University in August 2002. When he was in America, his father, Yueqin Zhang, passed away unfortunately at the age of seventy seven due to cancer. He was grieved at the contradiction of life. Changde Zhang is currently a candidate for the degree of Doctor of Philosophy in the Department of Chemistry at Louisiana State University and his area of specialization is polymer science.